Advanced Multiparametric Optimization and Control Studies for Anaesthesia

A thesis submitted to Imperial College London for the degree of Doctor of Philosophy

by

Ioana Nașcu

Centre for Process Systems Engineering, Department of Chemical Engineering, Imperial College London, United Kingdom.

January 2016

"Wonder is the beginning of knowledge."

Socrates

Declaration of Originality

I hereby declare that this is my own work and any published and unpublished work used here has been cited in the text, and the list of references in the bibliography section at the end of thesis.

Ioana Nașcu

Abstract

Anaesthesia is a reversible pharmacological state of the patient where hypnosis, analgesia and muscle relaxation are guaranteed and maintained throughout the surgery. Analgesics block the sensation of pain; hypnotics produce unconsciousness, while muscle relaxants prevent unwanted movement of muscle tone.

Controlling the depth of anaesthesia is a very challenging task, as one has to deal with nonlinearity, inter- and intra-patient variability, multivariable characteristics, variable time delays, dynamics dependent on the hypnotic agent, model analysis variability, agent and stability issues. The modelling and automatic control of anaesthesia is believed to (i) benefit the safety of the patient undergoing surgery as side-effects may be reduced by optimizing the drug infusion rates, and (ii) support anaesthetists during critical situations by automating the drug delivery systems.

In this work we have developed several advanced explicit/multi-parametric model predictive (mp-MPC) control strategies for the control of depth of anaesthesia. State estimation techniques are developed and used simultaneously with mp-MPC strategies to estimate the state of each individual patient, in an attempt to overcome the challenges of inter- and intra- patient variability, and deal with possible unmeasurable noisy outputs.

Strategies to deal with the nonlinearity have been also developed including local linearization, exact linearization as well as a piece-wise linearization of the Hill curve leading to a hybrid formulation of the patient model and thereby the development of multiparametric hybrid model predictive control methodology. To deal with the inter- and intra- patient variability, as well as the noise on the process output, several robust techniques and a multiparametric moving horizon estimation technique have been design and implemented.

All the studies described in the thesis are performed on clinical data for a set of 12 patients who underwent general anaesthesia.

Acknowledgments

Personal Acknowledgments

The four years of my PhD have been the most difficult as well as the most beautiful years of my life so far. It has been a period of learning, understanding, making mistakes but most of all, it has been a period in which I have truly shaped myself. The more I learned, the more I understood that there is so much I still don't know, and the more I would crave for knowledge. Like Socrates said "The only true wisdom is knowing you know nothing." Thankfully I was lucky in having around me great people that were able to guide me, feed my thirst for knowledge but most of all help me define my own path. Everything I have achieved so far and everything I will continue to do, I do for them.

For my supervisor, Professor Stratos Pistikopoulos, whom I greatly respect and admire not only as a mentor but as an example to follow. For being an inspiration in his passion for knowledge and life and above all for taking me to the next level.

For my parents for putting me and my brother above everything else, making me want to become a better person and providing me all the means to achieve it. Most of all for making me proud to be their daughter.

For my father, whom has passed onto me the love for control engineering, for teaching me about PID and model predictive control and helping me understand when I got lost; but very importantly for letting me play with electronic circuits (which I have all destroyed) and oscillators as a child. But most of all helping me understand my soul and for being one of the few people I admire in this world.

For my mother, for always knowing I can do better and never letting me give up no matter how hard it was. For being the one who has always pulled me up and for knowing me better than I know myself.

For my brother, for always being next to me, and one of the people I look up to. For teaching me strength, that I can achieve everything I imagine no matter how impossible it seems and that everything in this life has a solution.

For my friends, for being there for all the good and the bad things, for putting up with my craziness and for believing in me without the smallest doubt.

For those who are my heart and soul and showed me there is beauty and perfection in this imperfect world. For all the sacrifices made for me, to become who I am today.

And last, for myself, for always believing in my dreams, for never giving up on them…

Financial Support

I would like to thank the European Research Council (MOBILE, ERC Advanced Grant, No: 226462), the European Commission (OPTICO/G.A. No.280813) and the European Commission (PIRSES, G.A. 294987). Financial support from Texas A&M University and Texas A&M Energy Institute is also gratefully acknowledge.

Contents

List of Tables

List of Figures

List of abbreviations

BIS	-	Bispectral index
CHP	-	combined heat and power
DOA	-	depth of anaesthesia
EEG	-	electro-encephalogram
EMG	-	electromyographic
EPSAC	-	Extended Predictive Self Adaptive Control
GMDH	-	Group Method of Data Handling
GMDH-HDMR	-	Group Method of Data Handling - High Dimensional Model Representation
HDMR	-	High Dimensional Model Representation
hMPC	-	hybrid model predictive control
ICU	-	Intensive Care Unit
MHE	-	moving horizon estimation
MIMO	-	Multiple Input Multiple Output
MMG	-	mechanomyography
mp-MHE	-	multiparametric moving horizon estimation
mp-LP	-	multiparametric linear programming
mp-MILP	-	multiparametric mixed-integer programming
mp-MIQP	-	multiparametric mixed-integer quadratic programming
mp-QP	-	multiparametric quadratic programming
MPC	-	model predictive control
mp-MPC	-	Explicit/multiparametric model predictive control

PaN	-	Nominal patient
PAROC	-	PARametric Optimization and Control
PD	-	pharmacodynamic
(P)DAE	-	(partial) differential and algebraic equations
PID	-	Proportional Integrative Derivative
PK	-	pharmacokinetic
POP	-	Parametric Optimization toolbox
SI	-	Sensitivity Index
SISO	-	Single Input Single Output

Chapter 1
Introduction

1.1 Anaesthesia Process

Nowadays, general anaesthesia is an irreplaceable adjunct to modern surgery. Before the advent of anaesthesia, surgical procedures demanded extremely fast execution. The alteration of senses using drugs (opium, laudanum) and alcohol was well known since antiquity. The first recorded anaesthesia procedure was performed in 1842 using inhaled ether to deprive patient of their sense during surgery. The term “anaesthesia” (meaning no ability to sense, the word anaesthesia originates from the greek word "aisthesis" which means sensation and the prefix "an" is used for negation) was proposed to describe this new phenomenon.

General anaesthesia ensures that patients are unconscious, feel no pain, have no memory of the surgery, remain still during the operation and have adequate autonomic nervous system, respiratory and cardiac responses to keep them alive. Achieving this is possible by using a variety of drugs (anaesthetics).

The practice of modern clinical anaesthesia is based on the concepts of the anaesthesia triad and balanced anaesthesia shown in Figure 1.1. Anaesthesiologists administer a combination of drugs and adjust several infusion devices to achieve an adequate balance between hypnosis, analgesia and muscle relaxation of the patient.

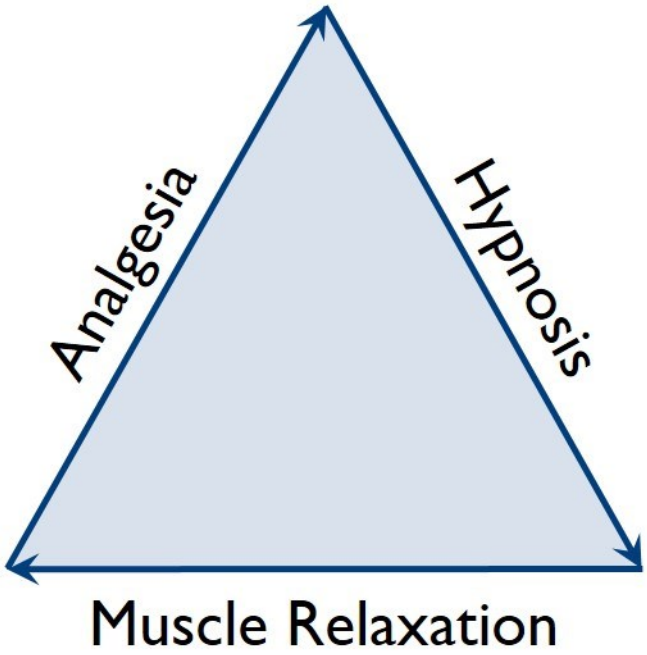

Figure 1.1: Anaesthesia components

Hypnosis describes a state of anaesthesia related to patient drug induced unconsciousness where the patient neither perceives nor recalls (amnesia) noxious stimuli i.e., stimuli associated with transmission of pain during events that occurred during surgery. The disability to recall is important because during surgery the patient might feel pain and be aware of the surgical procedures but cannot communicate this to the clinical staff. This awareness can be a traumatic experience, which is feared by the patients as well as the anaesthetists and should be avoided by maintaining sufficient hypnosis depth in the patient.

Analgesia describes a special state of anaesthesia related to the disability of the patient to perceive pain. Surgical procedures are painful and can discomfort the patient. Although the patient is unconscious, may perceive the pain and this can alter the general anaesthesia state, if analgesics are not administered. A stable analgesia state is partially responsible for a stable hypnosis and vice versa. It is important to have a balance between hypnosis and analgesia.

Skeletal muscles relaxation or neuromuscular blockade is a standard practice during general anaesthesia to facilitate the access to internal organs and to depress movement responses to surgical stimulations. Many surgical procedures require skeletal muscle relaxation to improve surgical conditions or to reduce surgical risks caused by movements of the patients.

There exists no single device, which accurately measures or estimates the anaesthetic state of the patient. However, the anaesthetic state is reflected in patient signs and biological signals. Patient signs reflecting the anaesthetic state involve response to speech, eyelash reflex, the constriction of the pupil of the eye, grimacing and other movement, breathing pattern, lachrimation and perspiration (Barash et al., 2009) and are relatively hard to measure online. Almost all mentioned patient signs indicate an excessively low anaesthetic depth. The heart rate, blood pressure, blood oxygen saturation and blood or end-tidal carbon dioxide concentrations are patient biological on-line measurable quantities reflecting the anaesthetic state. These are monitored in every modern operating room. For example, noxious stimulation increases blood pressure and heart rate when the anaesthesia depth is inadequately low. Monitoring the blood carbon dioxide concentrations provide surrogate measures of the analgesia depth.

Hypnosis and analgesia are the result of different pharmacological mechanisms within the central nervous system and it is not possible to be directly measured. Although there is no direct measure of unconsciousness or pain, there exist patient signs that can be sufficiently correlated with these anaesthesia states. Since consciousness is processed at the brain level, it is reasonable to assume that electroencephalogram signals (EEG), which reflect the brain activity, can be used to determine depth of drug induced unconsciousness. There are a number of signal processing tools and techniques available to quantify the EEG in order to derive an indirect measurement of hypnosis. To date there exist several anaesthesia monitors based on such indirect techniques, including the Bispectral Index (BIS) monitor (Johansen et al., 2000a), the State Entropy (SE) and Response Entropy (RE) monitors (Viertö-Oja et al.), the NeuroSENSE monitor (Bibian et al., 2011), the Cerebral State Index (CSI) monitor (Jensen et al., 2006) and the A-line monitor (Litvan et al., 2002). The BIS monitor is by far the clinically most wide-spread.

Bispectral analysis is a statistical technique that allows study of phenomena with nonlinear character such as surf beats and wave breaking (Rosenblatt et al., 1972). Bispectral analysis represents a different description of the EEG in that interfrequency phase relationships are measured, i.e., the bispectrum quantifies relationships among the underlying sinusoidal components of the EEG (Rampil, 1998, Sigl et al., 1994). Several variables from the EEG time domain (burst suppression) (Bruhn et al., 2000) and frequency domain (power spectrum, bispectrum, beta ratio, SynchFastSlow) are combined into a single index of hypnotic level. The weight factors of the various subparameters were assigned in a multivariate model based on a prospectively collected database of EEG recordings matched to corresponding states of hypnosis and to hypnotic drug levels. The BIS algorithm uses a complex formula (Johansen, 2006) with advanced artifact rejection techniques to define a dimensionless BIS value from 0 (isoelectric EEG) to 100 (alert and oriented) that is relatively independent of hypnotic agent. Awake, unpremedicated patients have BIS values at or above 93 (Figure 1.2). Loss of recall (<10%) occurs at BIS values of 75–80 (Iselin-Chaves et al., 1998). BIS correlates tightly with sedation scales such as the Observer's Assessment of Awareness and Sedation (OAA/S) (Glass et al., 1997) during midazolam (Liu et al., 1996), propofol (Liu et al., 1997, Irwin et al., 2002) or multiple hypnotic agents (Ibrahim et al., 2001, Mi et al., 1999) administration. In these studies, loss of response to mild prodding (transition OAA/S 2–1) was defined as loss of consciousness and correlated to BIS values between 68 and 75. BIS values of ≤60 have been associated with a low probability of recall and a high probability of unresponsiveness during surgery under general anaesthesia (Liu et al., 1997). BIS values between 40 and 60 have been recommended for anaesthetic maintenance during general anaesthesia (Johansen et al., 2000b). Blinded observation of practitioners attempting a rapid emergence resulted in hypnotic maintenance at BIS values in the high 30s to low 40s corresponding to deep sedation and near burst suppression (Gan et al., 1997). As the BIS falls from the mid 30 s to zero, EEG burst suppression increases to cortical silence. BIS responds monotonically to increasing hypnotic drug dose (volatile or intravenous) across the entire spectrum of awareness, independent of agent, and is not significantly influenced by opioids (Johansen and Sebel,

2000a) . BIS does not monitor analgesia and does not predict spinal cord reflexes to painful stimuli such as movement or hemodynamic responses (Johansen and Sebel, 2000a).

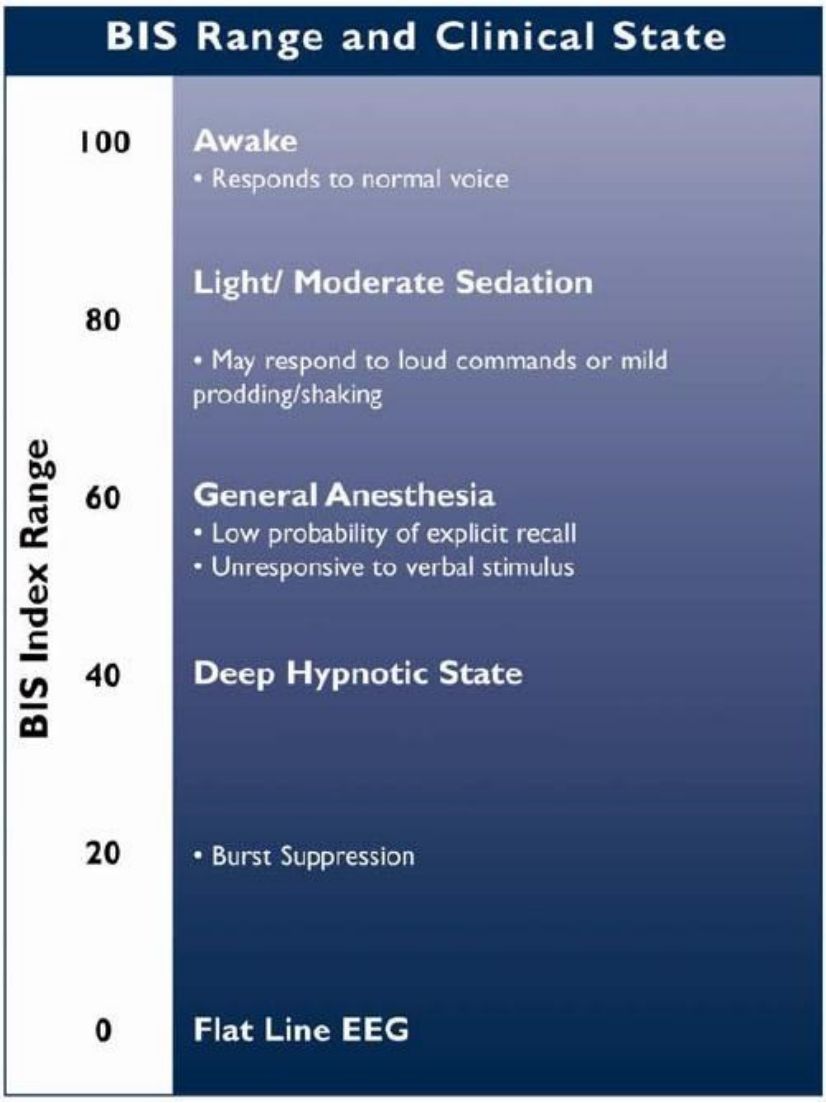

Figure 1.2: Bispectral index (BIS) scale. Dimensionless scale from 0 (complete cortical EEG suppression) to 100 (awake)

Significant EMG (electromyographic) activity may be present in sedated, spontaneously respiring patients, interfering with EEG signal acquisition and contaminating the BIS calculation. Conventionally, EEG signals are considered to exist in the 0.5–30 Hz band

and EMG signals in the 30–300 Hz band (although BIS uses EEG signals up to 47 Hz). This separation is not absolute, and low frequency EMG signals can occur in the conventional EEG band range. This EMG activity may be interpreted as high frequency, low amplitude waves, falsely elevating the BIS. Similarly, falsely elevated BIS values can also occur with high electrode impedances produced by inadequate electrode attachment or misplacement. Improvements in the BIS algorithm have focused on steadily decreasing the impact of EMG contamination in both anaesthetic and sedative ranges. An alert clinician needs to assess signal quality (SQI, Figure 1.3), EMG activity and BIS trend with relation to the clinical state of the patient prior to making any treatment decisions.

Figure 1.3: Bispectral index XP monitor(Johansen, 2006)

The analgesia functional component of anaesthesia has not received yet enough attention. In recent years there are several studies with the aim of developing such devices based on indirect indicators but without sufficient demonstration of their scientific base. The widely accepted indirect measures are the hemodynamic variables like blood pressure and heart rate variability. The changes in respiratory rate and blood carbon dioxide concentrations can also provide an indirect measurement for the depth of analgesia.

Monitoring the degree of muscle relaxation (neuromuscular blockade) can be performed by measuring the response to nerve stimulation using different techniques, by including mechanomyography (MMG), electromyography (EMG), acceleromyography (AMG). MMG is the measurement of evoked muscle tension, EMG is a method for evaluating the electrical activity produced by skeletal muscles and AMG is the measurement of acceleration of the contracting muscle. Small battery operated units are now available that are relatively inexpensive, easy to set up, and provide a measure the degree of neuromuscular blockade.

In general anaesthesia the choice of anaesthetic drug assumes a fundamental role. Drugs given to induce and maintain anaesthesia can be either as gases or vapours (inhalational anaesthetics), or as injections (intravenous anaesthetics). Intravenous medications are given directly into a vein. Intravenous anaesthetic agents are used commonly to induce anaesthesia, as induction is usually smoother and more rapid than that associated with most of the inhalational agents. Intravenous anaesthetics administered as repeated bolus doses or by continuous infusion may also be used for maintenance of anaesthesia, either alone or in combination with inhalational agents. An advantage of inhaled anaesthetics is that measuring the difference between inhaled and exhaled concentrations allows an accurate estimation of plasma or brain drug uptake.

Commonly used intravenous drugs are pure hypnotic drugs. Propofol is a relatively new intravenous drug, and has become widely accepted as the standard drug for intravenous anaesthesia. It has both fast redistribution and metabolism and does not accumulate in tissues as some of the other drugs. Unlike inhaled drugs, it is not possible to measure the effect site (brain) concentration of propofol in real-time. This disadvantage is outweighed by the possibility of precise titration by means of electronically controlled intravenous

infusion pumps. Besides, it is common practice to estimate the effect site drug concentration using mathematical patient models. The property of this drug to be purely hypnotic allows for decoupled control of the hypnotic and analgesic components of anaesthesia. Furthermore, the use of propofol is associated with low incidence of postoperative nausea and vomiting compared to other hypnotic drugs (Borgeat et al., 1992). This decreases the duration of postoperative care and ultimately patient mortality.

1.2 Control in anaesthesia

From an input-output point of view the anaesthesia process includes manipulated variables that can be intravenous anaesthetics, volatile anaesthetics, muscle relaxants, ventilation parameters and vasodilators as well as disturbances, such as surgical stimulus and blood loss (Figure 1.4). The three non-measurable main components of anaesthesia are hypnosis, analgesia and muscle relaxation and they represent the controlled outputs. Since these outputs can not be measured directly a connection to the measurable outputs such as EEG parameters, hart rate, blood pressure, Bispectral index should be inferred.

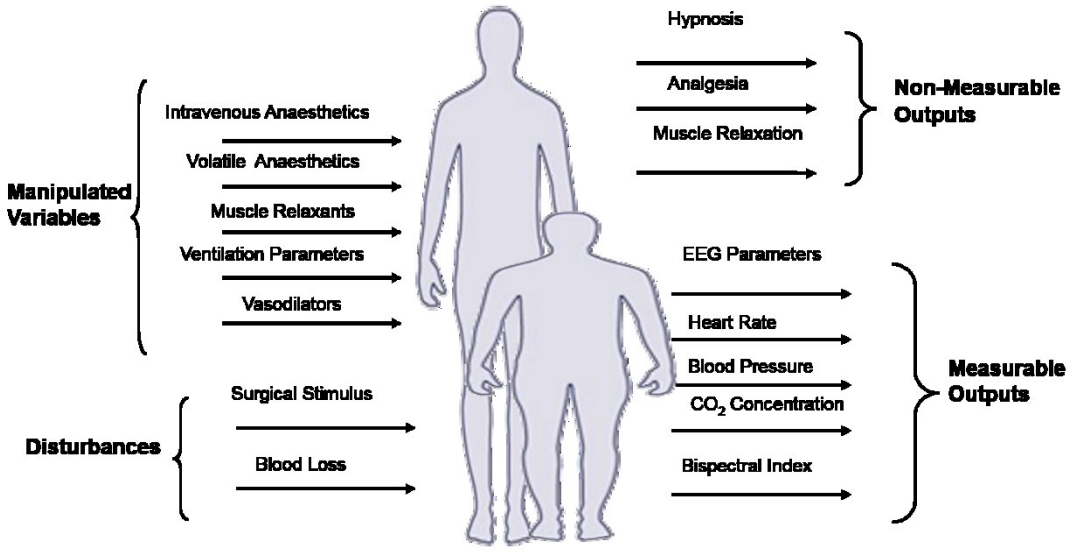

Figure 1.4: Input/Output representation of the anaesthesia

When inducing and maintaining anaesthesia, anaesthesiologists select initial doses based on a variety of considerations, they observe the results, and then make adjustments based on several factors, at irregularly varying intervals. In control engineering terminology, this constitutes a closed loop control system, due to the feedback present in the observations and interventions of the anaesthesiologist. This closed-loop control system has a special nature; (i) it has a human controller in the loop, and (ii) the control actions are intermittent and irregular in time due to the human controller.

The purpose of computer-controlled closed-loop systems is to formalize the process of observation and intervention in order to provide better and more accurate control. Such systems use a near continuous signal of drug effect, calculate the error between the observed value and the setpoint value (selected by the user), and use this error in an algorithm to make frequent and regular adjustments to drug administration rates. Moreover, some computer-control systems try to predict the future drug effect so that better adjustments can be done in advance (Absalom et al., 2011).

In order to have an accurate feedback control the process being controlled should be defined, and one or more real-time representative measures of the system state should be available. In engineering terms this means that the latter signals are designated as the process output/s, which have to be controlled according to certain agreed specifications. In an ideal case the control actuators or process input/s should, with minimal or known delay, cause predictable, linear changes in the process.

The process of anaesthesia is rather complex and not well understood, resulting in a challenging control problem. Our current state of the art understanding of consciousness and the mechanisms of anaesthetic-induced loss of consciousness is rather limited. Consciousness is so ethereal that it is difficult to model. At present models are available, such as the mean field models of drug action, (Absalom et al., 2011) which describe phenomena in the electroencephalogram associated with different brain states. The anaesthetic literature is replete with references to “depth of anaesthesia,” implies that anaesthesia is a continuous function of effect-site concentration; however systems such as the brain are commonly nonlinear, bistable systems (Foster et al., 2008, ASA, 2006).

The application of a closed-loop technology to drug delivery will assist physicians in

avoiding excessive over-dosages and under-dosages in their patients (Westenskow, 1997), optimizing the delivery of anaesthetics. Ideally, a robust controller would then tackle over-dosing and under-dosing by compensating for nonlinear drug responses, varying time delay, as well as inter and intra-patient variation. From a control engineering standpoint, Model Predictive Control (MPC) can play a crucial role in addressing some of the issues related to a closed loop technology, especially. (Torrico et al., 2007) Predictive control has advantages over other forms of automatic control in that it is robust against variable and unknown time-delay, over parameterization of system models, and has good disturbance rejection properties. It does, however, have a number of design parameters which must be adjusted carefully to suit the particular application and achieve the desired control performance. Model Based Predictive Control (MBPC) is a control methodology which uses on-line (=done while connected) a process model for calculating predictions of the future plant output and for optimizing future control actions. In fact MBPC is not a single specific control strategy but rather a family of control methods which have been developed with certain ideas in common (Keyser, 2003).

As shown in Figure 1.4, the control of anaesthesia poses a manifold of challenges: inter- and intra-patient variability, multivariable characteristics, variable time delays, dynamics dependent on the hypnotic agent, model analysis variability, agent and stability issues (Haddad et al., 2003), (Absalom et al., 2011), (Morley et al., 2000). In the open literature PID tuning techniques have been proposed. Since these classical controllers have no prior knowledge of the drug metabolism they cannot anticipate the response of the patient and their performance may be sub-optimal. Other authors developed model based strategies using fuzzy (Curatolo et al., 1996), predictive (Struys et al., 2003), (Ionescu et al., 2008), (Niño et al., 2009), (Hodrea et al., 2012), robust (Caiado Daniela et al., 2013), (Dumont et al., 2009) and adaptive (Haddad et al., 2003), (Nascu et al., 2012) control algorithms and applied them in clinical trials.

As discussed earlier, drugs that are given for the induction and maintenance of general anaesthesia can be either inhalational or intravenous anaesthetics. An individualised physiological based, patient specific, compartmental model for volatile anaesthesia is

presented and developed in (Krieger et al., 2012) and a combined strategy of model predictive control (MPC) and estimation under uncertainty is presented in (Krieger et al., 2014). For intravenous anaesthesia, robustness tests of MPC for depth of anaesthesia (DOA) control using the EPSAC (Extended Predictive Self Adaptive Controller) for a single input single output (SISO) model are presented in (Ionescu et al., 2011c), different protocols for the administration of Propofol and Remifentanil leading to a multiple input single output (MISO) model are evaluated in (Nascu et al., 2011) and in (Ionescu et al., 2012) a second output variable is determined, that originates from the effect of Remifetanil and leads to the implementation of a multiple input multiple output (MIMO) algorithm.

1.3 Project Objectives

As discussed in the previous sections, a suitable control system for anaesthesia must be reliable and robust, transparent to the anaesthetist and must be applicable in clinical routine environment.

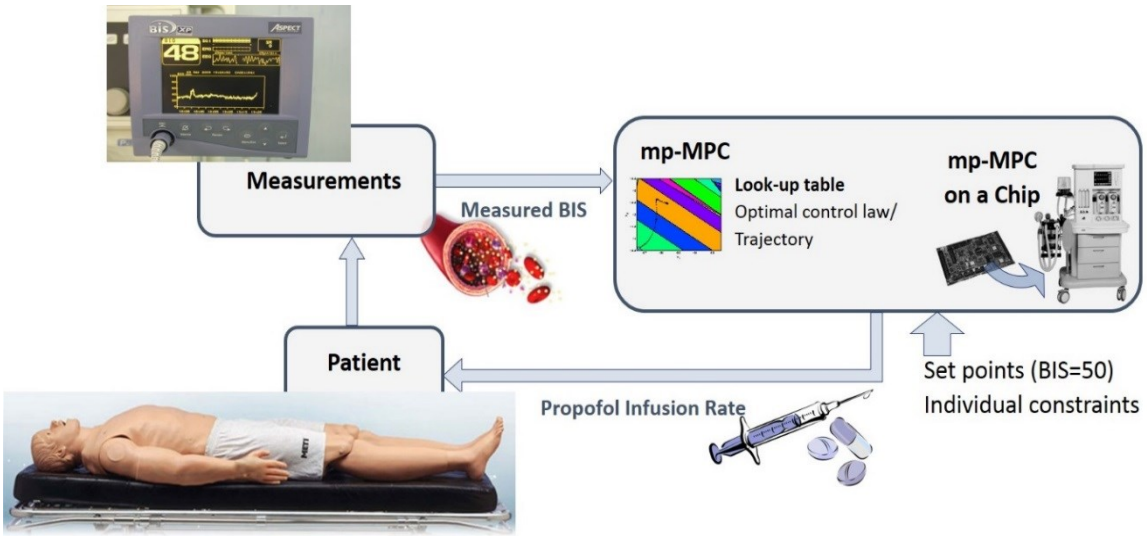

Figure 1.5: Automated control of depth of anaesthesia

The main objective of this research is to develop advanced control strategies for the control of intravenous anaesthesia. Specific aims include:

- The development of model based predictive control (MPC) strategies that account for the complex interactions in anaesthesia and the constraints imposed for patient safety
- The development of explicit MPC strategies to increase the transparency and reliability of the control system solution and it's acceptability to the anaesthetist
- The employment of robust control strategies to address issues related to inter- and intra- patient variability.
- The employment of estimation techniques to overcome issues related to unmeasurable data and process noise
- The employment of hybrid MPC to deal with the nonlinearity and the inter- and intra- patient variability

1.4 Thesis Outline

In this thesis we have developed explicit MPC strategies for the control of depth of anaesthesia in the induction and maintenance phases. State estimation techniques are developed and implemented simultaneously with mp-MPC strategies to estimate the state of each individual patient. Furthermore, a hybrid formulation of the patient model is performed leading to a hybrid mp-MPC that is further implemented using several robust techniques.

The thesis is organized as follows:

Chapter 2: describes strategies toward model-based automation of intravenous anaesthesia employing advanced control techniques. In particular, based on a detailed compartmental mathematical model featuring pharmacokinetic and pharmacodynamics information, two alternative model predictive control strategies are presented: a model predictive control strategy, based on online optimization, the extended predictive self-adaptive control and a multiparametric control strategy based on offline optimization, the multiparametric model predictive control.

Chapter 3: describes different design strategies for simultaneous muliparametric model predictive control and state estimation for intravenous anaesthesia. Three estimation techniques are implemented and compared: Kalman filter, offline and online moving horizon estimation. The state estimators are then implemented and tested simultaneously with multi-parametric model predictive controllers for real patient data. The estimators and the designed advanced control strategies are tested in both situations with and without noise influencing the measured output of the process.

Chapter 4: reformulates the intravenous anaesthesia model as a hybrid model leading to a hybrid model predictive control problem thus overcoming the nonlinearity issue. The resulting problem is solved explicitly via the solution of a multi-parametric mixed integer quadratic programming problem. To deal with the inter- and intra- patient variability, an estimation strategy and different robust algorithms are designed and implemented with the hybrid multiparametric model predictive control.

Chapter 5: describes PAROC, an integrated framework software platform for the development of explicit model predictive controllers. First, the main features of PAROC, including, high fidelity modelling, state-of-the-art multiparametric optimization techniques, explicit/multiparametric model predictive control strategies and a closed loop validation step are presented. The PAROC framework is applied on the anaesthesia process, in particular for the development of explicit/multiparametric model predictive controllers for the induction and maintenance phases of both intravenous and volatile anaesthesia.

Chapter 6 presents concluding remarks together with the future potential extensions of the current work.

Note that all theoretical aspects used throughout the thesis are presented in detail in the Appendix.

Appendix A presents the Sensitivity Analysis theory and current state of the art including: (i) Sobol's Sensitivity Analysis, (ii) High Dimensional Model Representation (HDMR), (iii) Group Method of Data Handling (GMDH) and (iv) GMDH – HDMR

Appendix B presents Model Reduction theory and current state of the art and presents both linear and nonlinear model order reduction

Appendix C depicts the theory on multiparametric programming

Appendix D presents theory on advanced model based control including the Extended Predictive Self Adaptive Control (EPSAC) and multiparametric Model Predictive Control (mp-MPC)

Appendix E depicts estimation techniques starting with the Kalman filter, followed by moving horizon estimation and the formulation as a multiparametric moving horizon estimation

Appendix D presents the application of the PAROC framework on a different case study – a distillation column

Chapter 2

A Multiparametric Model Based Approach to Intravenous Anaesthesia

2.1 Introduction

Anaesthesia plays a very important role in surgery and in the intensive care unit (ICU). Moreover, the role of the anaesthetist has become more complex and indispensable to maintain the patients' vital functions before, during, and after surgery. To estimate the drug effect in the patient's body and calculate the corresponding drug infusion rates, average population models are used. These strategies may not always be safe for the patient since they do not take into account any measured variable in a feedback control scheme and even if they reach the desired level of sedation fast, it can result in unsafe minimal values (undershoot) (Bailey et al., 2005). In stress situations the anaesthetist has to deal with routine assessments and simultaneously solve complex problems quickly. The automation of some routine actions of the anaesthetist can reduce the workload and consequently increase the safety of the patient.

Hitherto, many PID tuning techniques have been elaborated. Since these classical controllers have no prior knowledge of the drug metabolism they cannot anticipate the response of the patient and their performance may be sub-optimal. Therefore, model based strategies using fuzzy (Curatolo et al., 1996), predictive (Struys et al., 2003, Ionescu et al., 2008, Niño et al., 2009, Hodrea et al., 2012), robust (Caiado Daniela et al., 2013, Dumont et al., 2009) and adaptive (Haddad et al., 2003, Nascu et al., 2012) control algorithms have been developed and applied in clinical trials.

Model predictive control (MPC) is a model-based control technique that calculates the optimal control action considering constraints on the input, output, and state variables by solving an optimization problem. The downside of this control technique is that the optimization problem has to be solved online. One way to avoid this is to use

explicit/multiparametric model predictive control, which solves offline the optimization problem using multiparametric programming and derives the control inputs as a set of explicit functions of the system states. An important advantage of the multiparametric model predictive control (mp-MPC) is that the previously offline computed control laws can be easily implemented on embedded controllers. These types of devices use programming languages that cannot support powerful mathematical computations. The optimal control laws are retrievable immediately through simple function evaluations.

The aim of this chapter is to design and compare four different types of model-based controllers for administration of Propofol during the intensive care unit (ICU) sedation. Based on a compartmental pharmacokinetic (PK) and pharmacodynamic (PD) patient model, global sensitivity analysis is first presented to determine the relative influence of the uncertain pharmacokinetic and pharmacodynamic parameters and variables. Then, a model predictive controller is designed using an Extended Predictive Self Adaptive Control (EPSAC) strategy and three explicit model predictive controllers are designed using an mp-MPC strategy. The difference between the three controllers based on the mp-MPC strategy is that one of them uses the local linearized patient model, whereas the other two use the compensation of the nonlinear part of the patient model. In one of the two controllers using the nonlinear compensation, the states are estimated using an online estimator, while for the other one, the states are computed using the nominal patient model.

This chapter is organized as follows: The patient model including the pharmacokinetic and pharmacodynamic model as well as the patient data used throughout this work are presented in Section 2.2. Based on the presented mathematical model, global sensitivity analysis is presented in Section 2.3. Section 2.4 presents the multiparametric control strategy, the EPSAC strategy and the design of the controllers. The simulation results of the designed controllers in the induction and maintenance phase and discussions are presented in detail in Section 2.5. Finally, Section 2.6 summarizes the main outcome of this chapter.

2.2 Patient Model

For intravenous administration, the controlling drug enters the circulatory system, where under the action of the heart it is mixed and evenly distributed. The drug must diffuse out of the circulatory system into extracellular volumes before it reaches the target organ or cells. Because it acts on the target, the controlling drug may also be subject to excretion by the kidneys and intestines, as well as biotransformation and inactivation by organs such as the liver, the renal epithelium, and the intestinal mucosa. In this study, Propofol is used as the administrated hypnotic drug.

The model used for prediction should not be too complex, so as not to take too much computational time. On the other hand it should capture very well the dynamics of the patient in response to the applied Propofol infusion rate. The relationship between the infusion rate of Propofol and its effect can be described with pharmacokinetic (PK) and pharmacodynamic (PD) models. PK model describes the distribution of Propofol in the body and PD model describes the relationship between Propofol blood concentration and its clinical effect.

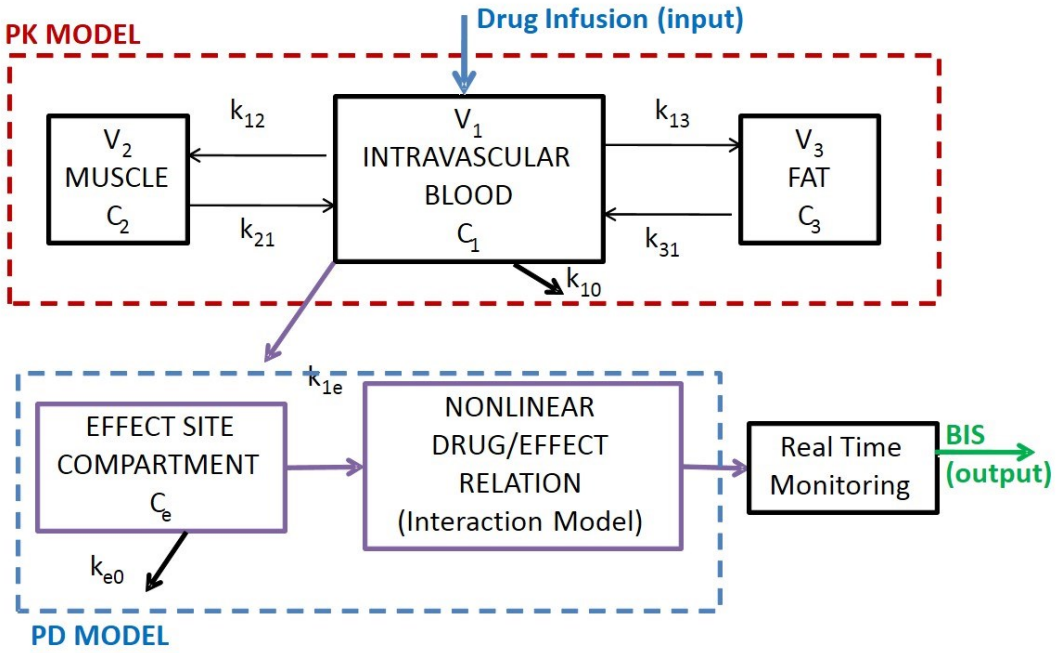

Figure 2.1: Intravenous anaesthesia - Compartmental model of the patient

The PK-PD models most commonly used for Propofol are the 4th order compartmental model introduced by Schnider (Schnider et al., 1999) and Minto (Minto et al., 1997) respectively and presented in Figure 2.1.

2.2.1 Pharmacokinetic Model

Pharmacokinetics, sometimes described as what the body responses to to a drug, refers to the movement of drug into, through, and out of the body - the time course of its absorption, bioavailability, distribution, metabolism, and excretion. Drug pharmacokinetics determines the onset, duration, and intensity of a drug's effect.

The pharmacokinetic model (PK) is expressed by linear relations as follows:

$$\begin{aligned}\dot{C}_1(t) &= -\left[k_{10}+k_{12}+k_{13}\right]\cdot C_1(t)+k_{21}\cdot C_2(t)\\ &+k_{31}\cdot C_3(t)+u(t)/V_1\\ \dot{C}_2(t) &= k_{12}\cdot C_1(t)-k_{21}\cdot C_2(t)\\ \dot{C}_3(t) &= k_{13}\cdot C_1(t)-k_{31}\cdot C_3(t)\end{aligned} \qquad \text{(Equation 2.1)}$$

where C_1 represents the drug concentration in the central compartment [mg/l]. The peripheral compartments 2 (muscle) and 3 (fat) model the drug exchange of the blood with well and poorly diffused body tissues. The concentrations of drug in the fast and slow equilibrating peripheral compartments are denoted by C_2 and C_3 respectively. The parameters k_{ij} for i=1:3, $i \neq j$, denote the drug transfer frequency from the i^{th} to the j^{th} compartment, k_{10} the frequency of drug removal from the central compartment and $u(t)$ [mg/min] is the infusion rate of the anaesthetic or analgesic drug into the central compartment. The parameters k_{ij} of the PK models depend on age, weight, height and gender and can be calculated for Propofol (Nascu et al., 2014c) as follows.

$$
\begin{aligned}
&V_1 = 4.27\,[l],\ \mathrm{V}_2 = 18.9 - 0.391\cdot(age - 53)\,[l],\ \mathrm{V}_3 = 2.38\,[l]\\
&\mathrm{Cl}_1 = 1.89 + 0.456(weight - 77) - 0.0681(lbm - 59) +\\
&\qquad + 0.264(height - 177)\,[l/\min]\\
&\mathrm{Cl}_2 = 1.29 - 0.024(age - 53)\,[l/\min],\ \mathrm{Cl}_3 = 0.836\,[l/\min]\\
&\mathrm{k}_{10} = \frac{Cl_1}{V_1}[\min^{-1}],\ \mathrm{k}_{12} = \frac{Cl_2}{V_1}[\min^{-1}],\ \mathrm{k}_{13} = \frac{Cl_3}{V_1}[\min^{-1}],\\
&\mathrm{k}_{21} = \frac{Cl_2}{V_2}[\min^{-1}],\ \mathrm{k}_{31} = \frac{Cl_3}{V_3}[\min^{-1}]
\end{aligned}
\qquad \text{(Equation 2.2)}
$$

where Cl_1 is the rate at which the drug is cleared from the body, and Cl_2 and Cl_3 are the rates at which the drug is removed from the central compartment to the other two compartments by distribution.

The lean body mass (*lbm*) for men (m) and women (f) are calculated as follows:

$$
\begin{aligned}
lbm\_m &= 1.1\cdot weight - 128\frac{weight^2}{height^2}\\
lbm\_f &= 1.07\cdot weight - 148\frac{weight^2}{height^2}
\end{aligned}
\qquad \text{(Equation 2.3)}
$$

2.2.2 Pharmacodynamic Model

The pharmacodynamics describe the link of concentration of the anaesthetic agent to the effect of the drug. The pharmacodynamic (PD) mathematical model is presented as follows:

$$
\dot{C}_e(t) = k_{e0}(C_e(t) - x_1(t)) \qquad \text{(Equation 2.4)}
$$

$$
BIS(t) = E_0 - E_{\max}\cdot\frac{C_e(t)^{\gamma}}{C_e(t)^{\gamma} + EC_{50}^{\gamma}} \qquad \text{(Equation 2.5)}
$$

An additional hypothetical effect compartment is added to represent the lag between plasma drug concentration and drug response. Its corresponding drug concentration is represented by the *effect-site compartment concentration* C_e. The effect compartment receives drug from the central compartment by a first-order process and is considered as a virtual additional compartment. Therefore, the drug transfer frequency for Propofol from the central compartment to the effect site-compartment is considered in clinical practice to be equal to the frequency of drug removal from the effect-site compartment $k_{e0}=k_{1e}=0.456$ [min^{-1}].(Schnider et al., 1998, Schnider et al., 1999, Nunes et al., 2009)

When considering the drug effect observed on the patient, the Bispectral Index (BIS) variable can be related to the effect drug concentration C_e by the empirical static nonlinear relationship (Equation 2.5), (Struys et al., 2003, Ionescu et al., 2008, Schnider et al., 1998, Schnider et al., 1999, Nunes et al., 2009) also called the *Hill curve, which corresponds to the second part of the PD model.* E_0 denotes the baseline value (awake state - without drug), which by convention is typically assigned a value of 100, E_{max} denotes the maximum effect achieved by the drug infusion, EC_{50} is the drug concentration at 50% of the maximal effect and represents the patient sensitivity to the drug, and γ determines the steepness of the curve.

As discussed in Chapter 1, the Bispectral Index (BIS) is a signal that is derived from the electro-encephalogram (EEG) used to assess the level of consciousness during anaesthesia.A BIS value of 0 equals EEG silence, while a BIS value of 100 is the value of a fully awake and conscious adult, 60 - 70 and 40 - 60 range represents light and moderate hypnotic condition, respectively. The target value during surgery is 50, giving us a range between 40 and 60 to guarantee adequate sedation.

The inverse of the Hill curve can also be defined as follows:

$$C_e(t) = EC_{50}\left(\frac{E_0 - BIS(t)}{E_{\max} - E_0 + BIS(t)}\right)^{\frac{1}{\gamma}} \qquad \text{(Equation 2.6)}$$

(Equation 2.1) – (Equation 2.6) complete the PK-PD patient model for intravenous anaesthesia.

2.2.3 Patient Data

For intravenous anaesthesia a data set of 12 virtually realistic generated patients (Ionescu et al., 2011c) plus an extra patient representing the average values of all 12 patients (PaN – patient nominal) is presented in Table 2.1 and used for the simulation studies. To generate the virtual patient population, the patient simulator was fed with 10 different pharamcodynamic profiles. The pharmacodynamic profile for a virtual patient was defined as a certain drug effect site concentration-versus-effect relation i.e., an E_{max} model combined with a certain additional delay that could be imposed by certain monitor types. To obtain realistic values, the E_{max} models derived from clinical work as calculated at the end of the induction phase using data points measured during the induction phase were used (Struys et al., 2001).

The parameter values of these patients are also used to calculate the parameters of the patient model. For a particular patient, E_0 can be measured in awake state and E_{max} is considered to have the same value, $E_{max}= E_0$. These parameters are considered known a priori in the studies.

Table 2.1: Biometric values of the 12 patients for intravenous anaesthesia

Patient	Age	Height (cm)	Weight (Kg)	Gender	EC_{50}	E_0	γ
1	40	163	54	M	6.33	98.8	2.24
2	36	163	50	M	6.76	98.6	4.29
3	28	164	52	M	8.44	91.2	4.1
4	50	163	83	M	6.44	95.9	2.18

5	28	164	60	F	4.93	94.7	2.46
6	43	163	59	M	12.0	90.2	2.42
7	37	187	75	F	8.02	92.0	2.1
8	38	174	80	M	6.56	95.5	4.12
9	41	170	70	M	6.15	89.2	6.89
10	37	167	58	M	13.7	83.1	1.65
11	42	179	78	F	4.82	91.8	1.85
12	34	172	58	M	4.95	96.2	1.84
Mean	38	169	65	M	7.42	93.1	3

2.3 Sensitivity Analysis

Based on the mathematical model presented in the previous subchapter, global sensitivity analysis is first applied, in particular, Sobol's method of sensitivity indices, the high dimensional model representation (HDMR) approach and GMDH-HDMR to determine the relative influence of the PK-PD parameters and variables. GMDH-HDMR, relies on the direct construction of the HDMR expansion through GMDH inductive modelling. The applied methodologies are presented in detail in Appendix A. By analysing the anaesthesia model, it can be observed that the dynamics of the linear part is influenced by the age, height, weight and gender parameters. The characteristic of the nonlinear part is influenced by EC50, E0 and γ parameters. The relative influence of the uncertain PK and PD parameters and the variables on the measurable outputs is investigated. The sensitivity index (SI) represents the relative influence of the parameter or variable on the output at a given time. To perform the analysis, using the mathematical models presented in Section 2.2, an anaesthesia experiment was simulated. A step of 50 [mg/min] was applied on the anaesthetic drug infusion rate that represents the input of the model. The

evolution of the output was investigated for an interval of 100 minutes, until steady state regime is reached. During simulations all parameters and variables were varied between their bounds. S1-S7 represents the sensitivity index for age, height, weight, EC50, E0, γ and gender respectively.

Figure 2.2 presents the evolution of the first order Sobol' sensitivity indices at different sample points starting from t=2 minutes to t=100 minutes. At the beginning of anaesthesia E0, the baseline value (the awake state, without drug) has the highest sensitivity index with respect to the BIS but it converges asymptotically to 0 with time as the patient enters the deep anaesthesia state. Analysing the sensitivities indices from Figure 2.2, it is observed that the most important parameter is EC50 (sensitivity index S4), the drug concentration at 50% of the maximal effect, representing the patient sensitivity to the drug. Note that EC50 (S4) increases exponentially and stabilizes when the BIS reaches its steady state regime. Also note that because the nonlinearity is represented by a sigmoid, the parameter γ *(S6),* which determines the steepness of the curve, has more influence in the beginning of anaesthesia due to the high nonlinearity of this zone. Note also that the sensitivity indices of the parameters of the linear part (PK) (Equation 2.1), increase with the nonlinearity slope but the corresponding values are less important than the ones for the parameters of the nonlinear part (Equation 2.5).

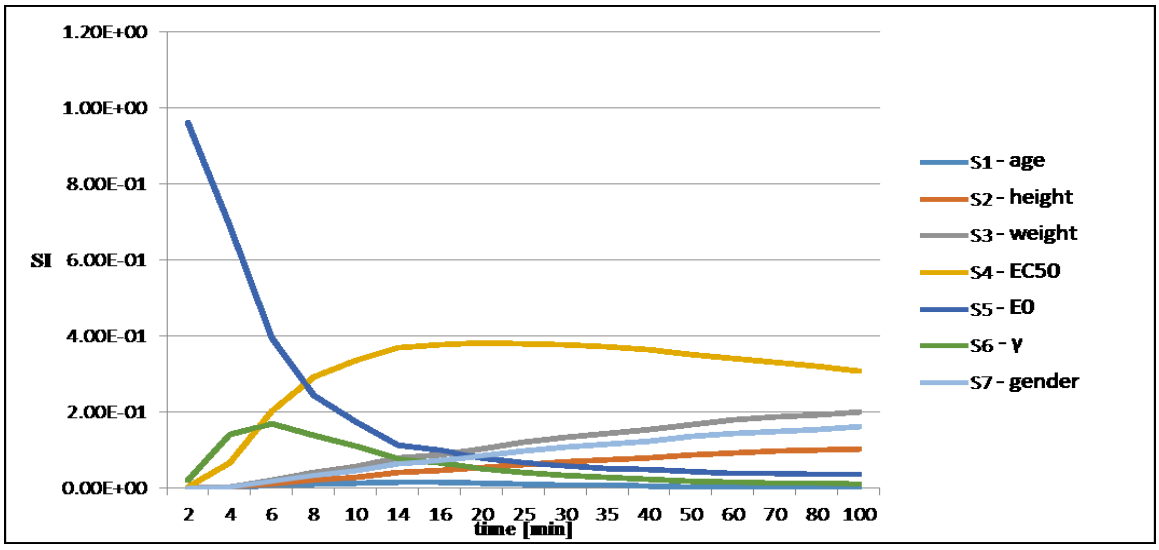

Figure 2.2: Evolution of the first order sensitivity indices

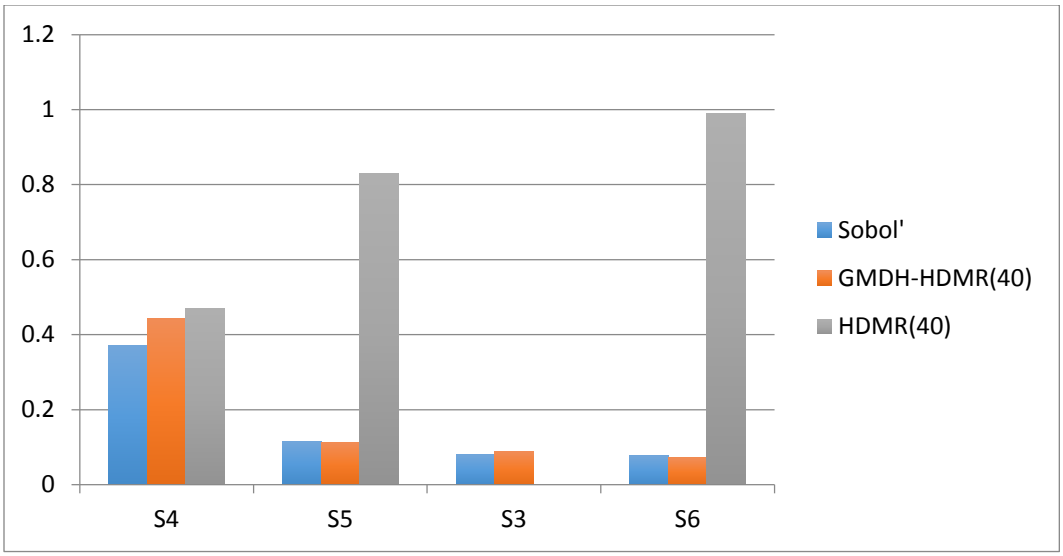

Figure 2.3: Comparison GMDH HDMR for small data samples (N=40) t=14

Table 2.2 further depicts a comparison of the results obtained with the various techniques (i) Sobol's Sensitivity Analysis, (i) GMDH-HDMR and (iii) HDMR reported for four of the parameters. These parameters are weight (S3), EC50 (S4), E0 (S5), γ (S6) and were chosen as they have the highest sensitivity index at t=14 minutes when using Sobol's sensitivity analysis as presented in Figure 2.2. The GMDH-HDMR approach only computes the indices for the parameter it selects as important, therefore S1 (age), S2 (height) and S7 (gender) are not calculated.

Table 2.2: Sensitivity Analysis. Comparison of GMDH and HDMR at t=14

	Sobol'	**GMDH-HDMR(40)**	**HDMR(40)**
S4 – EC50	0.,37122289	0.44268	0.47
S5 – E0	0.11501718	0.111865	0.8305
S3 - weight	0.07972202	0.08903	0
S6 - γ	0.07690754	0.0715	0.99

Sensitivity Analysis using GMDH-HDMR can be performed on a limited number of sample points and as a result, the most important individual contributions are detected. HDMR is able to do this with 256 Sobol' sample points but it will fail to operate properly for only 40 data points. For example, as depicted in Figure 2.3, the individual contribution of the third parameter (S3) is completely ignored and the interaction is not detected either. The advantage of GMDH-HDMR is that most of the time it gives more accurate results than HDMR with small number of data samples. HDMR becomes unreliable with limited sets of samples as it can miss important first order contributions. Moreover, the strength of GMDH-HDMR is the ability to be economical in the number of simulations required. This can be useful in the case of computationally expensive high fidelity models. GMDH inductively selects the most important parameters performing as a sparse method for calculating sensitivity indices, with scarce recourse to model simulations. HDMR on the contrary relies on the calculation of the sensitivity indices for all parameters and potential interactions. It captures non-linear system outputs as a summation of variable correlations in a hierarchical order. In a full model expansion, it considers all possible variable interactions and their contribution to the original function. The first term describes the average value of the fitness landscape near a reference point called cut-center. Second order terms express the independent effects of each variable if decision variables are deviated from the cutcenter. Higher order terms denote the residual group effect of variables. Therefore, the terms are independent or orthogonal to each other to form a mean convergent series. From Table 2.2 it can be observed that γ (S6) has the highest sensitivity index with respect to the BIS. Since this method exhibits better results for this type of model, γ (S6) shows which patient is most sensitive to the drug.

2.4 Advanced Model Based Control Strategies

Model Predictive Control (MPC) is a control methodology based on two main principles: explicit online use of a *process model* to *predict* the process output at future time instants, and the computation of an optimal control action by minimizing a cost function, including *constraints* on the process variables.

The main differences between the different types of MPC algorithms are: (i) the *type of model* used to represent the process and its *disturbances,* (ii) the *cost function(s)* to be minimized, with or without *constraints*, and (iii) the type of optimization performed. Details of the method formulation are presented in Appendix D.

2.4.1 EPSAC Strategy

Extended Predictive Self Adaptive Control (EPSAC) is one of the various NMPC design methods reported in literature (Su et al., 2016) and it adopts the approach of iterative optimization based on a predefined input trajectory (Keyser, 2003, De Keyser et al., 1985). A potential drawback of previous EPSAC methods is the incorporation of a convolution model in the formulation of the control algorithms. Since model parameters are obtained by introducing a step change to the current input value specified by the base input trajectory, the predicted outputs at sampling instants further away from the current sampling instant become less accurate due to process nonlinearity, leading to inevitable modelling error that degrades the achievable closed-loop performance. Another potential downside of this method is that the optimization problem has to be solved online. This issue is addressed in the following subchapters.

For the EPSAC approach (see Appendix D and (Keyser, 2003)), the controller output is obtained by minimizing the cost function:

$$\sum_{k=N_1}^{N_2}\left[r(t+k/t)-y(t+k/t)\right]^2+\lambda\sum_{k=0}^{N_u-1}\left[\Delta u(t+k/t)\right]^2 \qquad \text{(Equation 2.7)}$$

The design parameters are: N_1= the minimum costing horizon N_2= the maximum costing horizon, N_2-N_1 = the prediction horizon N_u=control horizon, λ=weight parameter. The signal *r* represents the *reference trajectory*.

In our case the process input is represented by the Propofol infusion rate applied to the patient. The process output is the BIS index and is predicted at time instant t over the prediction horizon N_2-N_1, based on the measurements available at that moment and the

future outputs of the control signal. The cost function is an extended EPSAC cost function that penalizes the control movements using the weight parameter λ.

2.4.2 Multiparametric Strategy

For the mp-MPC (see Appendix D), the generic optimization problem solved is:

$$\begin{aligned}
\min_{u} J &= \sum_{k=1}^{N} (BIS_k - BIS_k^R)^T QR_k (BIS_k - BIS_k^R) \\
&\quad + \sum_{k=0}^{N_u-1} \Delta u_k^T R_k \Delta u_k \\
s.t.\ & \mathrm{x}_{t+1} = Ax_t + Bu_t \\
& \mathrm{y}_t = Cx_t \\
& \mathrm{BIS}_{\min} \le y \le BIS_{\max} \\
& \Delta \mathrm{u}_{\min} \le \Delta u \le \Delta u_{\max} \\
& x_t \in X \subseteq \Re^p, u_t \in U \subseteq \Re
\end{aligned} \qquad \text{(Equation 2.8)}$$

where x denote the states, y *the* outputs and u the controls, all being (discrete) time dependent vectors, with the tracked output variables having time-dependent set points y^R. Finally, Δu correspond to changes in control variables, $\Delta u(k) = u(k) - u(k-1)$. The prediction horizon is denoted by N and control horizon by N_u. X, U are the sets of the state and input constraints that contain the origin in their interior. The weight matrix for manipulated variables R is a positive definite diagonal matrix ($R \succ 0$), QR is the weight for tracked outputs and $R1$ is a weight matrix for the control action changes (Δu). The control problem is posed as a quadratic convex optimization problem for which an explicit solution can be obtained. The key idea is to derive the optimal control inputs as a set of explicit affine functions of the current state of the system:

$$u = f(x) = \begin{cases} K_1 x + c_1 \text{ if } x \in CR^1 \\ \quad \ldots \\ K_s x + c_s \text{ if } x \in CR^s \end{cases} \qquad \text{(Equation 2.9)}$$

where s is the number of critical regions.

2.5 Control Design

The presence of the Hill nonlinearity (Equation 2.5) complicates the use of linear controller synthesis. Two methods to overcome this problem are proposed in this chapter: (i) exact and (ii) local linearization (note: Chapter 4 presents a hybrid formulation).

The local linearization is based on the linearized patient model (Equation 2.1), (Equation 2.4) and (Equation 2.5) using the parameter values of the nominal patient, a priori known, for a BIS value of 50 obtained using gPROMS ((PSE), 2010). The controller is designed using the linearized patient model as presented in Figure 2.4. Figure 2.5 depicts the control design scheme where the designed controller minimizes the error between the *BIS target* value and the measured *BIS* giving the patient the optimal *Propofol Drug infusion rate* that will derive the patient to the desired setpoint value.

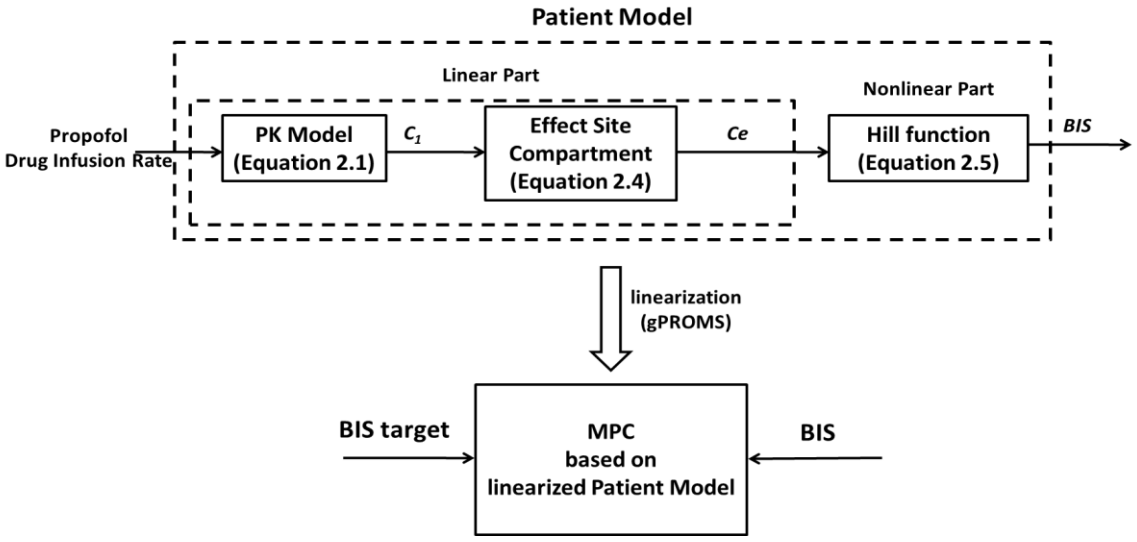

Figure 2.4: Controller design using local linearization

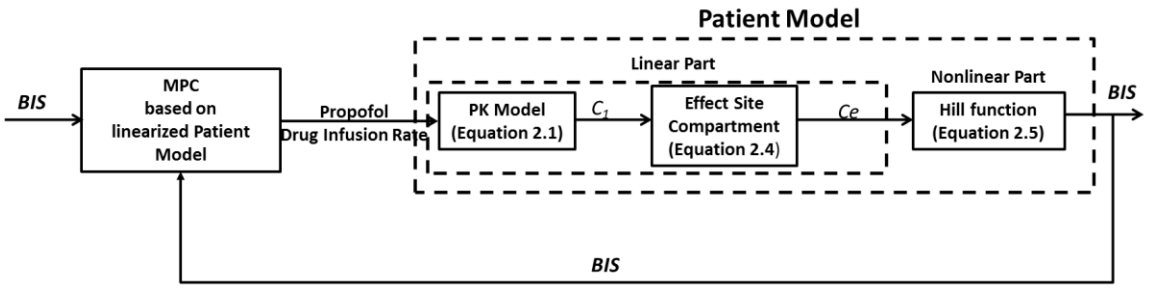

Figure 2.5: Control scheme using local linearization

Exact linearization is based on the compensation of the nonlinearity introduced by the Hill curve (Equation 2.5), in the PD model ((Equation 2.4) and (Equation 2.5)). Since the Hill nonlinearity is a monotonic function of the normalized effect site concentration, it has an inverse presented in (Equation 2.6). Using a parameter scheduling technique the inverse Hill function could be implemented in the control design scheme as illustrated by the block diagram in Figure 2.7. In the *Patient Model*, the *Hill curve* uses the nonlinear parameters of the real patient (E_0 , E_{max}, EC_{50} , γ), while the *inverse Hill function* is using the nonlinear parameter corresponding to the nominal patient a priori known (E_0^{mean}, E_{max}^{mean}, EC_{50}^{mean} , γ^{mean}).

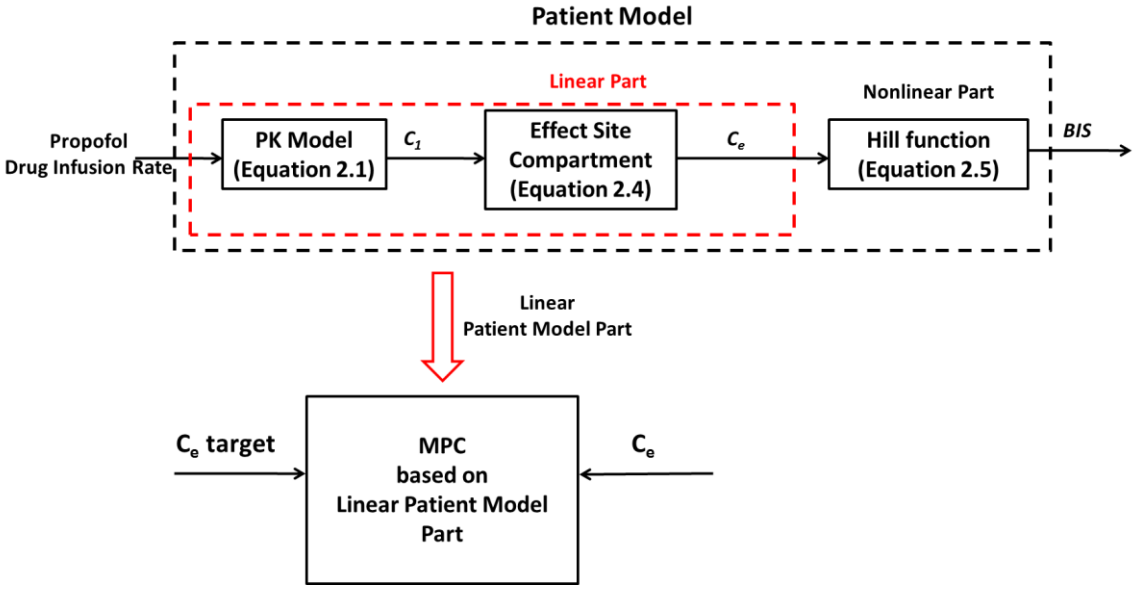

Figure 2.6: Controller design using exact linearization

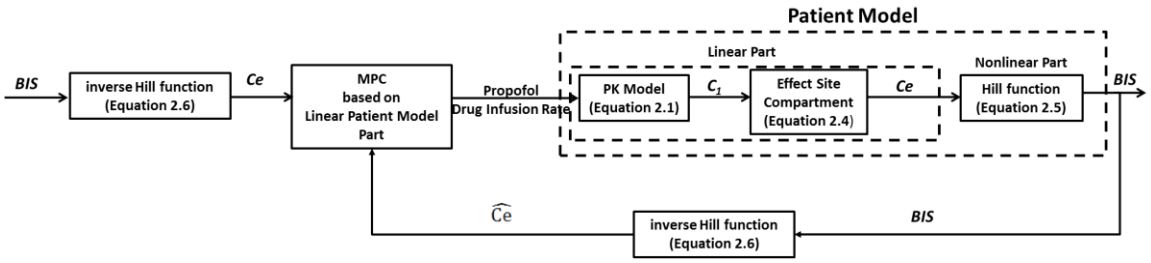

Figure 2.7: Control scheme using exact linearization

For this method the controller is designed using the *Linear Part* ((Equation 2.1) and (Equation 2.4)) of the patient model ((Equation 2.1), (Equation 2.4) and (Equation 2.5)) with the linear parameters of the nominal patient (*age, height, weight, gender*) as presented in Figure 2.6. Note that the *BIS target* here is transformed in C_e *target* using the *inverse Hill function* since the controlled variable is the estimated drug concentration $\hat{C}_e$.

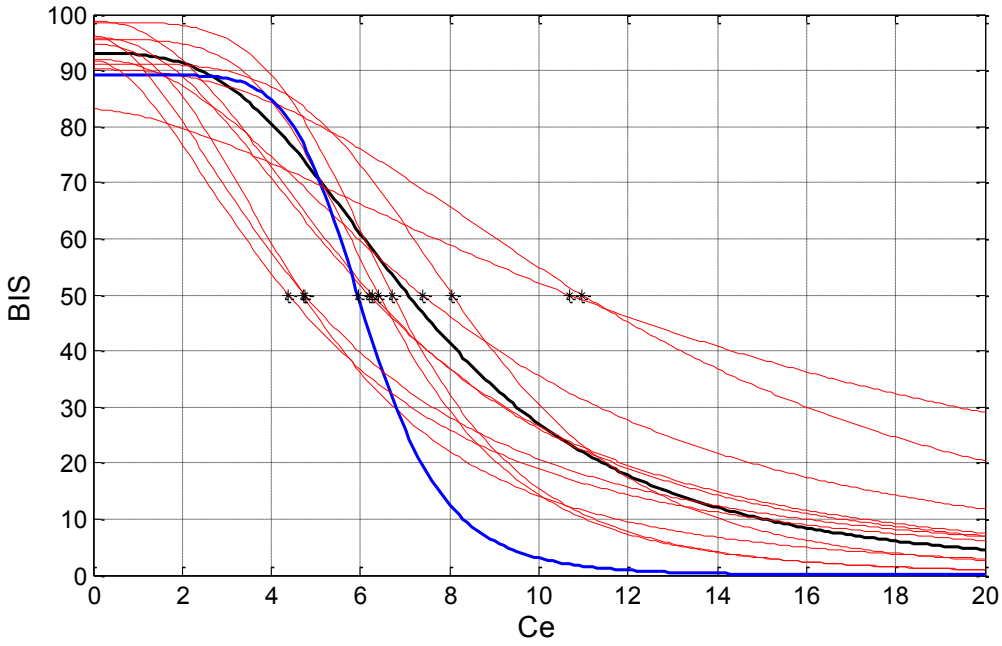

Figure 2.8: The nonlinear characteristic of the Hill curve for all patients

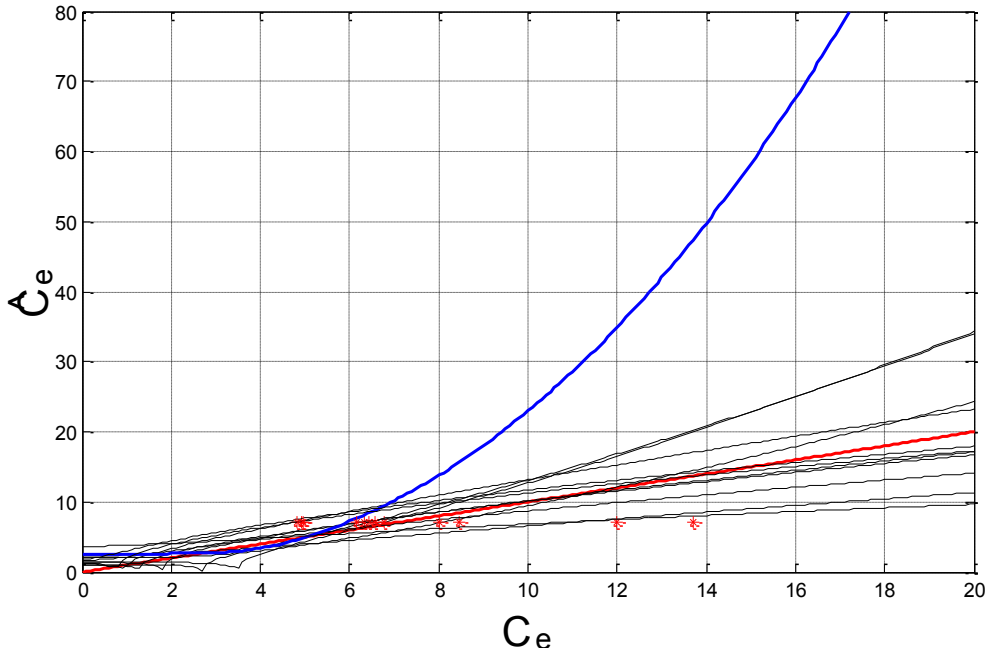

Figure 2.9: The nonlinearity compensation of the Hill curve for all patients

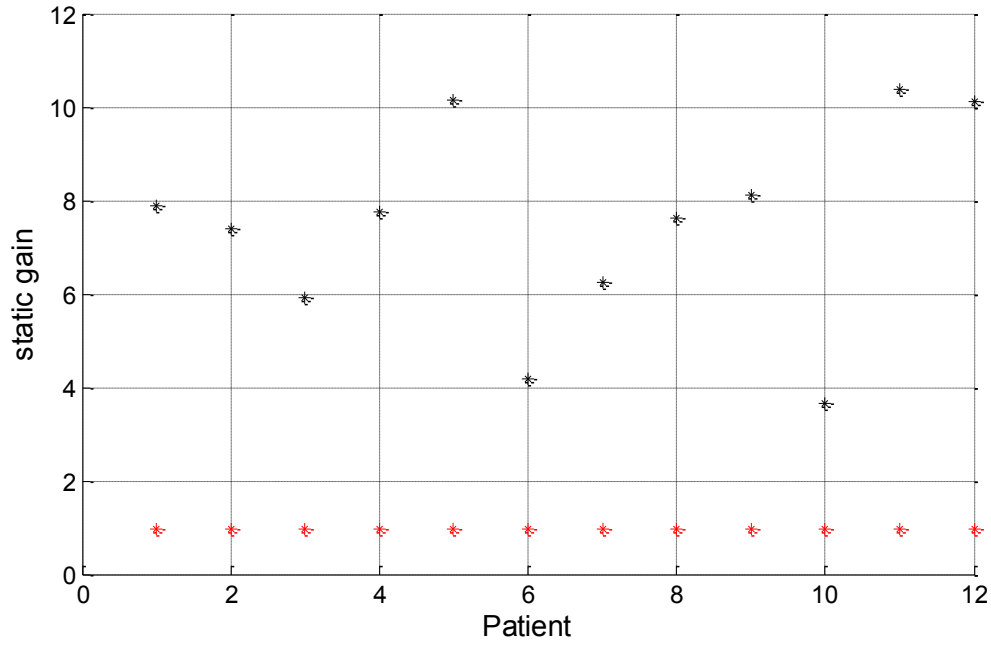

Figure 2.10: The static gain of the Hill curve for all patients

Figure 2.8 depicts the static characteristic of the Hill curve (Equation 2.5) from the Patient model for all patients in Table 2.1 where the nominal patient is represented with black and the black stars depict the BIS target value (=50). The nonlinearity compensation using the inverse of the Hill curve (Equation 2.6), based on the parameter values of the nominal patient from Table 2.1 is depicted in Figure 2.9 for all patients. At a first glance it can be observed that even after the nonlinearity compensation, some patients (especially patient 9 – represented with blue) still exhibit a nonlinear behaviour. Fortunately the nonlinear behaviour only appears at large values of the drug infusion rate (control action) which in clinical practice are not common. In this work the drug infusion is limited to 50 (mg/min) which ensures that the nonlinear behaviour of the patients is avoided. Moreover it can be observed that until the values of the control action corresponding to a BIS value of 50 are reached, denoted with a red star in Figure 2.9, all 12 patients have a linear behaviour. At the BIS target set at the value of 50, Figure 2.10 presents the static gain of the Hill function for different patients (represented by black stars), where it can be observed that we have variations between 3 and 10 for the static gain. The nonlinearity compensation should assure a static gain equal to 1 between C_e and $\hat{C}_e$, this is shown in Figure 2.10 (represented by red stars) where values between 0.98 and 1.1 can be observed.

An exact linearization takes place only for the case where the patient model is identical to the nominal model (red line in Figure 2.9); in this case the nonlinearity is cancelled out i.e., $\hat{C}_e = C_e$.

An important challenge of depth of anaesthesia (DOA) control is the high inter- and intra-patient variability. This results in different dynamics in the PK model, and changes in the parameters of the Hill function for each patient model. Four control strategies, a model predictive controller, EPSAC, and three different mp-MPC are designed and evaluated. The framework for the different ways of designing the controllers is presented in Figure 2.11.

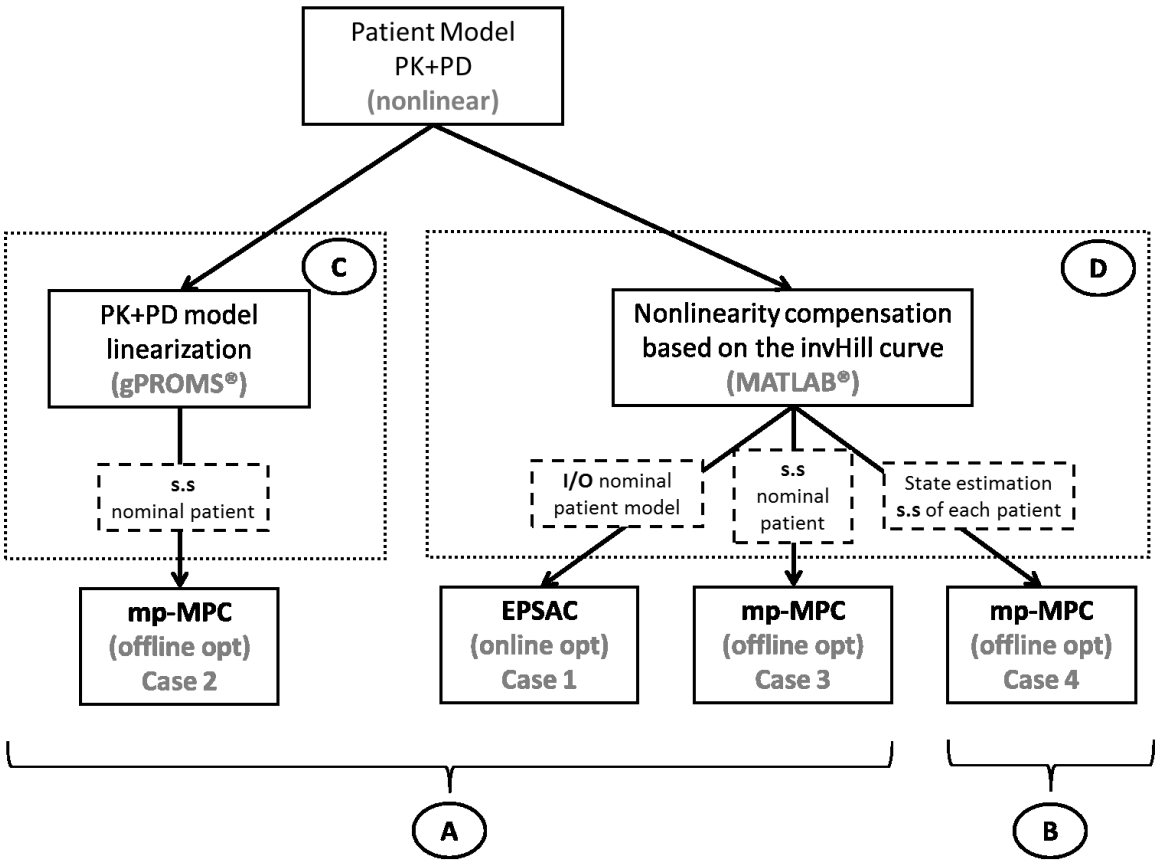

Figure 2.11: Control scheme development flowchart

The patient response is simulated using *Patient Model* block, composed of the PK–PD linear part ((Equation 2.1) and the effect site concentration (Equation 2.4)) and the nonlinear PD part composed of the Hill nonlinearity, (Equation 2.5). BIS can be measured; however, the states cannot and have to be estimated: either using the drug rate input and the nominal state-space patient model or by using the drug rate input and measured output (BIS) of the process, the state-space nominal model and a correction estimator based on the output changes.

To analyse the influence of the changes in the dynamics of the PK model on the control performances, two types of control schemes are implemented, one uses the states given by the nominal model (A) and the other uses an estimator to adjust the states based on the dynamics of each patient (B).

The influence on the changes of parameters of the Hill curve on the control performances is analysed by two types of control schemes, one using the local linearization of the complete PK–PD patient model (C) and the second is based on the exact linearization (D). The following design parameters are used: the weight matrix for tracked outputs (y), QR=1000, weight matrix for manipulated variables (u), R=1, the control horizon $N_u=1$ and the prediction horizon $N=20$ in both mp-MPC and EPSAC. The EPSAC has an extra weighting factor λ from (Equation 2.7) for which its default value λ=0 was used. The states used in the design of the controllers are C_1, C_2, C_3, C_e as described in (Equation 2.1). The clinically recommended sampling time is of 5 seconds (Ionescu et al., 2008). N_1, N_2, and N_u are chosen based on the characteristics of the process and the desired performances. Based on (Clarke et al., 1987, Mohtadi et al., 1987), N should be large, at least $2n-1$ but not larger than the rise time of the process. For anaesthesia, due to medical procedures, we are constrained to use a small sampling time leads to a choice of a greater value for N. Also, the dead time is not considered since it is very small and does not affect the process, therefore $N1 = 1$. In choosing Nu for processes with no unstable/underdamped poles, like anaesthesia, $Nu = 1$ is generally satisfactory. A choice of the Q, R, and QR is given by Bryson's rule (Franklin et al., 2001a). Usually the pump for the Propofol drug infusion is limited to 200 mg/min (3.3 mg/sec) but it can be observed from simulations as well as literature that the controller gives maximum values of 70 mg/min for the drug infusion. To test the ability of the controller in dealing with severe constraints as well as avoiding giving the patient unnecessary amounts of drug infusion (leading to longer recovery time) in this work the drug infusion is limited to 50 mg/min.

2.5.1 Case 1: Extended Prediction Self-Adaptive Control (EPSAC)

In this section, we apply a particular case of online MPC, the EPSAC strategy described in detail in Appendix D. The structure of the control system proposed in this section is shown in Figure 2.12.

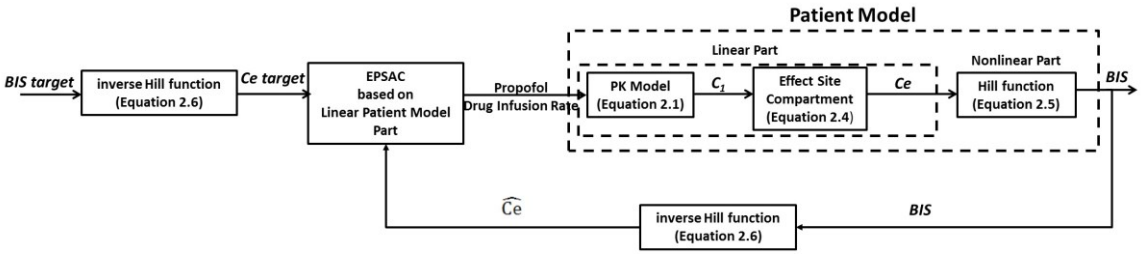

Figure 2.12: EPSAC control scheme

The *Patient Model* block is composed of the *PK Model* (Equation 2.1), *the Effect Site Compartment* (Equation 2.4) and the *Hill function* (Equation 2.5). The control strategy is based on the exact linearization (see Figure 2.6) and the I/O linear nominal part of the patient model (see Figure 2.6). The controller output is obtained by minimizing the cost function (Equation 2.7) with the design parameters in Section 2.5. The control algorithm uses for prediction a transfer function derived from the *Linear Part* ((Equation 2.1) and (Equation 2.4)) of the *Patient Model*. The inverse of the Hill curve (Equation 2.6) is used to compensate the nonlinearity as presented in Figure 2.7. The *Patient Model* uses the parameter values of the real patient while the inverse of the Hill curve and the linear model used for the controller use the parameter values of the nominal patient from Table 2.1.

2.5.2 Case 2: mp-MPC Without Nonlinearity Compensation

The structure of the control scheme is presented in Figure 2.13. This approach uses the explicit/multiparametric Model Predictive Control strategy based on local linearization of the *Patient Model* for the parameter values of the nominal patient from Table 2.1 as presented in Figure 2.4. The controller uses the error between the measured *BIS* and the *BIS target* value as well as the state space model of the nominal patient to give the patient the optimal *Propofol Drug Infusion Rate*.

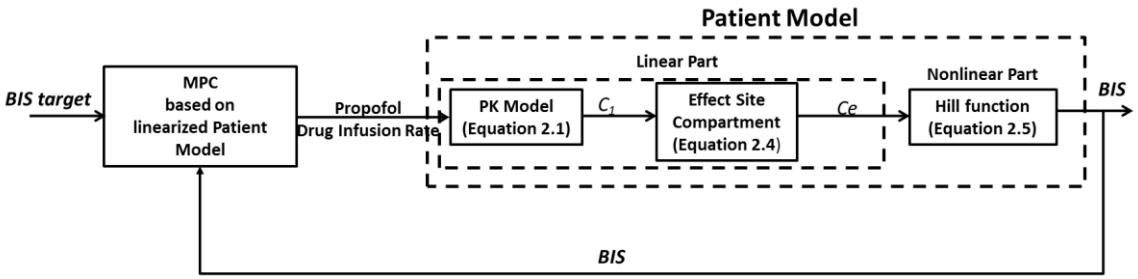

Figure 2.13 Case 2: mp-MPC without nonlinearity compensation - control scheme

To obtain the linearized patient model, the PK and PD model for the nominal patient is implemented in gPROMS ((PSE), 2010) and the state space of the linearized nominal patient model at BIS = 50 is determined. Using these matrices, the mp-QP optimization problem (Equation 2.8) is solved to obtain the control laws using a MATLAB implementation of multiparametric quadratic programming algorithm (ParOs, 2004, Pistikopoulos et al., 1999) and determine the mp-MPC control laws that will be used to calculate the optimal control action.

2.5.3 Case 3: mp-MPC With Nonlinearity Compensation

This approach uses explicit/multiparametric MPC based on exact linearization as presented in Figure 2.6. The controller is designed on the *Linear Part* of the *Patient Model* using the values of the nominal patient from Table 2.1 The optimization problem (Equation 2.8) is solved offline using POP(ParOs, 2004) to obtain the explicit control laws. Since the controller is now designed only on the linear part it will use the error between the C_e *target* and the $\hat{C}_e$ given by the *inverse Hill function* as well as the state space of the nominal patient values to give the optimal *opofol Drug Infusion Rate* as depicted in Figure 2.14. Note that here the *inverse Hill function* uses the values of the nominal patient while the *Patient Model* uses the real values of the real simulated patient.

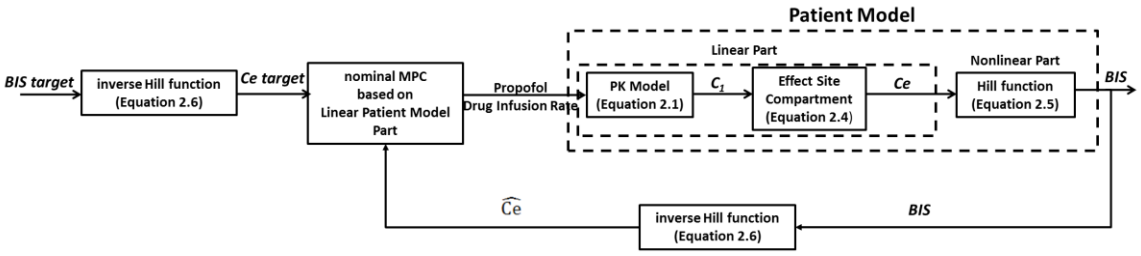

Figure 2.14: Case 3:mp-MPC with nonlinearity compensation - control scheme

2.5.4 Case 4: mp-MPC With Nonlinearity Compensation and Estimation

This approach, as the one presented in the previous subsection uses the explicit/multiparametric MPC strategy and has a similar control scheme Figure 2.15. the design of the controller is based on exact linearization (Figure 2.6).

The difference is the use of a state estimator that will give the controller the states of the real patient. The real patient states are estimated using a Kalman filter (Welch et al., 2001) based on the state space model of the nominal patient, the online *BIS* measurement, and the drug rate.

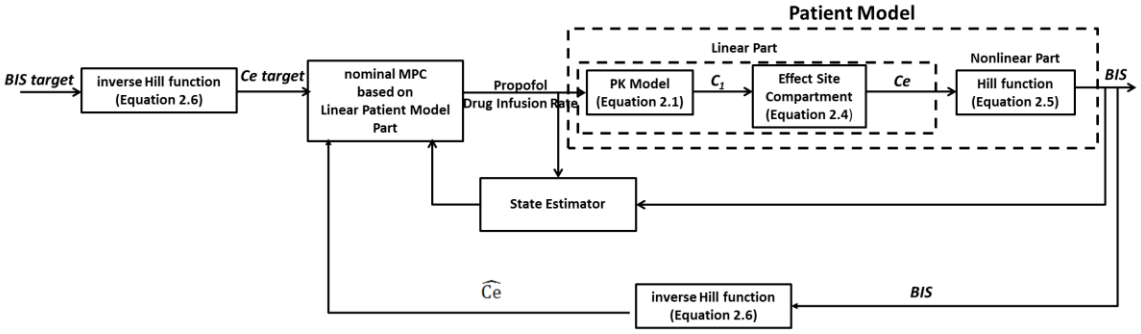

Figure 2.15: Case 4: mp-MPC with nonlinearity compensation and estimator - control scheme

2.6 Results

In this section, the results of a simulation study to evaluate the four control strategies for the administration of Propofol are presented. DOA is monitored using the BIS during the induction and maintenance phase of general anaesthesia. The closed-loop control tests are performed on a set of 12 patients (Ionescu et al., 2011a) plus an extra patient representing the nominal values of all 12 patients (PaN - patient nominal). The parameters values of these patients are given in Table 2.1 and are also used to calculate the parameters of the patient model. All designed controllers are simulated first for the set of data presented in Table I in order to have a better understanding of their behaviour on the different types of patients, and analyse the inter- and intra-patient variability. Next, the four controllers will be tested against each other and simulated for different patients so as to be able to compare their performances by means of the BIS index and the corresponding Propofol infusion rates.

In common practice the operation procedure does not start until the patient reaches an adequate DOA, usually taking up to 15 minutes. Thus, a rise time between 5 min and 7 min gives good performances. The target value during surgery is 50, giving us a range between 40 and 60 to guarantee adequate sedation, resulting in an overshoot/undershoot lower than 10%.

2.6.1 Induction Phase

Ideally, the induction phase of the patient in an operational DOA is performed as fast as possible, such that little time is lost before the surgeon can start operating. It is, therefore, desirable that the patient reaches the BIS = 50 target and remains within the target value without much undershoot or overshoot, i.e., values below BIS = 40 and above BIS = 60 should be avoided. In Figure 2.16, Figure 2.18, Figure 2.20 and Figure 2.21, we have the simulations of the four controllers for all 12 patients and the nominal one in the induction phase. Figure 2.17 presents the map of the critical regions (CR – the region in the space of the parameters where the objective and optimization variable obtained as a function of the varying parameters are valid) for the controller using local linearization (Case 2); and

in Figure 2.19, we have the map of the CR for the controllers designed using exact linearization, by using the inverse of the Hill curve (Cases 3 and 4).

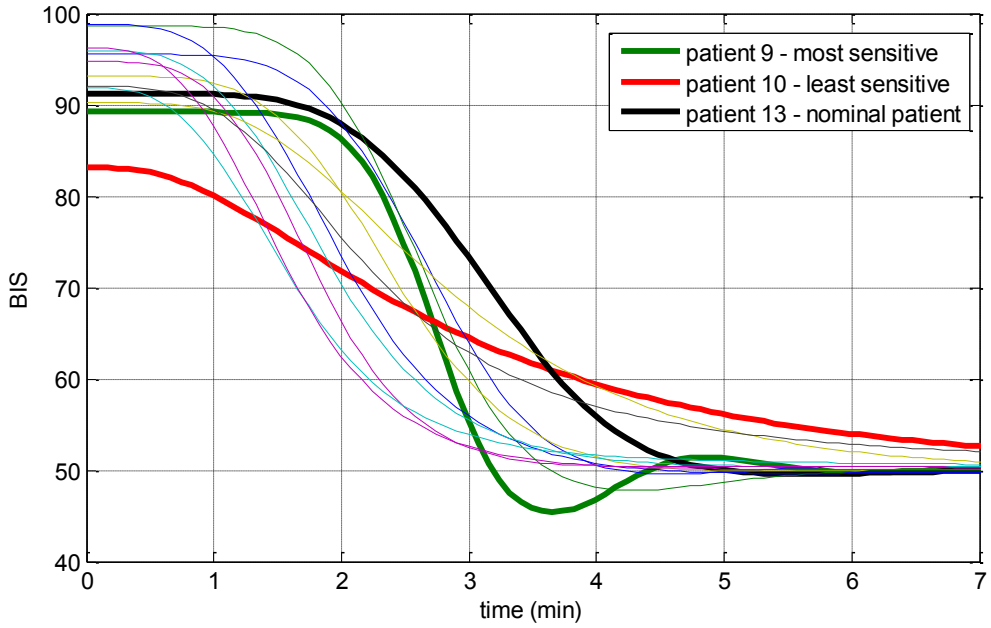

Figure 2.16: BIS output for all 13 patients for Case 1 – induction phase

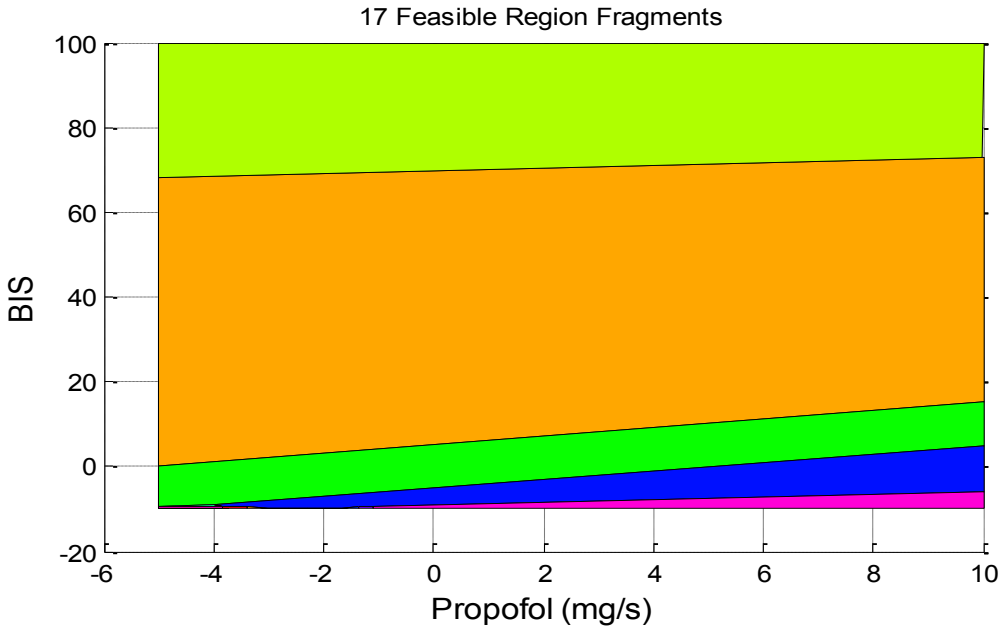

Figure 2.17: Map of critical regions Case 2

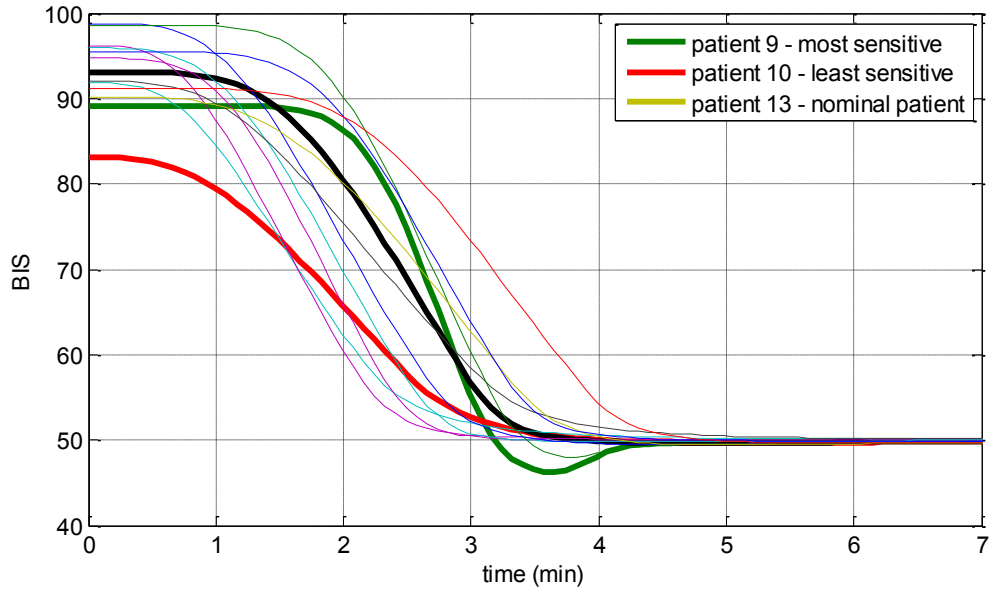

Figure 2.18: BIS output for all 13 patients for Case 2 – induction phase

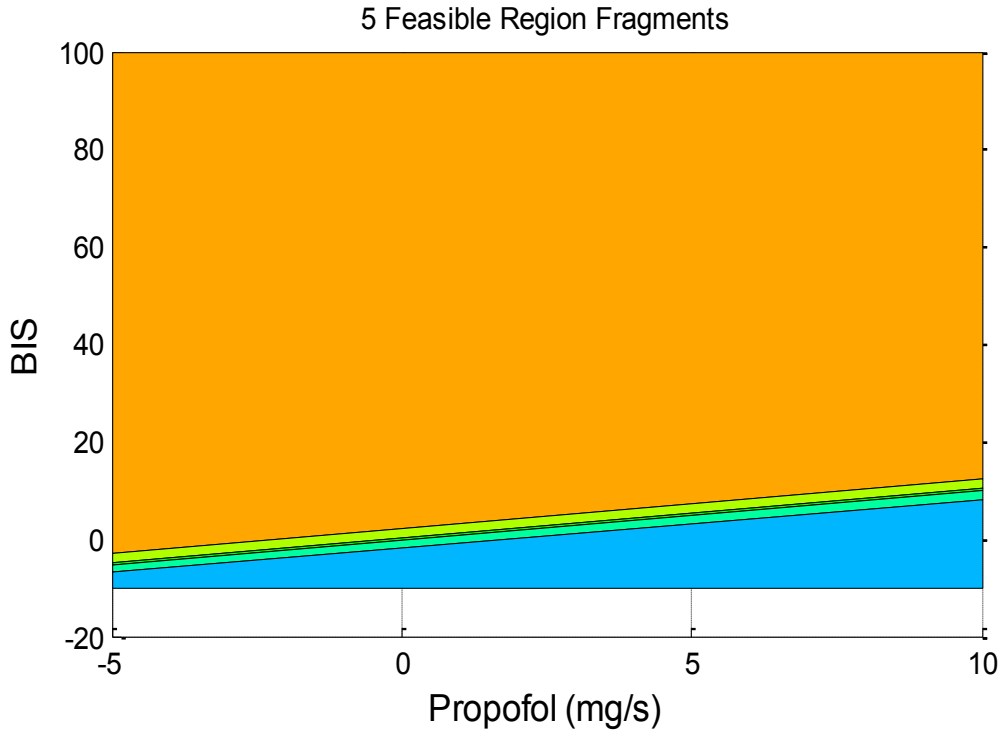

Figure 2.19: Map of critical regions Case 3 and Case 4

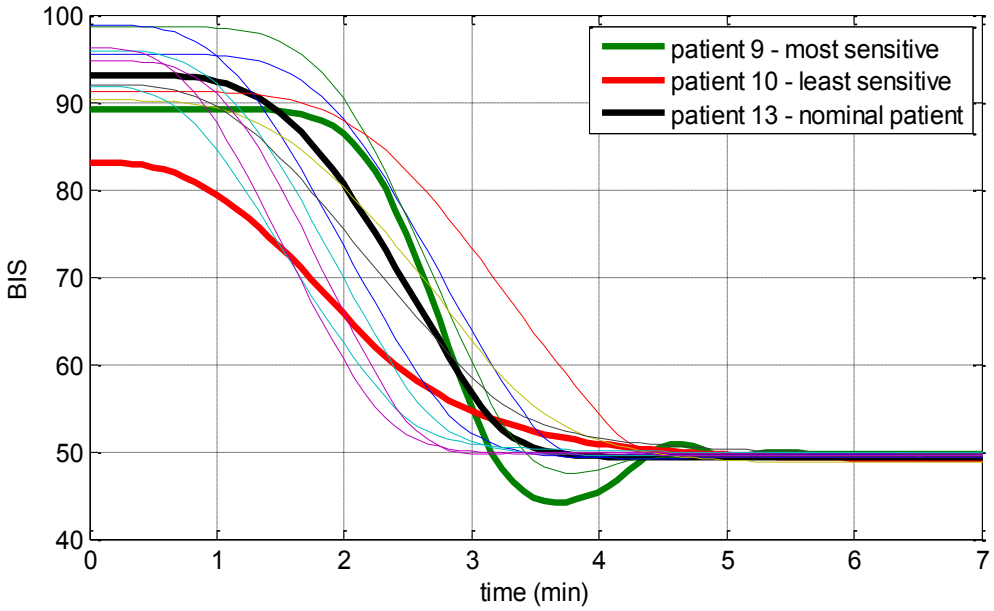

Figure 2.20: BIS output for all 13 patients for Case 3 – induction phase

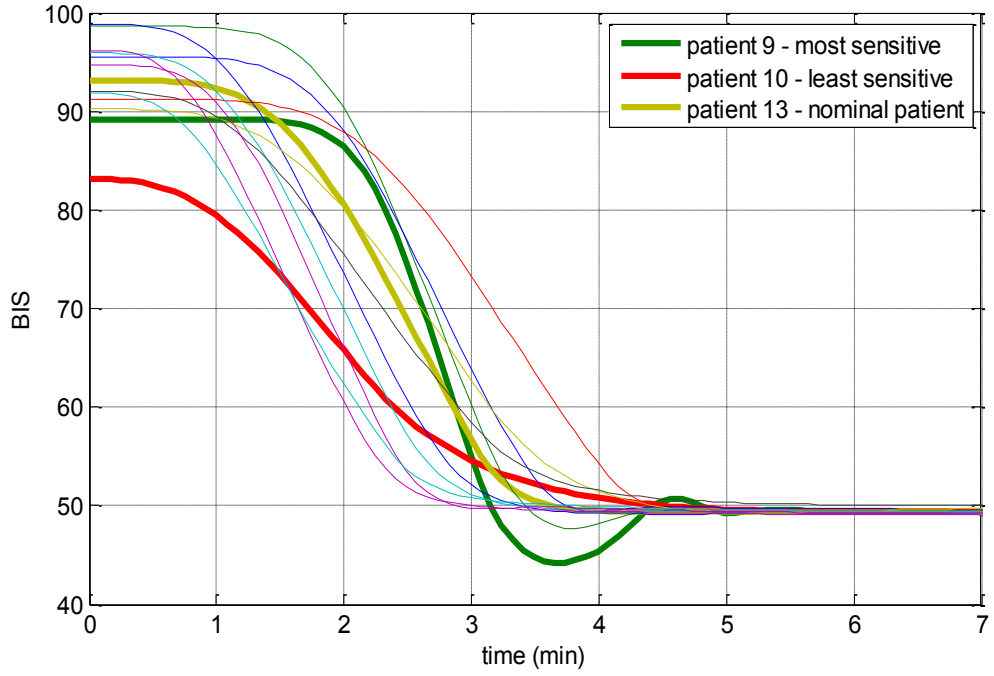

Figure 2.21: BIS output for all 13 patients for Case 4 – induction phase

Simulations of some patients show very small oscillations around the steady-state values. The average settling time for EPSAC is approximately 7 min, and for the mp-MPC controllers is approximately 5 min. In common practice, the operation procedure does not start until the patient reaches an adequate DOA, usually taking up to 15 min. Thus, a settling time between 5 and 7 min gives good performances. The best performances are obtained for Case 2. It seems that the local linearization is able to deal with inter- and intra-patient variability. Also, the process was linearized at BIS = 50, which is the value of the controller set point. The EPSAC controller is more influenced by interpatient variability and for some patients the settling time has greater values. For the nominal patient PaN, the four controllers: EPSAC and the mp-MPC controllers, are simulated, the results are compared and presented in Figure 2.22. For patient 9, the most sensitive patient, this simulation is presented in Figure 2.24. In Figure 2.23 and Figure 2.25, we have the corresponding Propofol infusion rates for the two patients. We can observe that due to the less aggressive behavior of the EPSAC controller, the output evolution will be smoother. In all the cases, the Propofol infusion rates are limited to 50 (mg/min). The same conclusions as for Figure 2.16 - Figure 2.21 valid here. For both simulated patients, the EPSAC controller has a slower response

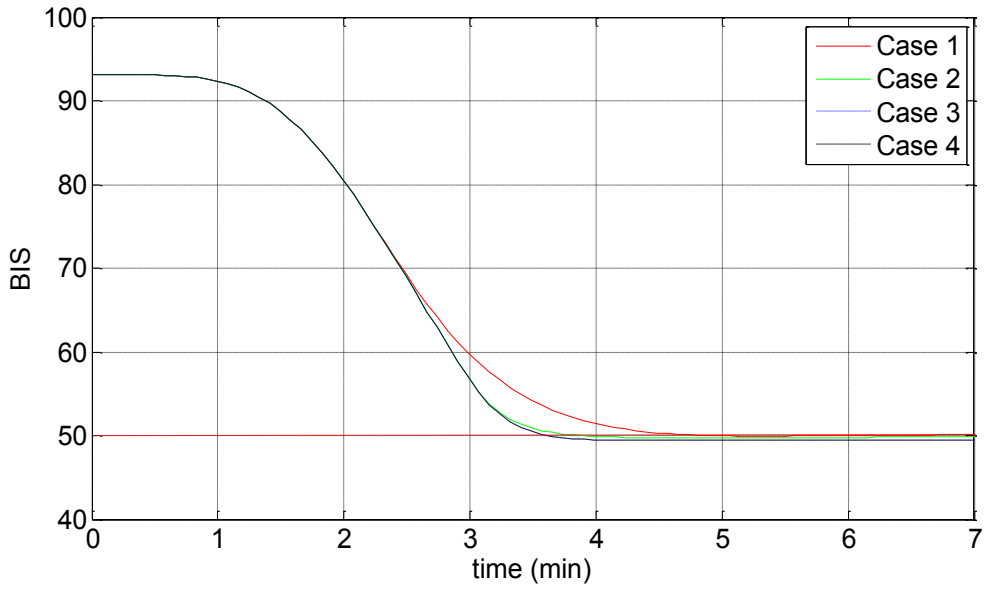

Figure 2.22: BIS response for the four controllers for PaN

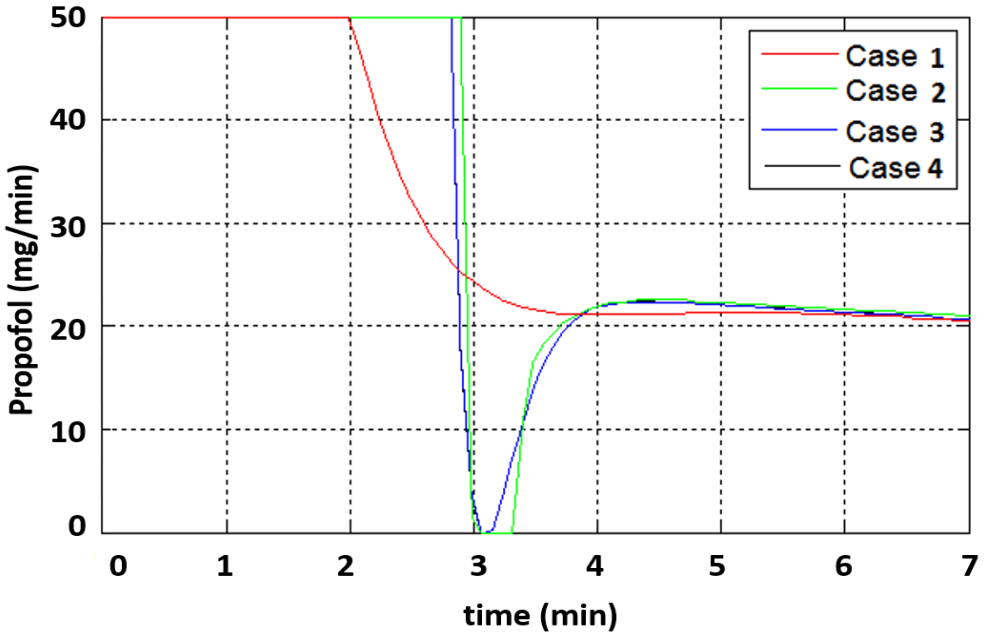

Figure 2.23: Output for the four controllers for the PaN

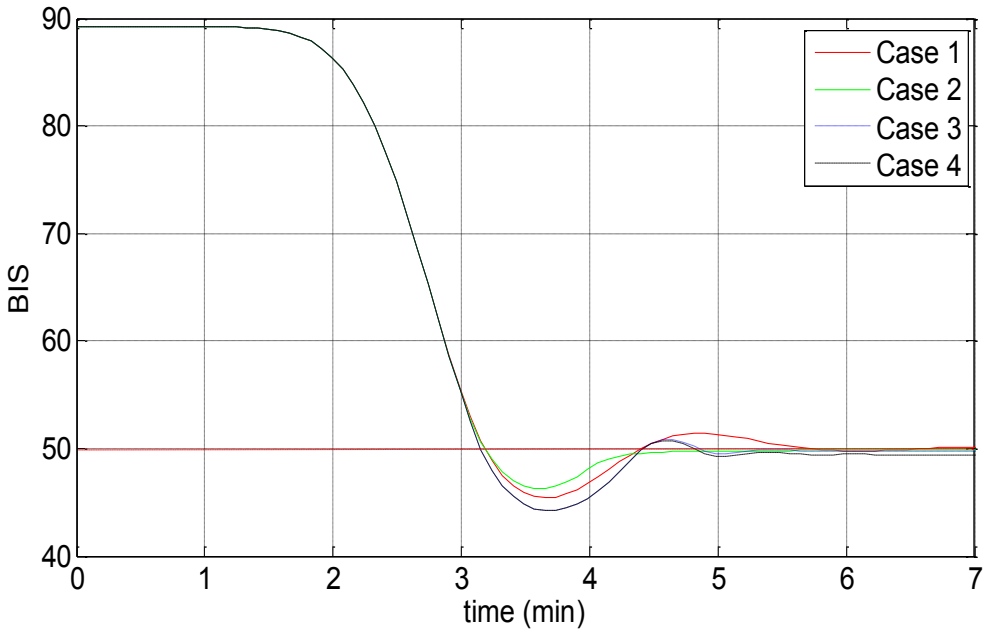

Figure 2.24: BIS response for the four controllers for patient 9

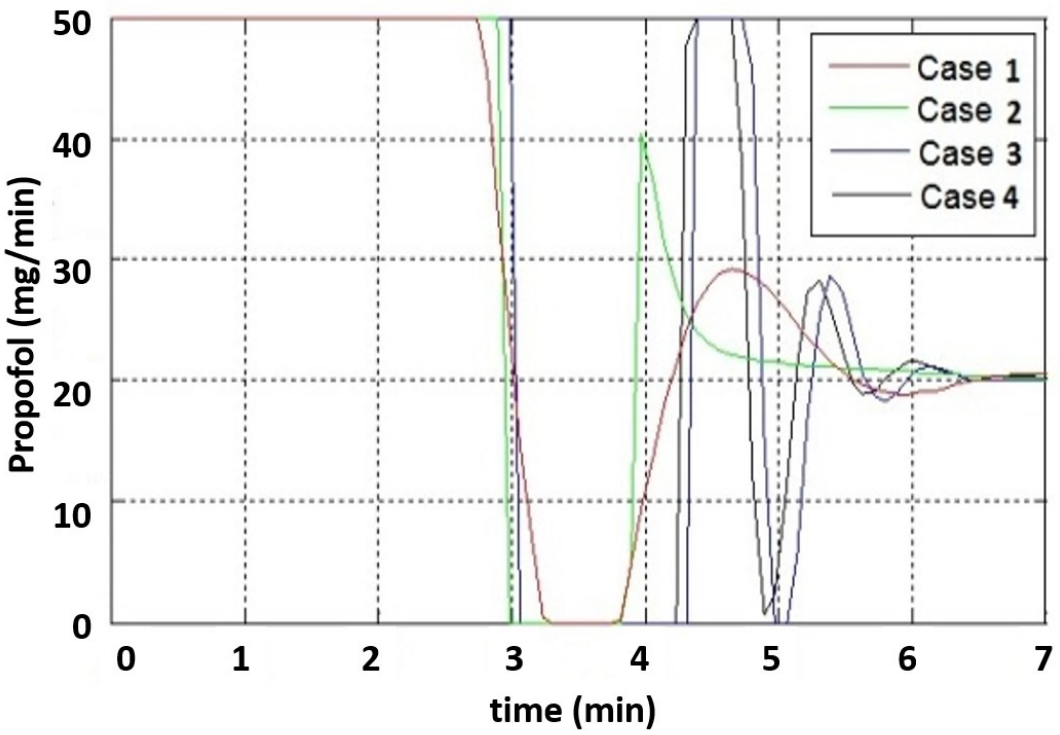

Figure 2.25: Output for the four controllers for patient 9

The optimal control action of the multiparametric controller from Case 3 is presented in Table 2.3, along with the corresponding closed loop simulation control action for the nominal patient and patient 9 (Figure 2.26). Although both patients are in the induction phase, due to the inter- patient variability, different critical regions of the multiparametric controller i.e., control laws provide the optimal control action at each time step for the two patients (for example at T=3, 4, 5). This results in different control policies as observed in Figure 2.26. T=1 corresponds to the control action at time 160 seconds. Since the sampling time is of 5 seconds the control action given at every T corresponds to the sampling time starting from 32 to 38.

Table 2.3: Optimal control action for Patient 9 and the nominal Patient

Step time	Patient 9 (control action)	Nominal Patient (control action)
T=1	$CR_{T=1} = 41$ $u_{opt}^{T=1} = 10$	$CR_{T=1} = 41$ $u_{opt}^{T=1} = 10$
T=2	$CR_{T=2} = 41$ $u_{opt}^{T=2} = 10$	$CR_{T=2} = 41$ $u_{opt}^{T=2} = 10$
T=3	$CR_{T=3} = 41$ $u_{opt}^{T=3} = 10$	$CR_{T=3} = 41$ $u_{opt}^{T=3} = 10$
T=4	$CR_{T=4} = 301$ $u_{opt}^{T=4} = -6.3382x_1 - 0.1001x_2 - 0.5335x_3 + + 7.7653x_e - 39.6582y + 39.6582y_{sp}$	$CR_{T=4} = 301$ $u_{opt}^{T=4} = -6.3382x_1 - 0.1001x_2 - 0.5335x_3 + + 7.7653x_e - 39.6582y + 39.6582y_{sp}$
T=5	$CR_{T=5} = 356$ $u_{opt}^{T=5} = 0$	$CR_{T=5} = 301$ $u_{opt}^{T=5} = -6.3382x_1 - 0.1001x_2 - 0.5335x_3 + + 7.7653x_e - 39.6582y + 39.6582y_{sp}$
T=6	$CR_{T=6} = 356$ $u_{opt}^{T=6} = 0$	$CR_{T=6} = 301$ $u_{opt}^{T=6} = -6.3382x_1 - 0.1001x_2 - 0.5335x_3 + + 7.7653x_e - 39.6582y + 39.6582y_{sp}$
T=7	$CR_{T=7} = 356$ $u_{opt}^{T=7} = 0$	$CR_{T=7} = 301$ $u_{opt}^{T=7} = -6.3382x_1 - 0.1001x_2 - 0.5335x_3 + + 7.7653\theta_e - 39.6582y + 39.6582y_{sp}$

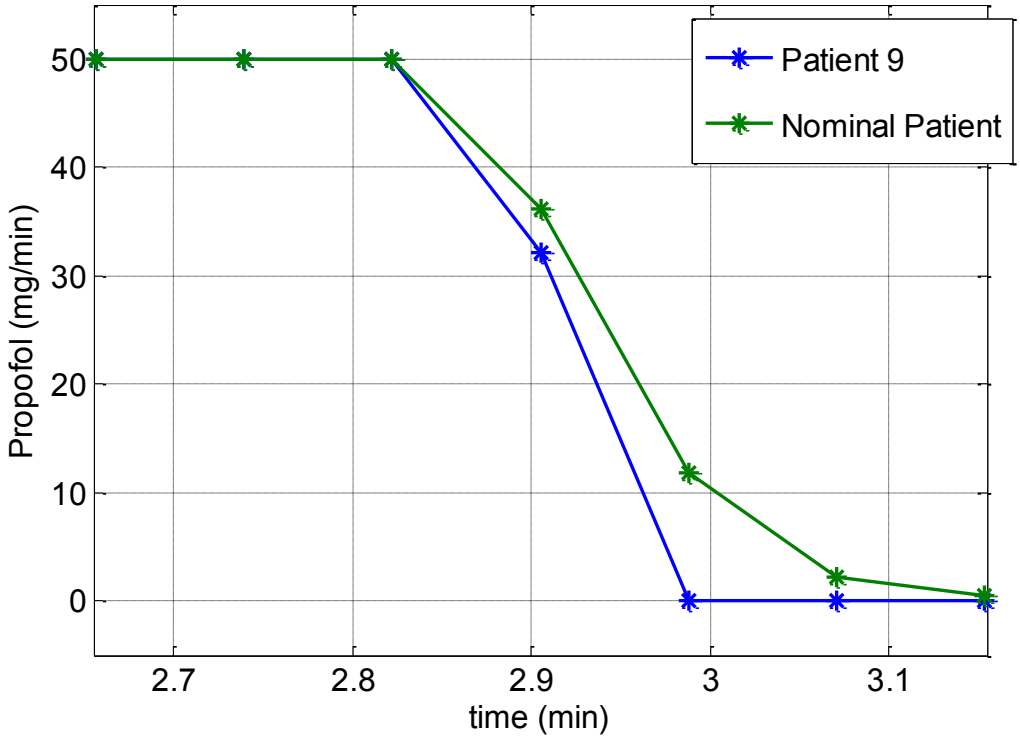

Figure 2.26: Optimal control action for Patient 9 and the nominal patient

2.6.2 Maintenance Phase

During the maintenance phase, it is important that the controller rejects the disturbances occurred during surgery as fast as possible and bring the patient to the BIS target value. In this phase, typical disturbances can be applied additively to the output of the process to check the controller's ability to reject them (West et al., 2013). A standard stimulus profile is defined and is presented in Figure 2.27. Each interval denotes a specific event in the operation theatre. Stimulus A represents response to intubation; B a surgical incision that is followed by a period of no surgical stimulation i.e., waiting for pathology result; C mimics an abrupt stimulus after a period of low level stimulation; D the onset of a continuous normal surgical stimulation; E, F, and G simulate short-lasting, larger stimulation within the surgical period; and H represents the withdrawal of stimulation during the closing period (Yelneedi et al., 2009).

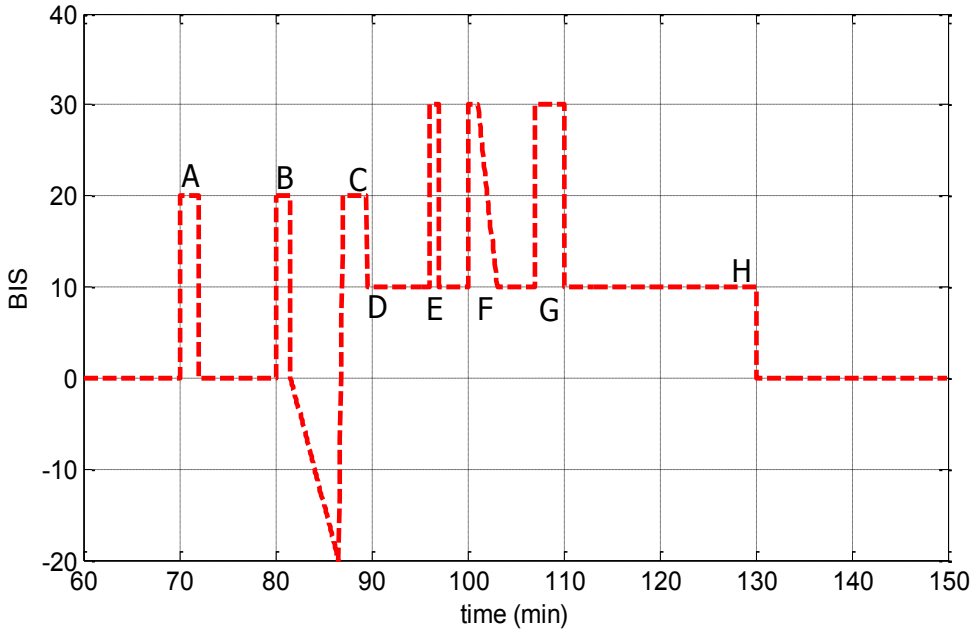

Figure 2.27: The artificially generated disturbance signal

In Figure 2.28 and Figure 2.30, the performance of the disturbance rejection of the four controllers for PaN and a more sensitive patient (patient 9) are shown. The figures present the most challenging part of the disturbance rejection test, namely B-C-D-E. In Figure 2.29 and Figure 2.31, we have the corresponding Propofol infusion rate for PaN and patient 9, limited between 0 and 50 mg/min. The simulations are performed for the maintenance phase using the disturbance signal (see Figure 2.27) between 60 and 140 min. The simulations show only small differences between the controllers and, thus, comparable performances of all four controllers. For the first control scheme, the behaviour of the controller is less aggressive; the response is slower but it also has the smallest values of the undershoot.

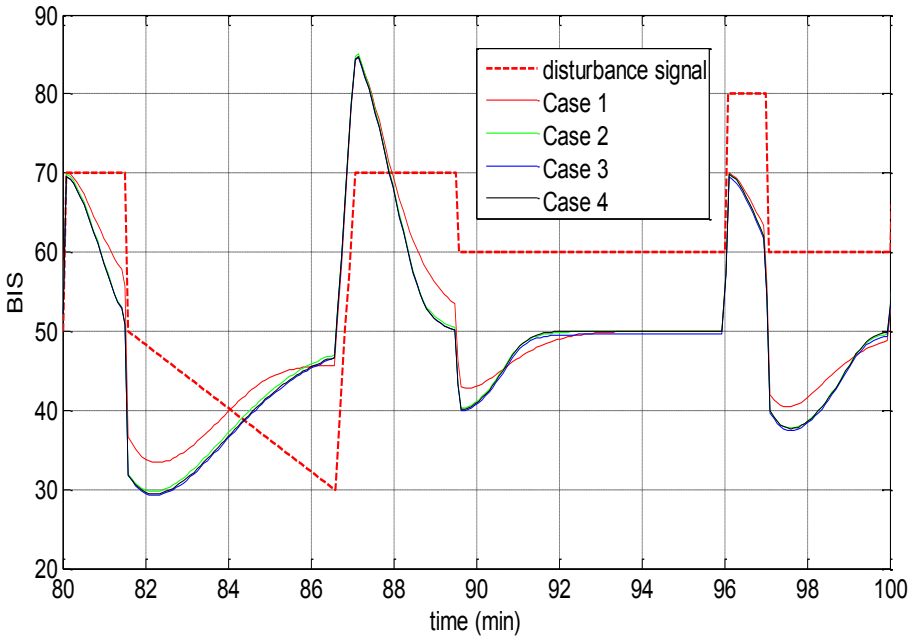

Figure 2.28: BIS response for the four controllers for PaN with disturbance

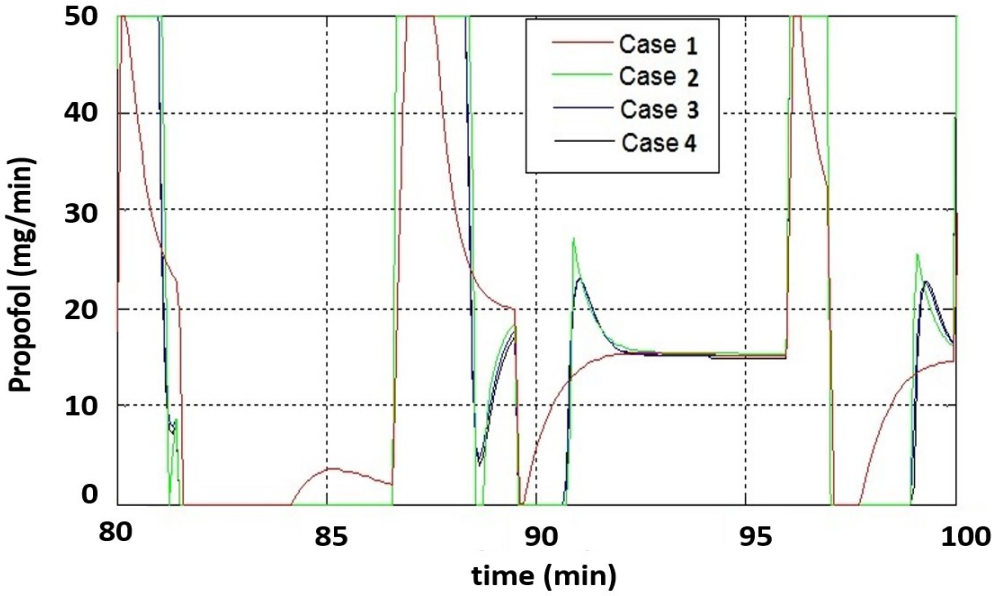

Figure 2.29: Output for the four controllers for PaN with disturbance

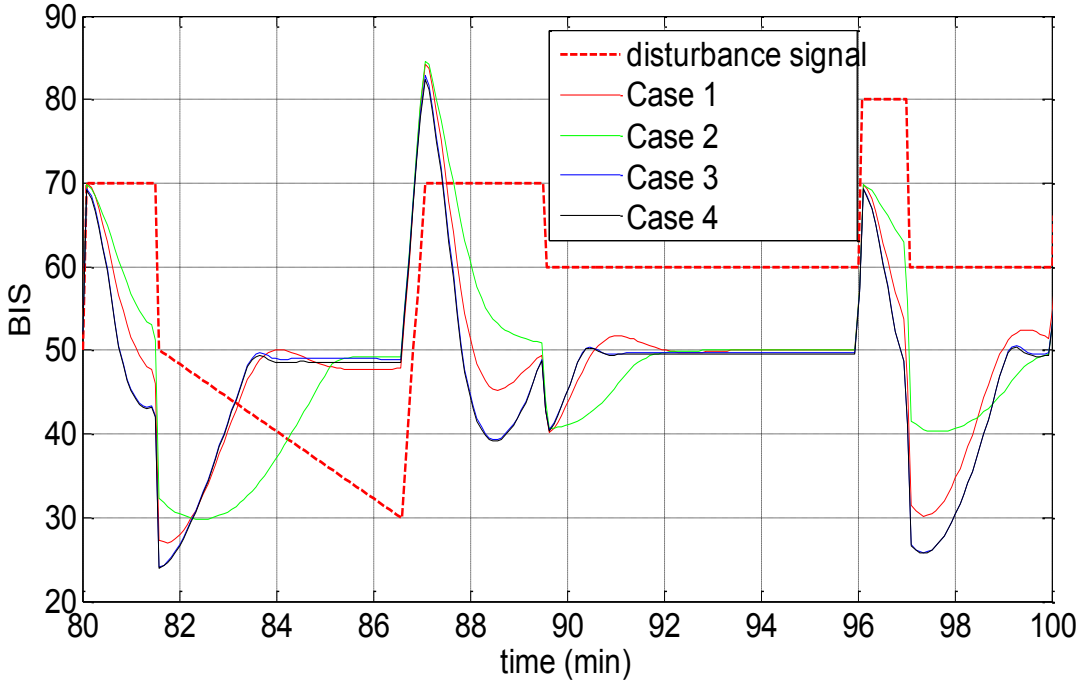

Figure 2.30: BIS response for the four controllers for patient 9 with disturbance

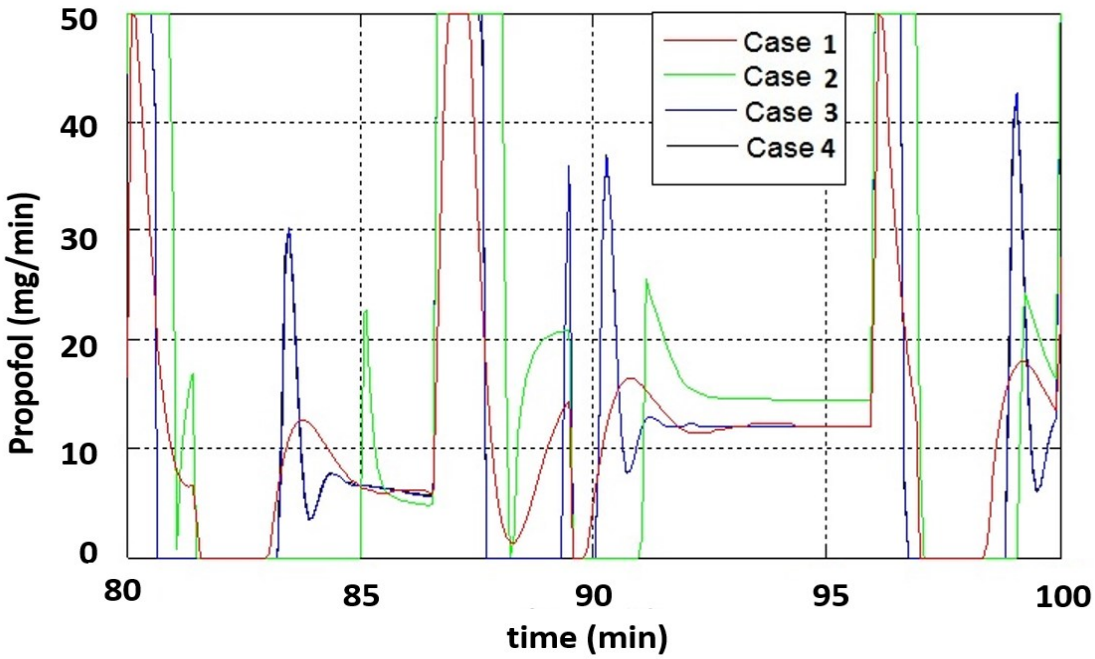

Figure 2.31: Output for the four controllers for patient 9 with disturbance

2.6.3 Discussion

The aim of this chapter is to evaluate the performance of a model-based predictive control algorithm and model predictive multiparametric control for automatic induction and control of DOA during the induction and the maintenance phases.

Some of the most important aspects of this application are the high inter- and intra-patient variability, variable time delays, dynamics dependent on the hypnotic agent, and model analysis variability. These are just some of the issues that are dealt with when trying to control the DOA.

The hypnotic agent Propofol is given as the input and the output is described by the BIS, resulting in a SISO system. SISO patient models for control of most anaesthetic drugs already exist in the literature and their parameters are estimated based on age, weight, gender, and height.

Four different types of controllers are designed and tested. The first controller is based on the online optimization EPSAC MPC technique. The other three controllers are based on the offline optimization mp-MPC: one uses the linearized patient model and the other two uses the compensation of the nonlinear part of the patient model. The difference between the two control strategies using nonlinearity compensation is that for one of them the states are computed using the nominal patient model, whereas the other one uses an online estimator.

In order to address the issue of inter- and intra-patient variability, each of the four controllers are first tested for the whole set of patients presented in Table 2.1 for the induction and the maintenance phase. The maps of the CR for the mp-MPC are presented in Figure 2.17 and Figure 2.19. One can observe that for the controllers using the nonlinearity compensation (exact linearization), there are less CR than for the controller using local linearization. This will make the controllers from Cases 3 and 4 easier to implement on embedded devices.

The undershoot of the most sensitive patient is of 4.6%. As it can be observed from Figure 2.18, Figure 2.20 and Figure 2.21, representing the BIS response of the mp-MPC controllers, the three cases have very similar settling time, lower than for the EPSAC strategy, an average of 270 seconds. For the undershoot evaluation we will consider the worst case scenario, meaning the most sensitive patient. We obtain for the first controller (Case 2) an undershoot of 3.7%, for Case 3 an undershoot of 5.8% and for Case 4, an undershot of 5.78%. All undershoots are below 10% which represents the maximum limit. For the induction phase it can be said that all four controllers perform well each of them having their own advantages: i.e., lower settling time, smaller undershoot.
The controllers are tested in the maintenance phase in order to see how well they can deal with the disturbance rejection. In Figure 2.28 and Figure 2.30, we can observe the four controllers response to a disturbance signal that mimics the events that occur in an operation theatre for PaN and for patient 9.

All four controllers are tested against each other for the induction and maintenance phase for two different patients. The first patient is PaN, and the second patient used for comparison, patient 9, represents the most sensitive patient. It is worth mentioning that the controllers are designed using the values of the nominal patient which means that for this patient, we will have the best behaviour of the controllers. As it can be observed from Figure 2.22, Figure 2.23, Figure 2.28 and Figure 2.29, the BIS response and the output for PaN in the induction phase and the maintenance phase, respectively, the three offline controllers have a very similar behavior. All the controllers present no undershoot and a fast settling time. The EPSAC controller has a less aggressive behaviour; hence, a longer settling time compared to the mp-MPC controllers, but as can be observed in the maintenance phase, it will have less undershoot. In Figure 2.24, Figure 2.25, Figure 2.30 and Figure 2.31, we have the BIS response and the output for patient 9 in the induction phase and the maintenance phase. This patient represents the worst-case scenario since it is the most sensitive patient. We can observe from the figures that all four controllers have good performances and their responses are very close to each other. However, the controller from Case 2 gives the best performances for this patient in the induction phase particularly lower undershoot, 3.7%, and faster settling time, 300 sec. This shows that the

combination between the linearization method based on gPROMS and optimization methods based on mp-MPC gives good results even without the nonlinearity compensation.

It is important to state that the design of the mp-MPC controller using the linearized patient model is the simplest design version of the four controllers since it does not use an estimator and it avoids using the nonlinearity compensation, which introduces additional complexity in the DOA control. Moreover, it obtains the best performances which can be explained through the fact that the nonlinearity of the Hill curve is more intense at extreme values of the BIS index and weaker around the BIS value of 50 where the model was linearized and where the BIS target is set. If the induction phase and the maintenance phase are kept around the value of 50%, Case 2 will give very good performances. But if the disturbances take the process out of the 50% area, we can observe that the performances are not as good as in the case of nonlinearity compensation. Case 2 does not provide good performances if the disturbances are substantial. Due to the Hill nonlinearity, the real-patient model has smaller gain at the extreme values of the control variable. In the case of substantial disturbances, the control variable goes to the extreme values and the controller has a slower response but also a lower undershoot/overshoot.

Using nonlinearity compensation is a good alternative in this case. Moreover, the computations required for the nonlinearity compensation are rather straightforward (the inverse of the Hill curve), and there are no recursive computations that might lead to accumulation of errors.

The estimator used for the mp-MPC with nonlinearity compensation can also be applied for the mp-MPC using local linearization. It was not used for this study because as it can be observed from the simulations, the case with nonlinearity compensation is more meaningful in the presence of disturbance.

The aim of the studies on control of anaesthesia is to be able to implement the controllers on embedded devices (see MOBILE project – MOBILE ERC Advanced Grant, No: 226462). These types of devices do not have the same computational power as the

computers where simulations are performed in real time. This would make classical MPC more difficult to implement since matrix operations are harder to program on embedded devices. The mp programming algorithms derive the explicit mapping of the optimal control actions as a function of the current states resulting in the implementation of a simple lookup table and simple function evaluations. This makes the mp-MPC controllers much easier to implement for the control of DOA.

For each patient, there will be a variable dose-response relationship. For the same reference value, the controller sends different drug rate and the blood and effect-site concentrations levels are different for each patient. The safety limit for Propofol blood concentration and effect-site concentration is fulfilled by maintaining the drug infusion below 50 mg/min. It can be observed from Figure 2.23, Figure 2.25, Figure 2.29 and Figure 2.31 that the drug infusion rates are maintained below this limit.

Note that the robustness of the performance is analyzed by having the controllers designed on a nominal model (Ionescu et al., 2008) and then tested on a wide set of patient models parameters where the impact of parameter uncertainties were analysed. Formal robust criteria can also be included as discussed in Chapter 4.

2.7 Conclusions

In this chapter, we have designed and evaluated four different controllers for the regulation of DOA during induction and maintenance phase. For the maintenance phase, a realistic disturbance signal was considered and applied. A simulation study was performed on a set of 12 virtually generated patients plus the mean patient. The performance of the four controllers was compared with each other for a sensitive patient and the nominal patient.

Some important aspects of this application are the high inter- patient variability and the presence of important disturbances during the maintenance phase. The results show a high efficiency, optimal dosage, and robustness of the MPC algorithm to induce and maintain the desired BIS reference while rejecting typical disturbances from surgery. The

mp-MPC approach, which is an offline optimization method, has similar performances with the online method and promising results.

Chapter 3

Simultaneous Estimation and Advanced Control for the Anaesthesia Process

3.1 Introduction

In the previous chapter we have designed and studied different controllers for the regulation of depth of anaesthesia during induction and maintenance phase. More specifically we presented: (i) a model predictive control strategy that is based on online optimization (EPSAC) and (ii) a multi-parametric model predictive control strategy based on offline optimization (mp-MPC). The implementation of these controllers, as discussed in Chapter 2 is based on the assumption that the state values are readily available from the system measurements and that we have a clear measurable output with not much noise influence. However, in reality, the measured output may be noisy (as discussed in Chapter1.1) and the system measurements may not produce this information directly - instead the state information needs to be inferred from the available output measurements. This can be done developing state estimators which is the subject of this chapter.

The use of estimation techniques will enable to: (i) estimate the state of each individual patient and adjust them based on his/her corresponding dynamics; (ii) overcome the noisy output measurements and (iii) deal with the system constraints (in conjunction with an MPC structure).

While in Chapter 2 for the Case 4 (Section 2.5.4), Kalman filter was implemented simultaneously with mp-MPC, it was observed that the performances of the controller was not significantly improved due to its limitations such as handling system constraints and noise. As a result, in this chapter, online and offline moving horizon estimator

(MHE) will be investigated and implemented simultaneous with mp-MPC. For comparison purposes, Kalman filter will be also tested. All resulting controllers with the corresponding estimation techniques are tested for both induction and maintenance phase for a set of 12 patient data.

This chapter is organized as follows: the design of three different estimation strategies as well as their performances on different patients are presented in Section 3.2. Section 3.3 presents the formulation and design of the simultaneous mp-MPC and estimation. The simulation results of the designed control strategies for the induction and maintenance phase are presented in Section 3.4 while discussions are presented in Section 3.5. Finally Section 3.6 summarizes the main outcome of this chapter.

3.2 Multiparametric Moving Horizon Estimation (mp-MHE)

The idea of moving horizon estimation is to estimate the state using a moving and fixed-size window of data. Once a new measurement becomes available, the oldest measurement is discarded and the new measurement is added. The concept is to penalize deviations between measurement data and predicted outputs. In addition – for theoretical reasons - a regularization term on the initial state estimate is added to the objective function. There are two main characteristics that distinguish MHE from other estimation strategies, such as Kalman filter: (i) prior information in the form of constraints on the states, disturbances and parameters can be included; (ii) since MHE is optimization based it is able to handle explicitly nonlinear system dynamics through the use of approximate nonlinear optimization algorithms. Here MHE is first formulated as a multiparametric problem and then combined with an explicit mp-MPC strategy. These concepts are discussed next.

3.2.1 Multiparametric Moving Horizon Estimation (mp-MHE) Formulation

Based on the moving horizon estimation theory presented in Appendix E the resulting multiparametric moving horizon estimation formulation can be obtained.

$$[\hat{x}_{T-N+1}, \{\hat{w}\}_{T-N+1}^{T-1}] = \min_{x_{T-N+1}, \{w\}_{T-N+1}^{T-N}} \sum_{k=T-N+1}^{T-N} (w_k - \overline{w})^T \cdot Q^{-1} \cdot (w_k - \overline{w}) + \sum_{k=T-N+1}^{T} (v_k^T \cdot R^{-1} \cdot v_k) +$$
$$+ (x_{T-N+1} - \bar{x}_{T-N+1/T-N})^T \cdot P_{SS}^{-1} \cdot (x_{T-N+1} - \bar{x}_{T-N+1/T-N})$$

(Equation 3.1)

subject to

$$x_{k+1} = A \cdot x_k + B \cdot u_k + G \cdot w_k \qquad \text{discrete state-space formulation}$$
$$y_k = C \cdot x_k + v_k \qquad \rightarrow v_k = y_k - C \cdot x_k$$
$$\text{BIS}_{\min} \le y \le BIS_{\max}$$
$$\Delta \text{u}_{\min} \le \Delta u \le \Delta u_{\max}$$
$$\begin{bmatrix} 1 & 0 & 0 & 0 \\ -1 & 0 & 0 & 0 \\ 0 & 1 & 0 & 0 \\ 0 & -1 & 0 & 0 \\ 0 & 0 & 1 & 0 \\ 0 & 0 & -1 & 0 \\ 0 & 0 & 0 & 1 \\ 0 & 0 & 0 & -1 \end{bmatrix} \cdot \begin{bmatrix} x_1 \\ x_2 \\ x_3 \\ x_e \end{bmatrix} \le \begin{bmatrix} 100 \\ 0 \\ 100 \\ 0 \\ 100 \\ 0 \\ 100 \\ 0 \end{bmatrix} \qquad \text{path constraints on state variables}$$
$$\begin{bmatrix} 1 \\ -1 \end{bmatrix} \cdot w \le \begin{bmatrix} 1 \\ -1 \end{bmatrix} \qquad \text{path constraints on the noise w}$$
$$\begin{bmatrix} 1 \\ -1 \end{bmatrix} \cdot v \le \begin{bmatrix} 1 \\ -1 \end{bmatrix} \qquad \text{path constraints on the noise v}$$
$$\bar{x}_{T-N+1/T-N} = A \cdot \hat{x}_{T-N/T-N} + B \cdot u_k + G \cdot \overline{w} \qquad \text{update of the cost to arrive}$$

Where N is the length of the horizon, T is the current point in time, Q and R are positive definite diagonal weighting matrices on the noises, P_{SS} is the steady state solution for the Kalman filter. $\{\hat{w}\}_{T-N+1}^{T-N}$ and $\{v\}_{T-N+1}^{T}$ are sequences of independent, normally distributed random numbers with mean values $\overline{w}$ for $\{w\}$ and zero-mean for $\{v\}$. $\bar{x}_{T-N+1/T-N}$ is the arrival cost which captures the previous measurements that are not considered any more. $\hat{x}_{T-N/T-N}$ is the solution of the MHE at the previous time step.

3.2.2 Estimation Design

The schematic of the estimator used for the different estimation techniques is presented in Figure 3.1. The *Estimator* block uses the input of the system, the *Drug Infusion Rate (u)* and the output measurements (from the sensor) of the system to estimate the states of the simulated patient. The process disturbances $w \in R^p$ and measurement disturbance $v \in R^p$ are considered unknown variables. The goal of the estimation is to construct an estimate of the trajectory of x for the simulated patient using only the process input values, the output measurements and the state space model of the nominal patient. Note that for control purposes we are usually interested in the estimate of the state at the current time, T, rather than the entire trajectory over the interval [0,T]. We have two sources of error: (i) the state transition is affected by an unknown process disturbance (or noise), w, and (ii) the measurement process is affected by another disturbance, v. In the MHE approach, we formulate the optimization objective to minimize the size of these errors thus finding a trajectory of the state that comes close to satisfying the (error-free) model while still fitting the measurements.

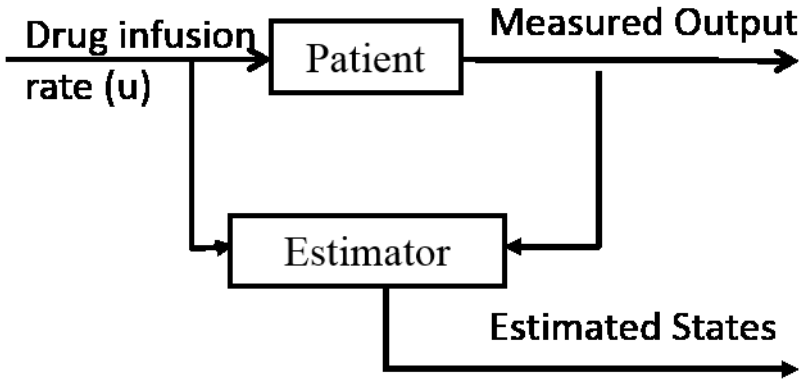

Figure 3.1 Intravenous anaesthesia - Schematic of the Estimator– General Case

State estimation is important as the controller requires the state space of the patient. Since there are no available measurements of the states nor do we have a model for each individual patient available 'a priori', usually the controller uses the state space model of the nominal patient. Estimation of the real states of individual patients is expected to

improve the overall performances of the controller while significantly increasing the safety of the patient.

Here three types of estimators, Kalman filter, online MHE and offline mp-MHE are used to estimate the current states of the patients using the nominal patient model, the patient measurements and the drug rate. Two approaches for the design of the estimators are employed: (i) the first case uses the output of the PD model (the nonlinear part) more precisely the measurement of the BIS index (ii) the second case considers the output $\hat{C}_e$ of the inverse Hill curve (Equation 2.6) (applied to the BIS index)– see Figure 3.2 and Figure 3.7.

The simulations were performed in open loop for a step on the input of 12 mg/min (Propofol drug infusion rate). The value was chosen such that steady state values of the states to reach the recommended range for the maintenance phase. For the design of the MHE, the following tuning parameters are used: a horizon of *N=3, Q=1* and *R=0.01*; the parameters vector includes the N past measurements and values for the manipulated variable.

3.2.2.1 Estimation Design – Case 1

As shown in Figure 3.2, the first estimation design strategy uses the *Drug Infusion Rate (u)* and the output of the *PD Model*, the *Measured BIS* in order to obtain the estimated states. This introduces nonlinearities in the estimation since the *PD Model* contains the nonlinear *Hill curve* –see (Equation 2.5). Three types of state estimators are implemented: the Kalman filter, online MHE and offline mp-MHE and tested against each other for the different patients of Table 2.1.

The results of the estimation are shown in Figure 3.3, Figure 3.4, Figure 3.5 and Figure 3.6. Note that the estimation using online MHE and mp-MHE show identical behaviour as expected with the difference between the two being that the mp-MHE can be implemented offline. The advantages of the mp-MHE is that by using a multiparametric approach it by passes the real time approach, thus overcoming the computational efficiency issues. Instead of solving the optimization problem at every sampling time, the mp-MHE uses the input and the output data to consult an off-line constructed look-up

table that indicates what closed-form expression from a finite collection must be used to estimate the values of state variables. Both the look-up table and the finite collection of closed-form expressions for state estimation are constructed once via off-line optimization (Darby et al., 2007). Hence, in the figures, online MHE is not shown.

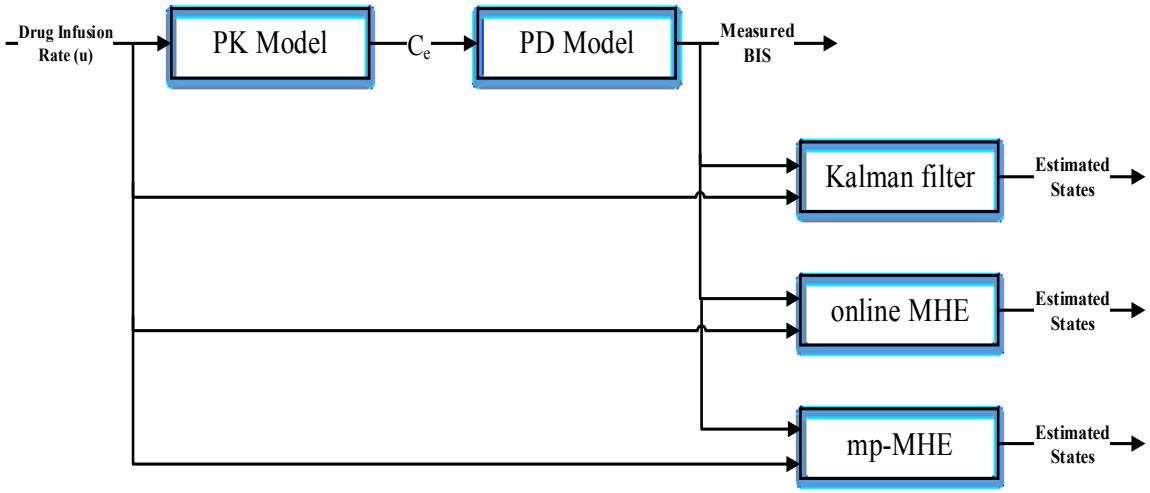

Figure 3.2: Intravenous anaesthesia - Schematic of the Estimation – Case 1

Note also that in all figures presented we have simulated the states of: (i) the nominal patient for which a state space model is a priori available; (ii) the actual patient; (iii) the actual patient estimated using mp-MHE; (iv) the actual patient estimated using Kalman filter.

The simulation of the estimators are performed first under the assumption that the measured output (BIS index) is noise free and the results are presented in Figure 3.3 - Figure 3.5 for patient 2 and 7, respectively. Figure 3.4 and Figure 3.5 present the results for patients 2 and 7 for two of the four states. The two states are chosen such as to best highlight the differences between the state estimators and they represent the concentration of drug in the muscles and the concentration of the effect site compartment respectively.

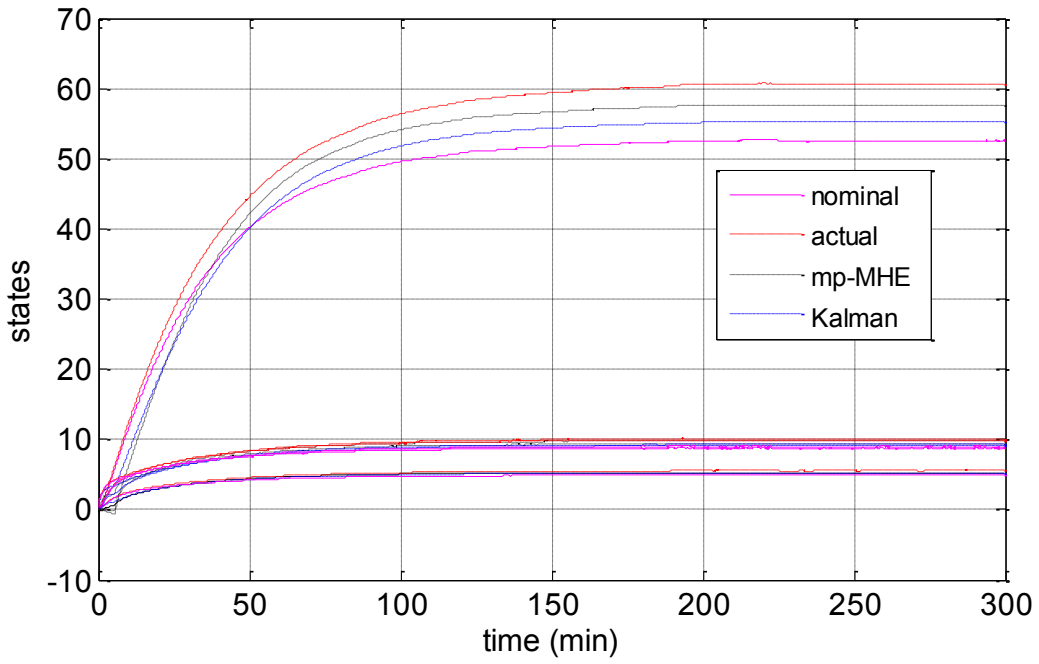

Figure 3.3: Intravenous anaesthesia - State estimation for patient 2 – all states– no noise

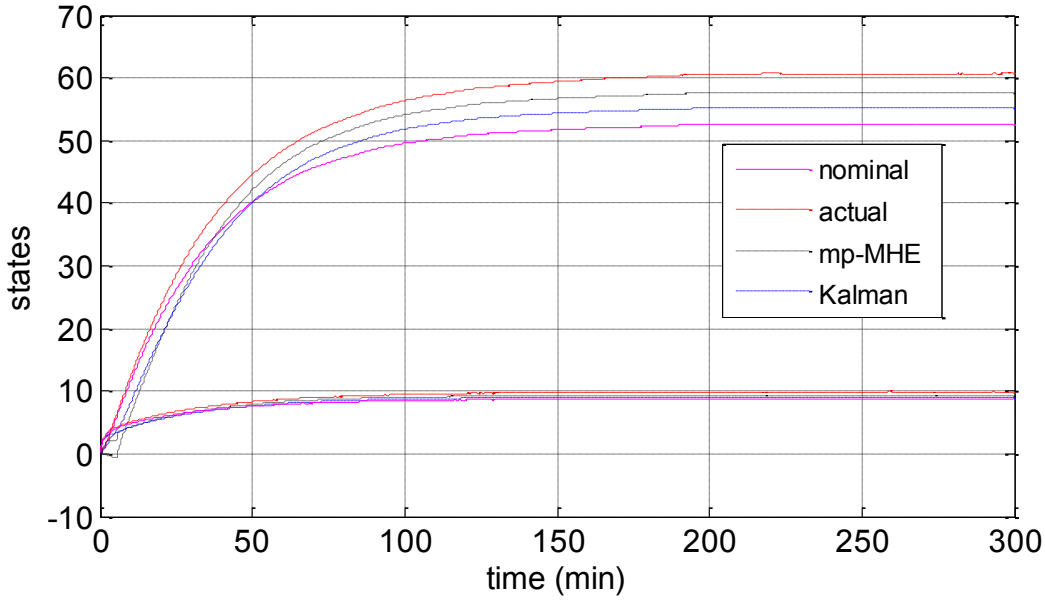

Figure 3.4: Intravenous anaesthesia - State estimation for patient 2 – 2 states – no noise

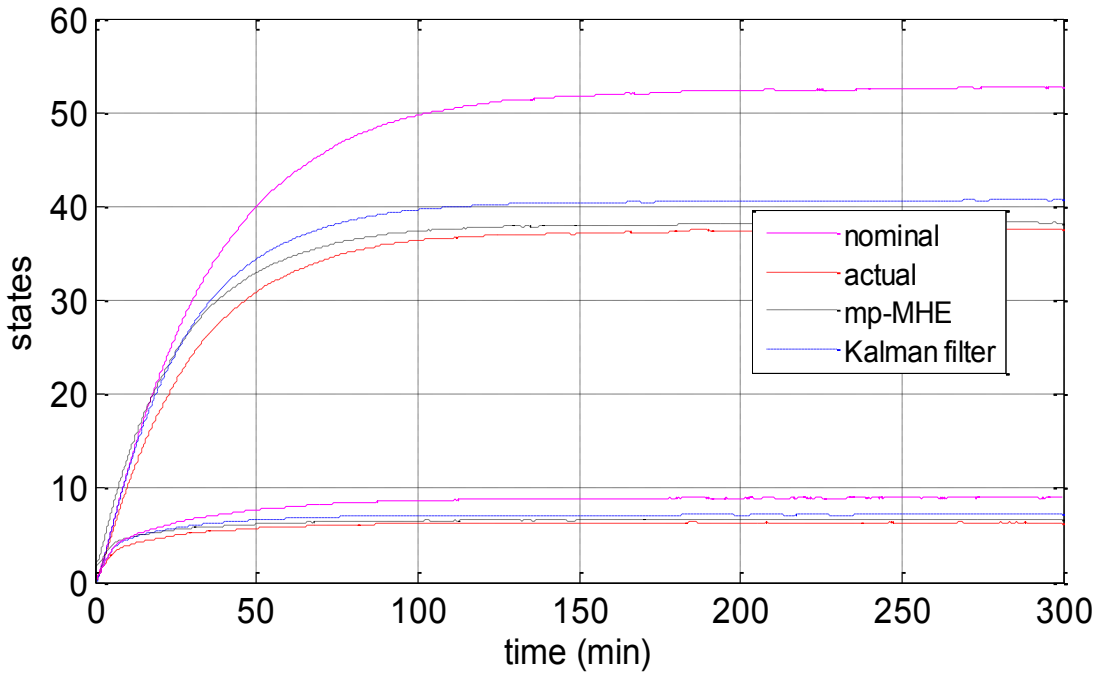

Figure 3.5: Intravenous anaesthesia - State estimation for patient 7 – 2 states – no noise

It can be observed that in the presence of no noise we obtain the weakest results for the estimator using the nominal state space model, followed by Kalman filter and the MHE has slightly better performances since it is able to deal with system constraints.

As discussed in Chapter 1.1 the Bispectral index (BIS) is highly influenced by noise and disturbances. Hence, noise has been added to the measured BIS index, and included for the moving horizon estimation; a Gaussian distribution with a 3% standard deviation is assumed. Figure 3.6 depicts the states in the presence of noise on the output. In this case estimation obtained with the mp-MHE estimation were improved, the estimated states being very close to the real patients despite the fact that the estimators were developed using the nominal patient state space model.

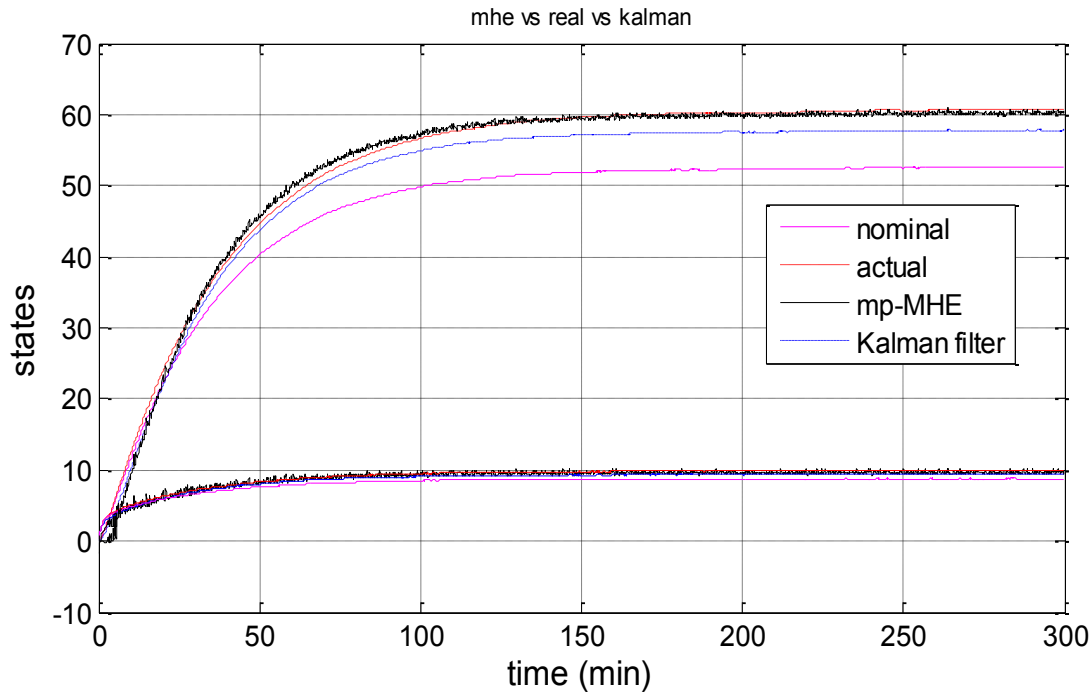

Figure 3.6: Intravenous anaesthesia - State estimation for patient 2 – 2 states – with noise

3.2.2.2 Estimation Design – Case 2

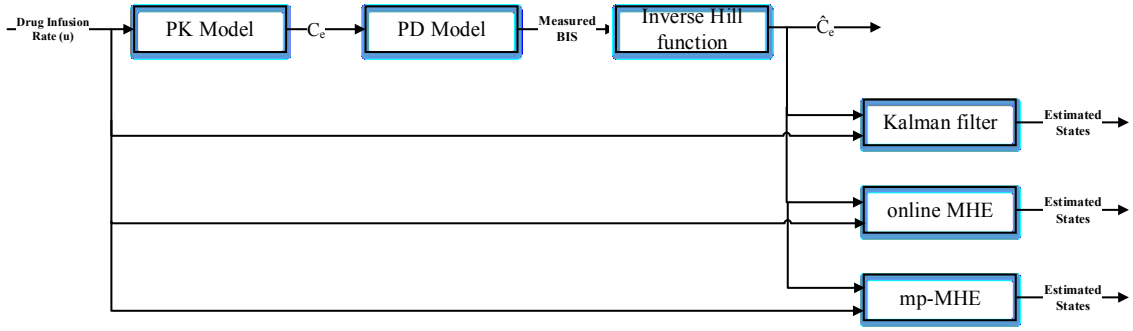

Figure 3.7: Intravenous anaesthesia - Schematic of the Estimation – Case 2

In the first case the output of the Hill function (BIS index) is used as an input for the estimators. In this case, to compensate for the nonlinearity, the inverse of the Hill curve is used on the measured output (Figure 3.7). This will make $\hat{C}_e$ as input for the estimators and will overcome the issues introduced by the nonlinearity.

Three types of state estimators are implemented, similar to Case 1: the Kalman filter, online MHE and offline mp-MHE and tested against each other for the different patients (Table 2.1). All three estimators are designed using the state space model of the nominal patient, the $\hat{C}_e$ concentration (obtained by using the inverse of the Hill curve on the measured output) and the *Drug Infusion Rate*.

In the case of the mp-MHE, the parameters of the multiparametric programming problem in (Equation 3.1) are the past and current measurements and inputs and the initial guess for the estimated states. Figure 3.8 presents the solution of the multiparametric programming problem in the form of 2-dimensional projection of the critical regions. The projections are based on the states of the parameter vectors while the values of the rest of the parameters are set to certain values within their feasible bunds so as to generate the graph. In this case θ_1 and θ_2 are the second state representing the drug concentration in the muscle compartment and the concentration in the effect site compartment.

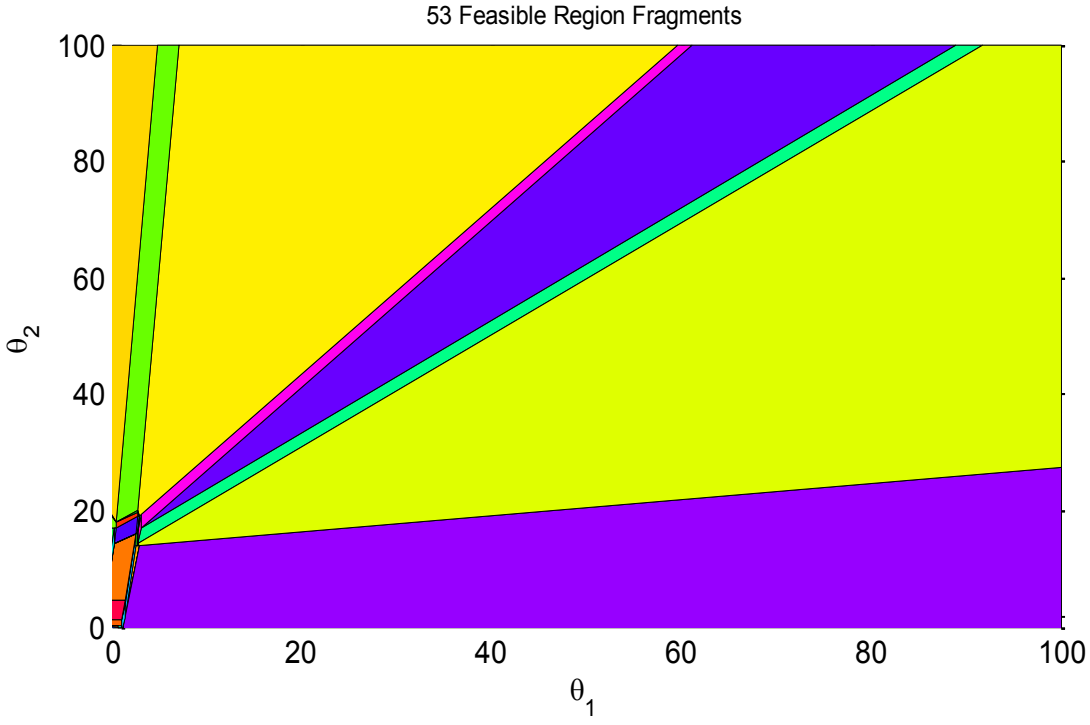

Figure 3.8: Intravenous Anaesthesia mp-MHE - critical regions

The simulations are performed following the structure in Figure 3.7. The results of the performances for the designed estimators using the output without being influenced by noise are presented in Figure 3.9 and Figure 3.10. It can be observed that without having the output corrupted by noise the estimators exhibit closer performances much better than the ones obtained by computing the states using the state space nominal model.

In Figure 3.11 an ideal case is presented where the nominal patient is the same as the one simulated and the process is not affected by noise. In this case all three estimators exhibit similar behaviour and estimate perfectly the real states.

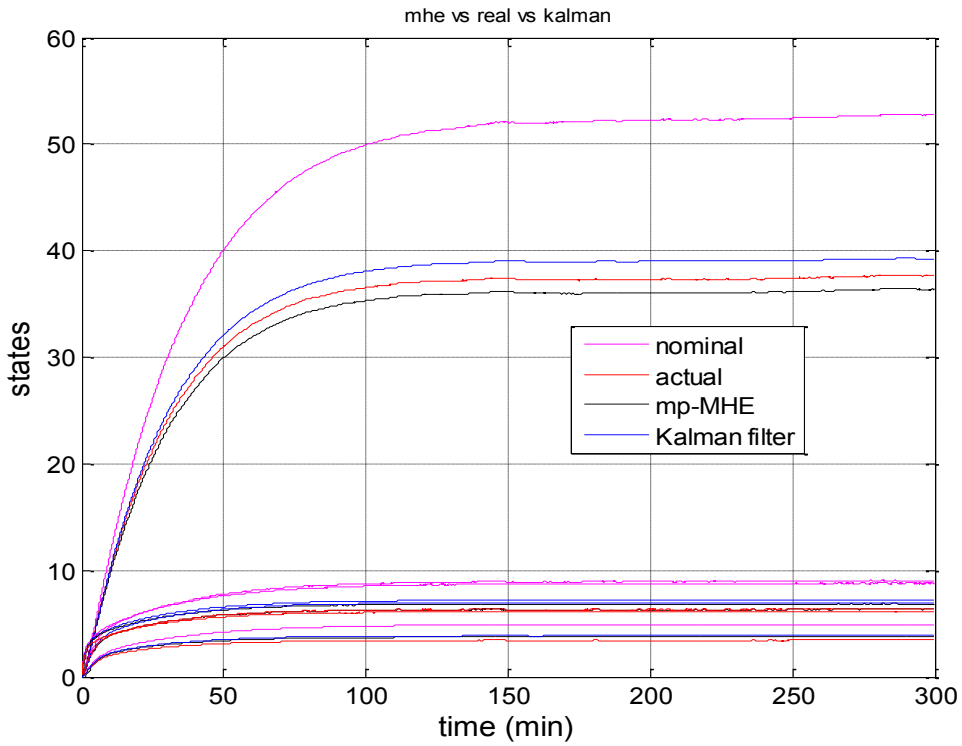

Figure 3.9: Intravenous anaesthesia - State estimation for patient 7 – no noise

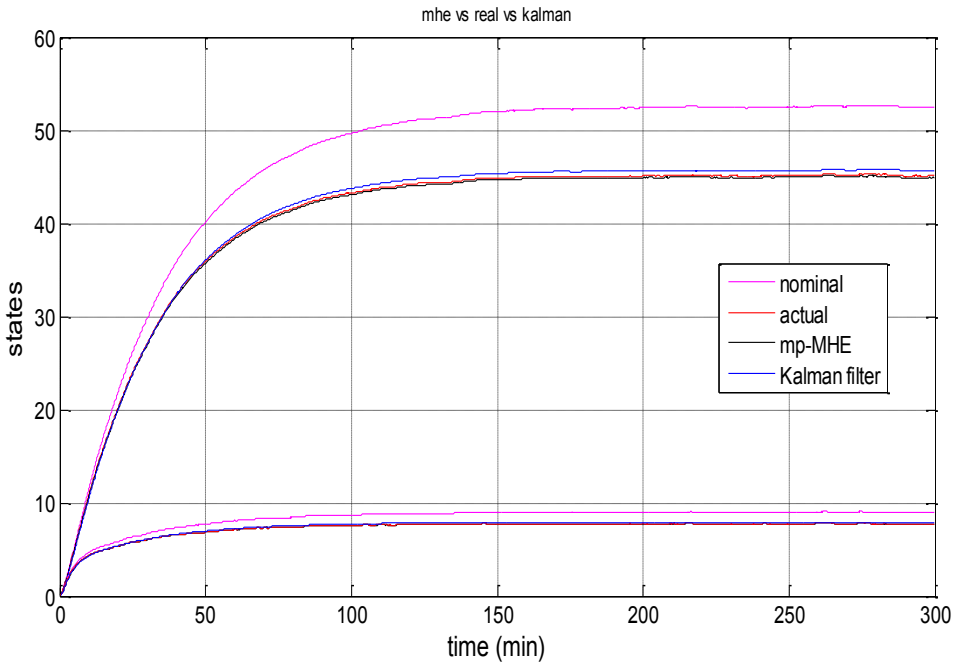

Figure 3.10: Intravenous anaesthesia - State estimation for patient 8 – 2 states –no noise

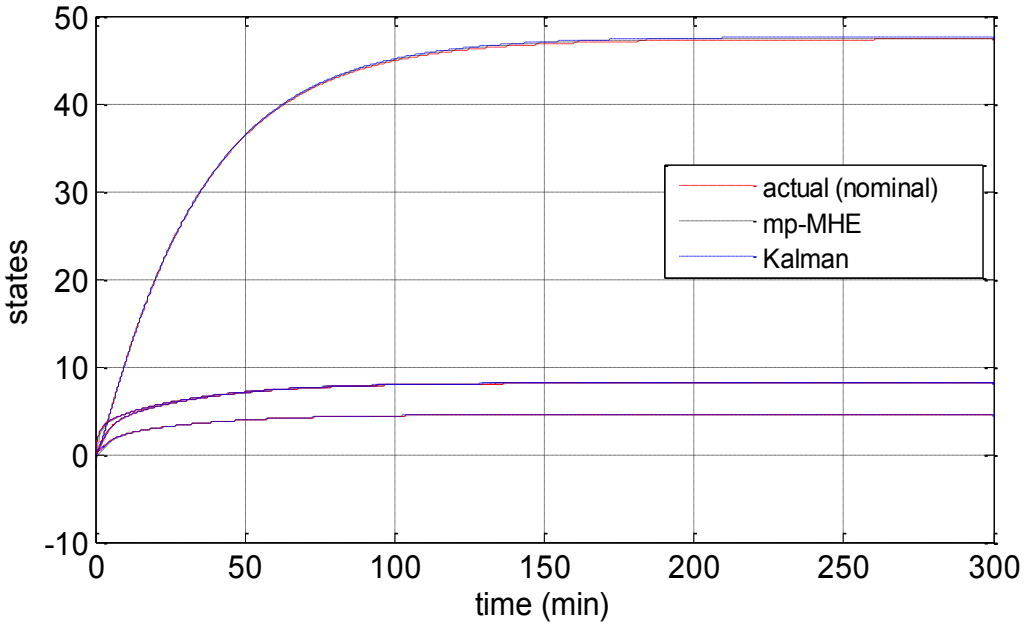

Figure 3.11: Intravenous anaesthesia - State estimation for the mean patient

In

Figure **3.12** and Figure 3.13 we show the results of the performance for the designed estimators using the output that is strongly corrupted by noise.

Figure 3.12 and Figure 3.13 show simulation results for the state estimation for patients 7 and 8 for two out of the 4 estimated states. The two states are chosen such as to best highlight the differences between the state estimators and they represent the concentration of drug in the muscles and the concentration of the effect site compartment.

For both patients as in the previous case the mp-MHE estimator exhibits better performance due to its capability of dealing with constraints and the non-gaussian noise in the process. As it can be observed from

Figure **3.12** and Figure 3.13, in this case the estimated states are very close to the real patients states.

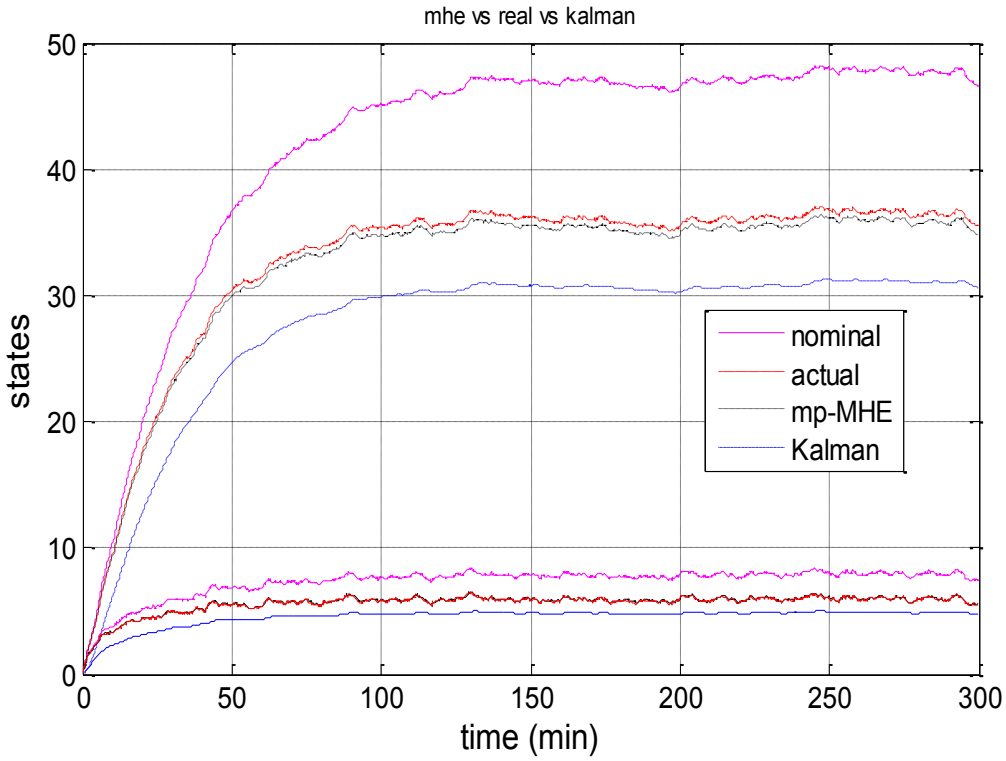

Figure 3.12: Intravenous anaesthesia - State estimation for patient 7- 2 states – with noise

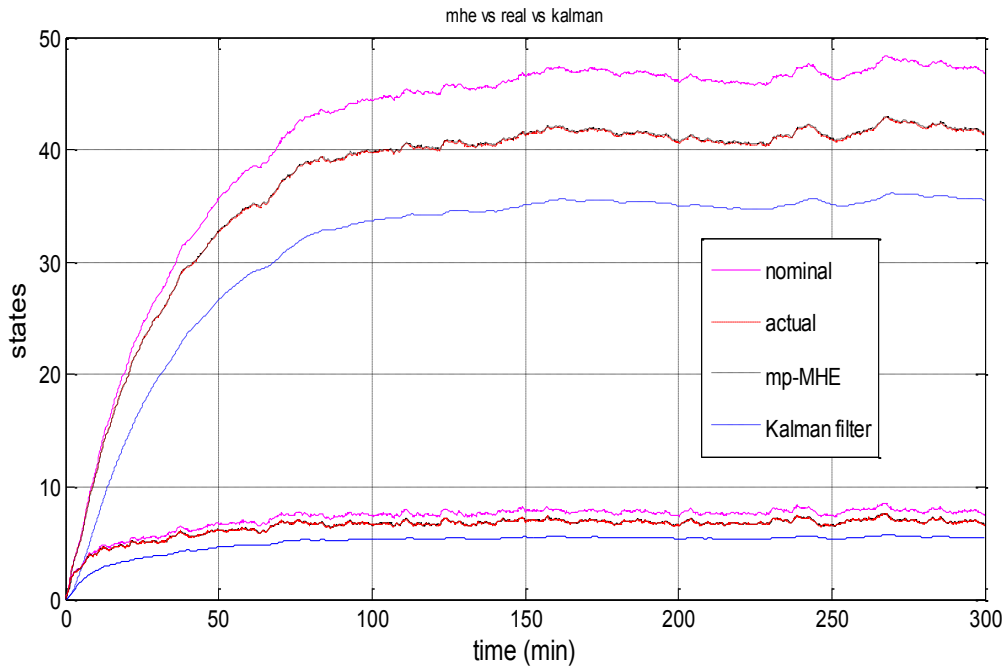

Figure 3.13: Intravenous anaesthesia - State estimation for patient 8 – 2 states – with noise

3.3 Simultaneous Estimation & MP-MPC Strategy

In this section developed estimation strategies are implemented simultaneously with mp-MPC for the control of intravenous anaesthesia. The proposed control design scheme for simultaneous estimation and mp-MPC is presented in Figure 3.14.

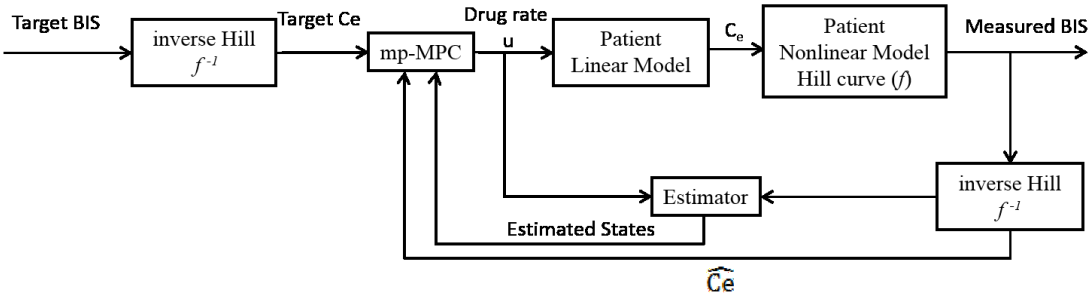

Figure 3.14: Schematic of simultaneous mp-MHE and mp-MPC for intravenous anaesthesia

The *Patient* is simulated using the mathematical model of the patient composed of the pharmacokinetic part (linear) and the pharamacodynamic part, including the *Hill curve* (nonlinear) as described in Chapter 2.1. The *inverse Hill function* block, designed based on the nominal patient model, is used to compensate for the nonlinearity introduced by the *Hill curve* in the Pharacodynamic model. This block uses the *Measured BIS* and provides the corresponding $\hat{C}_e$ to the *mp-MPC* block. The *BIS Target* can be set by the user but for general anaesthesia it is set to the value of 50. Since the *mp-MPC* block uses the corresponding $\hat{C}_e$ of the *Measured BIS*, the *BIS Target* will be transformed in *Ce Target* by using the *inverse of the Hill* curve block. The *Estimator* block is used to estimate the state of each individual patient. The commonly used technique to generate the states for the controller in the absence of the real state measurements is to compute them using the control action for the simulated patient and the nominal state space model. By estimating the states of every simulated patient, the controller instead of using the states computed using the nominal patient model will use the estimated values of states corresponding to each individual patient. Finally, the *mp-MPC* block, using the individual patient states given by the *Estimator* block, calculates the error between the $\hat{C}_e$ corresponding to the *Measured BIS* from the *Patient* and the *Target Ce* and provides the optimal *Drug rate u* to the *Patient* block in order to drive it to the desired target value.

The Hill curve (Equation 2.5) introduces nonlinearities in the system which complicate for the use of linear MPC controllers synthesis. To compensate for the nonlinearity, a parameter scheduling technique, as presented in Chapter 2.5, the inverse of the Hill curve (Equation 2.6), is implemented in the controller with the nominal patient model parameters as shown in Figure 3.14; f is using the nonlinearity parameter of the real patient (E_0 , E_{max}, EC_{50} , γ), while f^{-1} is using the parameter assumed by the controller (the nominal patient nonlinear parameters a priori known E_0^{mean}, E_{max}^{mean}, EC_{50}^{mean} , γ^{mean}). The controller then aims at controlling the estimated drug concentration $\hat{C}_e$ using a linear controller.

3.3.1 Simultaneous mp-MHE and mp-MPC formulation

Using the explicit/multiparametric MPC formulation described Appendix D, the control strategy is based on the nonlinearity compensation and the state space model of the PK-PD linear part for the nominal patient model. The following mp-QP optimization problem is solved to obtain the control laws using the POP toolbox (Pistikopoulos et al., 1999) and determine the controller.

$$\begin{aligned}
\min_u J = {} & \hat{x}^T{}_N P \hat{x}_N + \sum_{k=1}^{N-1} x_k Q_k x_k + \sum_{k=1}^{N-1} (y_k - y_k^R)^T QR_k (y_k - y_k^R) + \\
& + \sum_{k=0}^{N_u-1} (u_k - u^R)^T R_k (u_k - u^R) + \sum_{k=0}^{N_u-1} \Delta u_k R1_k \Delta u_k \\
s.t. \quad & \mathrm{x}_{t+1} = Ax_t + Bu_t + Gw_t \\
& \mathrm{y}_t = Cx_t + v_t \\
& \mathrm{BIS}_{\min} \le y \le BIS_{\max} \\
& \mathrm{u}_{\min} \le u \le u_{\max} \\
& \mathrm{w}_{\min} \le w \le w_{\max} \\
& \mathrm{v}_{\min} \le v \le v_{\max} \\
& x_t \in X \subseteq \Re^p, u_t \in U \subseteq \Re^s, w_t \in W, v_t \in V
\end{aligned} \qquad \text{(Equation 3.2)}$$

where $\hat{x}$ are the estimated states given by the state estimator, y outputs and u controls, w are the process disturbances and v the measurement noise all (discrete) time dependent vectors. The subsets of output variables that get tracked have time-dependent set points y^R. Finally, Δu are changes in control variables, $\Delta u(k) = u(k) - u(k-1)$. The prediction horizon is denoted by N and control horizon by N_u. X, U are the sets of the state and input constraints that contain the origin in their interior. Both $Q \succ 0$, the objective coefficient for the states and $P \succ 0$, the terminal weight matrix for the states, are positive definite diagonal matrices. The weight matrix for manipulated variables $R \succ 0$ is a positive definite diagonal matrix, QR is the weight matrix for tracked outputs and $R1$ is a weight matrix for the control action changes (Δu).

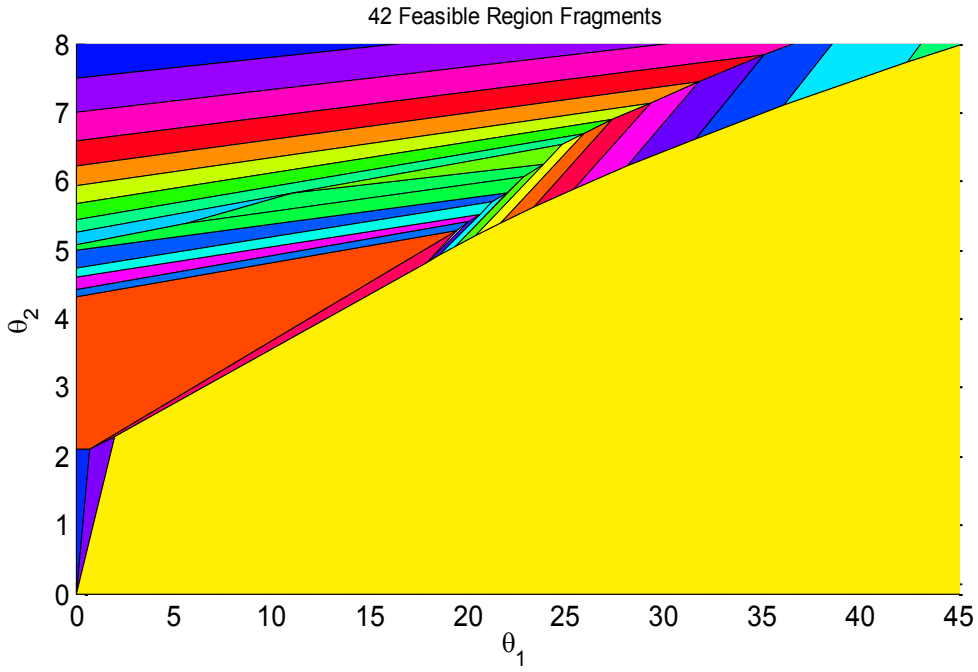

Figure 3.15: Map of critical regions - mp-MPC

For the design of the controller, the following tunning parameters are used: the objective coefficients for states (x), Q=0 when we have no state estimation and Q=1 in the case with state estimation, the weight matrix for tracked outputs (y), QR=1000, weight matrix for manipulated variables (u), R=1, the control horizon $N_u=1$ and the prediction horizon $N=20$. The states used in the design of the controllers are C_1, C_2, C_3, C_e as described in (Equation 2.1) and (Equation 2.4). The clinically recommended sampling time is of 5 seconds (Ionescu et al., 2008). N and N_u are chosen based on the characteristics of the process and the desired performances. Based on (Clarke et al., 1987, Mohtadi et al., 1987) N should be large, at least $2n-1$ but no larger than the rise-time of the process. For anaesthesia due to medical procedures we are constrained to use a small sampling time that will lead to a choice of a greater value for N. In choosing N_u, for processes with no unstable/underdamped poles, like anaesthesia, $Nu=1$ is generally satisfactory. A choice of the Q, R and QR is given by Bryson's rule (Franklin et al., 2001c).

Figure 3.15 presents a typical solution of the multiparametric programming problem in the form of 2-dimensional projection of the critical space. The parametric vector θ

consists of: the estimated states, the current time output and the output reference (*BIS=50*). Here θ_1 and θ_2 represent the concentration of the effect site compartment, C_e and the BIS index.

3.4 Results

In this section, the results of a simulation study to evaluate the three controllers for the administration of Propofol are presented. The three controller are: (i) the nominal controller that uses no state estimation, (ii) the simultaneous mp-MPC and Kalman filter and (iii) the simultaneous mp-MPC and mp-MHE. DOA is monitored using the BIS index during the induction and maintenance phase of general anaesthesia. The closed loop control sets are performed on a set of 12 patients plus an extra patient (Table 2.1) representing the nominal values of all 12 patients. The designed controllers are tested both under the assumption that the output of the system is not influenced by noise and with the output corrupted by noise and disturbances.

The simulations are performed first for the set of data presented in Table 1 so as to have a better understanding of their behaviour on different types of patients, and analyse the inter- and intra- patient variability. Next, the three controllers are tested against each other and simulated for different patients to be able to compare their performances by means of BIS and the corresponding Propofol infusion rates.

3.4.1 Induction Phase

Ideally the induction phase of the patient in an operational DOA is performed as fast as possible, so that little time is lost before the surgeon can start operating. It is therefore desirable that the patient reaches the BIS=50 target fast and remains within the target value without much undershoot or overshoot, i.e., values below BIS=40 and above BIS=60 should be avoided.

Figure 3.16 - Figure 3.21 present the simulations of the nominal controller and the two simultaneous mp-MPC and estimaton in the induction phase. Simulations of some patients show very small oscillations around the steady-state values. The average settling time for the designed controller is: (i) 280 seconds for nominal controller, (ii) 240 seconds for the simultaneous mp-MPC and Kalman filter and 225 seconds for the simultaneous mp-MPC and mp-MHE. The best performance is obtained for the simultaneous mp-MPC and mp-MHE. The mp-MHE is able to deal better with the inter- and intra- patient variability.

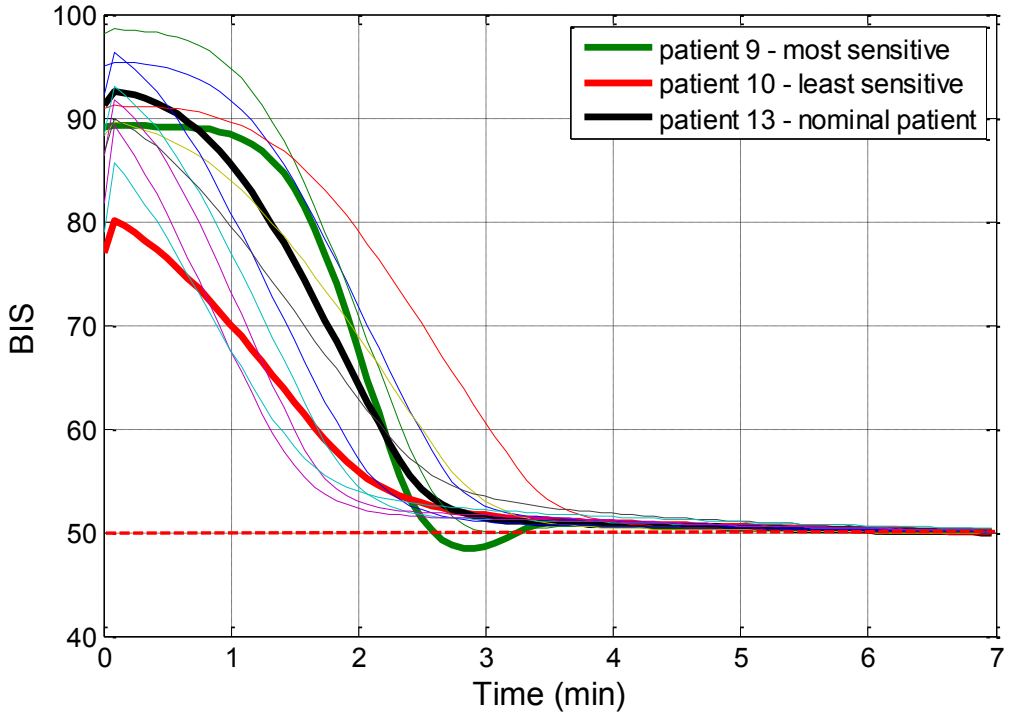

Figure 3.16: BIS response for all 13 patients in the induction phase – nominal mp-MPC

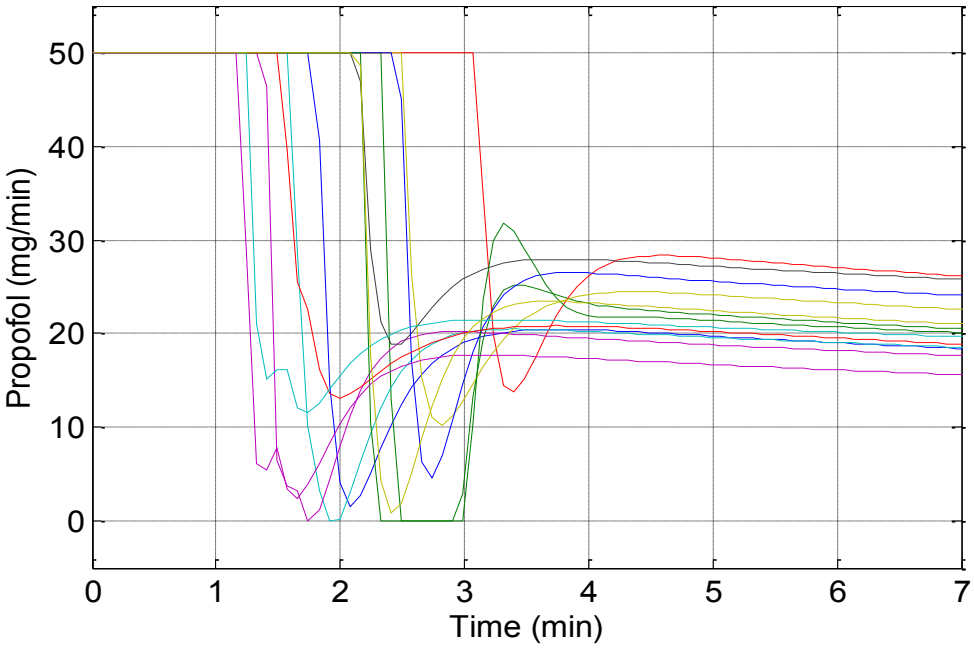

Figure 3.17: Propofol infusion rate for all 13 patients in the induction phase – nominal mp-MPC

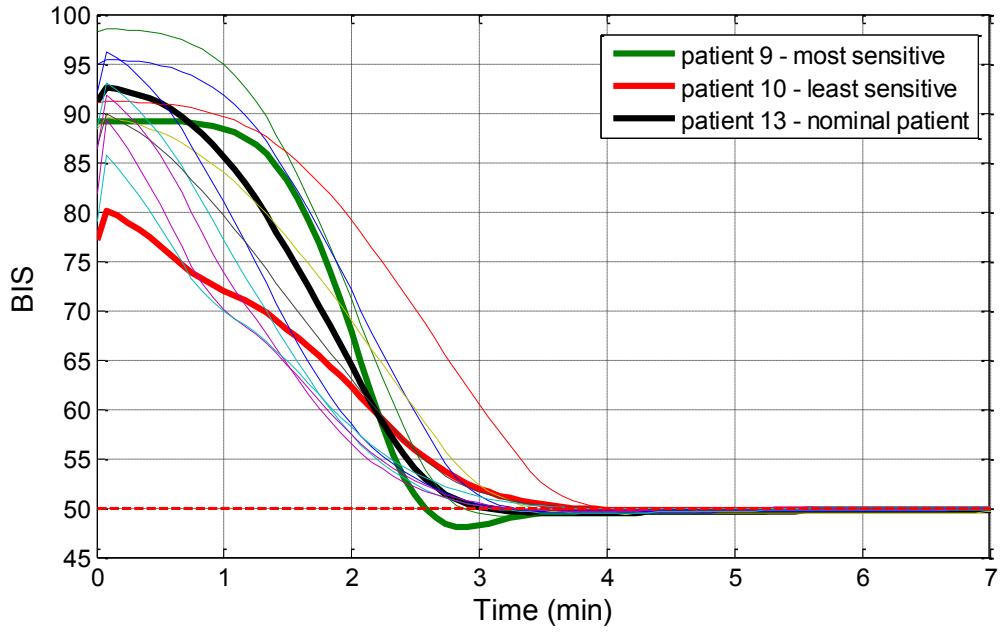

Figure 3.18: BIS response for all 13 patients in the induction phase – simultaneous mp-MPC and Kalman filter

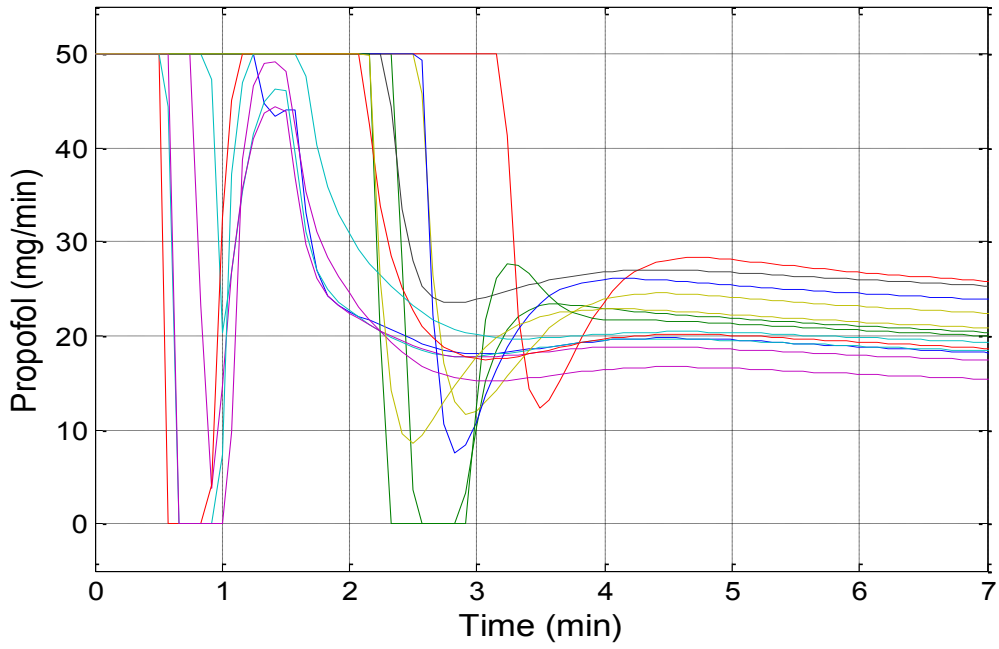

Figure 3.19: Propofol infusion rate for all 13 patients in the induction phase – simultaneous mp-MPC and Kalman filter

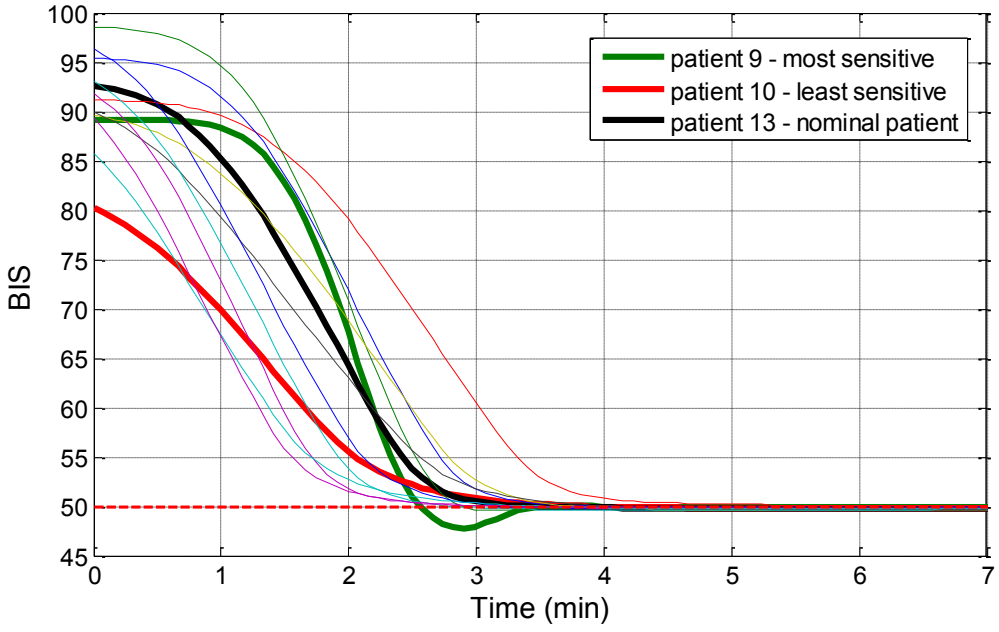

Figure 3.20: BIS response for all 13 patients in the induction phase – simultaneous mp-MPC and mp-MHE

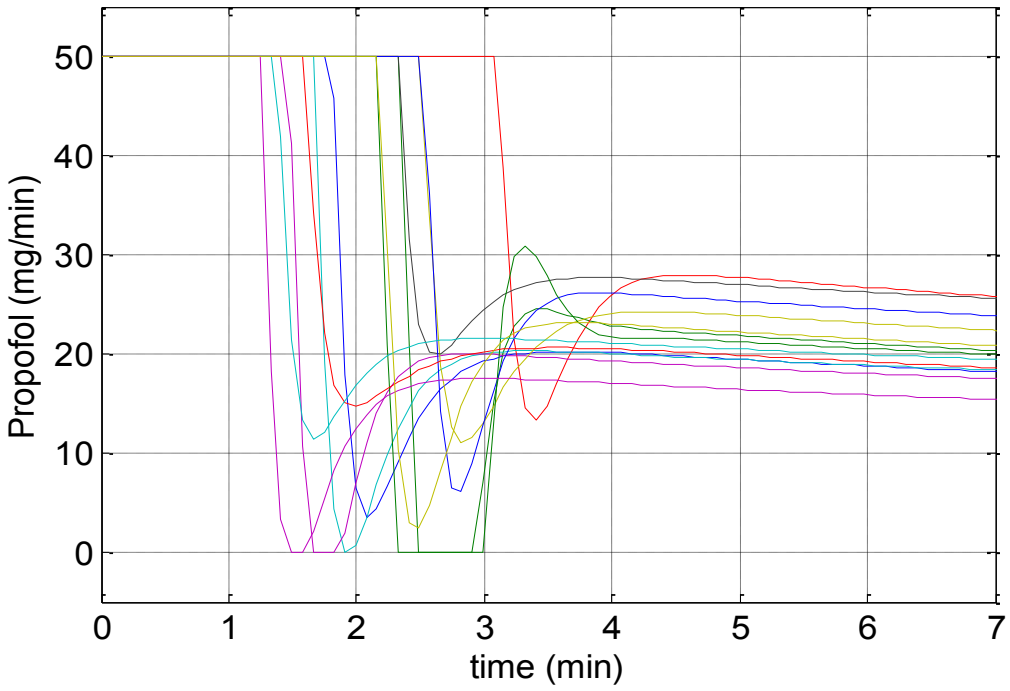

Figure 3.21: Propofol infusion rate for all 13 patients in the induction phase – simultaneous mp-MHE and mp-MPC

The designed controllers are tested for two different patients, patient 4 and patient 9 (patient 9 represents the most sensitive patient). Figure 3.22, Figure 3.23, Figure 3.25 and Figure 3.26 represent the BIS response of the 2 patients while Figure 3.24 and Figure 3.27 show the corresponding control action (drug infusion). It can be observed that all three controllers exhibit similar performances with a settling time of 200 seconds. Note that for all simulations we have: (i) with blue the mp-MPC without state estimation, (ii) with black the simultaneous mp-MPC and Kalman filter, (iii) with magenta the simultaneous mp-MPC and mp-MHE and (iv) with red the setpoint for the BIS index. From Figure 3.23 and Figure 3.26 where we have a zoom in on the BIS response of the three controllers we can observe that the undershoot of the most sensitive patient is of 2.2%. For the undershoot the worst case is considered meaning the most sensitive patient (patient 9). Also the simultaneous Kalman filter and mp-MPC as well as mp-MHE and mp-MPC have similar performances for this case where we have no noise corrupting the output. However, the simultaneous mp-MHE and mp-MPC has slightly better

performance for both patients since it is able to give better estimates of the states of the patients (see Section 3.2.2).

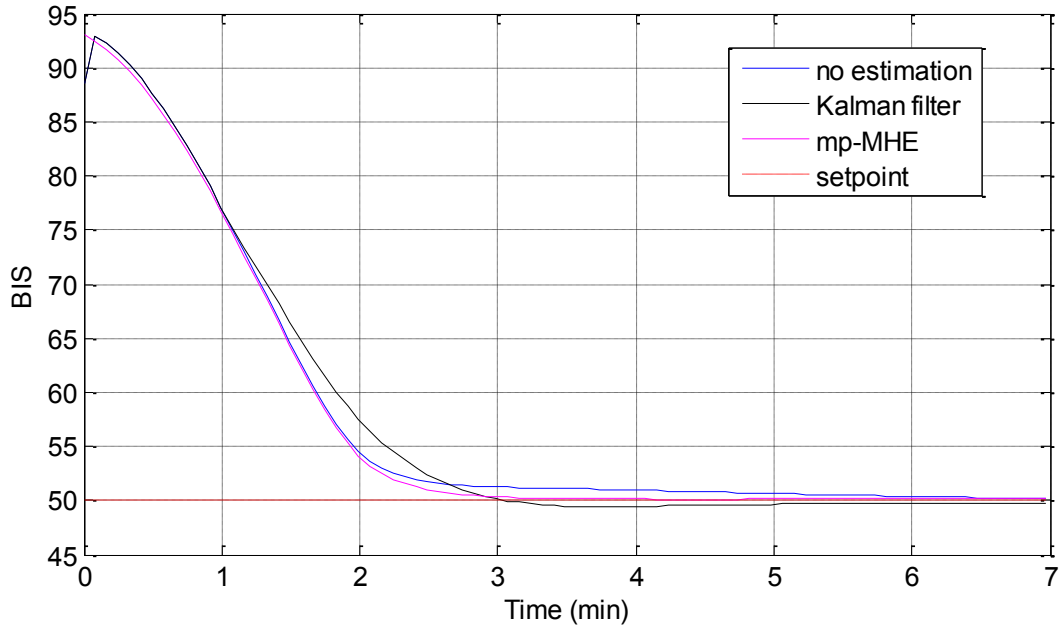

Figure 3.22: BIS response of the three controllers for patient 4 in the induction phase without noise

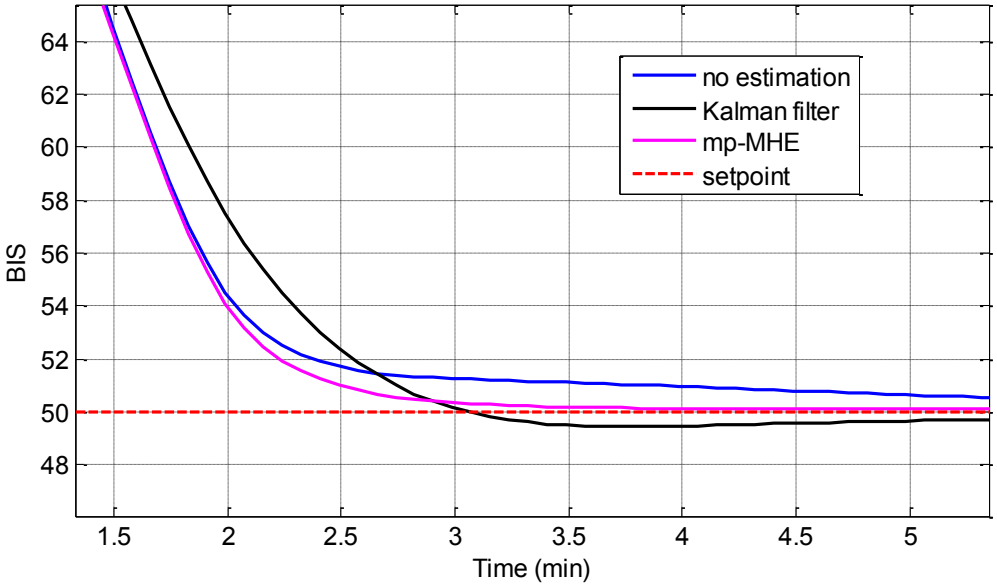

Figure 3.23: BIS response of the three controllers for patient 4 in the induction phase without noise – zoom in

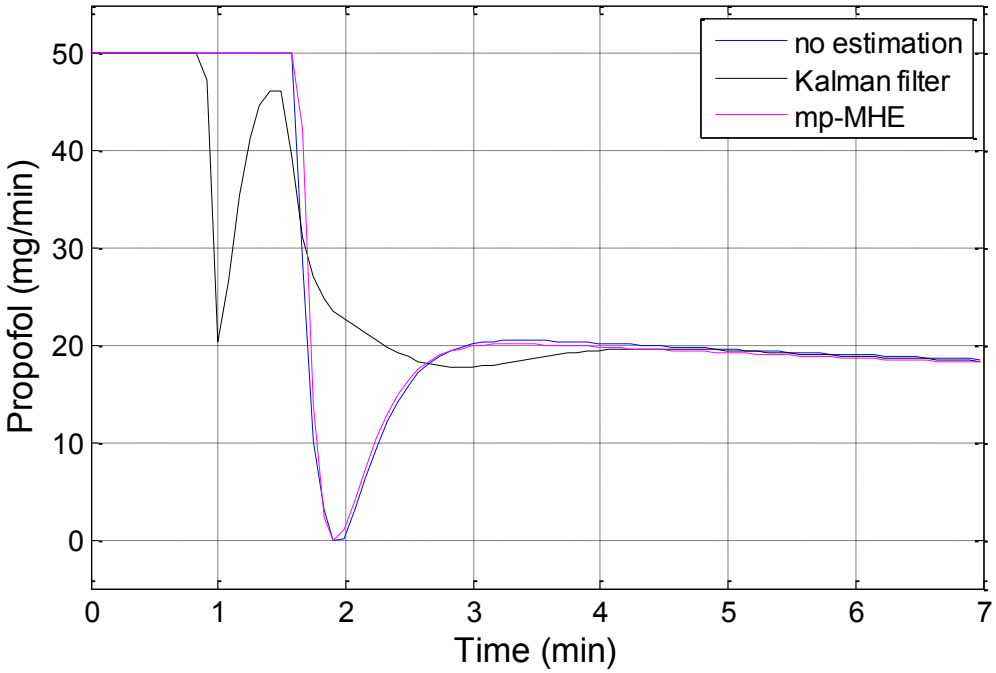

Figure 3.24: Propofol infusion rate of the three controllers for patient 4 in the induction phase without noise

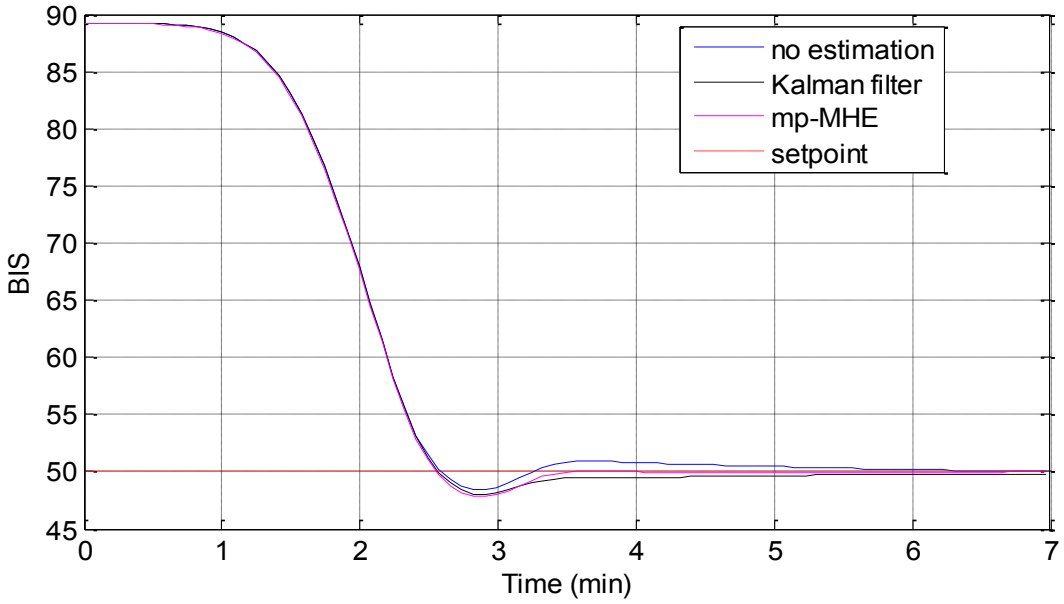

Figure 3.25: BIS response of the three controllers for patient 9 in the induction phase without noise

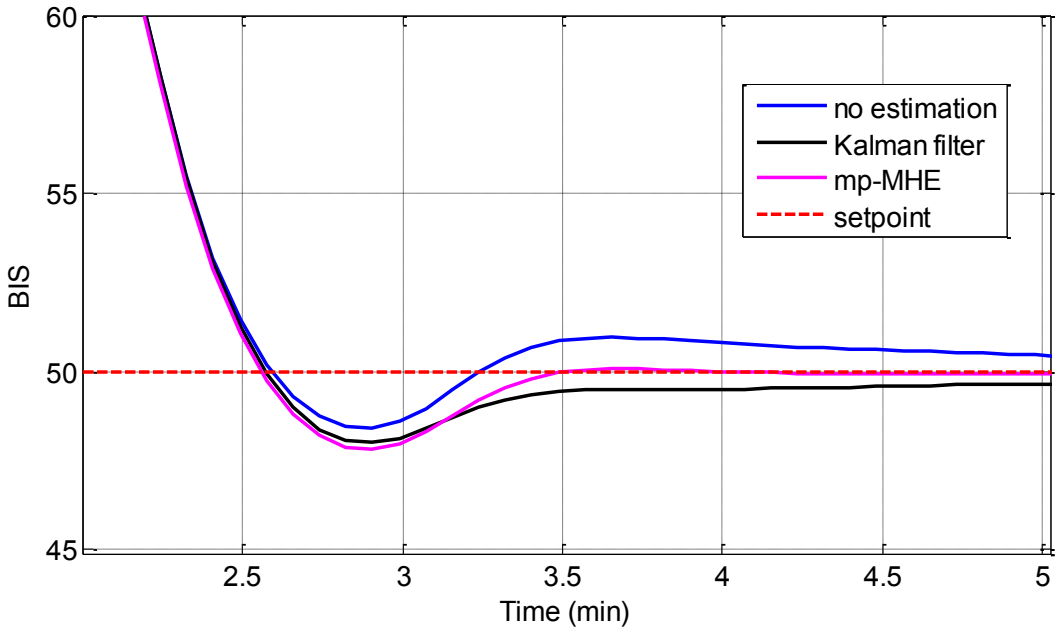

Figure 3.26: BIS response of the three controllers for patient 9 in the induction phase without noise – zoom in

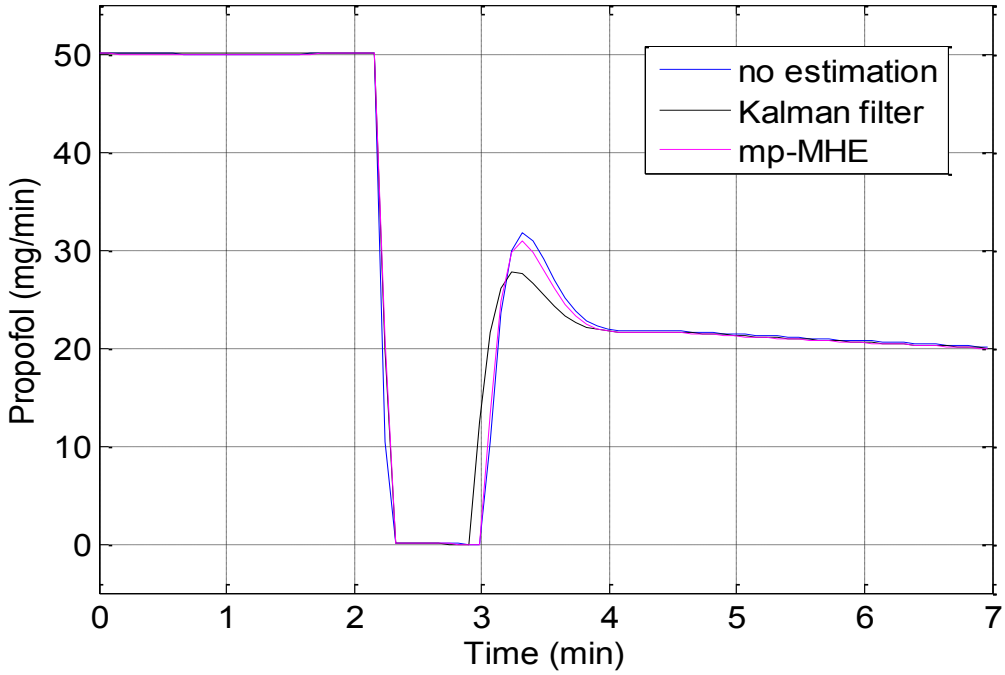

Figure 3.27: Propofol infusion rate of the three controllers for patient 9 in the induction phase without noise

The optimal control action of the simultaneous mp-MPC and mp-MHE is presented in Table 3.1, along with the corresponding closed loop simulation control action for the nominal patient and patient 9 (Figure 3.28). Although both patients are in the induction phase, due to the inter- patient variability, different critical regions of the multiparametric controller i.e., control laws provide the optimal control action at each time step for the two patients.

Table 3.1: Simultaneous mp-MHE and mp-MPC optimal control action for Patient 9 and the nominal Patient

Step time	Patient 9 (control action)	Nominal Patient (control action)
T=1	$CR_{T=1} = 356$ $u_{opt}^{T=1} = 0$	$CR_{T=1} = 301$ $u_{opt}^{T=1} = -6.3382x_1 - 0.1001x_2 - 0.5335x_3 + 7.7653x_e - 39.6582y + 39.6582y_{sp}$
T=2	$CR_{T=2} = 356$ $u_{opt}^{T=2} = 0$	$CR_{T=2} = 301$ $u_{opt}^{T=2} = -6.3382x_1 - 0.1001x_2 - 0.5335x_3 + 7.7653x_e - 39.6582y + 39.6582y_{sp}$
T=3	$CR_{T=3} = 301$ $u_{opt}^{T=3} = -6.3382x_1 - 0.1001x_2 - 0.5335x_3 + 7.7653x_e - 39.6582y + 39.6582y_{sp}$	$CR_{T=3} = 301$ $u_{opt}^{T=3} = -6.3382x_1 - 0.1001x_2 - 0.5335x_3 + 7.7653x_e - 39.6582y + 39.6582y_{sp}$
T=4	$CR_{T=4} = 301$ $u_{opt}^{T=4} = -6.3382x_1 - 0.1001x_2 - 0.5335x_3 + 7.7653x_e - 39.6582y + 39.6582y_{sp}$	$CR_{T=4} = 301$ $u_{opt}^{T=4} = -6.3382x_1 - 0.1001x_2 - 0.5335x_3 + 7.7653x_e - 39.6582y + 39.6582y_{sp}$
T=5	$CR_{T=5} = 301$ $u_{opt}^{T=5} = -6.3382x_1 - 0.1001x_2 - 0.5335x_3 + 7.7653x_e - 39.6582y + 39.6582y_{sp}$	$CR_{T=5} = 301$ $u_{opt}^{T=5} = -6.3382x_1 - 0.1001x_2 - 0.5335x_3 + 7.7653x_e - 39.6582y + 39.6582y_{sp}$

T=6	$CR_{T=6} = 301$ $u_{opt}^{T=6} = -6.3382x_1 - 0.1001x_2 - 0.5335x_3 +$ $+ 7.7653x_e - 39.6582y + 39.6582y_{sp}$	$CR_{T=6} = 301$ $u_{opt}^{T=6} = -6.3382x_1 - 0.1001x_2 - 0.5335x_3 +$ $+ 7.7653x_e - 39.6582y + 39.6582y_{sp}$
T=7	$CR_{T=7} = 301$ $u_{opt}^{T=7} = -6.3382x_1 - 0.1001x_2 - 0.5335x_3 +$ $+ 7.7653x_e - 39.6582y + 39.6582y_{sp}$	$CR_{T=7} = 301$ $u_{opt}^{T=7} = -6.3382x_1 - 0.1001x_2 - 0.5335x_3 +$ $+ 7.7653\theta_e - 39.6582y + 39.6582y_{sp}$

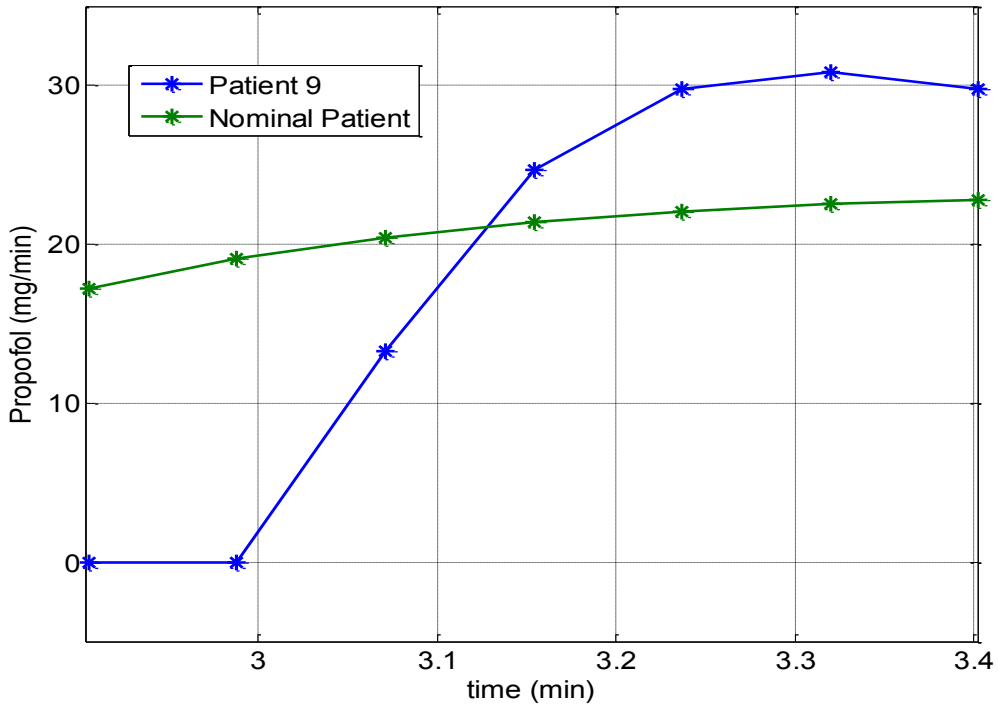

Figure 3.28:Optimal control action for Patient 9 and the nominal patient

As presented in Chapter 1.1 the measured BIS index is strongly influenced by process noise and disturbances (due to sensors, EMG interfering with the EEG, etc.). Therefore, noise will be added on the output and the three different controllers will be tested on the

set of patients from Table 2.1. The results are presented for two of the patients, patient 4 and the most sensitive patient, patient 9. Figure 3.29, Figure 3.30, Figure 3.32 and Figure 3.33 present the BIS output for the simulated patients while Figure 3.31 and Figure 3.34 depict the corresponding control action. It can be observed that the simulations exhibit a similar settling time as the case where there is no noise, around 200 seconds. In this case, due to the noise on the output we observe that the simultaneous mp-MHE and mp-MPC has significantly better performances then the controller that uses no estimation and the simultaneous Kalman filter and mp-MPC. For patient 4 the undershoot for the mp-MPC using no estimation is of 5.4%, the simultaneous Kalman filter and mp-MPC is of 3.6% and the simultaneous mp-MHE and mp-MPC has an undershoot of under 0.7% which can be considered as insignificant. For patient 9, representing the worst case scenario by being the most sensitive patient we have an undershoot of 5.9% for the mp-MPC without estimation, 4% for the simultaneous Kalman filter and mp-MPC and only 2.2% for the simultaneous mp-MHE and mp-MPC. Moreover, the better performances of the simultaneous mp-MHE and mp-MPC are justified due to the fact that the MHE is able to deal with noise and system constraints. The performances of the three controllers can be better observed in Figure 3.30 and Figure 3.33 where we have a zoom in on the most significant part of the simulation.

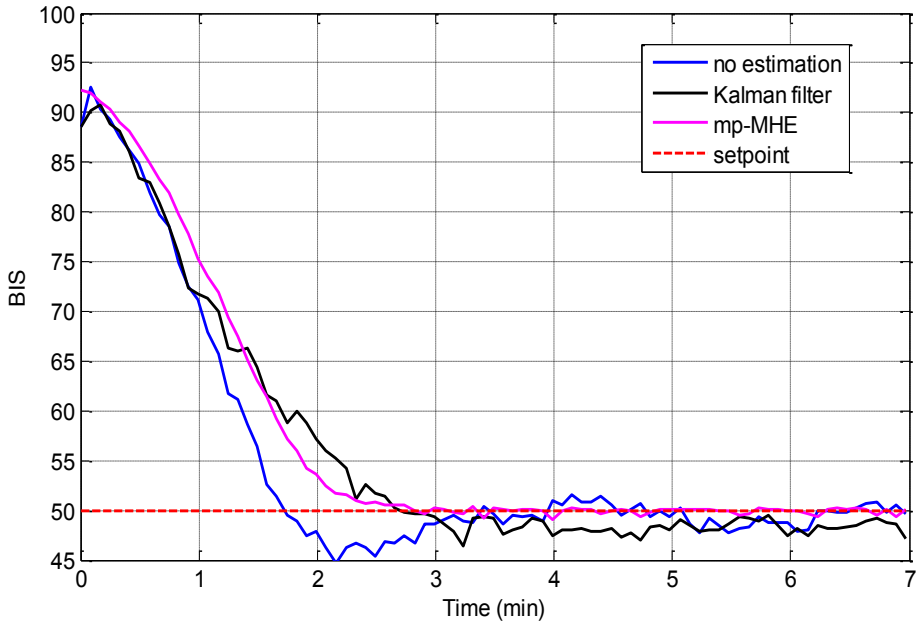

Figure 3.29: BIS response of the three controllers for patient 4 in the induction phase with noise

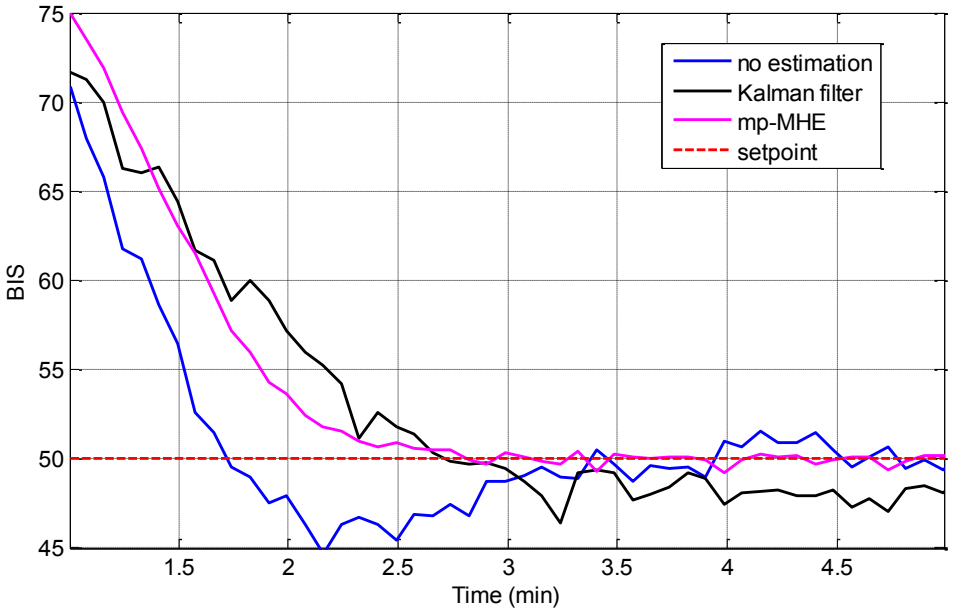

Figure 3.30: BIS response of the three controllers for patient 4 in the induction phase with noise – zoom in

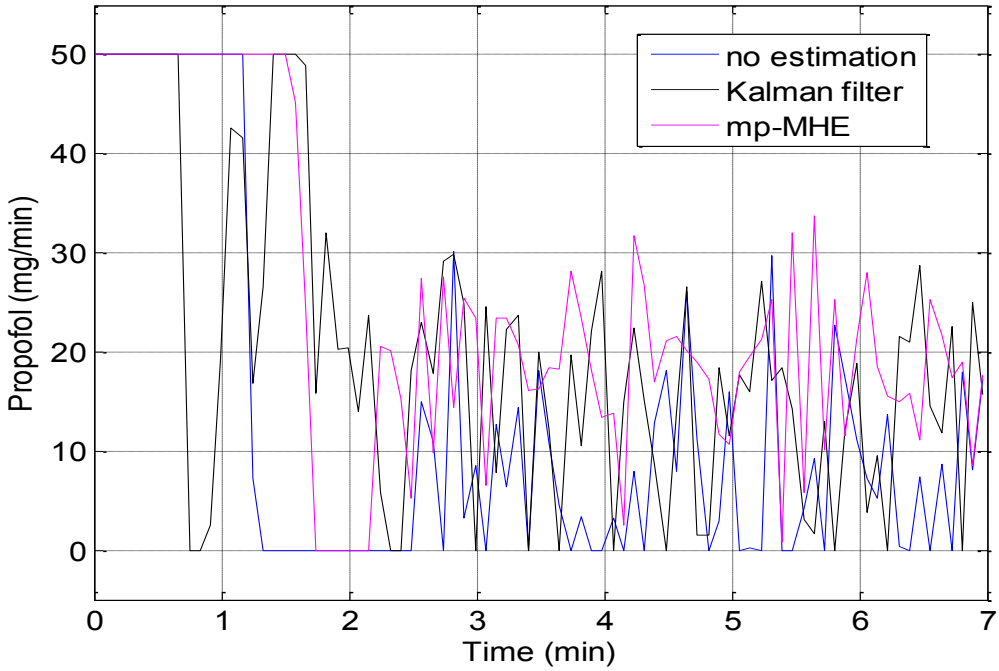

Figure 3.31: Propofol infusion rate of the three controllers for patient 4 in the induction phase with noise

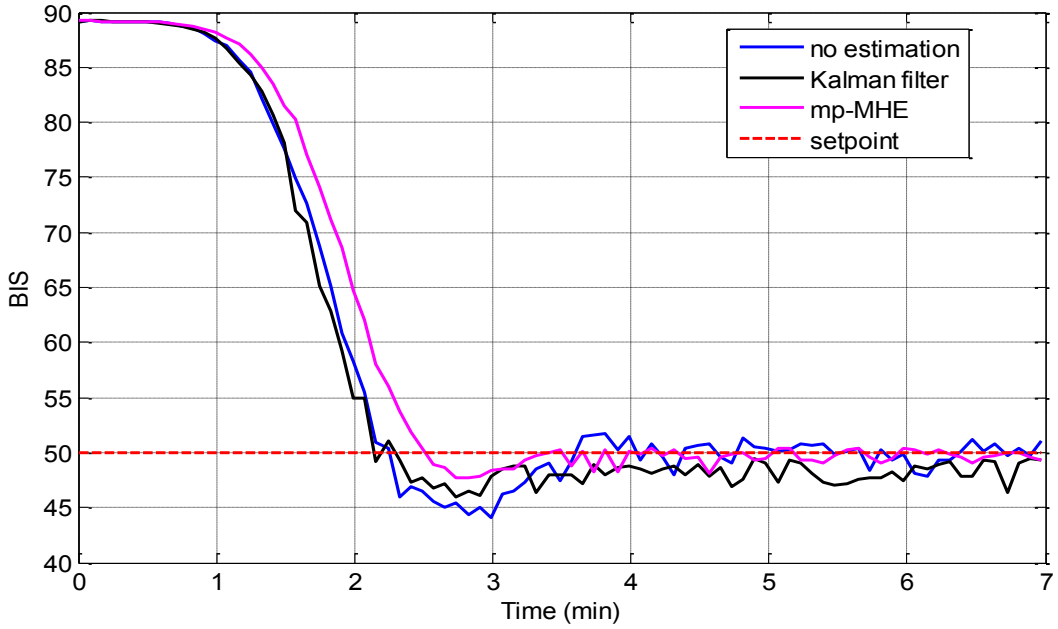

Figure 3.32: BIS response of the three controllers for patient 9 in the induction phase with noise

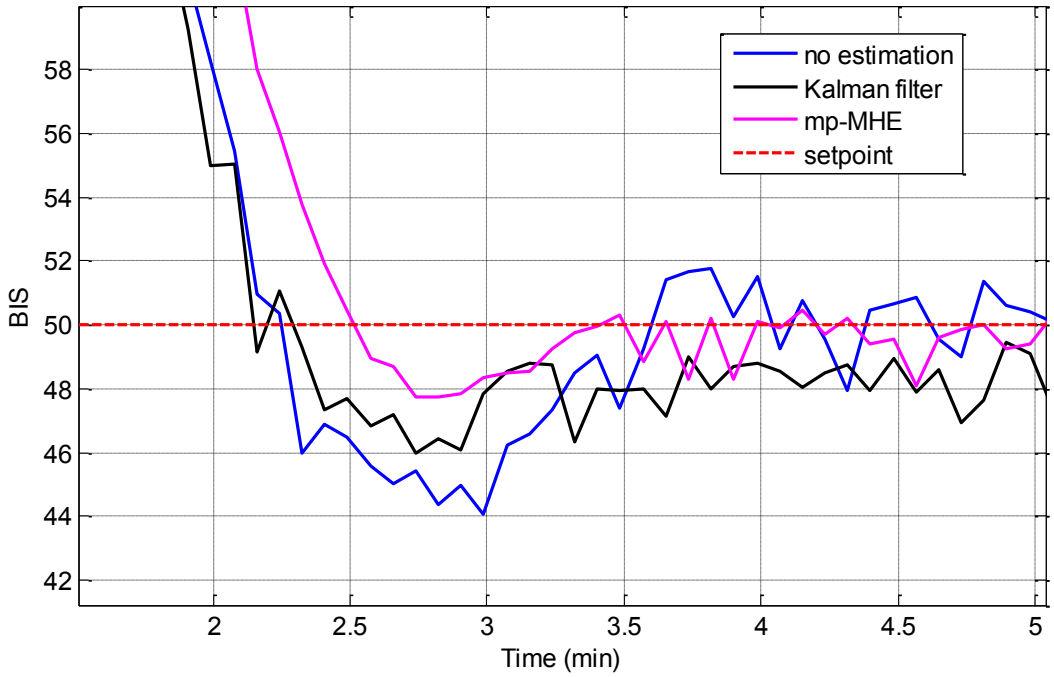

Figure 3.33: BIS response of the three controllers for patient 9 in the induction phase with noise – zoom in

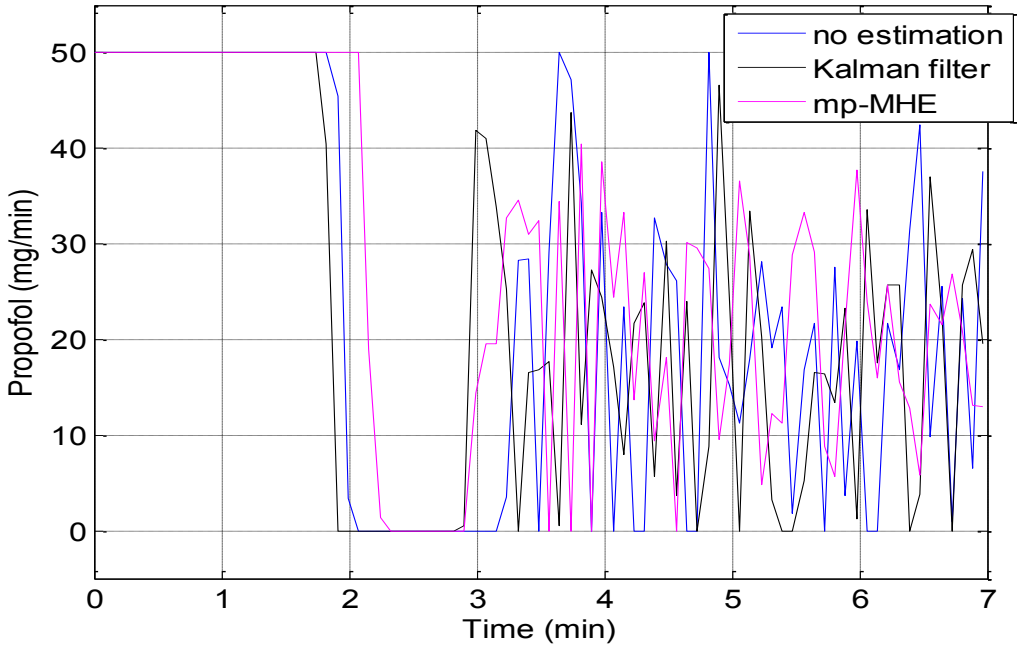

Figure 3.34: Propofol infusion rate of the three controllers for patient 9 in the induction phase with noise

For an in depth understanding of the need of using state estimation simultaneous with mp-MPC the controllers have been tested comparatively (also with a mp-MPC using no estimation) both under the assumption that the output is noise free and corrupted by noise. It can be observed that (i) the controllers provides maximum amount of drug infusion in order to drive the output to the desired setpoint value; (ii) as soon as the setpoint value is reached, the controller focuses on ensuring that over- and under- shoot of the system is avoided until reaching steady state; (iii) for the case where the output is strongly influenced by noise, the controllers exhibit satisfactory performances, especially fast settling time and avoids any significant undershoot/overshoot; (iv) the controller using mp-MHE estimation exhibits better overall performance, especially in the case where the output is noisy, with no significant undershoot and a settling time of 200 seconds.

3.4.2 Maintenance Phase

During the maintenance phase, it is important that the controller rejects the disturbances occurred during surgery as fast as possible and bring the patient to the BIS target value. In this phase, typical disturbances can be applied additively to the output of the process to check the controller's ability to reject them (West et al., 2013). A standard stimulus profile is defined and is presented in Figure 3.35. Each interval denotes a specific event in the operation theatre. Stimulus A represents response to intubation; B a surgical incision that is followed by a period of no surgical stimulation i.e., waiting for pathology result; C mimics an abrupt stimulus after a period of low level stimulation; D the onset of a continuous normal surgical stimulation; E, F, and G simulate short-lasting, larger stimulation within the surgical period; and H represents the withdrawal of stimulation during the closing period (Yelneedi et al., 2009).

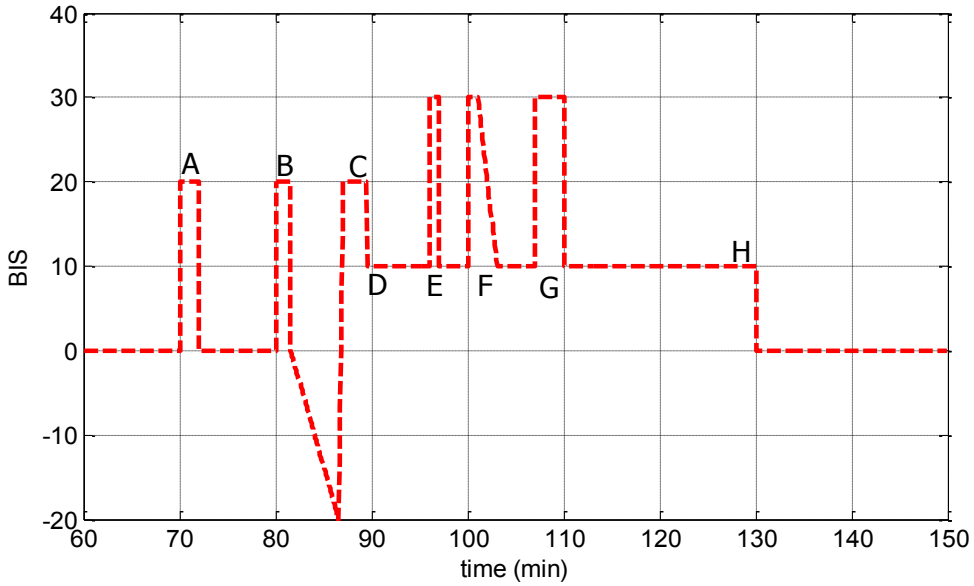

Figure 3.35: The artificially generated disturbance signal

In Figure 3.36 - Figure 3.41 we have the simulations of the three controllers and the nominal one in the maintenance phase. The controllers are tested for the whole set of patients in order to address the issue of inter- and intra- patient variability for each controller.

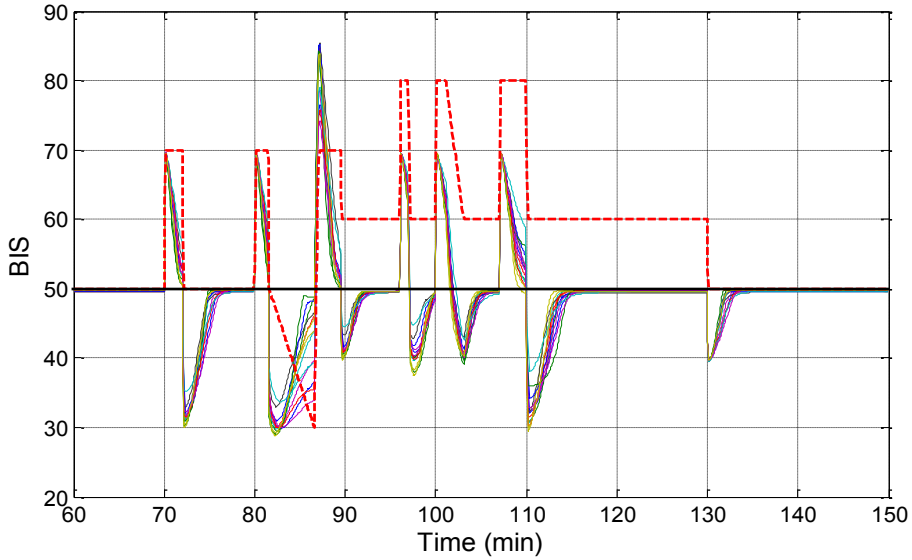

Figure 3.36: BIS response for all 13 patients in the maintenance phase – nominal mp-MPC

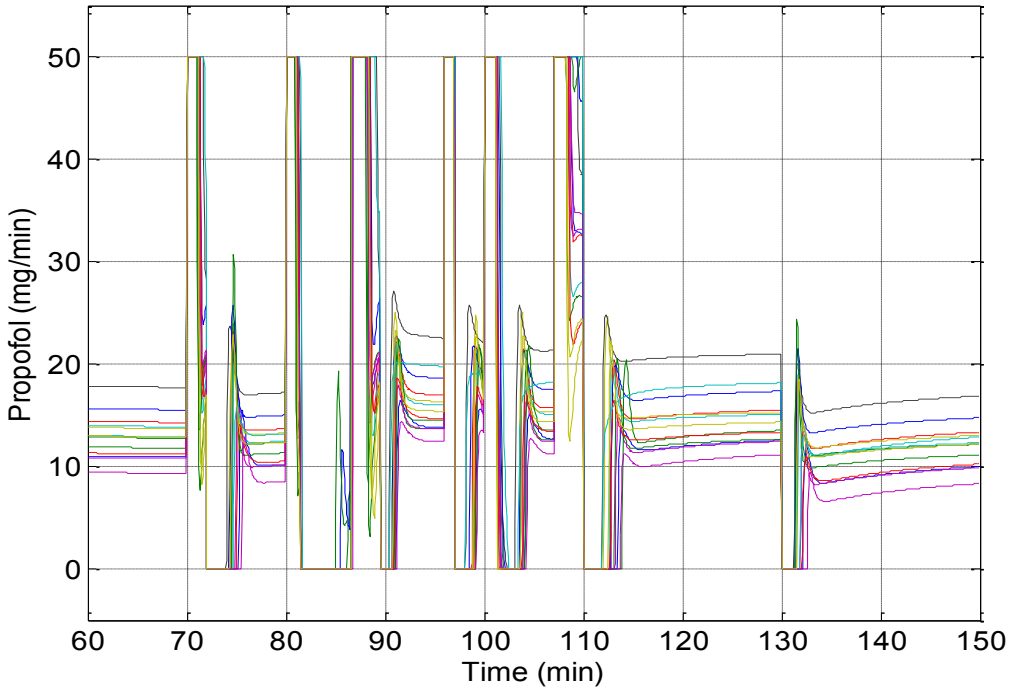

Figure 3.37: Propofol infusion rate for all 13 patients in the maintenance phase – nominal mp-MPC

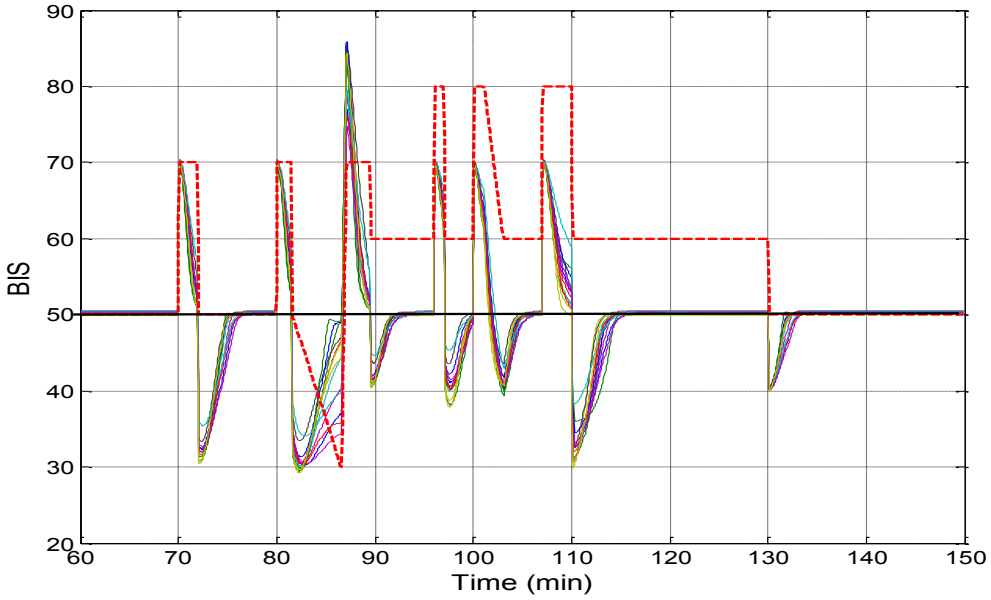

Figure 3.38: BIS response for all 13 patients in the maintenance phase – simultaneous mp-MPC and Kalman filter

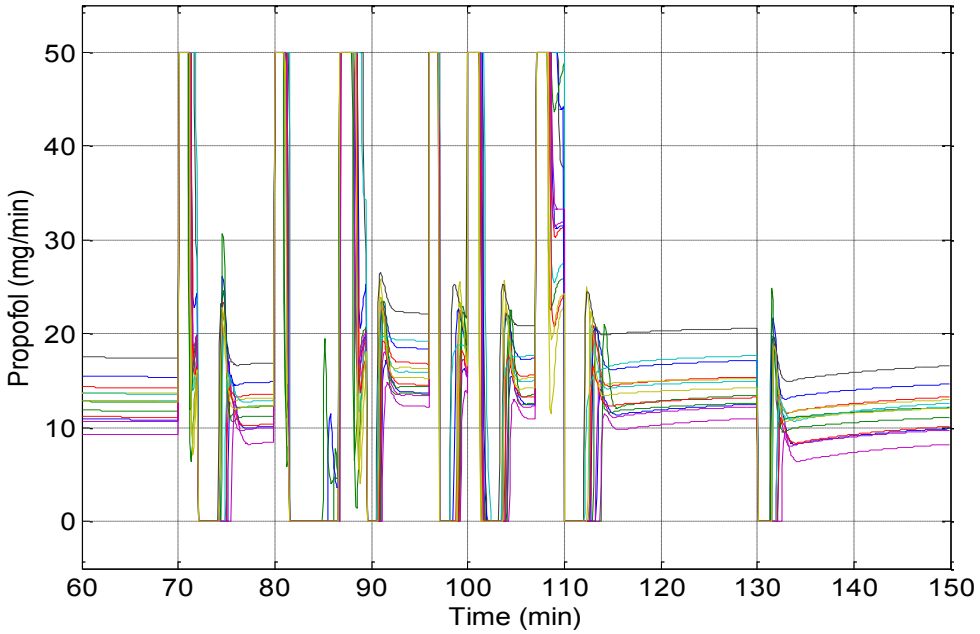

Figure 3.39: Propofol infusion rate for all 13 patients in the maintenance phase – simultaneous mp-MPC and Kalman filter

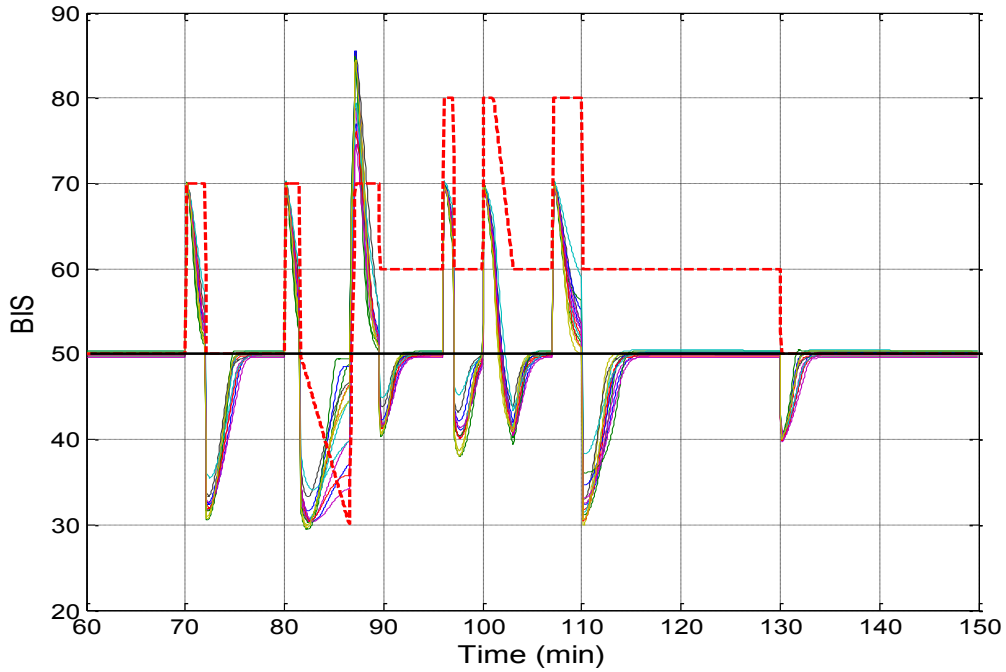

Figure 3.40: BIS response for all 13 patients in the maintenance phase – simultaneous mp-MPC and mp-MHE

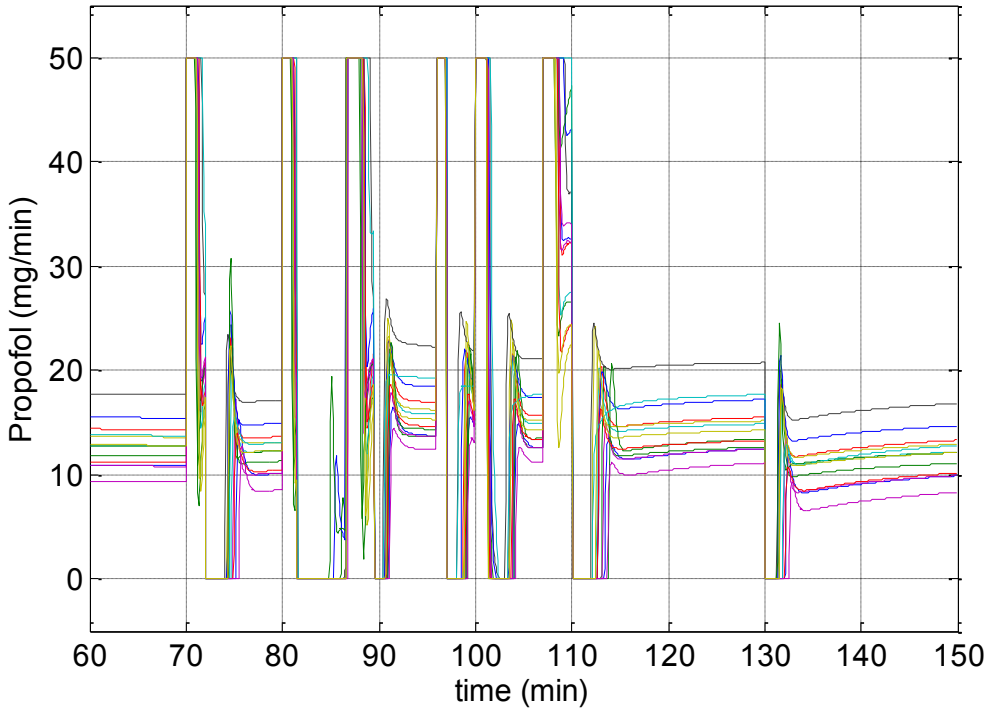

Figure 3.41: Propofol infusion rate for all 13 patients in the maintenance phase – simultaneous mp-MPC and mp-MHE

In Figure 3.42, Figure 3.43, Figure 3.46 and Figure 3.47, the performance of the disturbance rejection for patient 4 and the most sensitive patient (patient 9) are shown. Figure 3.44 and Figure 3.48 present the BIS response for the most challenging part of the disturbance rejection test, namely B-C-D-E while in Figure 3.45 and Figure 3.49 we have the corresponding Propofol infusion rate for patient 4 and patient 9. The simulations are performed for the maintenance phase using the disturbance signal (see Figure 3.35). The simulations show only small differences between the controllers. The controller using mp-MHE has a less aggressive behaviour, thus a smaller value for the undershoot.

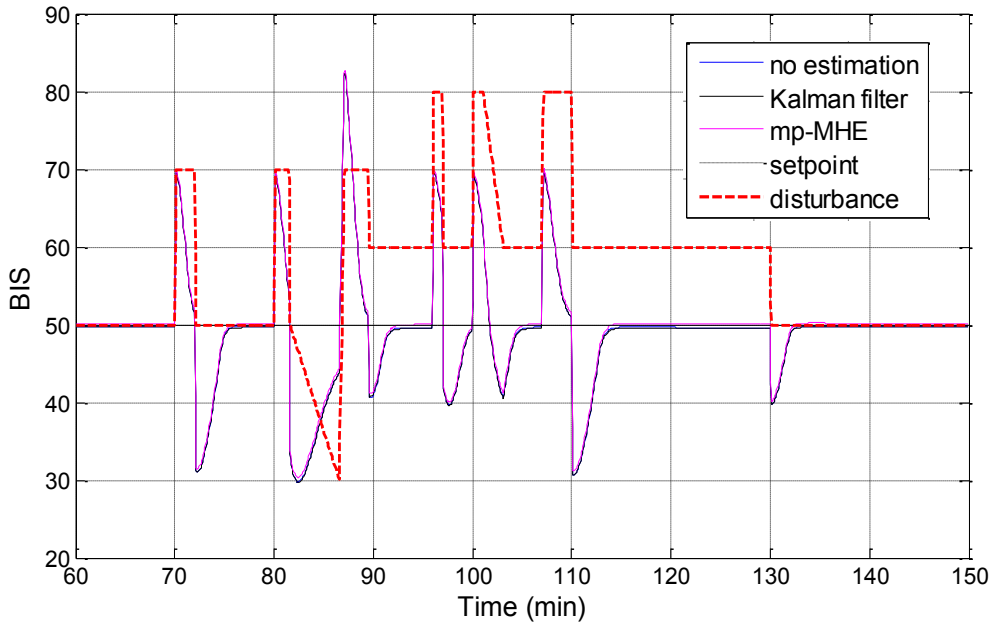

Figure 3.42: BIS response of the three controllers for patient 4 in the maintenance phase without noise

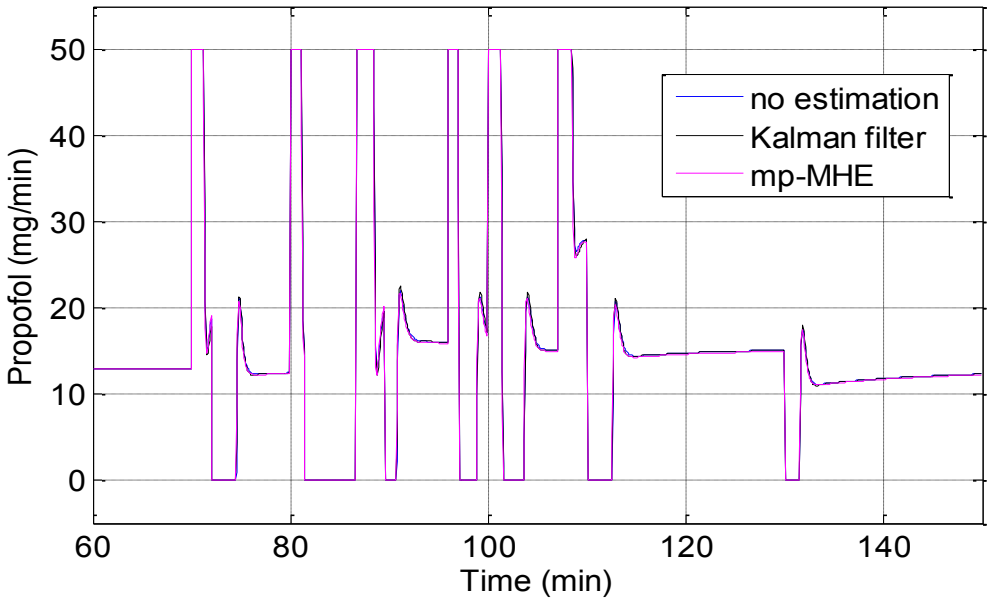

Figure 3.43: Propofol infusion rate of the three controllers for patient 4 in the maintenance phase without noise

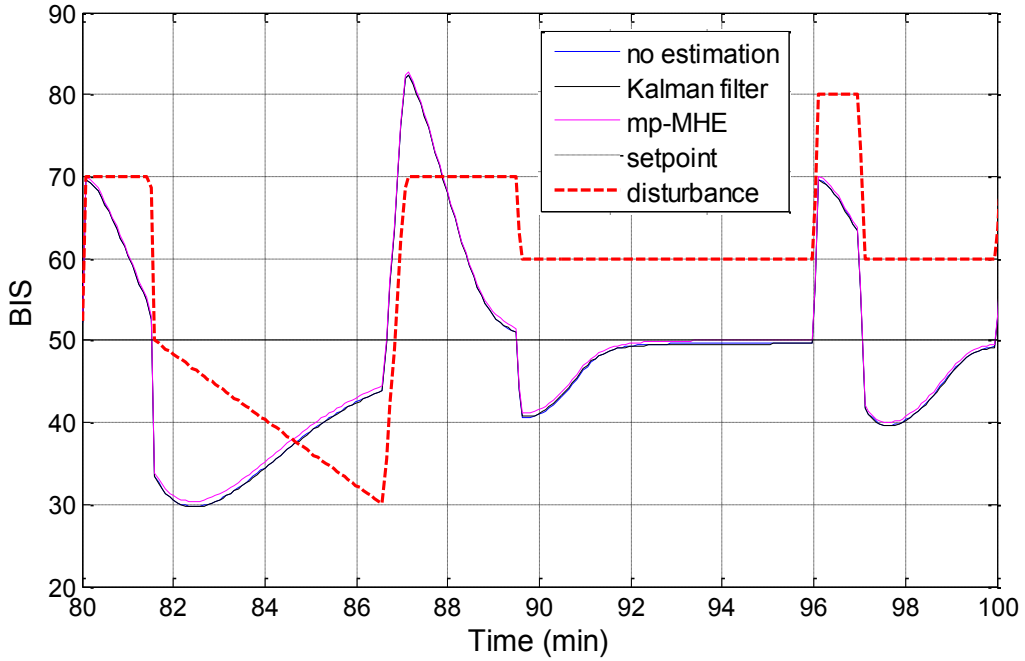

Figure 3.44: BIS response of the three controllers for patient 4 in the maintenance phase - B-C-D-E interval - without noise

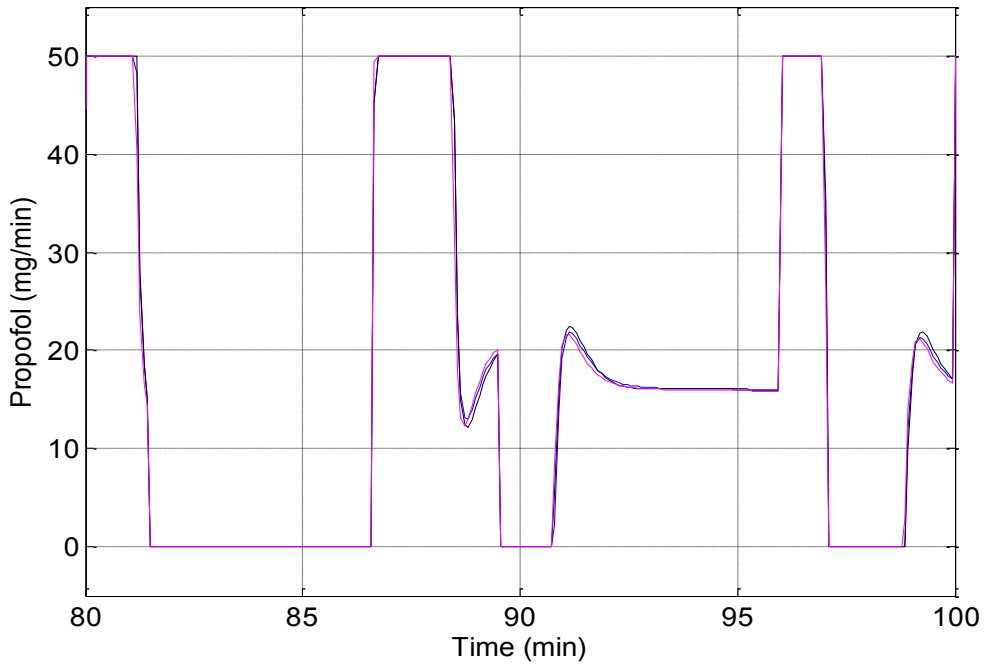

Figure 3.45: Propofol infusion rate of the three controllers for patient 4 in the maintenance phase - B-C-D-E interval - without noise

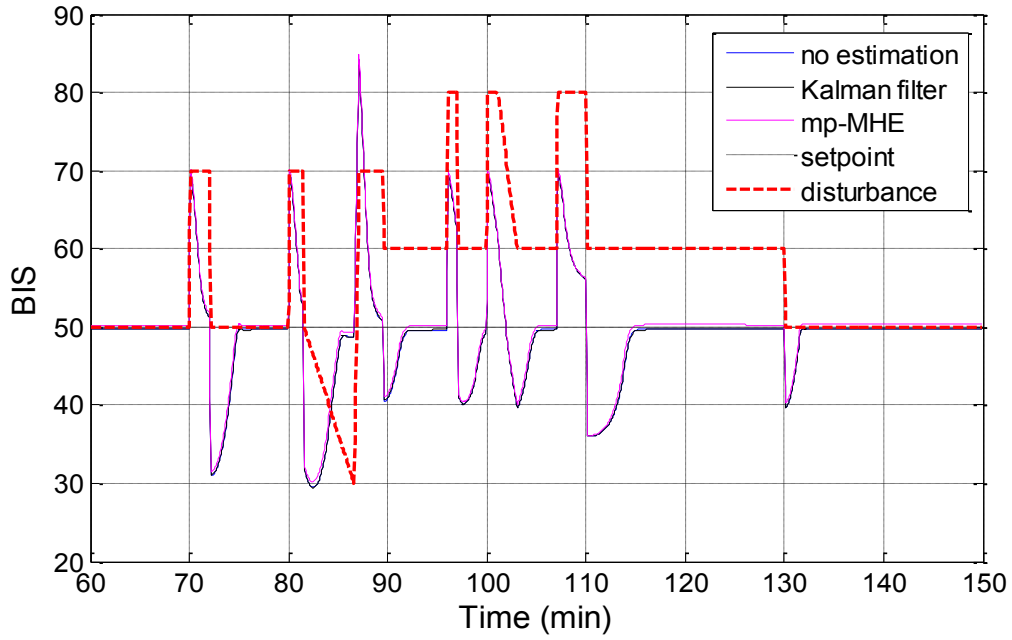

Figure 3.46: BIS response of the three controllers for patient 9 in the maintenance phase without noise

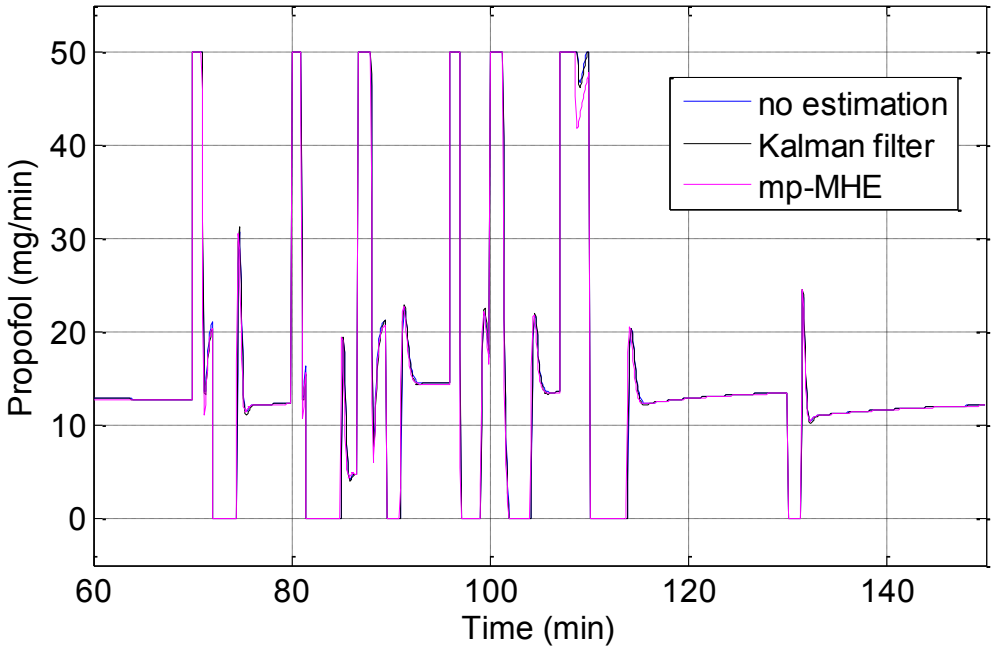

Figure 3.47: Propofol infusion rate of the three controllers for patient 9 in the maintenance phase without noise

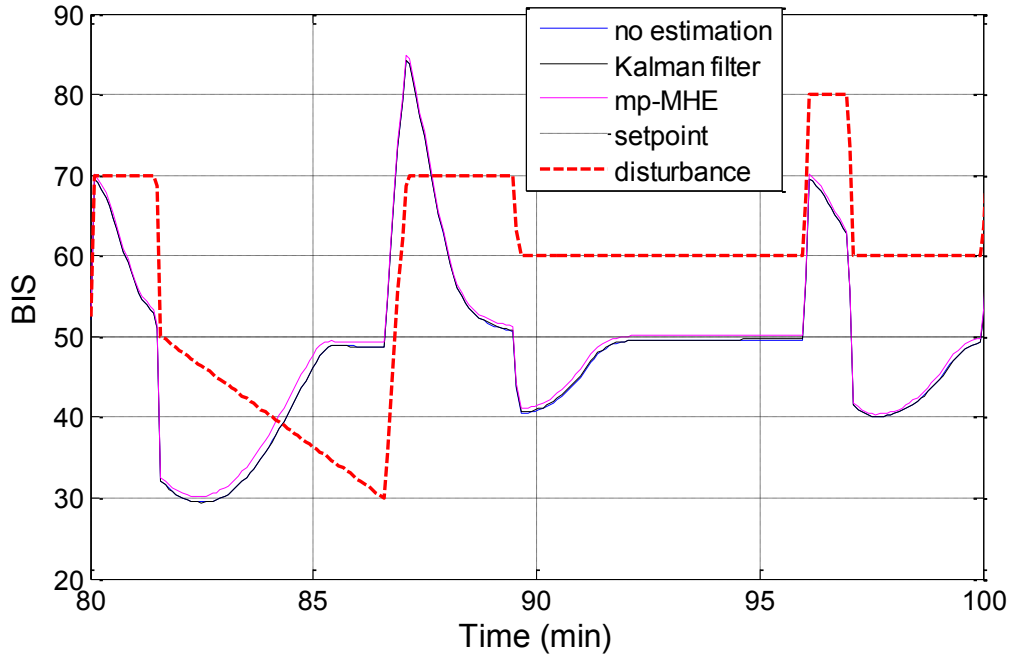

Figure 3.48: BIS response of the three controllers for patient 9 in the maintenance phase - B-C-D-E interval - without noise

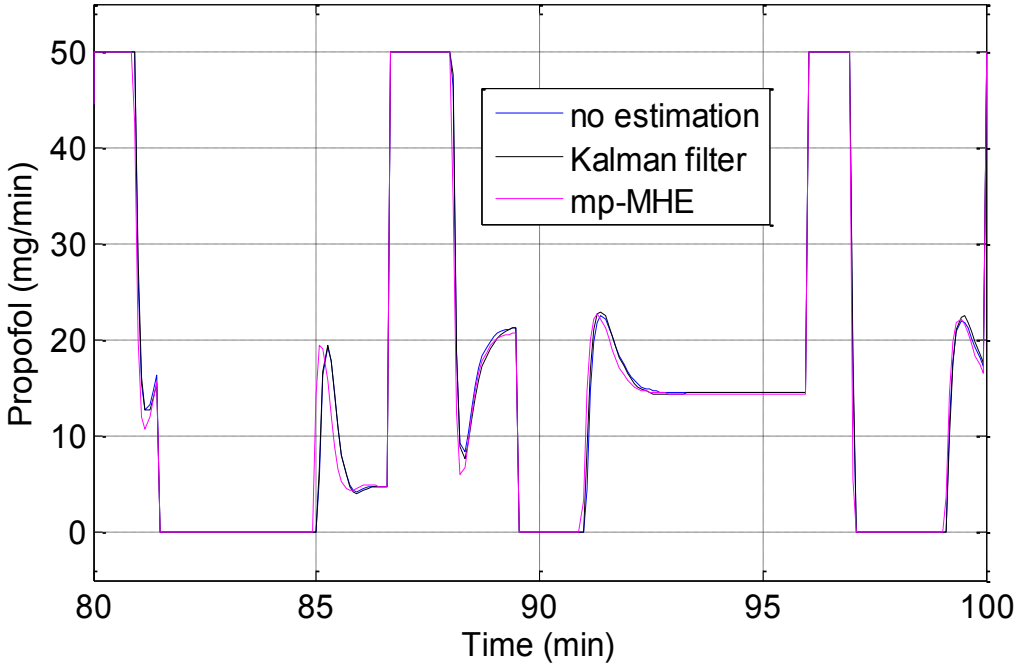

Figure 3.49: Propofol infusion rate of the three controllers for patient 9 in the maintenance phase - B-C-D-E interval - without noise

In Figure 3.50 - Figure 3.57 the three controllers are tested for the maintenance phase under the influence of noise (see Chapter1.1) for patient 4 and the most sensitive patient (patient 9). Figure 3.50 and Figure 3.54 depict the BIS output for the simulated patients for the whole disturbance signal while Figure 3.52 and Figure 3.56 depict the BIS output for the most challenging part of the disturbance signal (B-C-D-E). In Figure 3.51, Figure 3.53, Figure 3.55, and Figure 3.57 we have the corresponding Propofol infusion rates. It can be observed that under the influence of noise the best results are obtained for the controller using mp-MHE followed by the controller using the Kalman filter.

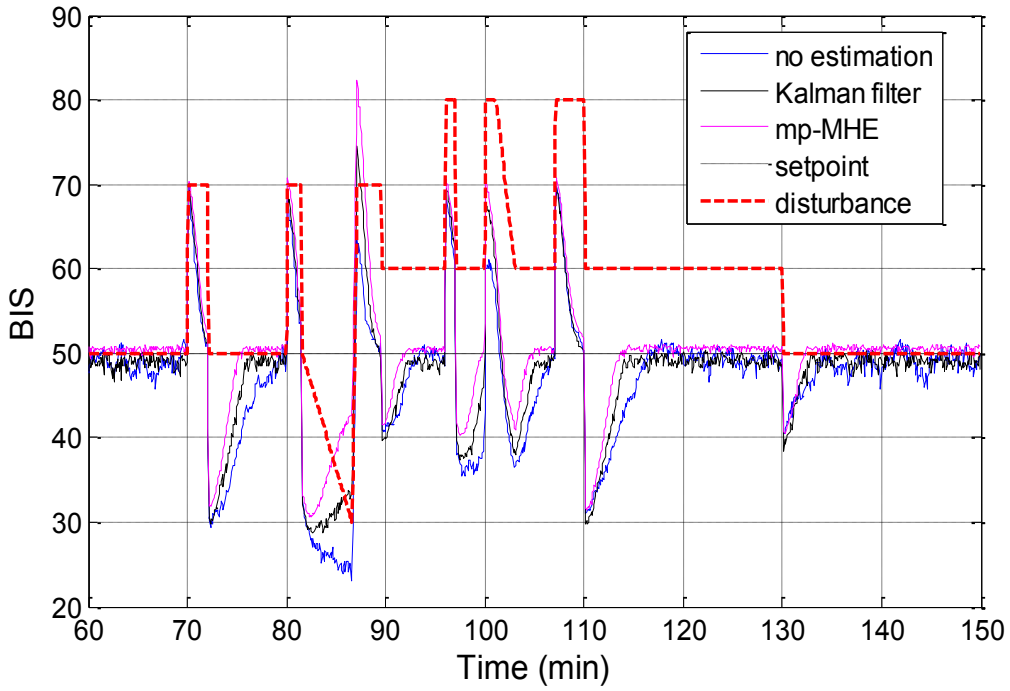

Figure 3.50: BIS response of the three controllers for patient 4 in the maintenance phase with noise

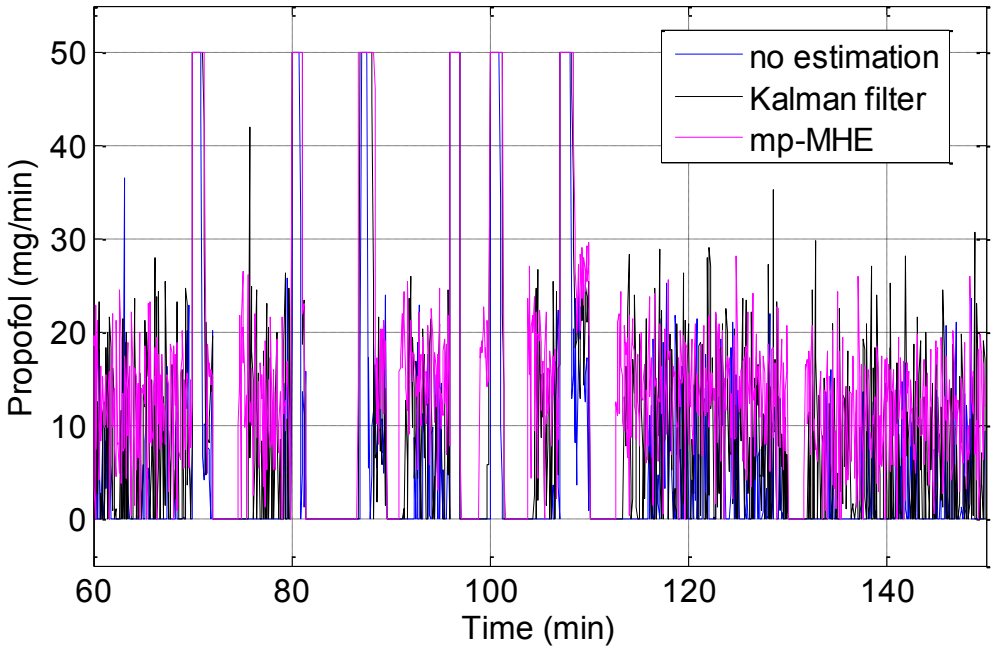

Figure 3.51: Propofol infusion rate of the three controllers for patient 4 in the maintenance phase with noise

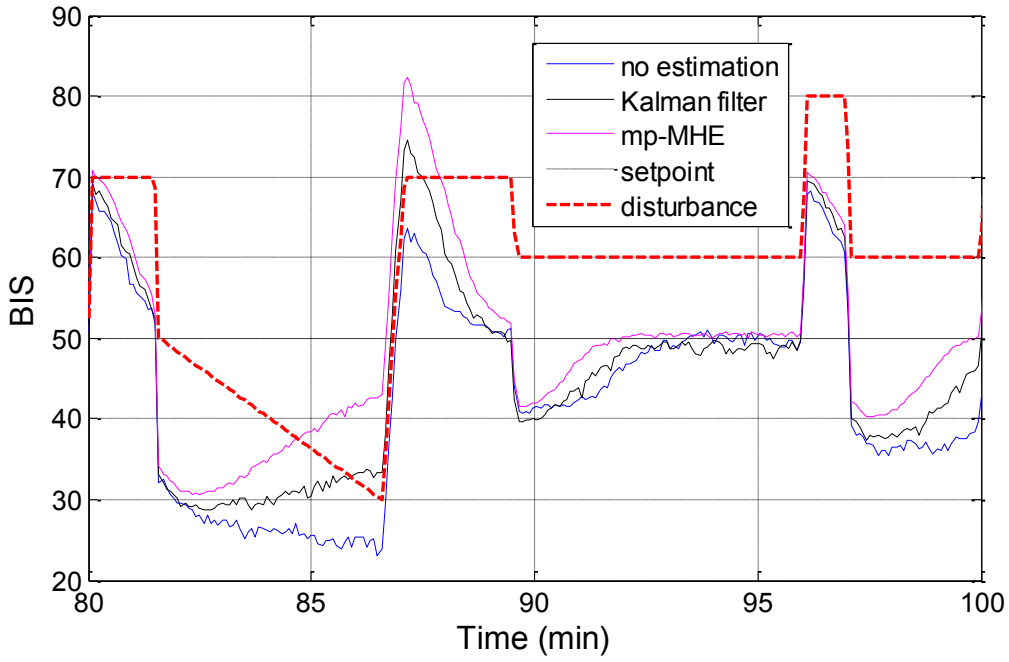

Figure 3.52: BIS response of the three controllers for patient 4 in the maintenance phase - B-C-D-E interval - without noise

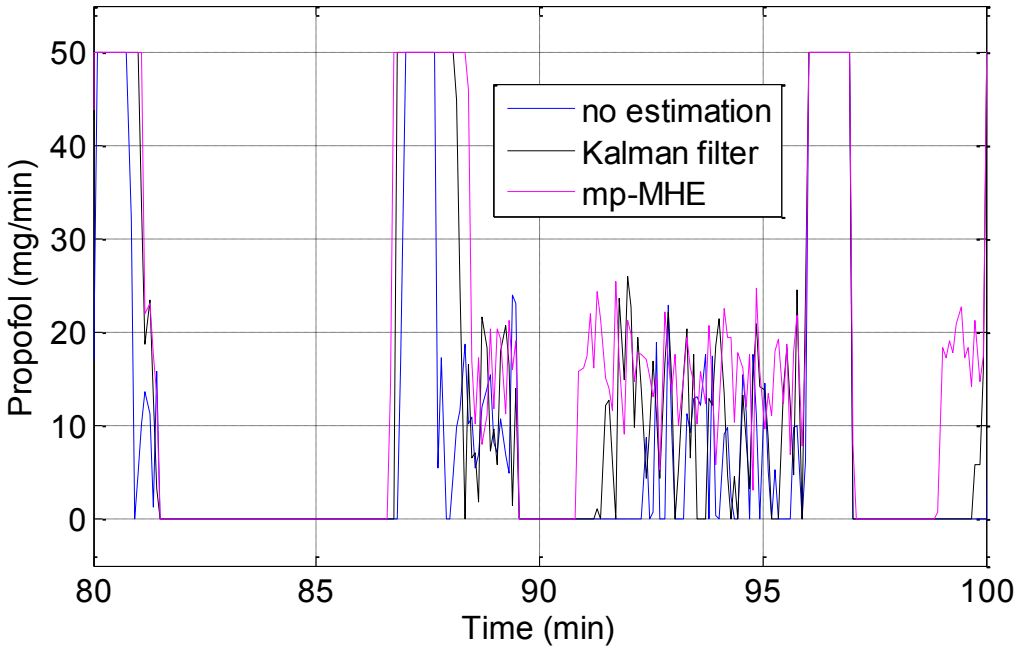

Figure 3.53: Propofol infusion rate of the three controllers for patient 4 in the maintenance phase - B-C-D-E interval - with noise

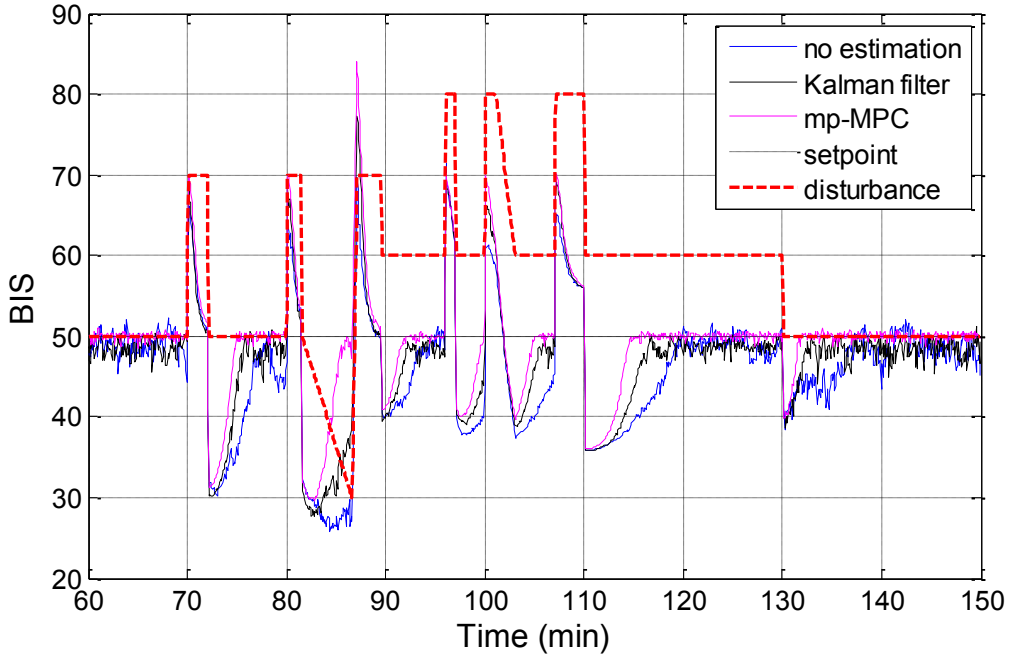

Figure 3.54: BIS response of the three controllers for patient 9 in the maintenance phase with noise

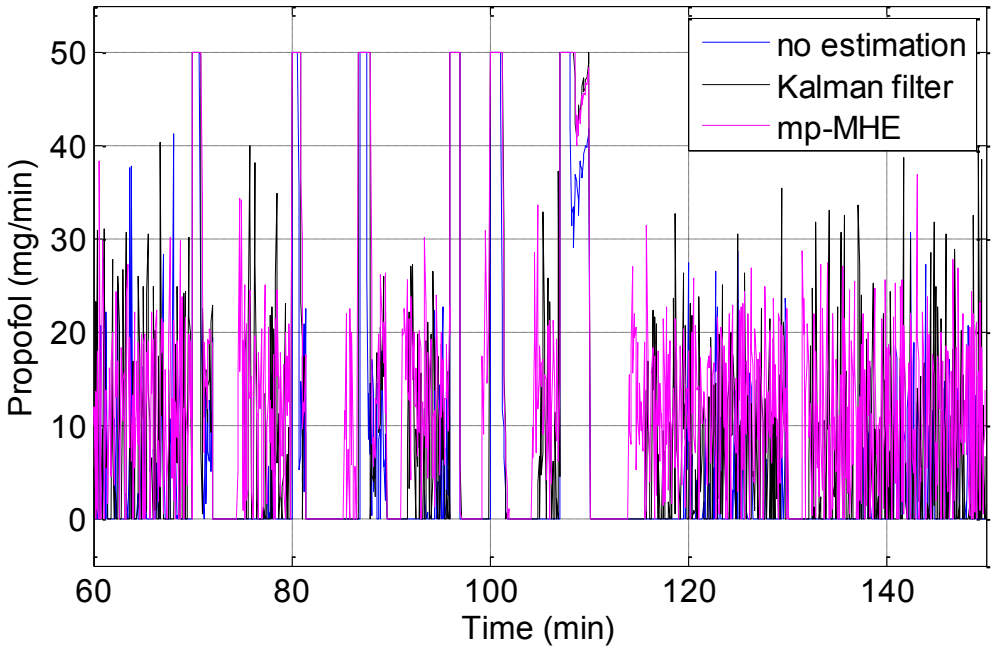

Figure 3.55: Propofol infusion rate of the three controllers for patient 9 in the maintenance phase with noise

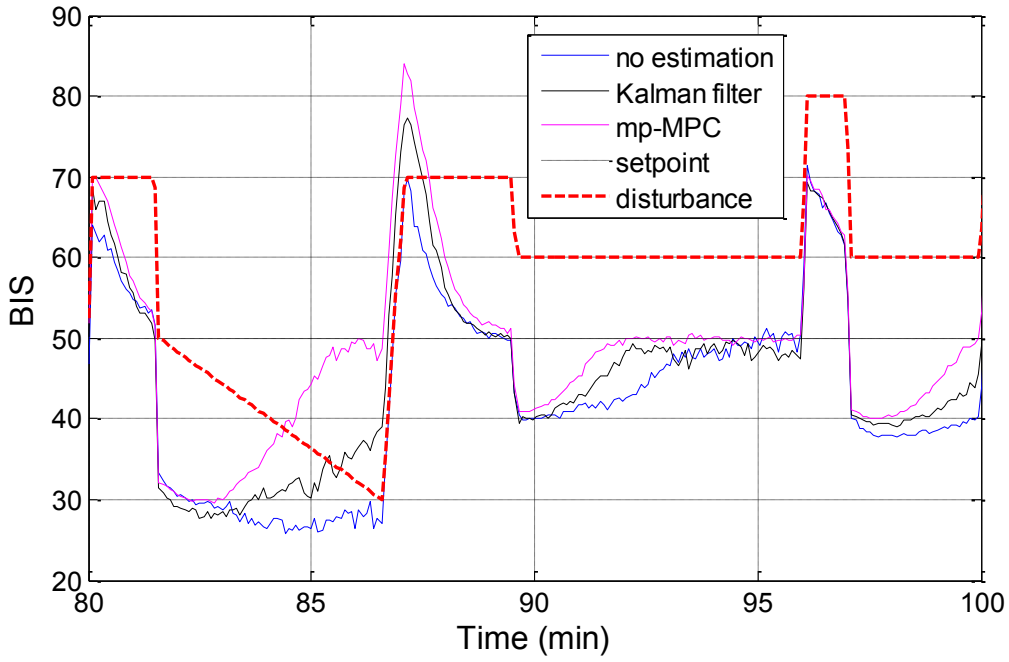

Figure 3.56: BIS response of the three controllers for patient 9 in the maintenance phase - B-C-D-E interval - without noise

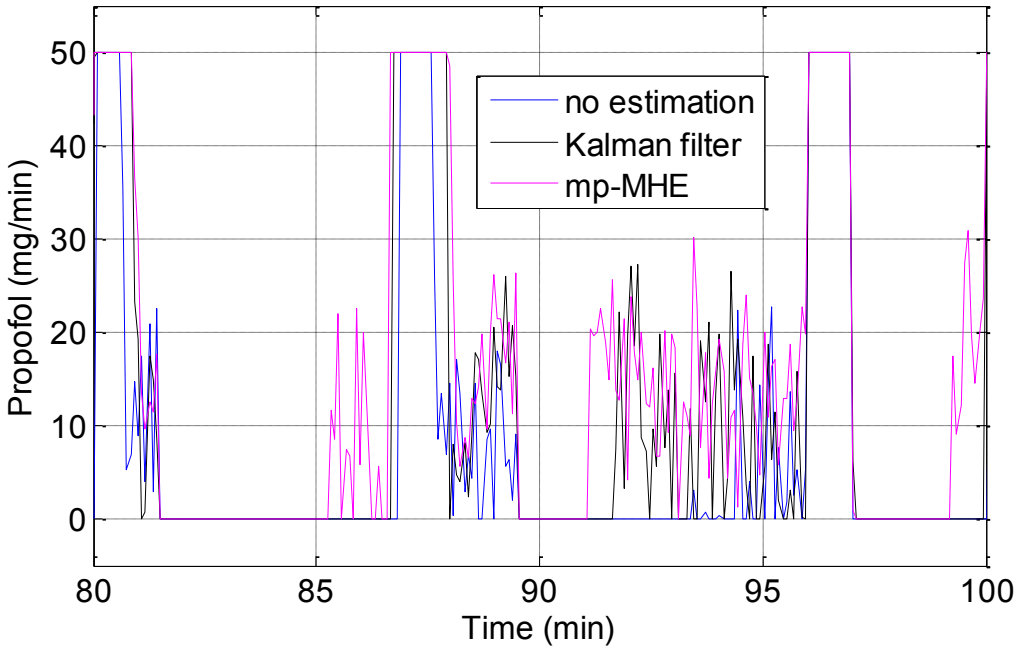

Figure 3.57: Propofol infusion rate of the three controllers for patient 9 in the maintenance phase - B-C-D-E interval - with noise

3.5 Discussion

The aim of this chapter is to design and evaluate different estimation techniques that can be implemented simultaneously with mp-MPC for the automatic induction and control of DOA during induction and maintenance phase. The performance of the controllers are analysed both with and without noise influencing the output (BIS index).

Three different types of estimation techniques are designed and tested: (i) Kalman filter, (ii) online moving horizon estimation and (iii) offline moving horizon. Two different design schemes are presented for the implementation of the estimators that use as input: (i) the output of the Hill curve (BIS index) and (ii) the $\hat{Ce}$ by applying the inverse of the Hill curve to compensate for the nonlinearity introduced by the Hill function. Since the second scheme avoids the use of the nonlinearity in the design of the estimators it will show better overall performances. The MHE estimators show better performances than

the Kalman filter especially under the influence of noise. The online and offline MHE exhibit similar performances, the mp-MPC has the advantage that by using multiparametric programming, it manages to avoid the computation expenses of online MHE by solving the optimization problem once and offline. This will further facilitate the implementation of such techniques on embedded devices. Due to these advantages of the mp-MHE the online MHE is not considered in further studies.

The Kalman filter and mp-MHE are simultaneously implemented with mp-MPC and along with the nominal controller tested in the induction and maintenance phase for the set of patients in Table 2.1. To address the inter- and intra- patient variability each of the three controllers are tested for the whole set of patients.

In the induction phase, for the nominal controller we have an average settling time 280 seconds, for the simultaneous Kalman filter and mp-MPC, an average of 240 seconds and an average of 225 seconds for the simultaneous mp-MHE and mp-MPC. For the undershoot evaluation, the worst case scenario is considered, meaning the most sensitive patient. Without the presence of noise, we obtain a maximum undershoot of: (i) 5.9% for the nominal mp-MPC without state estimation, (ii) 4% for the simultaneous Kalman filter and mp-MPC and (iii) 2% for the simultaneous mp-MHE and mp-MPC. All undershoots are below 10% which represents the maximum limit. We can say that as an overall performance the simultaneous mp-MHE and mp-MPC shows better results especially under the influence of noise.

The controllers are tested in the maintenance phase in order to see how well they can deal with disturbance rejection. In Figure 3.42 - Figure 3.57 we can observe the four controllers response to a disturbance signal that mimics the events that occur in an operation theatre for patient 4 and for patient 9 with and without the influence of noise.

For each patient there will be a variable dose-response relationship. For the same reference value, the controller sends different drug rate and the blood and effect-site concentrations levels are different for each patient.

3.6 Conclusions

In this chapter we have designed and evaluated three different state estimation techniques (Kalman filter, offline moving horizon estimation and online moving horizon) for the intravenous anaesthesia process. For intravenous anaesthesia the performances were analysed and tested comparatively on a set of 12 patients. The state estimators are implemented simultaneously with mp-MPC and simulated for the same set of patients in the induction and maintenance phase both with and without noise influencing the output.
It is therefore desirable that the patient reaches the BIS=50 target and remains within the target value without much undershoot or overshoot, i.e., values below BIS=40 and above BIS=60 should be avoided. In common practice the operation procedure does not start until the patient reaches an adequate DOA, usually taking up to 15 minutes. Thus, a rise time between 5 min and 7 min gives good performances.

The designed methodologies show good performances: fast settling time and no significant overshoot or undershoot. Good performances for the control of DOA are defined by maintaining the BIS between the values of 40 and 60 as well as having a settling time lower than 15 minutes (in common practice it usually takes up to 15 minutes to reach DOA). The moving horizon estimator exhibits better performance compared to the other estimation techniques especially under the influence of noise and constraints. Moreover since the BIS output is influenced by strong noise, the use of the mp-MHE brings improvements to the control strategies. The estimators provide sufficiently accurate information to the parametric controllers to induce and maintain the desired Bispectral Index reference based only on the measured information.

Furthermore the proposed strategies were able to deal with two of the main challenges in controlling the depth of anaesthesia: (i) nonlinearity by using the inverse of the Hill function and (ii) inter- and intra- patient variability by using estimation techniques to estimate the state of each individual patient. Alternative strategies that are able to deal with these challenges are further investigated in the following chapter.

Chapter 4

Hybrid and Robust Explicit Model Predictive Control Strategies

4.1 Introduction

In most drug delivery systems such as controlling the depth of anaesthesia, the nonlinearities are typically present in the pharmacodynamic model of the system and are described by the Hill curve representing the relation between the concentration of the drug and the effect observed on the patient. For the case of infusion of anaesthetic agents, the nonlinear Hill curve approximation has been used in both volatile (Krieger et al., 2014) and intravenous (Nascu et al., 2012, Nascu et al., 2014a) anaesthesia

In this chapter we further focus on different ways in dealing with the most important two challenges in controlling the depth of anaesthesia (DOA): nonlinearity and inter- and intra- patient variability. Advanced control strategies using either hybrid and robust multiparametric model predictive control or simultaneous hybrid multiparametric model predictive control and state estimation techniques are developed and tested. Here we first generate a piece-wise linearization of the Hill curve. The main advantage of this procedure is that the parameter space is linearized and that the uncertainty in some key parameters of the Hill curve is compensated for. As a result of the linearization, the anaesthesia model is described by a piece-wise affine system. This will lead to a hybrid model predictive control (hMPC) problem formulation (Bemporad et al., 1999a) and thus a mixed-integer quadratic programming (MIQP) problem formulation. However, the online implementation of hMPC involves the online solution of the MIQP problem, which introduces a high computational burden. To overcome this, the hMPC problem is

solved explicitly offline via the solution of state-of-the-art multi-parametric mixed integer quadratic programming problem (mp-MIQP) (Dua et al., 2002i, Oberdieck et al., 2015).
Another important challenge in the control of DOA that is addressed in this chapter is the high inter- and intra- patient variability, which introduces a high degree of uncertainty in the system. A number of robust control strategies and a state estimation technique are developed and presented simultaneously with the hybrid multiparametric model predictive control (mp-hMPC). State estimation is used for the unavailable states as well as in order to overcome issues that arise from noisy outputs. In particular, moving horizon estimators (MHE), implemented in a multi-parametric fashion (Nascu et al., 2014j, Darby and Nikolaou, 2007, Voelker et al., 2013) is used simultaneously with the hMPC control. The control strategies are tested on a set of 12 patients for the induction and maintenance phase of general anaesthesia.
The chapter is organized as follows: the pharmacokinetic and pharmacodynamic patient model as well as the formulation of the hybrid patient model is presented in Section 4.2. Section 4.3 presents the design of the hybrid multiparametric model predictive controller along with the robust control strategies and the moving horizon estimation strategy. The simulation results of the designed controllers using the presented robust and estimation strategies for the induction and maintenance phase are presented in Section 4.4. In section 4.5 we present the discussions following the results section while in Section 4.6 we summarize the main outcome of this chapter.

4.2 Patient Model formulation

4.2.1 Patient Model

The patient model for the administration of intravenous anaesthesia is composed of the pharmacokinetic (PK) and pharmacodynamic (PD) models. PK model describes the distribution of Propofol in the body and PD model describes the relationship between Propofol blood concentration and its clinical effect. The PK-PD models most commonly

used for Propofol are the 4th order compartmental model introduced by Schnider (Schnider et al., 1999) and Minto (Minto et al., 1997)

The PK model is expressed by linear relations as follows:

$$\begin{aligned}\dot{x}_1(t) &= -\left[k_{10}+k_{12}+k_{13}\right]\cdot x_1(t)+k_{21}\cdot x_2(t)\\ &+k_{31}\cdot x_3(t)+u(t)/V_1\\ \dot{x}_2(t) &= k_{12}\cdot x_1(t)-k_{21}\cdot x_2(t)\\ \dot{x}_3(t) &= k_{13}\cdot x_1(t)-k_{31}\cdot x_3(t)\end{aligned} \qquad \text{(Equation 4.1)}$$

where x_1 represents the drug concentration in the central compartment [mg/l]. The peripheral compartments 2 (muscle) and 3 (fat) model the drug exchange of the blood with well and poorly diffused body tissues. The concentrations of drug in the fast and slow equilibrating peripheral compartments are denoted by x_2 and x_3 respectively. The parameters k_{ij} for i=1:3, $i \neq j$, denote the drug transfer frequency from the i^{th} to the j^{th} compartment, , k_{10} the frequency of drug removal from the central compartment. $u(t)$ [mg/min] is the infusion rate of the anaesthetic or analgesic drug into the central compartment. The parameters k_{ij} of the PK models depend on age, weight, height and gender and can be calculated for Propofol as presented in Table 2.1. A more detailed description of the patient model can be found in Chapter 1.1.

The PD mathematical model is presented as follows:

$$\dot{C}_e(t) = k_{e0}(C_e(t)-x_1(t)) \qquad \text{(Equation 4.2)}$$

$$BIS(t) = E_0 - E_{\max}\cdot\frac{C_e(t)^{\gamma}}{C_e(t)^{\gamma}+EC_{50}^{\gamma}} \qquad \text{(Equation 4.3)}$$

The additional hypothetical effect compartment is added to represent the lag between plasma drug concentration and drug response. Its corresponding drug concentration is represented by the *effect-site compartment concentration* C_e. The drug transfer frequency

for Propofol from the central compartment to the effect site-compartment is considered in clinical practice to be equal to the frequency of drug removal from the effect-site compartment $k_{e0}=k_{1e}=0.456$ [min^{-1}].(Schnider et al., 1998, Schnider et al., 1999, Nunes et al., 2009)

The *Hill curve* (Equation 4.3)*, corresponds to the second part of the PD model.* E_0 denotes the baseline value (awake state - without drug), which by convention is typically assigned a value of 100, E_{max} denotes the maximum effect achieved by the drug infusion, EC_{50} is the drug concentration at 50% of the maximal effect and represents the patient sensitivity to the drug, and γ determines the steepness of the curve.

4.2.2 Hybrid Patient Model

A feature of the PD model for DOA control is the presence of nonlinearities corresponding to the Hill curve. Due to its S shape profile, a piecewise linearization of the Hill curve which divides the BIS into three partitions, where each partition i is associated with a different linear function $BIS = C_i C_e + e_i$. The resulting piece-wise affine formulation is shown in Table 4.1 where the parameters describing the PK model can be found in Table 2.1.

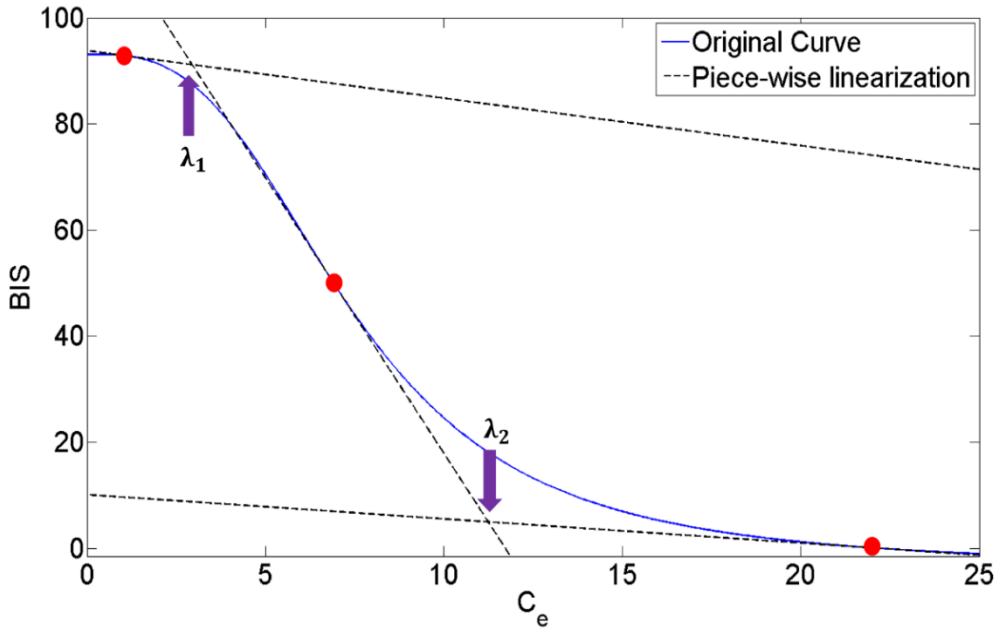

Figure 4.1: The original Hill curve and a piece-wise linearized version. The red dotes denote the points around which the linearization was performed while the purple arrows show the switching points λ_1 and λ_2, respectively

The binary variables δ thereby denote whether a certain partition is active. As a result, this system belongs to the class of hybrid systems, i.e., systems which are described by continuous as well as discrete dynamics and/or logical constraints.

Table 4.1: Hybrid model for intravenous anaesthesia

Intravenous Anaesthesia	
PK model	$\dot{x}_1(t) = -[k_{10} + k_{12} + k_{13}] \cdot x_1(t) + k_{21} \cdot x_2(t)$ $+ k_{31} \cdot x_3(t) + u(t)/V_1$ $\dot{x}_2(t) = k_{12} \cdot x_1(t) - k_{21} \cdot x_2(t)$ $\dot{x}_3(t) = k_{13} \cdot x_1(t) - k_{31} \cdot x_3(t)$
Effect site compartment	$\dot{C}_e(t) = k_{e0} \cdot (C_e(t) - C_p(t))$

PD model (Hill curve)	$BIS = C_i C_e + e_i$ $0 \le C_{e1} \le \lambda_1 \delta_1$ $\lambda_1 \delta_2 \le C_{e2} \le \lambda_2 \delta_2$ $\lambda_2 \delta_3 \le C_{e3} \le \lambda_3 \delta_3$ $C_e = C_{e1} + C_{e2} + C_{e3}$ $\delta_1 + \delta_2 + \delta_3 = 1$ $C_i = f[E_0, E_{\max}, EC_{50}, \gamma]$

Where $\delta \in [0,1]^3$; $C_i, e_i, i \in \{1,2,3\}$ are found using the first order Taylor expansions at the points for the linearization; $\sum_i \delta_i = 1$.

Note that $\sum_i \delta_i = 1$ holds, as only one linearization is active for every drug concentration C_e, and the choice of which linearization is active is described via the switching points λ_1 and λ_2 (see Figure 4.1)

Systems which can be described via the equations presented in Table 4.1 are part of the mixed-logical dynamical (MLD) systems, which are a well-studied class of systems (Bemporad et al., 1999b, Heemels et al., 2001). The basic principle is thereby that additionally to the commonly encountered continuous parts, discrete elements are present in the problem formulation, either as inputs, states, variables or outputs. Additional information can be found in Appendix C.

4.3 Control Design

4.3.1 Hybrid formulation of the control problem –intravenous anaesthesia

Based on the piece-wise affine formulation presented in Table 4.1, the following hybrid explicit MPC can be obtained (Bemporad and Morari, 1999a):

$$\min_{u} J = \sum_{k=1}^{N} (BIS_k - BIS_k^R)^T QR_k (BIS_k - BIS_k^R) + \sum_{k=0}^{N_u-1} \Delta u_k^T R_k \Delta u_k$$

$$s.t. \quad \mathrm{x}_{t+1} = \begin{bmatrix} -(k_{10}+k_{12}+k_{13}) & k_{21} & k_{31} & 0 \\ k_{12} & -k_{21} & 0 & 0 \\ k_{13} & 0 & -k_{31} & 0 \\ k_{41} & 0 & 0 & -k_{e0} \end{bmatrix} x_t + \begin{bmatrix} 1 \\ 0 \\ 0 \\ 0 \end{bmatrix} u_t$$

$$BIS = C_i C_e + e_i$$
$$0 \le C_{e1} \le \lambda_1 \delta_1$$
$$\lambda_1 \delta_2 \le C_{e2} \le \lambda_2 \delta_2$$
$$\lambda_2 \delta_3 \le C_{e3} \le \lambda_3 \delta_3$$
$$C_e = C_{e1} + C_{e2} + C_{e3}$$
$$\delta_1 + \delta_2 + \delta_3 = 1$$
$$C_i = f[E_0, E_{\max}, EC_{50}, \gamma]$$
$$\mathrm{u}_{\min} \le u \le u_{\max}$$
$$x_t \in X \subseteq \Re^p, u_t \in U \subseteq \Re^s, y \in [0,1]^3$$

(Equation 4.4)

where x are states, y outputs and u controls, all (discrete) time dependent vectors. The prediction horizon is denoted by N and control horizon by N_u. X, U are the sets of the state and input constraints that contain the origin in their interior. The weight matrix for manipulated variables $R \succ 0$ is a positive definite diagonal matrix and QR is the weight matrix for tracked outputs. Thus, if a certain combination of integer variables is fixed, (Equation 4.4) results in a convex QP. For the design of the controller the following design parameters were used: the objective coefficients for states (x), the weight matrix for tracked outputs (y), QR=10^2, weight matrix for manipulated variables (u), R=1.

(Equation 4.4) can be recast as an mp-MIQP problem for which we have recently proposed the first exact solution reported in the literature (Oberdieck and Pistikopoulos, 2015) (see also Figure 4.2). Once the algorithm is initialized, a candidate solution is found, which is fixed in the original problem thus transforming it into a mp-QP problem.

The mp-QP problem is solved using available solvers. Next, the objective values of the mp-QP problem and the upper bound in the critical region considered are compared against each other to form a new, tighter upper bound. The algorithm terminates if a termination criterion is reached. More details on the exact solution can be found in Appendix C.

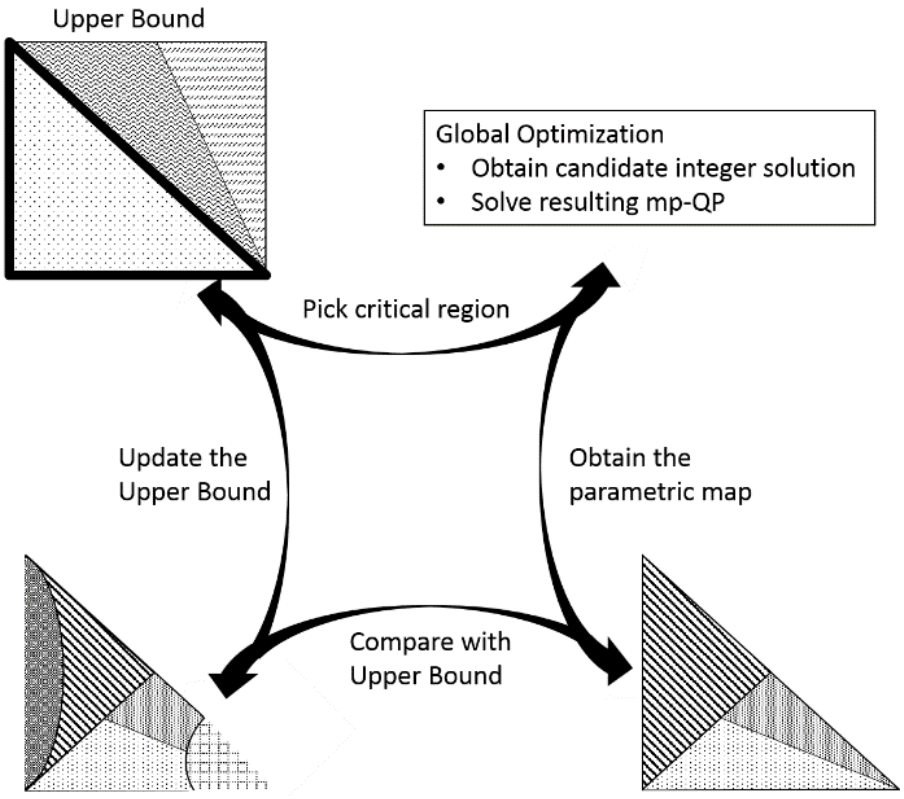

Figure 4.2: The general framework for the solution of mp-MIQP problems

Figure 4.3 presents a typical solution of the multiparametric programming problem in the form of 2-dimensional projection of the critical space. The parametric vector θ consists of: the estimated states, the current time output and the output reference (*BIS=50*). Here θ_1 and θ_2 represent the concentration of the effect site compartment, C_e and the first state x_1.

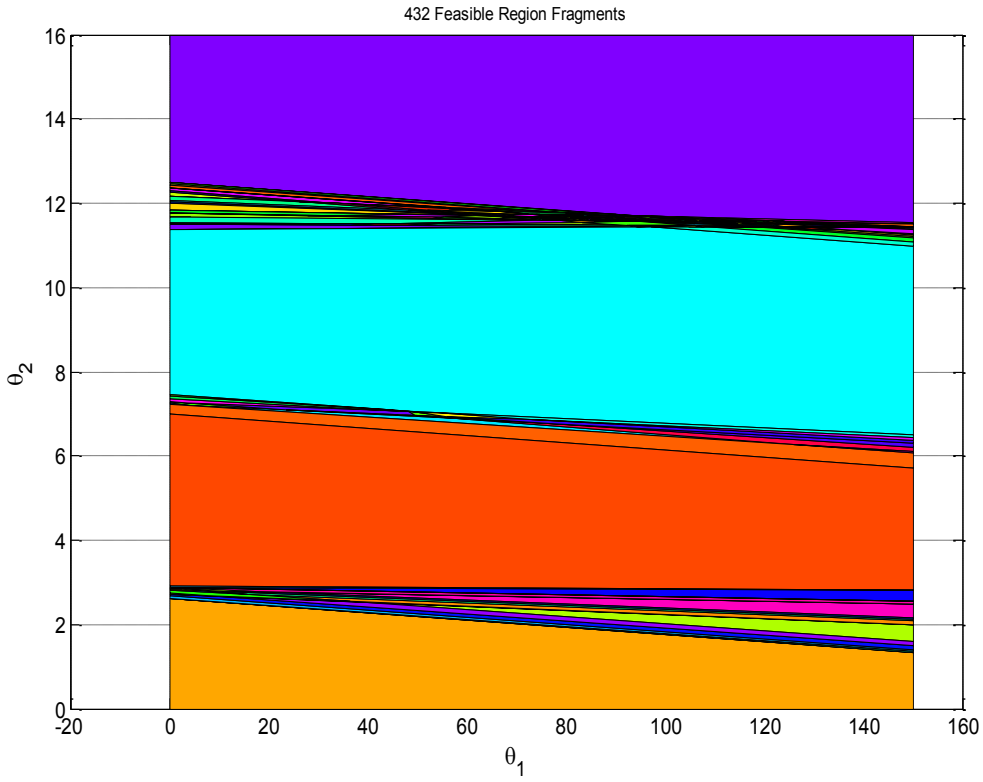

Figure 4.3: Map of critical regions - mp-hMPC

4.3.2 Robust & estimation of the hybrid mp-MPC control strategy

Another challenge for the DOA control is the high inter- and intra- patient variability, which introduces a high degree of uncertainty in the system. Thus, robust control strategies or estimation techniques are required. Robust techniques and a multiparametric moving horizon estimation technique which are able to deal with these types of problems have been developed.

4.3.2.1 Strategy 1 – Moving Horizon Estimation (MHE)

Moving horizon estimation (MHE) is an estimation method that considers a limited amount of past data. It provides information about the states of the system when measurements are unavailable, noisy or unreliable (Voelker et al., 2013, Nascu et al., 2014j). Moreover, it has the advantage of incorporating system knowledge as constraints in the estimation problem. In MHE the system states and disturbances are derived by solving (Equation 4.5)

Using simultaneous mp-MHE and mp-hMPC the state of each individual patient will be estimated and used by the controller (Nascu et al., 2014e) by formulating and solving a constrained moving horizon estimator with multiparametric programming (Nascu et al., 2014e) as follows: the mp-MHE is obtained by substituting the state space formulation of the estimated system $\hat{x}_{t+1} = A\hat{x}_t + Bu_k + G\hat{w}_t$, $\hat{v}_t = y_t - C\hat{x}_t$ into:

$$x_{k+1} = A \cdot x_k + B \cdot u_k + G \cdot w_k \qquad \text{discrete state-space formulation}$$

$$y_k = C \cdot x_k + v_k \qquad \rightarrow v_k = y_k - C \cdot x_k$$

$$\mathrm{BIS}_{\min} \le y \le BIS_{\max}$$

$$\Delta \mathrm{u}_{\min} \le \Delta u \le \Delta u_{\max}$$

$$\begin{bmatrix} 1 & 0 & 0 & 0 \\ -1 & 0 & 0 & 0 \\ 0 & 1 & 0 & 0 \\ 0 & -1 & 0 & 0 \\ 0 & 0 & 1 & 0 \\ 0 & 0 & -1 & 0 \\ 0 & 0 & 0 & 1 \\ 0 & 0 & 0 & -1 \end{bmatrix} \cdot \begin{bmatrix} x_1 \\ x_2 \\ x_3 \\ x_e \end{bmatrix} \le \begin{bmatrix} 100 \\ 0 \\ 100 \\ 0 \\ 100 \\ 0 \\ 100 \\ 0 \end{bmatrix} \qquad \text{path constraints on state variables}$$

$$\begin{bmatrix} 1 \\ -1 \end{bmatrix} \cdot w \le \begin{bmatrix} 1 \\ -1 \end{bmatrix} \qquad \text{path constraints on the noise w}$$

$$\begin{bmatrix} 1 \\ -1 \end{bmatrix} \cdot v \le \begin{bmatrix} 1 \\ -1 \end{bmatrix} \qquad \text{path constraints on the noise v}$$

$$\bar{x}_{T-N+1/T-N} = A \cdot \hat{x}_{T-N/T-N} + B \cdot u_k + G \cdot \bar{w} \qquad \text{update of the cost to arrive}$$

(Equation 4.5)

Where N is the length of the horizon, T is the current point in time, Q and R are positive definite diagonal weighting matrices on the noises, P_{SS} is the steady state solution for the Kalman filter. $\{\hat{w}\}_{T-N+1}^{T-N}$ and $\{v\}_{T-N+1}^{T}$ are sequences of independent, normally distributed random numbers with mean values $\overline{w}$ for $\{w\}$ and zero-mean for $\{v\}$. $\bar{x}_{T-N+1/T-N}$ is the arrival costwhich captures the previous measurements that are not considered any more.

4.3.2.2 Strategy 2 – Offset Free

One key problem of inter- patient variability is the presence of an offset in the output of the process. Hence, the first (intuitive) approach is to introduce a new parameter Δy, which captures this offset. In a mathematical form, it can be understood as expanding the definition of the output y_k:

$$x_{q,k+1} = x_{q,k} + \underbrace{(y^R - y_k)}_{error}, \ \forall k = 1,\ldots,N \qquad \text{(Equation 4.6)}$$

and added penalties in the objective function of problem:

$$\min_u J = x'_{q,N} P_q x_{q,N} + \sum_{k=1}^{N-1} x'_{q,k} Q_{q,k} x_{q,k} \qquad \text{(Equation 4.7)}$$

Note that the offset Δy is assumed to be the same for the entire horizon. At each step, this offset is calculated, and fed as a parameter to the system, thus resulting in an offset-free approach. The advantage of this approach is its simplicity (in fact, (Sakizlis et al., 2004a) proposed a similar strategy), however it only provides a symptomatic approach, rather than tackling the underlying issue.

4.3.2.3 Strategy 3 –State Output Correction

This approach is inspired by the work of (Chang et al., 2013, Chang et al., 2014a, Chang et al., 2014c), who proposed an "error compensator", i.e., to feed the parametric controller a "nominal" state which is corrected for disturbance. However, the key problem in anaesthesia is the scarsity of information, i.e., how to quantify this disturbance. The idea here is to assume that we know the correct value of the state $x_{k,4}$. Based on this, we can collect the data which represents what the nominal Hill-curve would predict compared to the actual patient. This data is then used to (a) adjust the values of C_i and e_i and (b) correct the value of $x_{k,4}$ when it is fed to the controller so as to obtain a better control action. Mathematically, this can be understood as follows:

$$\arg\min_{C,e}(y - y^{pred})^2 \qquad \text{(Equation 4.8)}$$

where y is the actual output and

$$y^{pred} = \sum_{i=1}^{3} C_i \delta_i x_{0,4} + \sum_{i=1}^{3} e_i \delta_{i,1} \qquad \text{(Equation 4.9)}$$

The values of *C* and *e* are adjusted over time and the "corrected" state is then calculated as:

$$\tilde{x}_{0,4} = C_i^{-1}(y - e_i) \qquad \text{(Equation 4.10)}$$

where *i* is based on *y*.

Simulations have shown that the direct application of (Equation 4.8) does not yield satisfactory results, as the change in *C* can be substantial, altering the S-shaped nature of the Hill-curve. Hence, we have adopted a two-stage procedure where *e* is determined by finding the average difference between *y* and y^{pred} and *C* is only adjusted based on the difference corrected values.

4.3.2.4 Strategy 4 – Prediction Output Correction

While the approach of adjusting C and e provides a theoretically more attractive approach, it also requires a new source of information. This last approach uses the state-space prediction x_{k+1} in order to obtain data regarding the mismatch between y and y_{pred}. The idea is the following: assume you have calculated $x_{k,4}$ using (Equation 4.10), we get to stage k + 1 via the state-space model

$$x_{k+1} = Ax_k + Bu_k \qquad \text{(Equation 4.11)}$$

The new state x_{k+1} results in (a) a real output y, but (b) we can obtain the data according to (Equation 4.9) as we can predict how $x_{k,4}$ would behave in the state-space model. This allows for the quantification of the mismatch between the linearization and the actual output without requiring any new parameters nor extra measurements.

4.3.3 Hybrid Control Design

In this section developed strategies are implemented with the hybrid mp-MPC for the control of intravenous anaesthesia. The proposed control design scheme for the simultaneous mp-MHE and mp-hMPC is presented in Figure 4.5 while in Figure 4.4 we have the design scheme for the mp-hMPC and the robust control strategies.

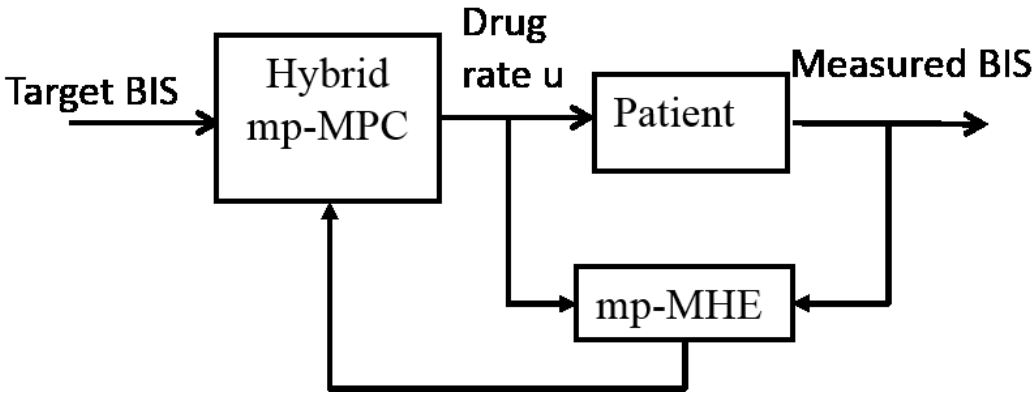

Figure 4.4: Simultaneously hybrid mp-MPC and mp-MHE control scheme

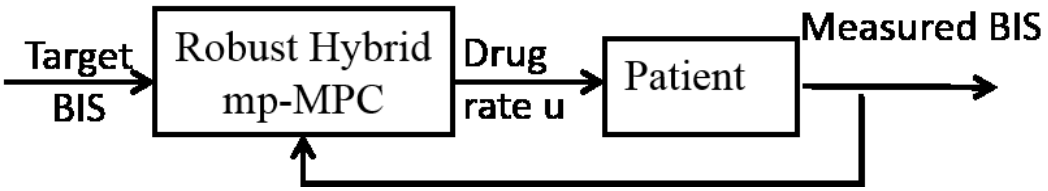

Figure 4.5: Robust Hybrid mp-MPC control scheme

The *Patient* in both design schemes, is simulated using the mathematical model of the patient composed of the pharmacokinetic part (linear) (Equation 4.1) and the pharamacodynamic part (Equation 4.2) and (Equation 4.3).

For the design of the simultaneous mp-MHE mp-hMPC, the *Estimator* block is used to estimate the state of each individual patient. By estimating the states of every simulated patient, the controller instead of using the states computed using the nominal patient model will use the estimated values of states corresponding to each individual patient. Finally, the *mp-hMPC* block, using the individual patient states given by the *Estimator* block, calculates the error between the *Measured BIS* from the *Patient* and the Target BIS and provides the optimal *Drug rate u* to the *Patient* block.

For the design of the robust mp-hMPC the developed robust strategies presented in Section 4.3.3 are implemented within the design of the mp-MPC. The *Robust Hybrid mp-MPC* block, calculates the error between the *Measured BIS* from the *Patient* and the Target BIS and provides the optimal *Drug rate u* to the *Patient* block in order to drive it to the desired target value.

4.4 Results

In this section the results of a simulation study to evaluate the control strategies designed in this chapter, for the administration of Propofol are presented. The controllers are based on model based predictive control algorithm for automatic induction and

control of DOA. DOA is monitored using the Bispectral Index (BIS) during the induction and maintenance phase of general anaesthesia.
The closed loop control tests are performed on a set of 12 patients (Ionescu et al., 2011c) plus an extra patient representing the nominal values of all 12 patients (PaN – patient nominal) presented in Table 2.1. For a particular patient E_0 can be measured in awake state and E_{max} is considered to have the same value, $E_{max}= E_0$. These parameters are considered known a priori in the simulations.

All of the designed controllers are simulated first for the whole set of data presented in **Table** 2.1 in order to have a better understanding of their behaviour on the different types of patients, and also to be able to analyse the inter- and intra- patient variability. Next, the controllers showing the most relevant performances will be tested against each other and simulated for different patients so as to be able to compare their performances by means of the BIS index and the corresponding Propofol infusion rates. The performances of the five controllers are evaluated both in the induction and maintenance phase of DOA and the results are analysed comparatively. Note that the controllers are designed using the values of the nominal patient which means that for this patient we will have the best behaviour of the controllers.
Ideally the induction phase of the patient in an operational DOA is performed as fast as possible, such that little time is lost before the surgeon can start operating. It is therefore desirable that the patient reaches the BIS=50 target and remains within the target value without much undershoot or overshoot, i.e., values below BIS=40 and above BIS=60 should be avoided. In common practice the operation procedure does not start until the patient reaches an adequate DOA, usually taking up to 15 minutes. Thus, a rise time between 5 min and 7 min gives good performances

During the maintenance phase, it is important that the controller rejects the disturbances occurred during surgery as fast as possible and bring the patient to the BIS target value. In this phase, typical disturbances can be applied additively to the output of the process to check the controller's ability to reject them. A standard stimulus profile is defined and is presented in Figure 4.6. Each interval denotes a specific event in the

operation theatre. Stimulus A represents response to intubation; B a surgical incision that is followed by a period of no surgical stimulation i.e., waiting for pathology result; C mimics an abrupt stimulus after a period of low level stimulation; D the onset of a continuous normal surgical stimulation; E, F, and G simulate short-lasting, larger stimulation within the surgical period; and H represents the withdrawal of stimulation during the closing period (Yelneedi et al., 2009).

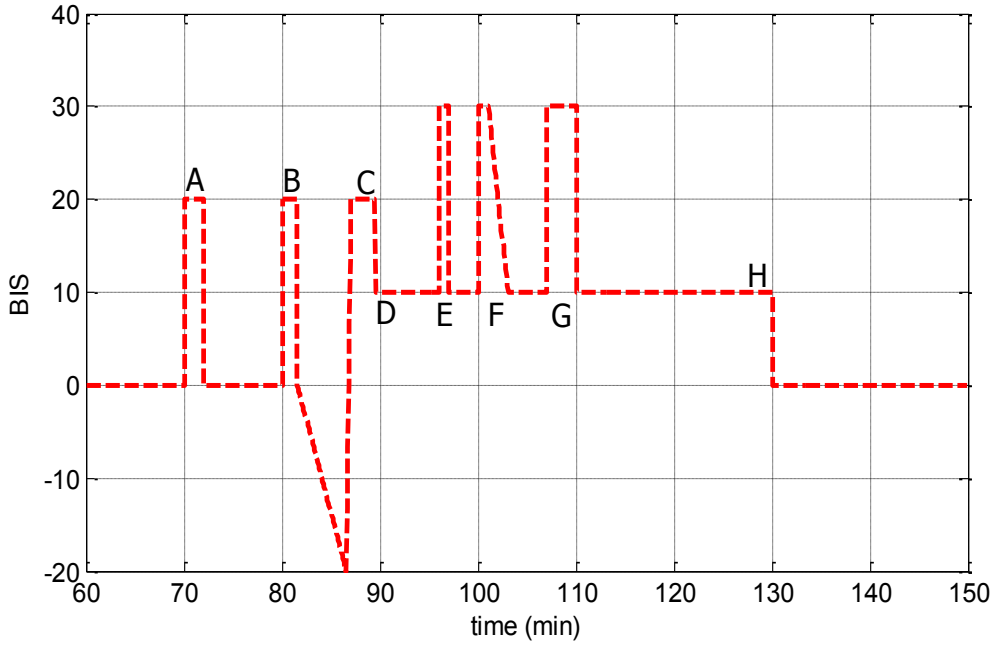

Figure 4.6: The artificially generated disturbance signal

4.4.1 No Offset Correction

In Figure 4.7 and Figure 4.8 we have the simulations of all the patients and the nominal one in the induction phase for the mp-hMPC controller without any robust techniques or state estimation. Figure 4.7 represents the BIS response of the patients while Figure 4.8 represents the corresponding control action. It can be observed that except the nominal patient (which was used for the design of the controller) all patients present an offset from the setpoint. Such behaviour is explained due to the high inter- and intra- variability. Figure 4.9 and Figure 4.10 present the simulations of all the patients and the nominal one

for the maintenance phase and it can be observed that, similar to the induction phase all patients (except the nominal one) present an offset from the setpoint.

The average settling time for the whole set of patients is of 240 seconds and the undershoot for the most sensitive patient (patient 9), representing the worst case scenario is of 5.7%.

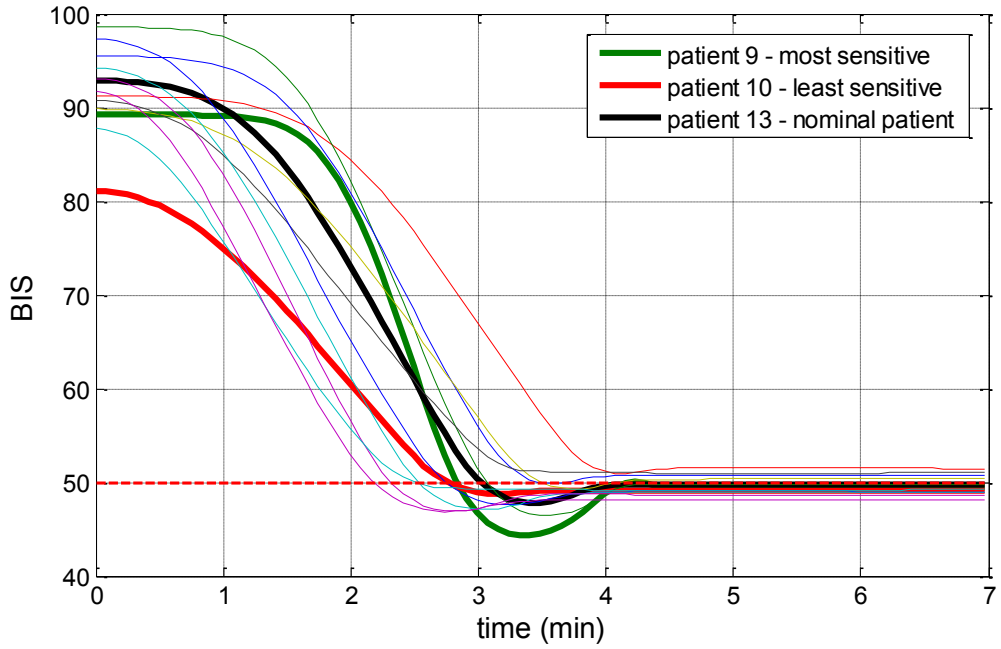

Figure 4.7: BIS output for all 13 patients without offset correction – induction phase

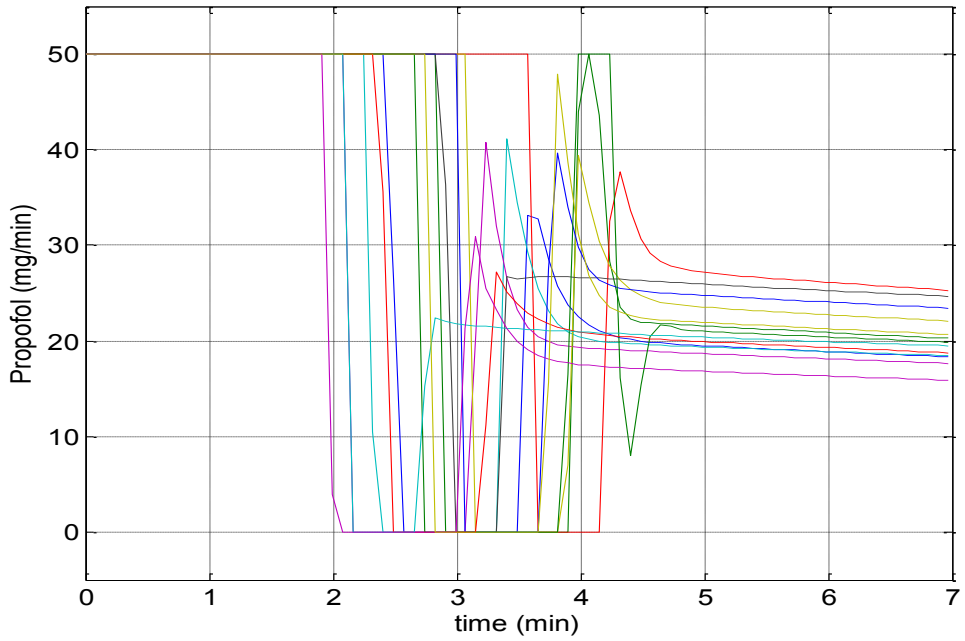

Figure 4.8: drug infusion for all 13 patients without offset correction – induction phase

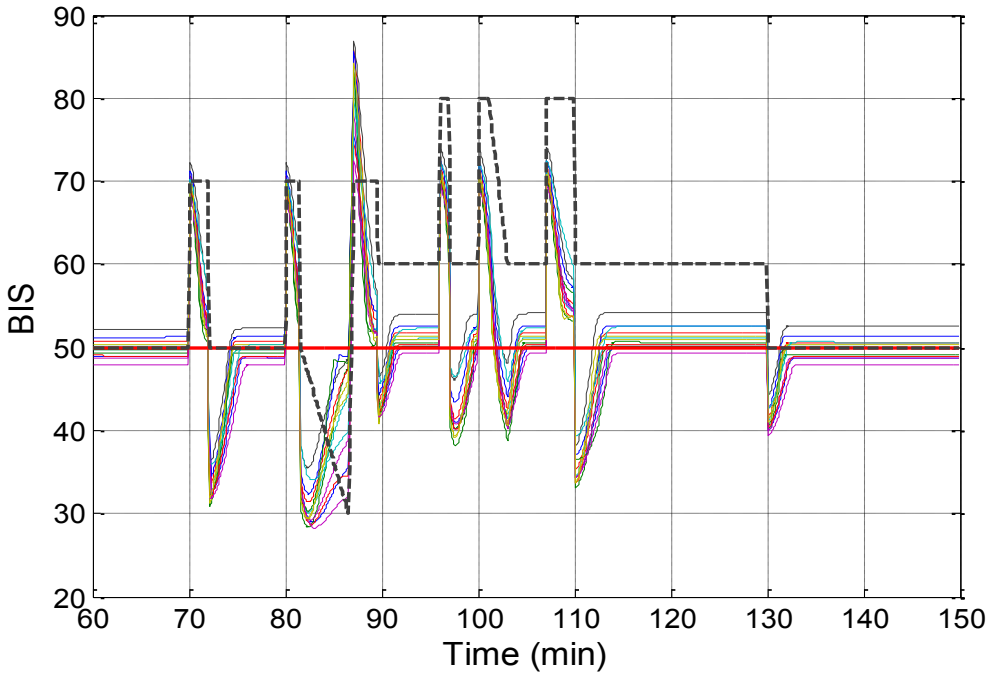

Figure 4.9: BIS output for all 13 patients without offset correction – maintenance phase

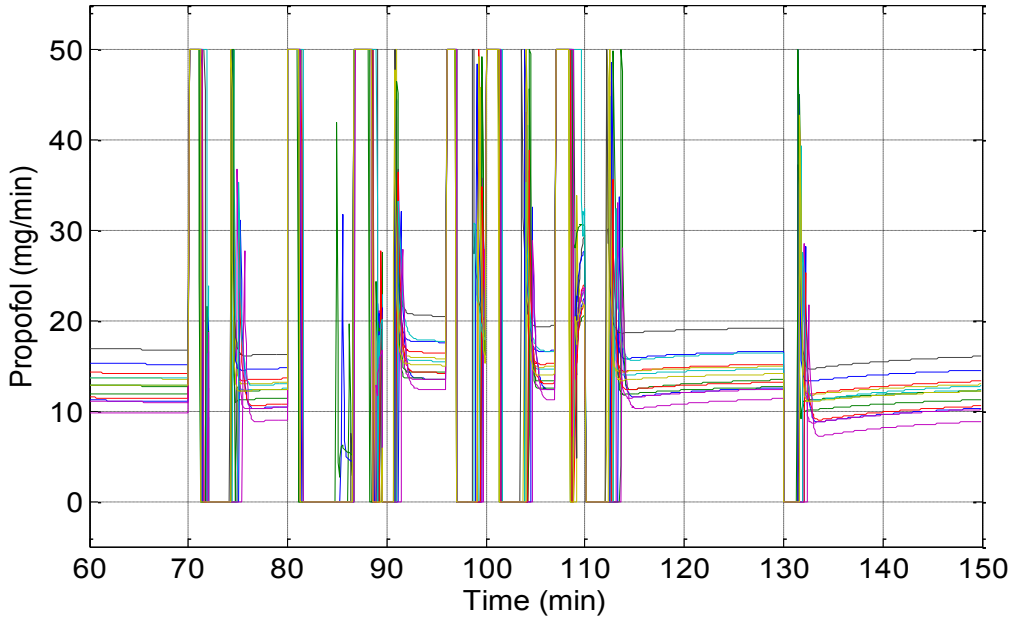

Figure 4.10: drug infusion for all 13 patients without offset correction – maintenance phase

The optimal control action of the multiparametric controller is presented in Table 4.2, along with the corresponding closed loop simulation control action for the nominal patient and patient 9 (Figure 4.11). Although both patients are in the induction phase, due to the inter- patient variability, different critical regions of the multiparametric controller i.e., control laws provide the optimal control action at each time step for the two patients.

Table 4.2: mp-hMPC optimal control action for Patient 9 and the nominal Patient

Step time	**Patient 9 (control action)**	**Nominal Patient (control action)**
T=1	$CR_{T=1} = 46$ $u_{opt}^{T=1} = 10$	$CR_{T=1} = 72$ $u_{opt}^{T=1} = -13.4028x_1 - 0.123x_2 -$ $- 0.6308x_3 - 135.7109x_e$

T=2	$CR_{T=2} = 46$ $u_{opt}^{T=2} = 10$	$CR_{T=2} = 72$ $u_{opt}^{T=2} = -13.4028x_1 - 0.123x_2 -$ $- 0.6308x_3 - 135.7109x_e$
T=3	$CR_{T=3} = 72$ $u_{opt}^{T=3} = -13.4028x_1 - 0.123x_2 -$ $- 0.6308x_3 - 135.7109x_e$	$CR_{T=3} = 72$ $u_{opt}^{T=3} = -13.4028x_1 - 0.123x_2 -$ $- 0.6308x_3 - 135.7109x_e$
T=4	$CR_{T=4} = 72$ $u_{opt}^{T=4} = -13.4028x_1 - 0.123x_2 -$ $- 0.6308x_3 - 135.7109x_e$	$CR_{T=4} = 72$ $u_{opt}^{T=4} = -13.4028x_1 - 0.123x_2 -$ $- 0.6308x_3 - 135.7109x_e$
T=5	$CR_{T=5} = 72$ $u_{opt}^{T=5} = -13.4028x_1 - 0.123x_2 -$ $- 0.6308x_3 - 135.7109x_e$	$CR_{T=5} = 72$ $u_{opt}^{T=5} = -13.4028x_1 - 0.123x_2 -$ $- 0.6308x_3 - 135.7109x_e$
T=6	$CR_{T=6} = 72$ $u_{opt}^{T=6} = -13.4028x_1 - 0.123x_2 -$ $- 0.6308x_3 - 135.7109x_e$	$CR_{T=6} = 72$ $u_{opt}^{T=6} = -13.4028x_1 - 0.123x_2 -$ $- 0.6308x_3 - 135.7109x_e$
T=7	$CR_{T=7} = 72$ $u_{opt}^{T=7} = -13.4028x_1 - 0.123x_2 -$ $- 0.6308x_3 - 135.7109x_e$	$CR_{T=7} = 72$ $u_{opt}^{T=7} = -13.4028x_1 - 0.123x_2 -$ $- 0.6308x_3 - 135.7109x_e$

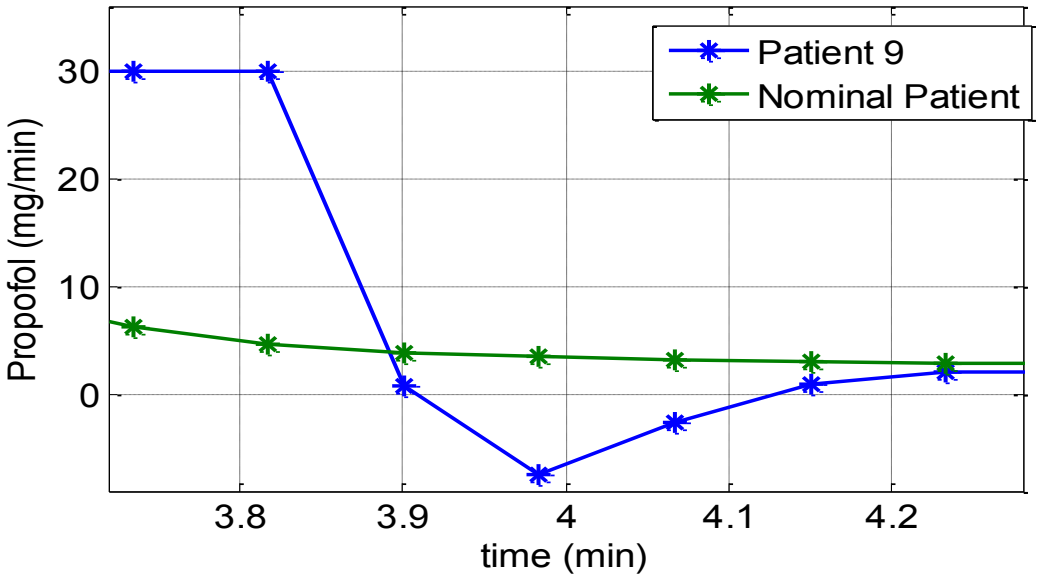

Figure 4.11: Optimal control action for Patient 9 and the nominal patient

In Figure 4.12 we show how the multiparametric hybrid model predictive controller operates for the nominal patient by presenting the correlation between the measured BIS output, the corresponding drug infusion rate, the active partition of the controller, the C_e, representing the fourth state of the process and the Hill function.

1. At the first point (1), the second partition of the controller becomes active and the Hill function switches from the first linearization to the second. The control action gives the maximum infusion of Propofol to drive the patient to the desired BIS value.
2. At the second point (2), the measured BIS reaches the target value of 50 and the controller stops providing the patient Propofol infusion rate. We can observe an undershoot on the BIS action since we have a more aggressive controller (which can be adapted by the tunning parameters of the controller). We are still in the second partition and the second linearization of the Hill function.
3. At the third point (3), we reach the maximum value of the undershoot therefore the controller will still operate at zero infusion rate. We are still in the second partition and the second linearization of the Hill curve. We can observe that the C_e reaches its maximum.
4. At the fourth point (4), the BIS settles at the value of 50, again providing the concentration C_e settles at the value of 42 [mg/min] and the controller starts giving Propfol infusion rate while it is also stabilising. Again the second partition remains active (second part of the linearization).

Note that in this case only the first and second linearization of the Hill curve become active i.e., only the first and second partition of the hybrid controller are activated. The third one will activate only when we have larger values of the concentration C_e therefore when the BIS value moves towards lower values. This will happen in the case of high disturbances in the maintenance phase. Also note that the concentration C_e is the inverse of the BIS output.

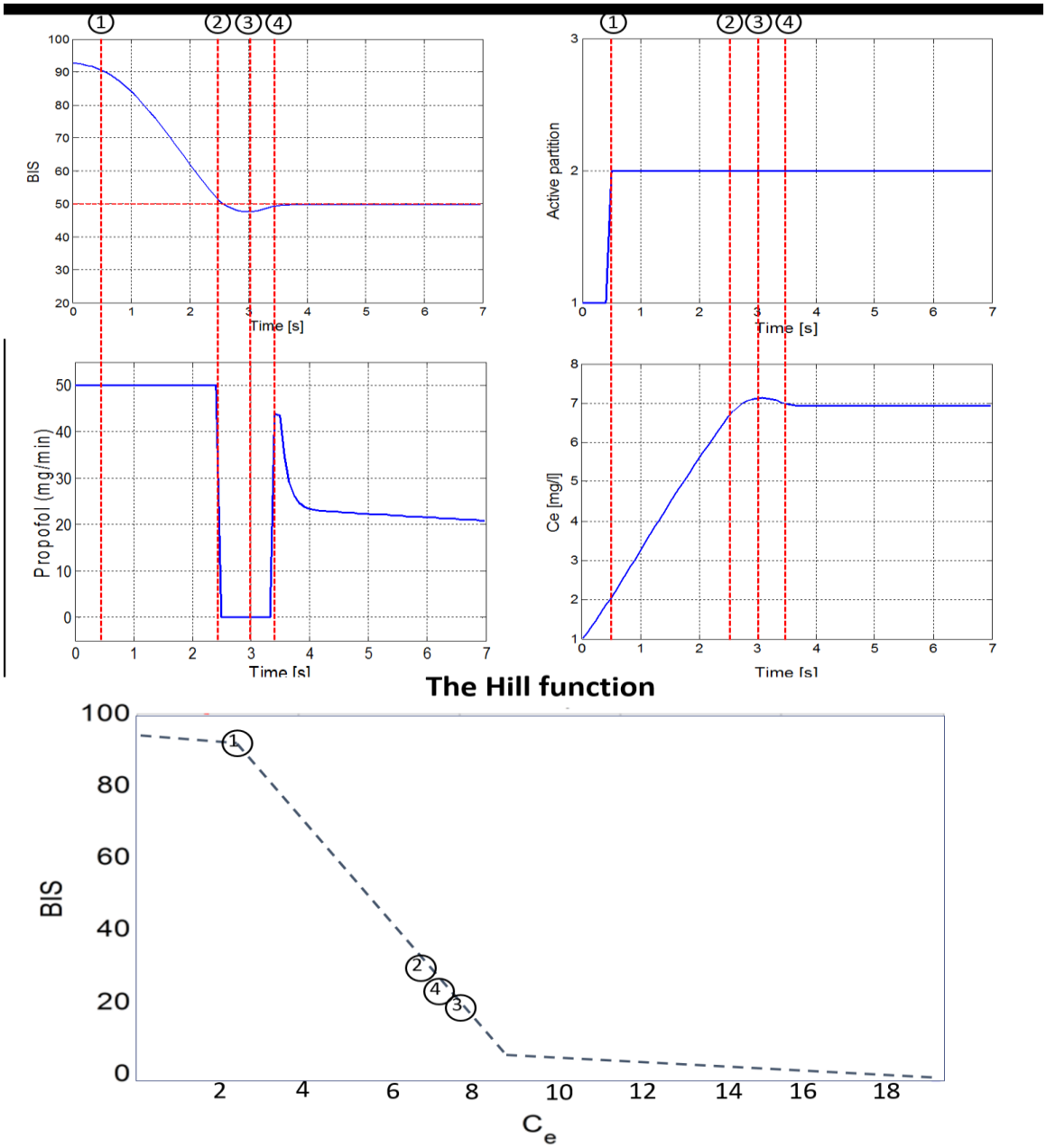

Figure 4.12: Nominal mp-hMPC simulation for the nominal patient – induction phase

4.4.2 Strategy 1 – Moving Horizon Estimation (MHE)

For the simultaneous mpMHE and mp-hMPC case we deal with the inter- and intra-patient variability by estimating the states of each simulated patient. The states are then used by the mp-hMPC to give the patient the optimal Propofol infusion rate. Therefore, the controller will be able to compensate for the offset from the setpoint. This can be observed in Figure 4.13 where we have the BIS response for all 13 patients and the nominal one and Figure 4.14 where we have the corresponding Propofol infusion rate. The average settling time is of 240 seconds and the undershoot of the most sensitive patient (patient 9) is of 3.5%.

In Figure 4.15 and Figure 4.16 we have the simulations of all patients in the maintenance phase.

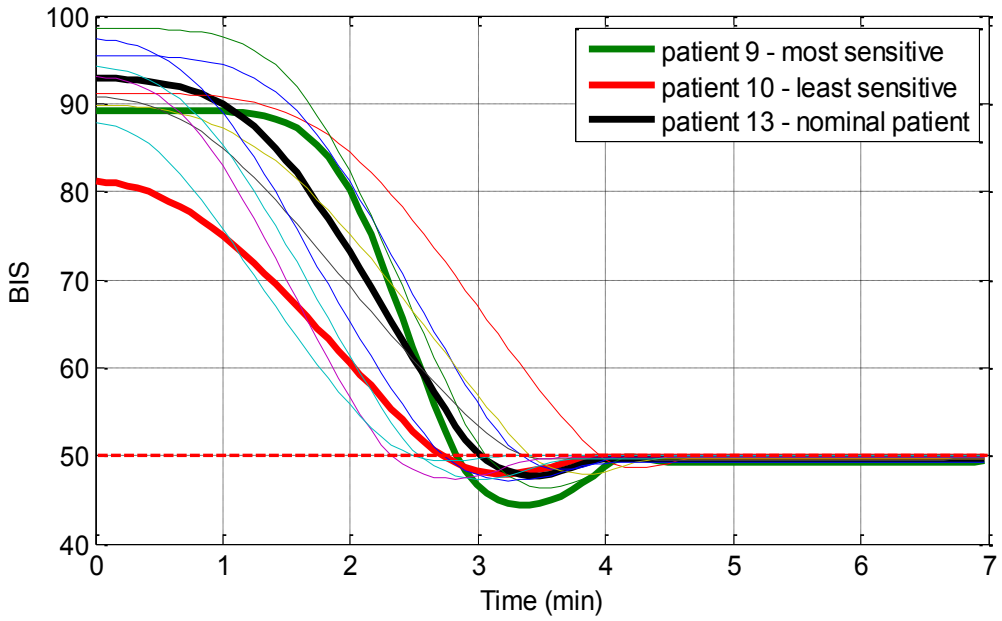

Figure 4.13: BIS output for all 13 patients – strategy 1 (mp-MHE and mp-hMPC) – induction phase

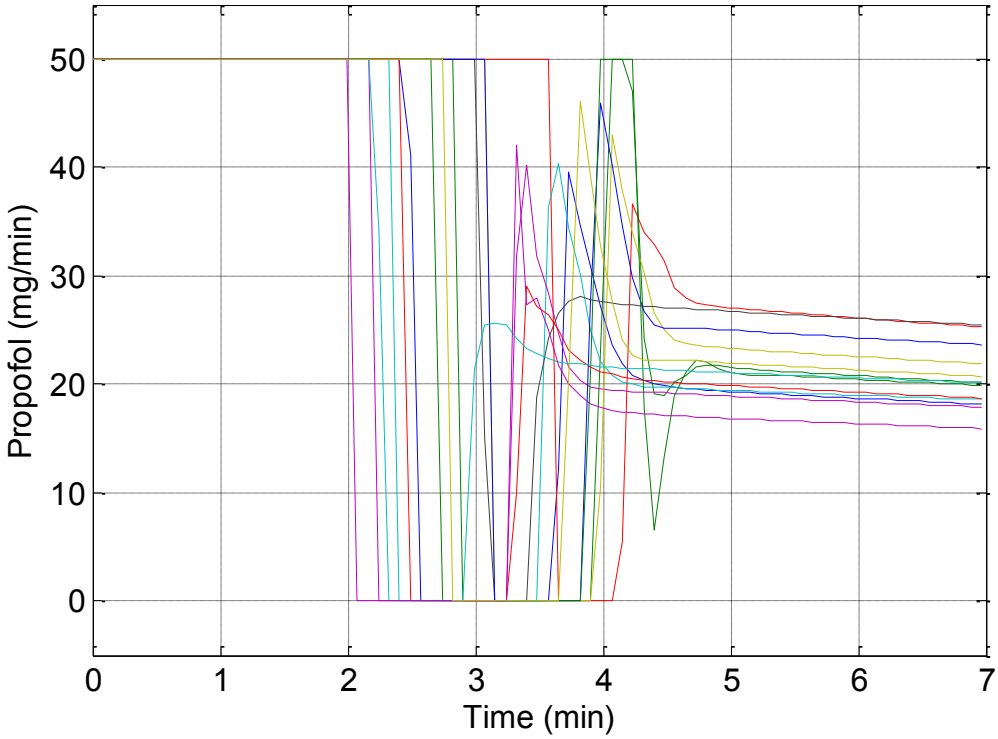

Figure 4.14: drug infusion for all 13 patients – strategy 1 (mp-MHE and mp-hMPC) – induction phase

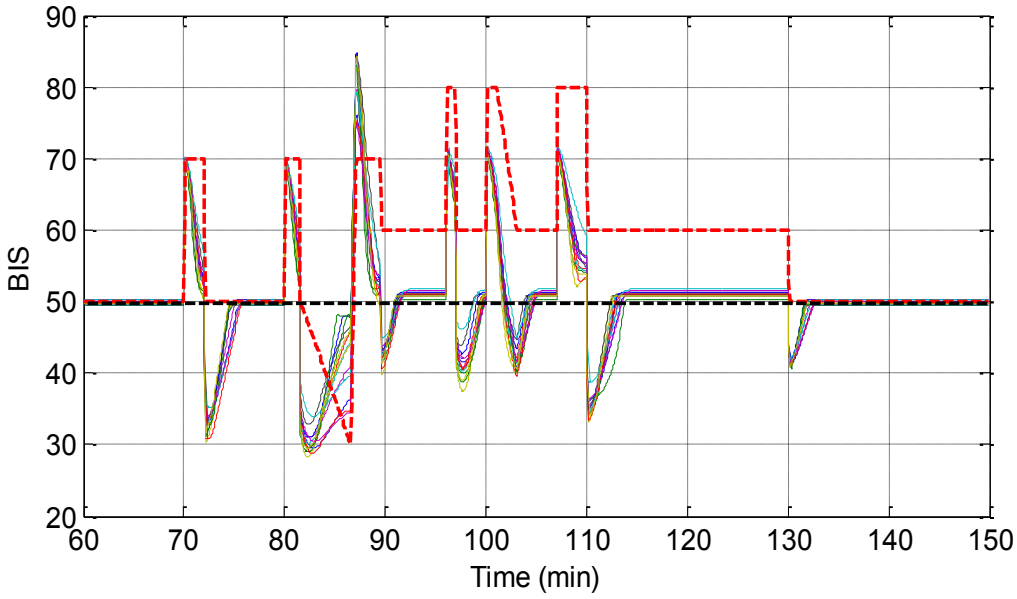

Figure 4.15: BIS output for all 13 patients – strategy 1 (mp-MHE and mp-hMPC) – maintenance phase

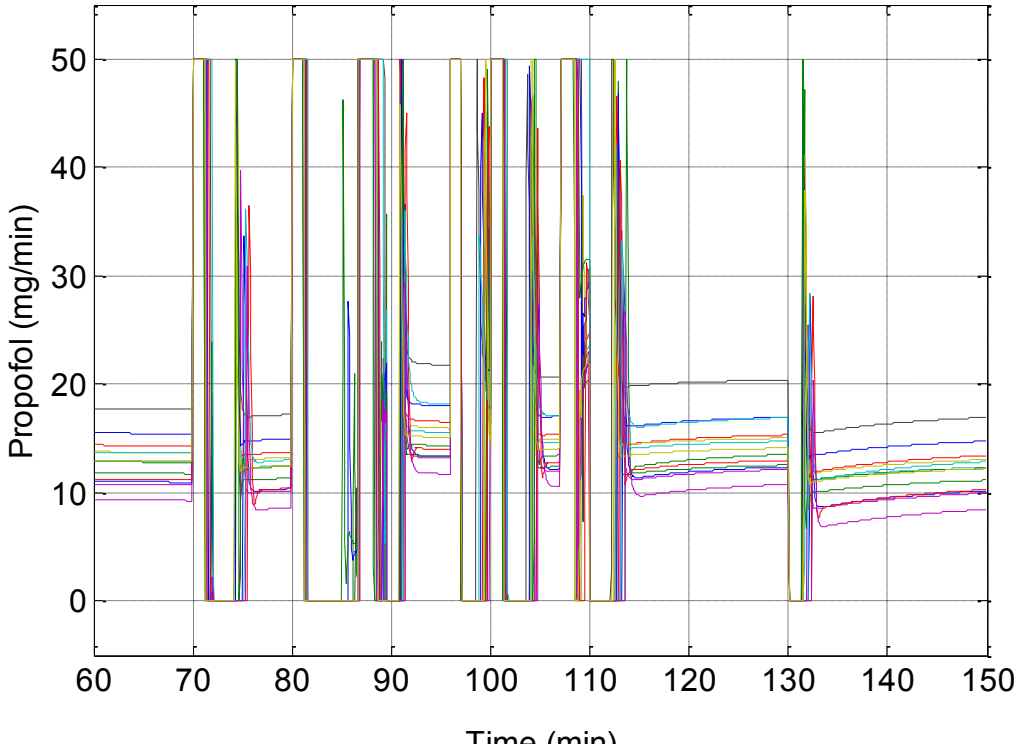

Figure 4.16: drug infusion for all 13 patients – strategy 1 (mp-MHE and mp-hMPC) – maintenance phase

4.4.3 Strategy 2 - Offset-Free

Figure 4.17 and Figure 4.18 present the simulations of all the patients and the nominal one in the induction phase for the mp-hMPC using the offset correction. It can be observed from Figure 4.17 where we have the BIS response of the patients that the controller is able to compensate for the offset and brings all the patients to the setpoint value of 50. In Figure 4.18 we have the corresponding Propofol infusion rate. Simulations of some patients show very small oscillations around the steady state values. The average settling time is of 250 seconds.

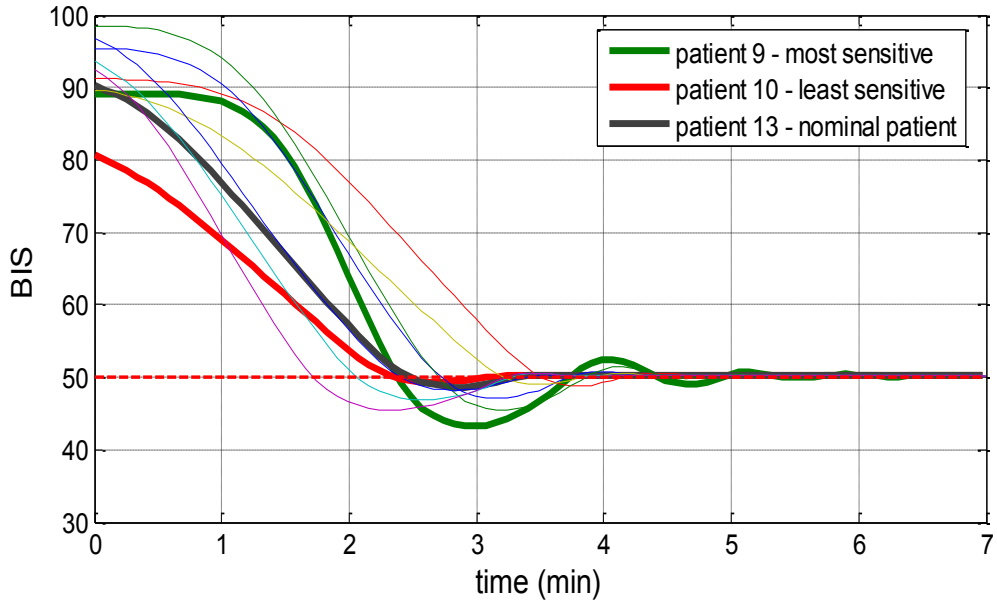

Figure 4.17: BIS output for all 13 patients – strategy 2 – induction phase

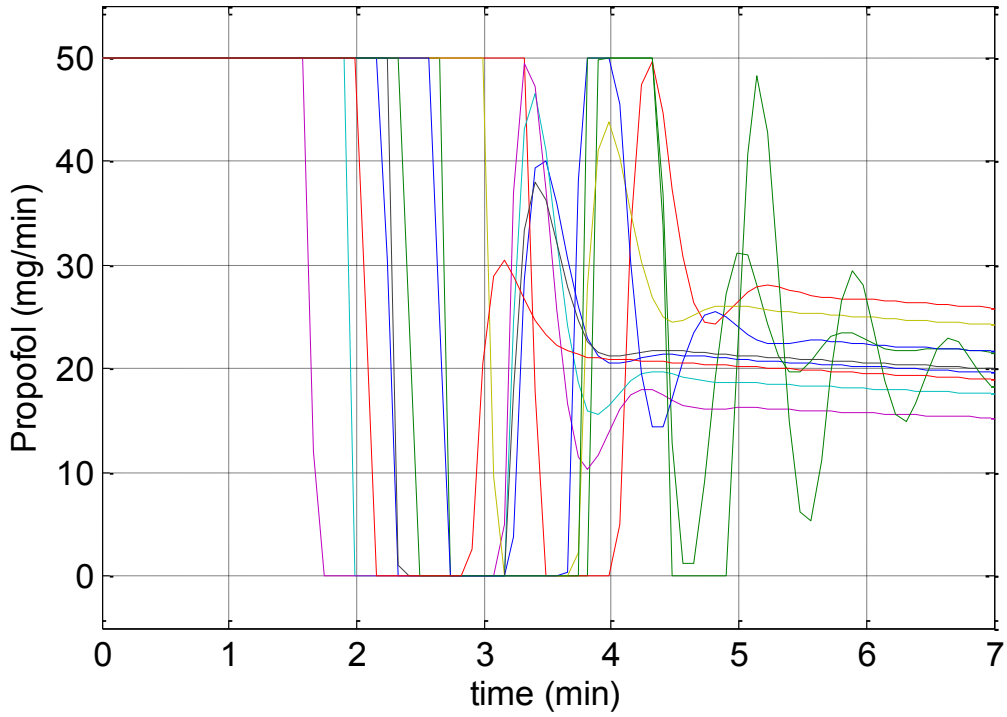

Figure 4.18: drug infusion for all 13 patients – strategy 2 – induction phase

The BIS response of all patients in the maintenance phase is depicted in Figure 4.19 while Figure 4.20 depicts the corresponding drug infusion rate. The controller compensates for disturbances but due to pump limitation the simulations exhibit some offsets from the setpoint.

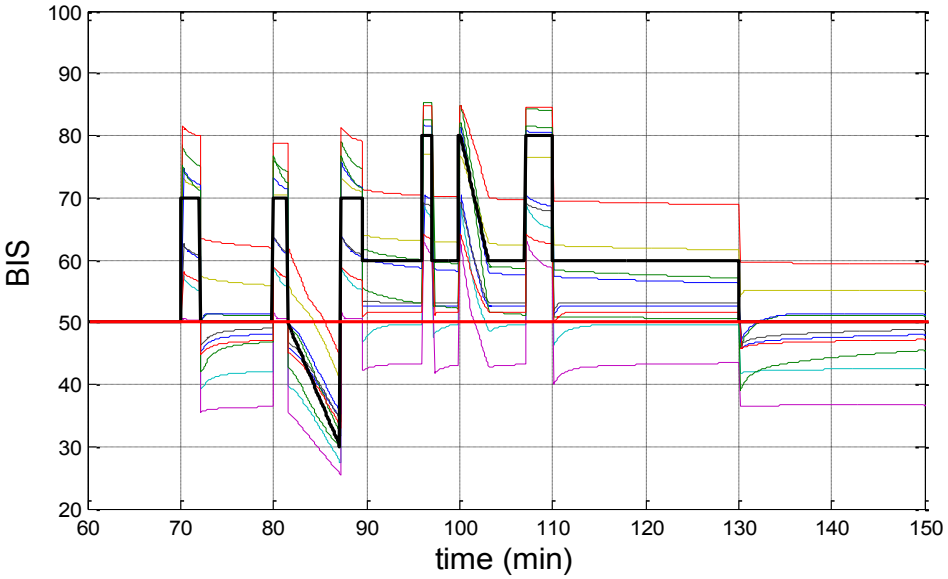

Figure 4.19: BIS output for all 13 patients – strategy 2 – maintenance phase

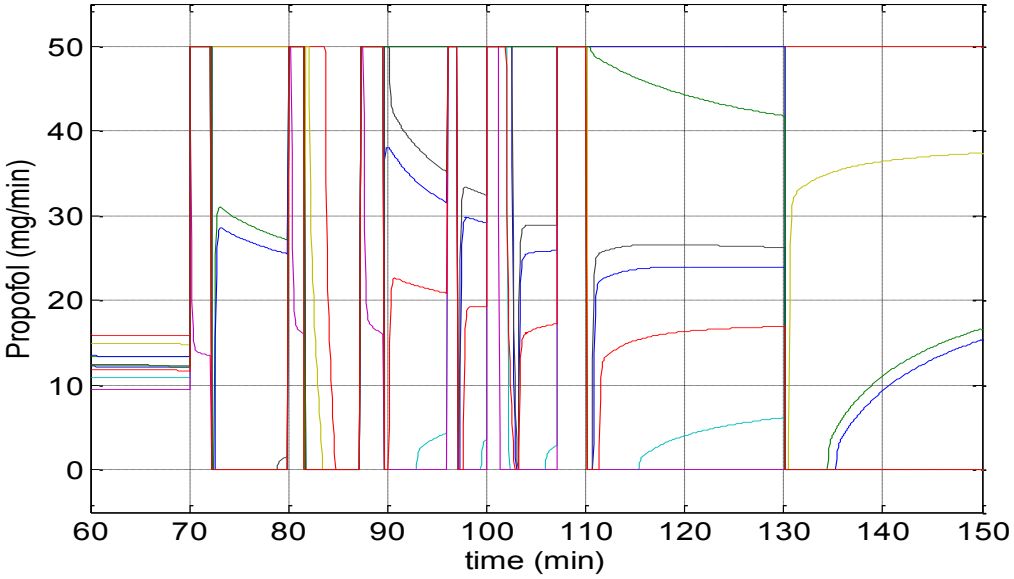

Figure 4.20: drug infusion for all 13 patients – strategy 2 – – maintenance phase

4.4.4 Strategy 3 - State-Output Correction

The advantage of this approach is that it tackles the underlying problem of the varying coefficients of the Hill-curve, and hence is conceptually more advanced. Additionally, it does not require an additional parameter in the system. However, it does require the measurement of the fourth state (which is the concentration of the drug in the blood), which would require additional equipment or the use of the inverse of the Hill curve using the nominal patient data (introducing extra errors). Hence from a practical point of view this approach seems to be infeasible at the current state of the art.

Figure 4.21 and Figure 4.22 we have the simulations of all patients and the nominal one for the induction phase where we have the BIS response and the corresponding Propofol infusion rate. Note that for this strategy the controller is only simulated in the induction phase since it can be observed that the performances of the offset free controller (Strategy 2) exhibits better performances.

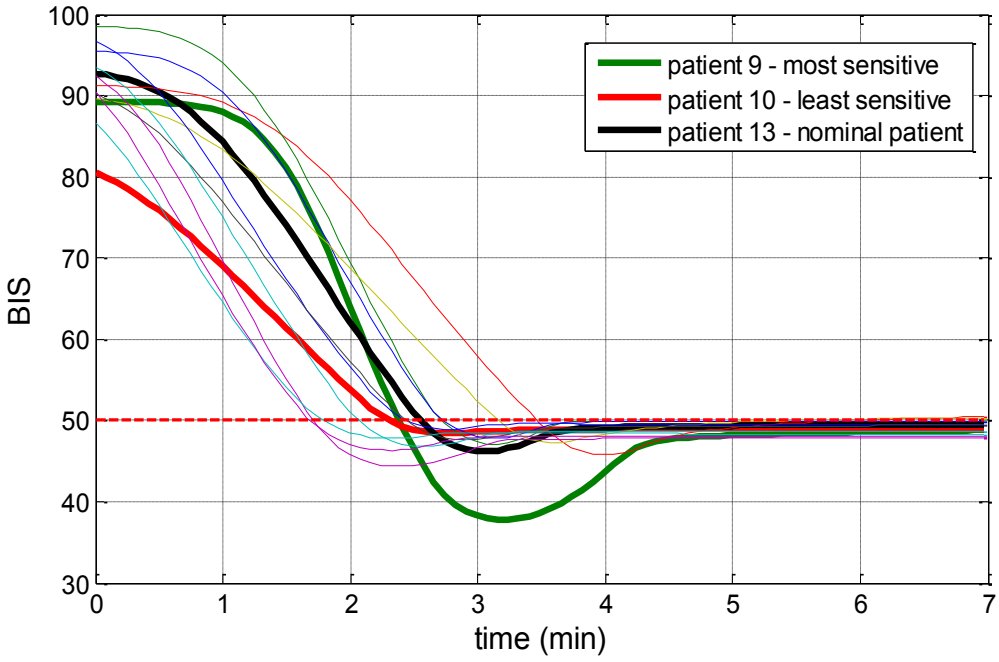

Figure 4.21: BIS output for all 13 patients – strategy 3 – induction phase

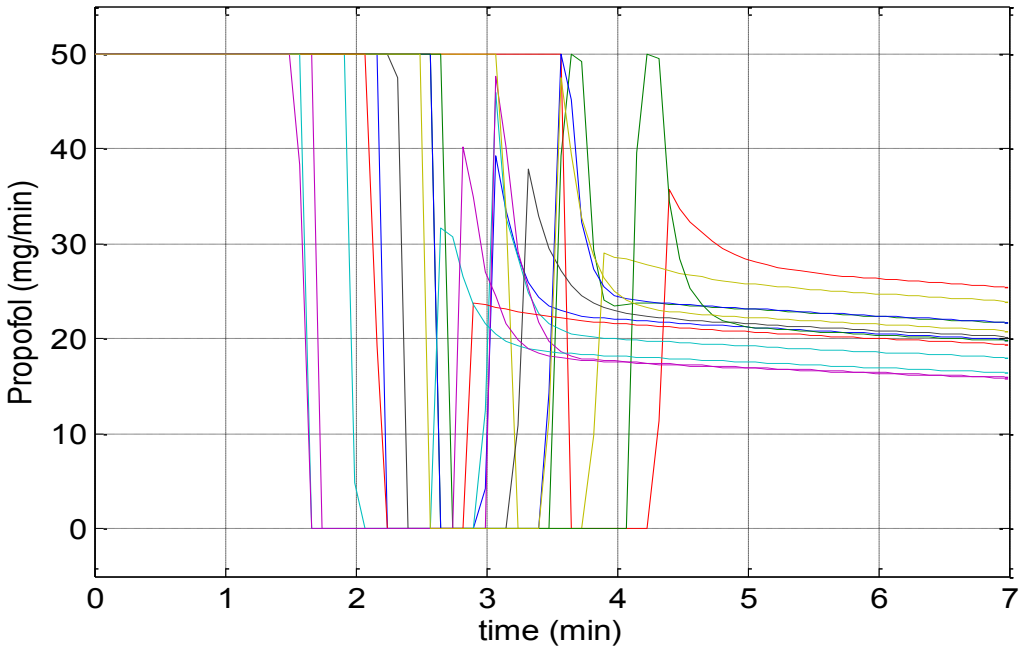

Figure 4.22: drug infusion for all 13 patients – strategy 3 – induction phase

4.4.5 Strategy 4 - Prediction-Output Correction

Unlike the previous method, this method allows for the quantification of the mismatch between the linearization and the actual output without requiring any new parameters nor extra measurements. The only obstacle is that it needs be ensured that during the fitting process no other disturbances are present. However, in the setting of the surgery, such disturbances can be avoided as the real disturbances occur during the incisions/loss of blood etc. which can be controlled.

In Figure 4.23 and Figure 4.24 we have the BIS response of all 13 patients and the nominal one in the induction phase and the corresponding Propofol infusion rate respectively. The average settling time is of 220 seconds and the maximum undershoot is 5.8%. It can be observed from the simulations performed in the induction phase that the mp-hMPC using offset correction (Strategy 2) exhibits better performances, hence the controller using Strategy 4 will be tested only in the induction phase.

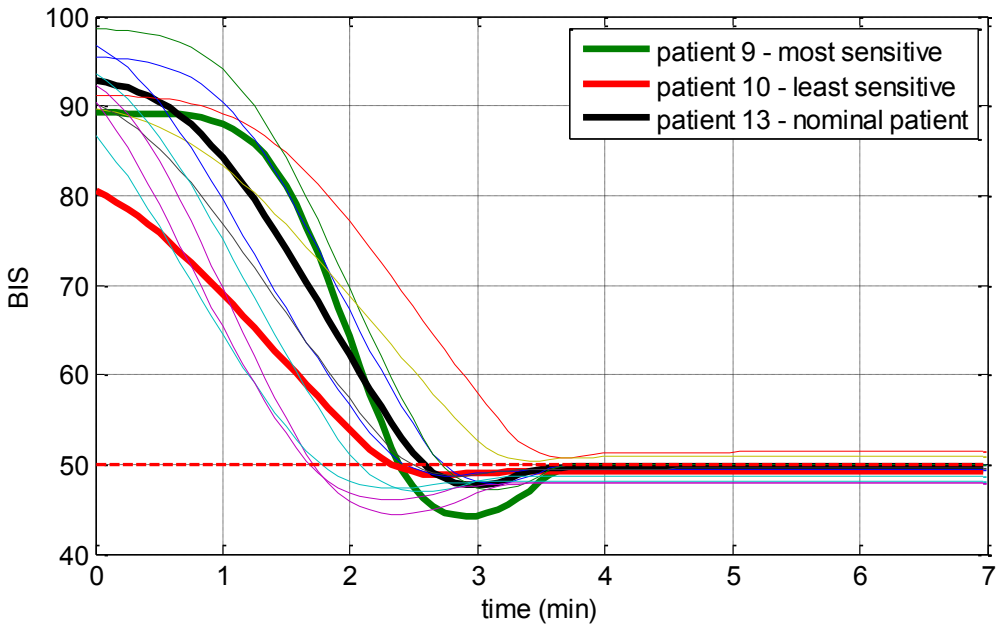

Figure 4.23: BIS output for all 13 patients – strategy 3 – induction phase

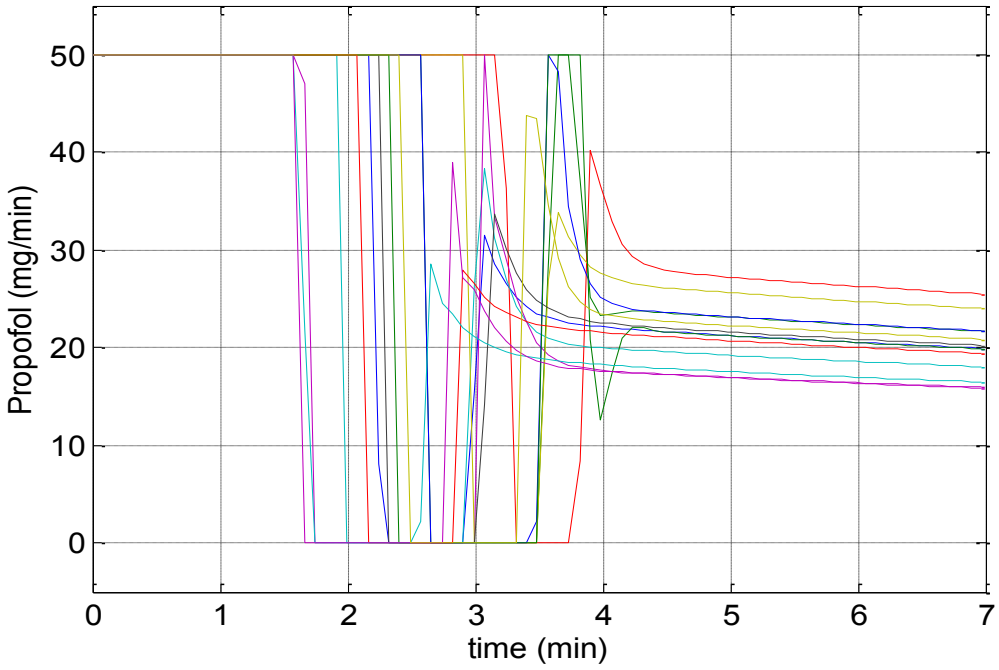

Figure 4.24: drug infusion for all 13 patients – strategy 3 – induction phase

4.4.6 Comparison

The nominal mp-hMPC controller (without any offset correction) is compared with the controller using estimation techniques and with one of the controllers using robust techniques, the simultaneous mp-MHE and mp-hMP, and the Offset Free mp-hMPC. The simulations are performed in the induction phase for two different patients: patient 2 and the most sensitive patient, patient 9.

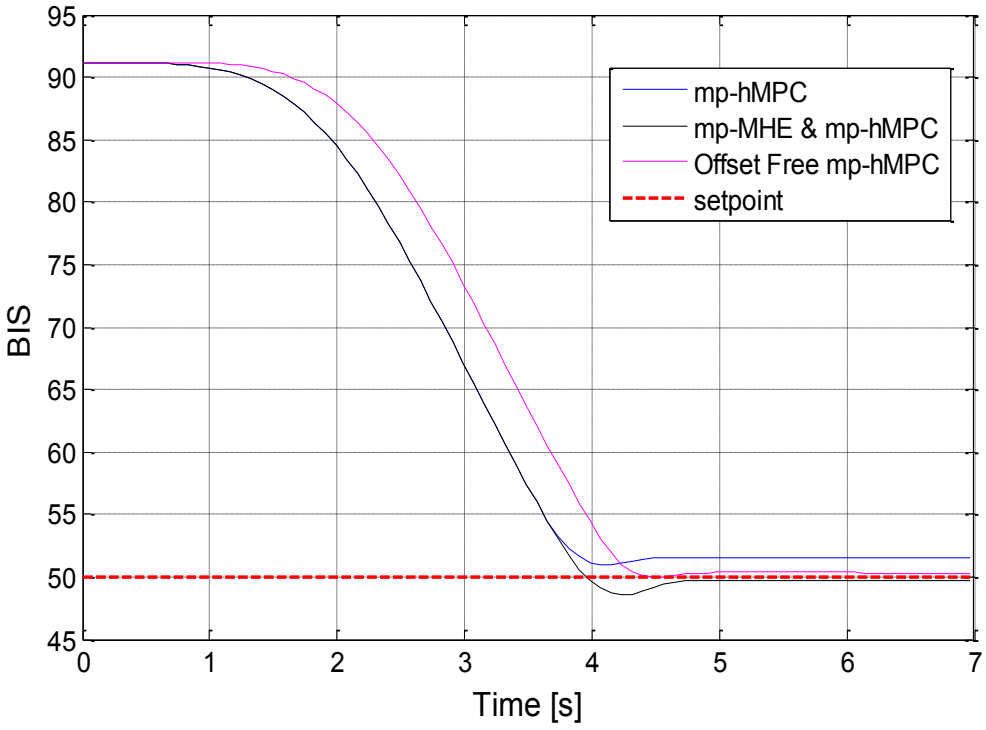

Figure 4.25: BIS response of the three controllers for patient 2 – induction phase

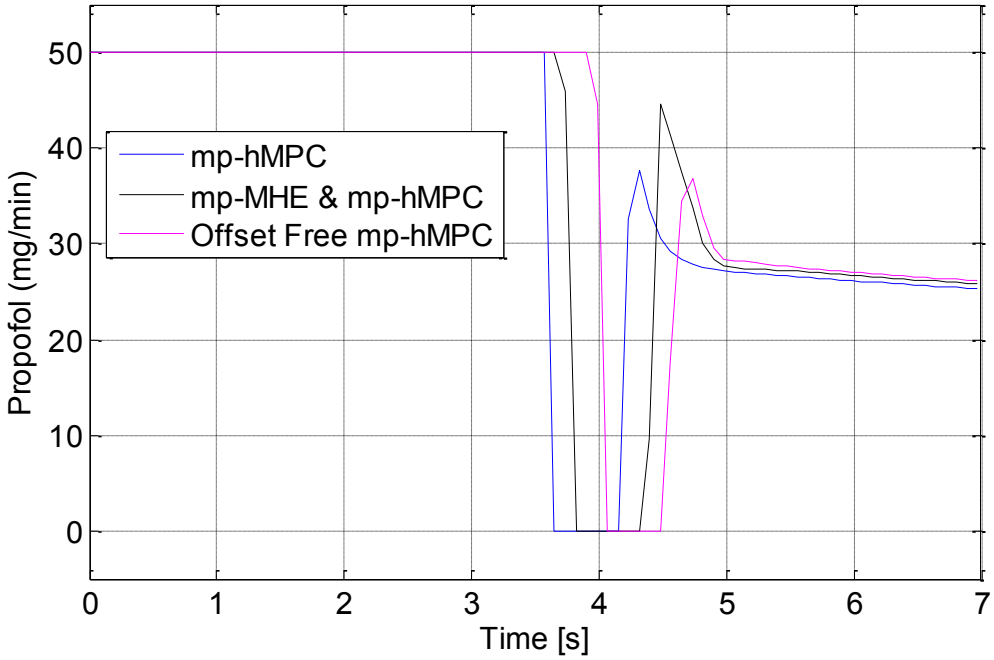

Figure 4.26: drug infusion of the three controllers for patient 2 –induction phase

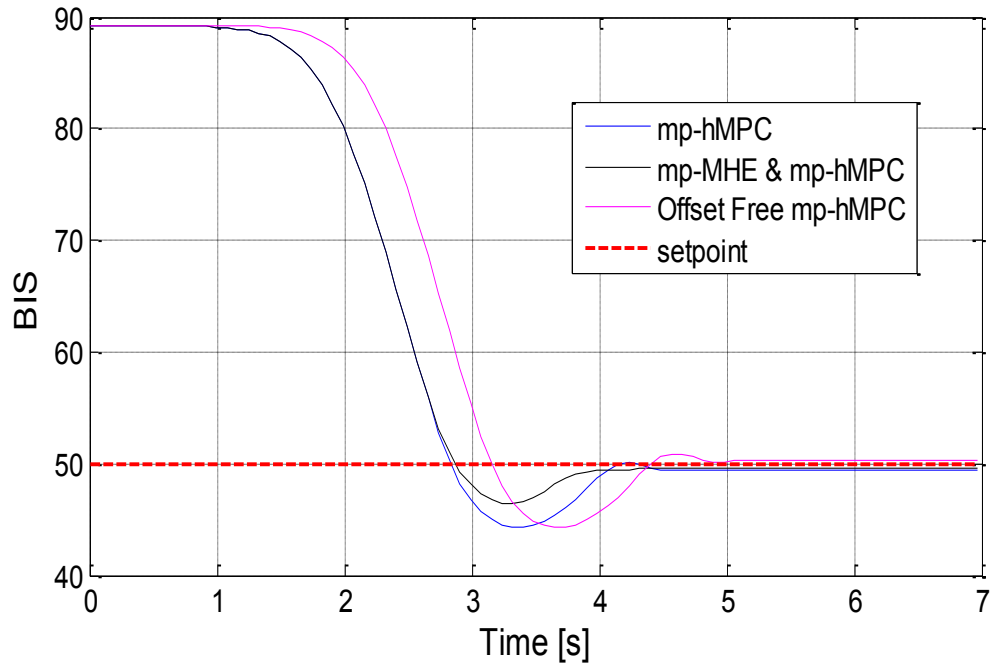

Figure 4.27: BIS response of the three controllers for patient 9 – induction phase

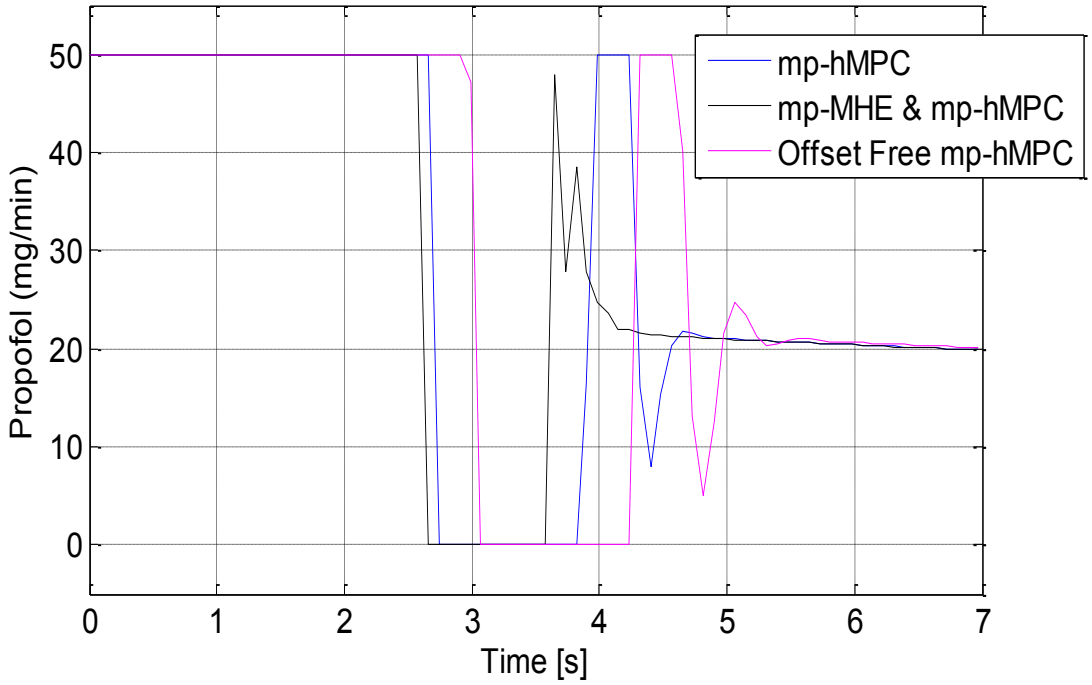

Figure 4.28: drug infusion of the three controllers for patient 9 – induction phase

The simulations of the comparison of the three controllers for patient 2 is presented in Figure 4.25 where we have the BIS response and Figure 4.26 where we have the corresponding control action. It can be observed that for the nominal controller there is an offset from the setpoint due to the inter- and intra- patient variability. By using robust or estimation techniques the offset can be corrected and the controllers will take the patient closer to the desired BIS setpoint of 50.

In Figure 4.27 we have the BIS response for patient 9 and Figure 4.28 presents the corresponding control action. As for patient 2, the controller that has no offset correction, presents an offset from the setpoint. The simultaneous mp-MHE and mp-hMPC gives the best performances: faster settling time, 240 seconds and an undershoot of 3.5%. The mp-hMPC using offset correction has a settling time of 288 seconds and an undershoot of 5.6%.

The comparison results show that the controller that uses the state estimates of each patient that is simulated is able to compensate better for the offset from the setpoint and also deal with the inter- and intra- patient variability.

4.5 Discussion

We have proposed a piece-wise affine formulation for a compartmental anaesthesia patient model, based on which a hybrid explicit/multiparametric MPC strategy is being developed. For the case when variability is not considered, it is shown that this requires the solution of a novel multiparametric mixed integer quadratic problem. In the presence of variability, a moving horizon estimation procedure and robust explicit MPC techniques were also incorporated within the overall hybrid explicit MPC strategy. These advanced control strategies are tested on a set of 12 patients and a nominal one for the automatic induction and control of DOA during induction and maintenance phase.

The resulting mp-hMPC controller was tested for the set of patients in the induction. For the nominal case with no offset correction, we can observe from Figure 4.7 - Figure 4.10 that, all patients present an offset from the desired target value with the exception of course of the nominal patient. This is due to the high inter- and intra- patient variability and can be compensated by making the control robust or using estimation techniques. Thus a number of robust techniques and an estimation strategy have been developed: (i) offset correction, (ii) state output correction, (iii) prediction output strategy, and (iv) moving horizon estimation. All the strategies have been tested for the set of patients in the induction phase. It can be observed that the applied strategies manage to correct the offset from the nominal case, therefore improving the performances of the controller. In the induction phase, the average settling time is of 250 seconds. The operation procedure does not start until the patient reaches an adequate DOA, usually taking up to 15 minutes. Thus, a rise time between 4 and 5 min gives good performances.

Even though some patients show small oscillations around the steady state values, the highest undershoot or overshoot is of 5.8%. For DOA undershoots or overshoots of up to

10% are acceptable provided that the setpoint is reached as soon as possible. This further confirms the satisfactory performance of the derived hybrid controller.

The nominal mp-hMPC as well as the simultaneous mp-MHE and mp-hMPC and the mp-hMPC using offset correction (the second strategy) are tested in the maintenance phase in order to see how well they can deal with disturbance rejection. In Figure 4.19, and Figure 4.15 the controllers response to a disturbance signal that mimics the events that occur in an operation theatre for all patients is shown. It can be observed that the robust controllers and the controller using mp-MHE are able to overcome the offset, especially around the value of 50, with the remaining offset due to limits imposed on the controller.

The performance of the nominal controller are also compared with two strategies: (i) moving horizon estimation and (ii) offset free. The simulations are performed in the induction phase for two of the patients: patient 2 and patient 9 (the most sensitive patient) and presented in Figure 4.25 - Figure 4.28. As expected, the simultaneous mp-MHE and mp-hMPC and the hybrid offset free are able to deal with the inter- and intra- patient variability showing better overall performance.

4.6 Conclusions

In this chapter we have dealt with two of the main challenges in the control of the intravenous depth of anaesthesia: nonlinearity and inter-and intra- patient variability. To deal with the nonlinearity, a piece-wise linearization of the Hill curve was presented leading to a hybrid model-predictive control formulation which was solved explicitly offline via multiparametric quadratic programming algorithms. To account for the inter- and intra- patient variability, multiparametric moving horizon estimation as well as several robust algorithms were implemented simultaneous with multiparametric model predictive control. A simulation study was performed on a set of 12 patients for the induction and maintenance phase of intravenous anaesthesia for the designed strategies. Moreover, the performance of the most relevant strategies and the nominal controller

were compared with each other for two of the patients, including the most sensitive one. It is shown that the designed controllers are able to deal with the nonlinearities introduced by the Hill curve and exhibit good performances with no significant undershoot or overshoot and a fast settling time. The hybrid controllers using the simultaneous mp-MPC and mp-hMHE as well as the offset correction show better performances and are able to deal with the offset problem. Furthermore, they are able to overcome the inter- and -intra patient variability proving a high-efficiency, optimal dosage and robustness of the model predictive control algorithm to induce and maintain the desired Bispectral Index reference while rejecting typical disturbances from surgery.

Another important characteristic of using hybrid formulation and multiparametric model predictive control on the intravenous anaesthesia process is that it can be adapted to other drug delivery systems since the Hill curve is used to describe the nonlinearity in most of them.

Chapter 5

PAROC Framework for the Anaesthesia Process

5.1 Introduction

Model based optimization techniques have been proven to be essential for the control and operation of complex processes. In this context, model predictive control (MPC) - a model based control technique that calculates the optimal control action considering constraints on the input, output and state variables by solving an optimization problem at every sampling point (online) is perhaps the most widely accepted technology for advanced control applications.

Explicit/multiparametric MPC where the solution of the online optimization problem can be obtained using off-line multiparametric programming has also received a lot of attention in the last fifteen years. A key feature of explicit/multiparametric MPC is that the governing control laws of the system at hand i.e., the control input as a function of the system states can be explicitly obtained, facilitating the implementation of MPC on embedded devices.(Bemporad et al., 2002g, Pistikopoulos et al., 2007a, Pistikopoulos, 2009)

The ability to derive in an explicit form the underlying control laws is particularly important for safety-critical applications, such as the control of drug delivery systems. Here we focus on the control of the depth of anaesthesia (DOA), which plays an important role in surgery and the intensive care unit. As the role of the anaesthetist has become more complex and indispensable to maintain the patients' vital functions before, during and after surgery, the automation of the drug/anaesthetic administration may reduce workload while offering additional support during critical situations. Optimization of the drug infusion rates is also important for the safety of the patient and reduction of potential side-effects. While the control of DOA has been studied in the open literature,(Krieger et al., 2012, Krieger et al., 2014, Gentilini et al., 2001, Ionescu et al.,

2011c, Nascu et al., 2011, Nascu et al., 2015c, Curatolo et al., 1996, Struys et al., 2003, Ionescu et al., 2008, Hodrea et al., 2012, Caiado Daniela et al., 2013, Dumont et al., 2009, Haddad et al., 2003, Nascu et al., 2012, Sartori et al., 2005, Nascu et al., 2014e) it still remains a rather challenging task, mainly due to features such as inter-/intra- patient variability, variable time delays and nonlinearities.(Haddad et al., 2003, Absalom et al., 2011).

Complex systems such as the control of depth of anaesthesia presented in this chapter, control of drug delivery systems and in general biomedical processes often require advanced techniques for modelling, optimization and control. Complexity typically arises from the physical and operational characteristics of the processes such as periodicity, discontinuities, nonlinearity, time delays and large scale models. For advanced control applications, there is a clear need to address complexity issues in a systematic way in tandem with contemporary simulation software tools. Moreover, there is a need to address complex systems such as biomedical systems in a systematic way (Bogle, 2012).

The development of PAROC (PARametric Optimization and Control),(Pistikopoulos et al., 2015) targets these issues in a step-by-step procedure including advanced modelling, approximation and state-of-the-art multi-parametric programming and explicit control techniques. A key feature of the framework is the closed-loop validation of the advanced controller against the high fidelity model. The PAROC framework is particularly suitable for safety-critical applications, and is applied to the process of intravenous and volatile anaesthesia process with the specific aim to overcome issues related to patient variability.

This chapter is organized as follows: the PAROC framework is described step by step in Section 5.2. Section 5.3 presents the application of the presented framework on the process of intravenous anaesthesia while Section 5.4 presents the framework through the volatile anaesthesia process. Discussions are presented in Section 5.5 while the main outcome of this chapter is presented in Section 5.6.

5.2 The PAROC framework

The PAROC framework presented in Figure 5.1,(Pistikopoulos et al., 2015) enables the solution of complex optimization control problems using a step-by-step-procedure to obtain explicit MPC control strategies. The framework starts from the development of a high-fidelity model of the system that could be approximated using discrete time models in state space form via model order reduction techniques or system identification techniques. The reduced model is then used to formulate an mp-MPC problem subject to the state space model and constraints. The resulting multiparametric programming problem is solved with state-of-the-art techniques and the map of the optimal control actions is acquired. Due to the fact that in many processes the measured output may be noisy and the system measurements do not produce this information directly, the state information needs to be inferred from the available output measurements. Therefore, a state estimator is implemented in the framework simultaneously with the mp-MPC. In the last step, the solution is validated against the original high fidelity model, thus closing the loop.

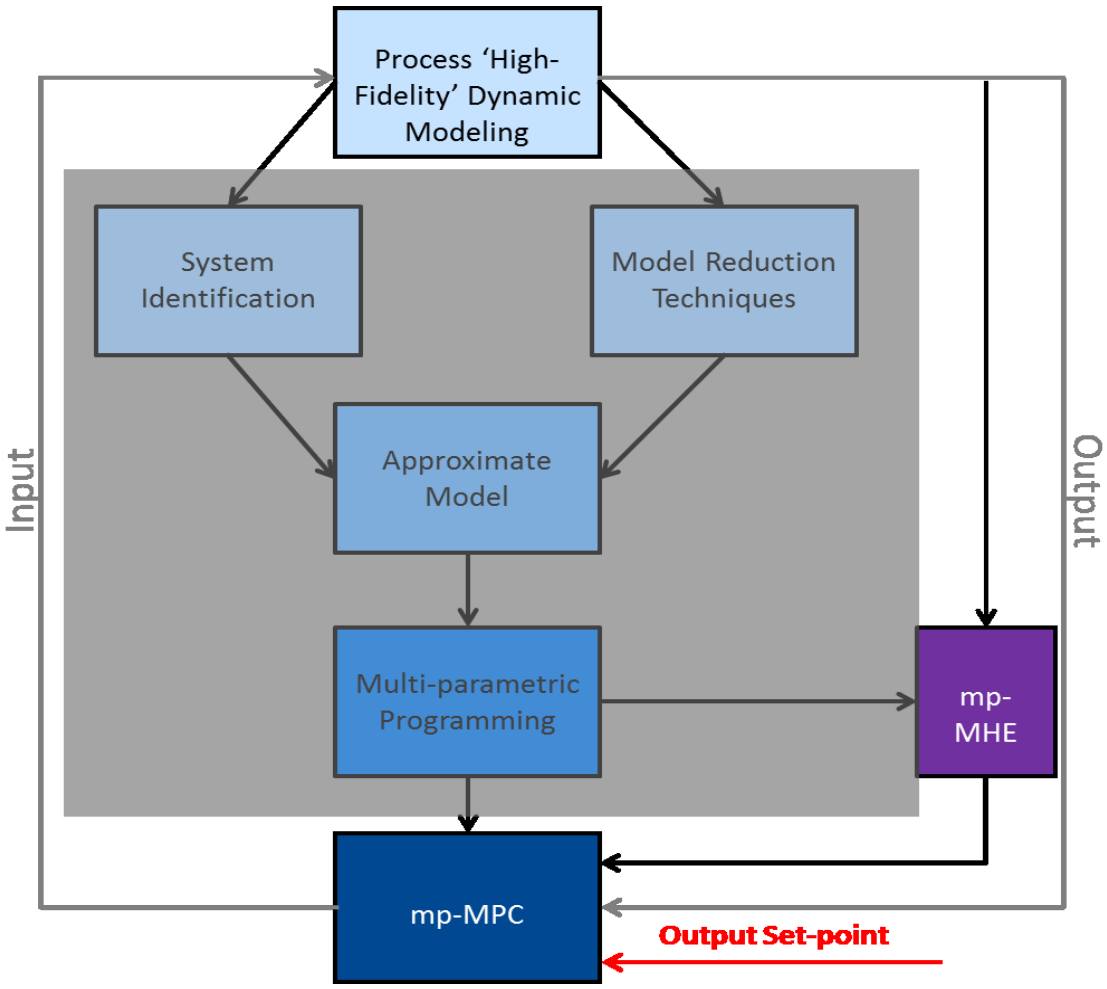

Figure 5.1: The PAROC framework

One of the key advantage of the PAROC framework is that it follows a multiparametric approach for the controller design that transfers the computational burden offline(Pistikopoulos, 2000). Furthermore the framework is versatile and process-independent with wide applicability;(Nascu et al., 2015a) implemented to systems including: (i) a combined heat and power (CHP) cogeneration system for residential use, (Diangelakis et al., 2014, Diangelakis et al., 2015) (ii) distillation column, (Nascu et al., 2014e) (iii) a periodic chromatographic separation system of monoclonal antibodies, (Papathanasiou et al., 2015) (iv) pressure swing absorption, (Khajuria et al., 2011) (v) PEM fuel cell energy systems, (Panos et al., 2012, Ziogou et al., 2011) (vi) hydrogen storage tank, (Panos et al., 2010) (vii) batch polymerization system, (Asteasuain et al.,

2006) (viii) wind turbines, (Kouramas et al., 2011a) and (ix) drug delivery systems including anaesthesia, (Nascu et al., 2015c) type-1 diabetes, (Zavitsanou et al., 2014, Zavitsanou et al., 2015) and leukemia (Fuentes-Garí et al., 2015, Velliou et al., 2014). PAROC addresses different classes of control problems such as: (i) nominal mp-MPC, (ii) hybrid mp-MPC, (iii) robust mp-MPC, (iv) simultaneous mp-MPC and moving horizon estimation, (v) integration of scheduling and control, (vi) development of mp-MPC for periodic systems. The main features of PAROC are briefly discussed next.

5.2.1 High – Fidelity Modelling

The first step of the framework corresponds to the development of a high-fidelity model of the process, model analysis (for example through global sensitivity analysis), (Saltelli et al., 2006, Kiparissides et al., 2009) parameter estimation and dynamic optimization of the developed model. The validated high-fidelity model most commonly features nonlinear (partial) differential and algebraic equations ((P)DAEs) which can be developed in a high-level environment such as PSE's gPROMS® ModelBuilder (PSE, 1997-2014).

5.2.2 Model Reduction

Sometimes it is necessary to reduce the original high fidelity model to a linear state space of lower dimensionality. In PAROC this can be done in two ways: either through (i) system identification or (ii) model reduction techniques. System identification is most commonly performed using the System Identification Toolbox in MATLAB®. Model order reduction techniques are also available (Narciso et al., 2008, Lambert et al., 2013) and presented in detail in Appendix B.

5.2.3 Multiparametric Optimization & Control Strategy

Once an accurate state-space model is obtained the corresponding MPC problem is formulated explicitly by treating the states, output setpoints, measured disturbances and past inputs as parameters (Bemporad et al., 2002g). The solution of such an explicit/multiparametric model predictive control (mp-MPC) formulation requires the solution of a multiparametric programming problem. The main characteristic of mp-MPC is its ability to obtain: (i) the objective and optimization variable as a function of the varying parameters, and (ii) the regions in the space of the parameters where these functions are valid (critical regions) (Pistikopoulos et al., 2007a). This reduces the online implementation of the MPC to simple function evaluation, facilitating real time applications. To facilitate the solution of such problems the Parametric Optimization toolbox (POP), (ParOs, 2004) is used. POP is a solver for multiparametric linear and quadratic programming problems based on a variable step-size geometrical approach (Baotic, 2002). Key developments in multiparametric programming and multiparametric/explicit MPC are shown in Table 5.1 and Table 5.2.

Table 5.1: Key developments in multiparametric programming

Types	Theoretical development	Authors
mp-LP	finding the optimal basis by evaluating a connected graph	(Gal et al., 1972)
	explores the parameter space using the properties of the generated polytopes	(Bemporad et al., 2002a)
mp-QP	a geometrical approach as presented for mp-LP problems	(Dua et al., 2002i) (Bemporad et al., 2002g) (Baotic, 2002)

	combinatorial (also called 'reverse transformation') approach where the combination of all possible active sets of constraints are considered	(Gupta et al., 2011a) (Seron et al., 2000)
mp-MILP	branch-and-bound approach in conjunction with suitable comparison and fathoming procedures	(Acevedo et al., 1997a, Acevedo et al., 1999) (Oberdieck et al., 2014g)
	decomposition-type approach which alternates between a mixed-integer linear programming (MILP) and a mp-LP problem	(Dua et al., 2000) (Wittmann-Hohlbein et al., 2012, Wittmann-Hohlbein et al., 2013)
mp-MIQP	a decomposition-type approach that relies on global optimization	(Dua et al., 2002i) (Oberdieck and Pistikopoulos, 2015)
	branch-and-bound approach	(Oberdieck et al., 2014g) (Axehill et al., 2014a)

Table 5.2: Key developments in multiparametric model predictive control

Types	**Theoretical development**	**Authors**
nominal MPC	Nominal mp-MPC problems	(Bemporad et al., 2002g) (Pistikopoulos, 2009, Pistikopoulos et al.,

		2007) (Nikandrov et al., 2009)
hybrid mp-MPC	multiparametric model-based control of systems that are described by both linear as well as logical dynamics	(Dua et al., 2002i) (Oberdieck and Pistikopoulos, 2015) (Axehill et al., 2014a) (Nascu et al., 2015e) (Trifkovic et al., 2014)
robust mp-MPC **(the immunity of a system against perturbations)**	Additive disturbances	(Sakizlis et al., 2004c) (Alamo et al., 2005) (Olaru et al., 2006) (Raković et al., 2008)
	Model uncertainities	(Pistikopoulos et al., 2009) (Ricardez Sandoval et al., 2008)
	Min-max robust mp-MPC	(Alamo et al., 2005) (Bemporad et al., 2003) (Ricardez Sandoval et al., 2008) (Muñoz De La Peña et al., 2006)

	Linear input/output model	(Olaru and Ayerbe, 2006) (Muñoz de la Peña et al., 2005)

5.2.4 Moving Horizon Estimation

A main assumption in the implementation of the previous presented strategies is that accurate, noise-free information i.e., measurements is available for all system states. Since this is rarely the case, state estimators is used for the unavailable states as well as in order to overcome issues that arise from noisy outputs. In particular, moving horizon estimators (MHE), implemented in a multiparametric fashion are used (Darby and Nikolaou, 2007, Voelker et al., 2013). The resulting mp-MHE can be used simultaneously with mp-MPC within the PAROC framework.

5.2.5 Validation

The last step of the PAROC framework is the off-line closed loop validation, aiming to test the controller against the original high fidelity model developed in the first step. This (i) establishes the accuracy and robustness of the controller and (ii) the consistency of the approximate model; depending on the outcome of the validation step the explicit controller can be redesigned and revaluated.

5.2.6 Software Platform

Within the PAROC framework, the high-fidelity modelling and analysis step is performed in gPROMS® ModelBuilder or in MATLAB® for simpler models. The formulation and solution of the multiparametric programming problem is carried out in POP, (ParOs, 2004) within MATLAB®. The closed-loop validation of the developed controller can be performed in two ways. The first approach includes the simulation of the high-fidelity model as well as the controller through MATLAB® using PSE's

gO:MATLAB to simulate the high fidelity model as a single function call in the MATLAB® environment. This approach provides an effortless way of closing the loop but the user is unable to utilize the capabilities of the gPROMS® family to their full extent. As a result a tool that inserts the mp-MPC solution directly in gPROMS® has been developed. A dynamic link library (dll) is generated in C++ that contains the solution of the multiparametric programming control problem provided by POP. The dll is then called within the gPROMS® environment. A representation of the PAROC software platform is presented Figure 5.2.

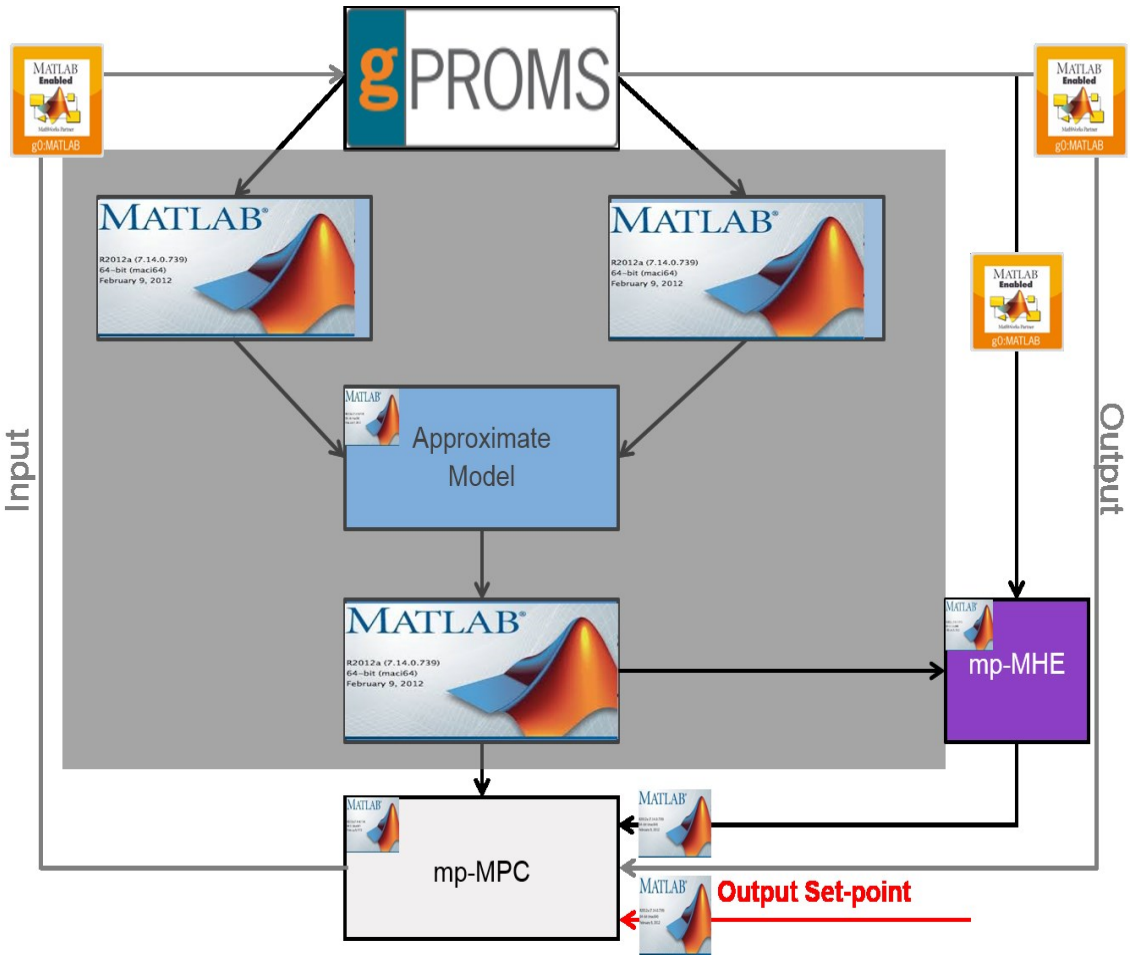

Figure 5.2: The PAROC platform software

5.3 The PAROC Framework for Intravenous Anaesthesia

This section presents the application of the PAROC framework for the design and development of multiparametric model predictive controllers for the induction and maintenance phases of intravenous anaesthesia. As presented in the previous section, for the automatic depth of anaesthesia (DOA), the intravenous agent Propofol is the input with the Bispectral Index (BIS) as the output of the system.

5.3.1 High – Fidelity Modelling

The high fidelity model used for intravenous control of depth of anaesthesia is presented in detail in Chapter 2.1.

5.3.2 Model Reduction

The intravenous anaesthesia model presented in Chapter 2.1 and used for this study does not require model reduction. Hence it can be used directly for optimization and control via multiparametric programming. Model reduction has been applied for the case of volatile anaesthesia, (Nascu et al., Krieger et al., 2012) where the mathematical model is more complex.

5.3.3 Multiparametric Optimization & Control Strategy

The anaesthesia/patient mathematical model presented in the Chapter 2.1 together with the patient data provided in Table 2.1 provide the basis for the development of the explicit/multiparametric model predictive control strategy, which is described Chapter 2 Chapter 3 and Chapter 4.

5.3.4 Moving Horizon Estimation

The moving horizon estimation formulation is presented in Chapter 3 along with the simultaneous multiparametric model predictive control and multiparametric moving horizon estimation formulation.

5.3.5 Validation

In this step the simultaneous estimator and controller for automatic induction and control of DOA is tested against the original high fidelity model both for the induction and maintenance phases of general anaesthesia. The closed loop control tests are performed on the set of the 12 patients presented Table 2.1. In chapter 2 we have the results for the multiparametric model predictive control of DOA, in Chapter 3 the results for simultaneous multiparametric model predictive control and multiparametric moving horizon estimation and in Chapter 4 we present the simulations for the hybrid multiparametric model predictive control.

5.4 The PAROC Framework for Volatile Anaesthesia

This section presents the application of the PAROC framework for the design and development of multiparametric model predictive controllers for volatile anaesthesia. The PAROC framework applied on the process of anaesthesia is presented in Figure 5.3

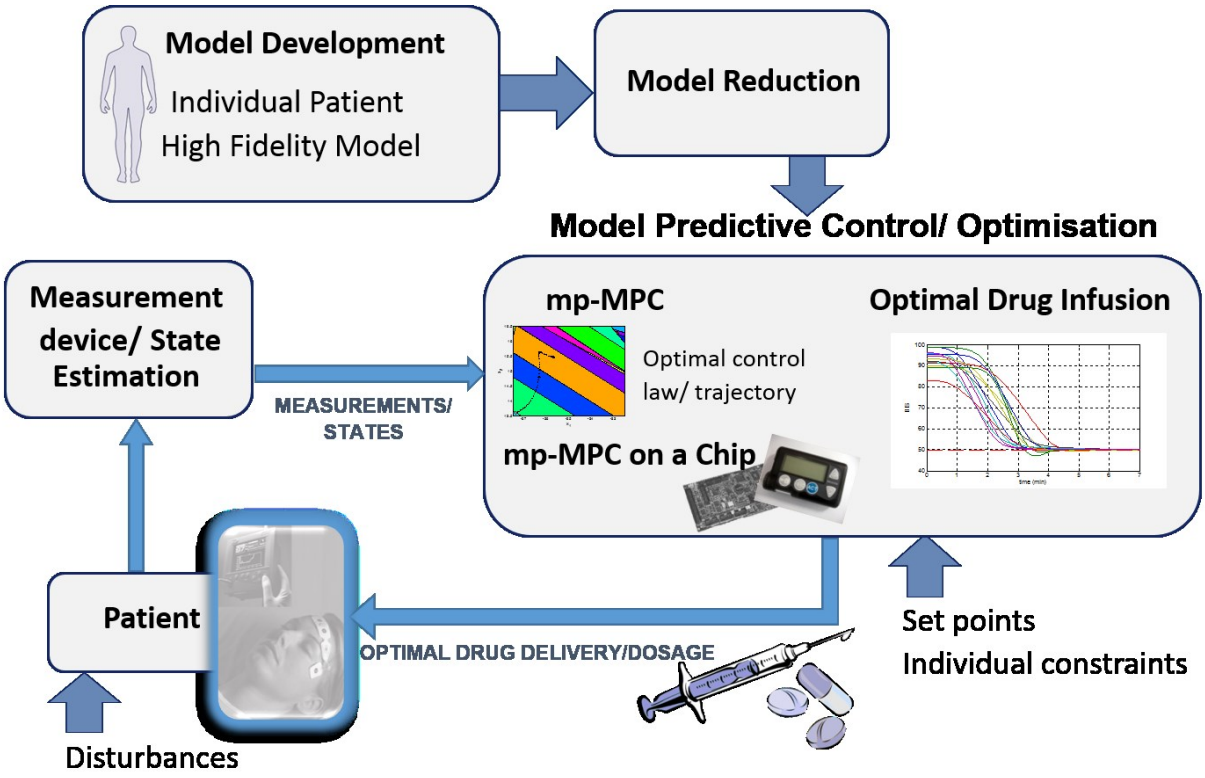

Figure 5.3: PAROC framework for anaesthesia system

5.4.1 High – Fidelity Modelling

A suitable model for prediction should capture the dynamics of the patient in response to the applied anaesthetic signal. The relationship between the drug infusion rate and its effect can be described with pharmacokinetic (PK) and pharmacodynamic (PD) models used to represent the distribution of drugs in the body. The PK model follows the distribution of the drug in the body while the PD model describes the relationship between the drug blood concentration and its clinical effect.

5.4.1.1 Pharmacokinetic Model

The physiologically based four compartmental model was developed by Eger (Eger, 1974) and is presented in Figure 5.4 (a). These compartments are the vessel rich group

(VRG), the muscle group (M), the adipose tissue (F) and the vessel poor group (VPG). Each compartment is further sub-divided into an ideally mixed blood and ideally mixed tissue part as presented in Figure 5.4 (b). All compartments are further sub-divided into blood and tissue parts. A detailed description of the model can be found in (Krieger et al., 2014).

The equations describing the uptake of the anaesthetic in the body compartments are presented below:

$$
\begin{aligned}
V_{b,i}\frac{dC_{b,i}}{dt} &= Q_i(C_a - C_{b,i}) - Q_i(\lambda_i C_{b,i} - C_{t,i}) \\
V_{t,i}\frac{dC_{t,i}}{dt} &= Q_i(\lambda_i C_{b,i} - C_{t,i}) \\
V_{t,VRG}\frac{dC_{t,VRG}}{dt} &= u_{t,VRG} - \dot{Q}_{liv} C_{t,VRG} m_{liv} \\
\dot{Q}_i &= r_{\dot{Q},i}\dot{Q} \\
V_{t,i} &= r_{V,i} V \\
V_{b,i} &= r_{V_{b,i}} V_b
\end{aligned}
\qquad \text{(Equation 5.1)}
$$

where V_b is the blood volume, V_t, the tidal volume, Q is the cardiac output, C_b, the concentration of the anaesthetic in the blood, C_t, is the concentration of the drug in the tissue, u_t is the anaesthetic uptake by the tissue, r_Q is the ratio of the cardiac output, r_V the ratio of the total lung volume and λ is the blood gas partition coefficient and C_a is the concentration of the blood in the arterial blood.

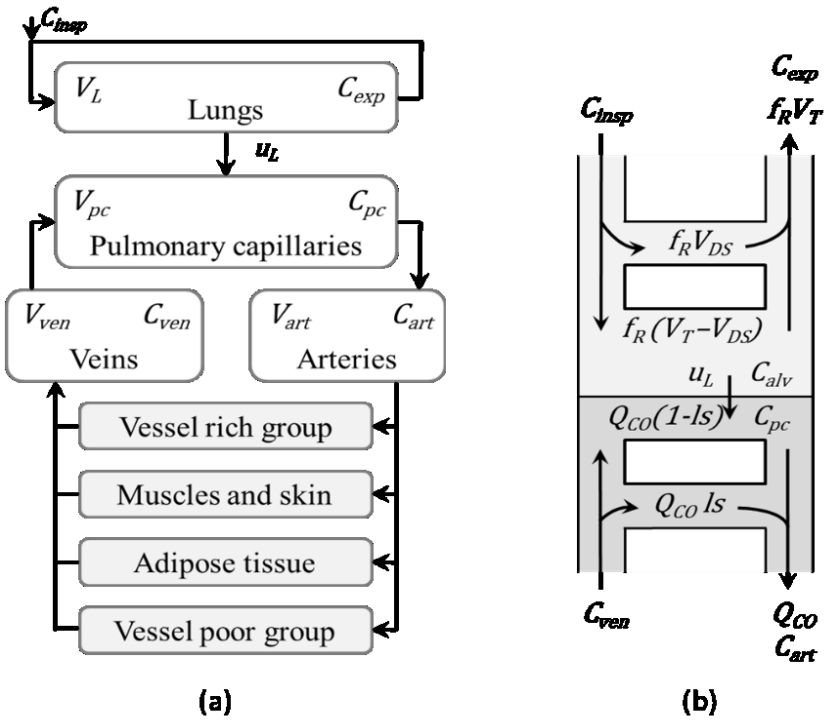

Figure 5.4: Volatile anaesthesia - (a) Structure of the physiological based model (b) detailed fluxes of gas and blood in the lungs

Two factors, the ventilation of air and the perfusion of blood through the lungs determine the uptake of the anaesthetic agent occurring in the lungs. The equations describing the anaesthetic uptake in the lungs are given as follows:

$$
\begin{aligned}
&\dot{V}_A = \dot{V} - \dot{V}_D = f_R(V_T - V_D) \\
&V_A = V_L - V_D \\
&C_{A_I}(V_A + V_T) = C_I V_T + C_E V_A \\
&C_E = \frac{C_{\bar{v}}}{\lambda} \\
&u_L = (\dot{Q} - \dot{Q}_s)(\lambda C_{A_I} - C_{\bar{v}}) \\
&C_a \dot{Q} = C_{\bar{v}} \dot{Q} + u_L \\
&C_{\bar{v}} = \sum_i r_{\dot{Q},i} C_{b,i} + (1 - \sum_i r_{\dot{Q},i}) C_a
\end{aligned}
\qquad \text{(Equation 5.2)}
$$

where V is the total minute ventilation, V_A is the alveolar ventilation, V_L, the lung volume, V_D is the dead-space ventilation, V_T, the tidal volume, C_a is the concentration of the drug in the arterial blood, C_A the is the concentration of the drug in the alveoli just after inspiration, C_E the end-tidal expired concentration, C_v is the mixed venous blood concentration and u_L is the anaesthetic uptake by the lungs.

To obtain an individualized patient model the parameters and variables in (Equation 5.1) and (Equation 5.2) described as a function of the patient's weight, age, height and gender (male=1, female=0).

Calculation of patient specific tissue mass:

$$\begin{aligned} m_{ideal} &= 22 \cdot h^2 \quad \text{with } BMI = \frac{m[kg]}{(h[m])^2} \\ m_F &= (1.2BMI - 10.8gender + 0.23age - 5.4) \cdot 0.01m \\ m_{VPG} &= 0.2m \\ m_{VRG} &= 0.1m \\ m_M &= m - m_F - m_{VPG} - m_{VRG} \end{aligned} \qquad \text{(Equation 5.3)}$$

Calculation of the patient specific blood volume

$$\begin{aligned} V_{B,f} &= 0.3561h^3 + 0.03308m + 0.1833 \\ V_{B,m} &= 0.3669h^3 + 0.03219m + 0.6041 \end{aligned} \qquad \text{(Equation 5.4)}$$

Calculation of patient specific cardiac output

$$\dot{Q} = 5.84 + 0.08BMI - 0.03age - 0.62(1 - gender) \qquad \text{(Equation 5.5)}$$

Calculation of patient specific lung volume

$$V_L = 11.97 \exp(-0.096 BMI) + 0.46 \qquad \text{(Equation 5.6)}$$

C[vol%] is the concentration, Q_{CO} *[mL/min]* the cardiac output, *Q [mL/min]* the blood flow, *V [mL]* the volume, V_T *[mL]* the tidal volume, V_{DS} *[mL]* the dead space, f_R *[1/min]* the respiratory frequency, *ls* the lung shunt.

Assuming a constant tidal volume, V_T, and a constant respiratory frequency, f_R, the PK equations result in a linear state space system with the arterial blood concentration, C_a, as output and the inhaled concentration of the anaesthetic agent, C_I, as input of the system.

5.4.1.2 Pharmacodynamic Model

The pharmacodynamics describe the link of concentration of the anaesthetic agent to the effect of the drug.

An additional hypothetical effect compartment is added to represent the lag between plasma drug concentration and drug response. Its corresponding drug concentration is represented by the *effect-site compartment concentration* $C_{e,}$ and k_{e0} denotes the delay of the drug action. The effect compartment receives drug from the central compartment by a first-order process and is considered as a virtual additional compartment. For volatile anaesthesia C_a denotes the concentration in the arterial blood calculated in (Equation 5.2) and the PD mathematical model is presented as follows:

$$\dot{C}_e(t) = k_{e0} \cdot (C_e(t) - C_a(t)) \qquad \text{(Equation 5.7)}$$

$$BIS(t) = E_0 - E_{\max} \cdot \frac{C_e(t)^{\gamma}}{C_e(t)^{\gamma} + EC_{50}^{\gamma}} \qquad \text{(Equation 5.8)}$$

5.4.2 Model Reduction

For the design of a simultaneous control and estimation strategy, in the cases where the models are too complicated to be used directly for control studies, reduced models are first derived based on the model reduction scheme described in (Nascu et al., 2014e). This approach (i) reduces the computational complexity on both the controller and estimator since they no longer require full state information, and (ii) avoids any estimation errors due to poor/inadequate observability of some of the states (Singh et al., 2005). For volatile anaesthesia, since the model in use is more complicated than for the intravenous anaesthesia, model order reduction is performed before proceeding to control studies.

The state space matrices for the full volatile anaesthesia model are presented below:

$$A = \begin{pmatrix} 0.68 & 0.07 & 0.04 & 0.01 & 0.01 & 0.0003 & 0.0002 \\ 0 & 0.02 & 0.32 & 0.01 & 0.01 & 0.002 & 0.0003 \\ 0 & 0.31 & 0.75 & 0.009 & 0.004 & 0.002 & 0.0001 \\ 0 & 0.04 & 0.04 & 0.05 & 0.28 & 0 & 0.0002 \\ 0 & 0.003 & 0.001 & 0.02 & 0.99 & 0 & 0 \\ 0 & 0.002 & 0.003 & 0.0002 & 0.001 & 0.001 & 0.02 \\ 0 & 0.001 & 0.001 & 0.0002 & 0 & 0.01 & 0.99 \end{pmatrix}$$

$$B = \begin{pmatrix} 0.18 \\ 0.22 \\ 0.099 \\ 0.159 \\ 0.006 \\ 0.012 \\ 0.004 \end{pmatrix}$$

$$C = \begin{pmatrix} 1 & 0 & 0 & 0 & 0 & 0 & 0 \end{pmatrix}$$

$$D = 0$$

(Equation 5.9)

Model order reduction techinques are applied on the full anaesthesia model as presented in Appendix B and the resulting reduced model is presented below:

$$A = \begin{pmatrix} 0.827 & -0.063 & -0.041 & -0.064 \\ -0.063 & 0.961 & -0.033 & -0.056 \\ -0.041 & -0.033 & 0.968 & -0.059 \\ -0.064 & -0.056 & -0.059 & 0.886 \end{pmatrix}$$

$$B = \begin{pmatrix} -0.409 \\ -0.086 \\ -0.049 \\ -0.073 \end{pmatrix} \quad \text{(Equation 5.10)}$$

$$C = \begin{pmatrix} -0.409 & -0.086 & -0.049 & -0.073 \end{pmatrix}$$

$$D = 0$$

5.4.3 Moving Horizon Estimation

For the design of the estimation strategy in this case, the volatile anaesthesia model presented in Chapter 5.4.1 is reduced from 7 states to 4 (see chapter 5.4.3). This approach (i) reduces the computational complexity on the estimator since they no longer require full state information, and (ii) avoids any estimation errors due to poor/inadequate observability of some of the states (Singh and Hahn, 2005). The three types of estimators (the Kalman filter, online MHE and mp-MHE) are designed and implemented similar to the intravenous anaesthesia cases.

For the mp-MHE, the vector of 9x1 parameters system consisting of: the measured/calculated state vector, the previous and current measured outputs and the previous control action is given to the multiparametric moving horizon estimator which computes the estimate for the reduced states of the system. These estimates are then used by the multiparametric controller to calculate the optimal control value that will be applied to the system. In the case of the mp-MPC, the vector of parameters is a 6x1 system consisting of: the estimated states, the current time output and the output setpoint.

The measurement noise is included as noise for the moving horizon estimation. A Gaussian distribution with a 3% standard deviation is assumed. The state estimator is considered for a horizon of N=3. In this case the parameters vector therefore includes the N past measurements and values for the manipulated variable.

Figure 5.5 presents the solution of the multiparametric programming problem in the form of 2-dimensional projection of the critical space.

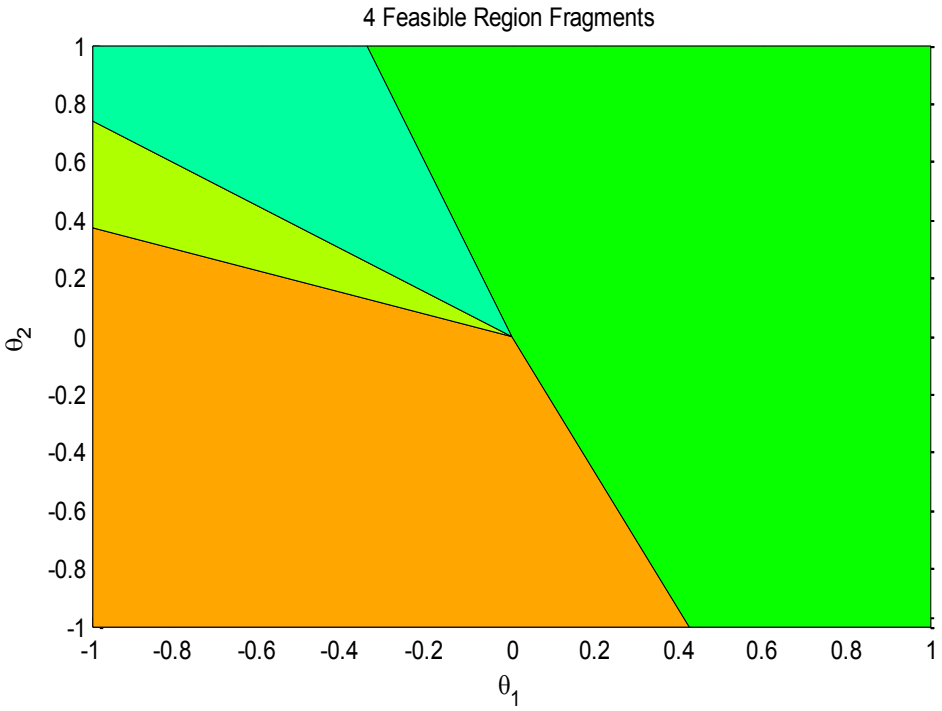

Figure 5.5: critical regions for Volatile Anaesthesia mp-MHE

The results are presented in Figure 5.6 for one patient where it can be observed that better results are obtain with the use of MHE estimation.

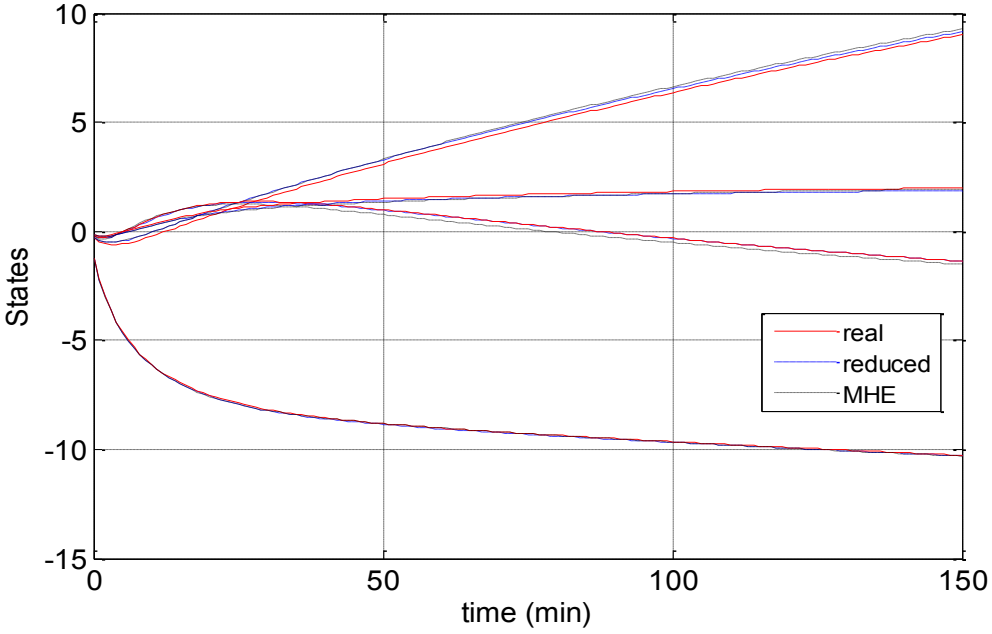

Figure 5.6: Volatile anaesthesia - Comparison of actual and estimated reduced order state and MHE

5.4.4 Multiparametric Optimization & Control Strategy

The control design scheme of the simultaneous design strategies and mp-MPC is illustrated in Figure 5.7:

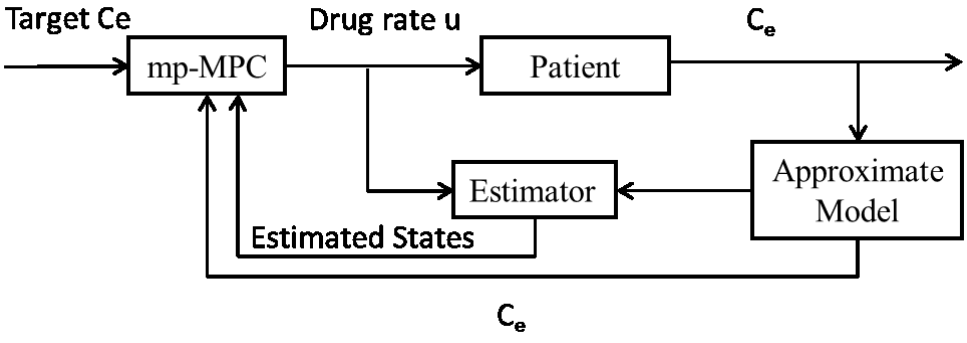

Figure 5.7: Volatile anaesthesia - Schematic of simultaneous reduced order mp-MHE and mp-MPC for volatile anaesthesia

The *Patient* block represents the high fidelity model of the patient composed of the PK and PD part as described in Section 5.4.1.1 and Section 5.4.1.2. The *Estimator* block uses the approximate model of the patient described in Section 5.4.2 and the drug infusion to estimate the state of each individual patient. Furthermore, the estimated states, the approximate model as well as the target of the concentration is used by the *mp-MPC* block to give the optimal control action.

Using the explicit/multiparametric MPC formulation described in (Pistikopoulos et al., 2007a), the control strategy is based on the nonlinearity compensation and the state space model of the PK-PD linear part for the nominal patient model. The following mp-QP optimization problem is solved to obtain the control laws using the POP toolbox (Pistikopoulos et al., 1999) and determine the controller.

$$\begin{aligned}
&\min_{C} J = \sum_{k=1}^{N-1} (C_{e,k} - C_e^R)^T QR_k (C_{e,k} - C_e^R) + \sum_{k=0}^{N_u-1} \Delta C_{I,k}^T R1_k \Delta C_{I,k} \\
&s.t. \qquad C_{k+1} = AC_k + BC_{I,k} \\
&\qquad\quad \mathrm{C_{e,k}} = CC_k \\
&C_{I,\min} \le C_{I,0},\ldots,C_{I,N_u} \le C_{I,\max} \\
&C_{e,\min} \le C_{e,1},\ldots,C_{e,N} \le C_{e,\max} \\
&\Delta C_{I,\min} \le C_{I,-1} - C_{I,0},\ldots,C_{I,N_u-1} - C_{I,N_u} \le \Delta C_{I,\max}
\end{aligned} \qquad \text{(Equation 5.11)}$$

where N is the output horizon, N_u the control horizon, QR the weight matrix on reference tracking error, $R1$ the weight matrix on change in control input, A, B, C state space matrices, C_e effect site concentration (control output), C_e^R reference point on effect site concentration, C_I inspired concentration (control input), ΔC_I change in inlet concentration (change in control input).

Although the first state of the original system of ODEs is also the measured variable, it is possible to reconstruct it from the estimated reduced states.The objective coefficients for states (x), Q=0 when we have no state estimation and Q=1 in the case with state estimation, the weight matrix for tracked outputs (y), QR=1000, weight matrix for

manipulated variables (u), R=1, the control horizon $N_u=1$ and the prediction horizon $N=10$.The initial system consists of 7 states. Using the model reduction techniques presented in the previous chapter the full model is reduced to 4 states. An mp-MHE is used to estimate the reduced states and a comparison between the estimated states and the reduced states are presented in Figure 5.6. The estimator is designed using the nominal patient.

Figure 5.8 depicts the solution of the mp programming problem in the form of 2-dimensional projections of the critical space. The projections are based on the states variables of the parameter vectors. The values of the rest of the parameters are set to fixed values within their feasible bounds in order to generate the graphs.

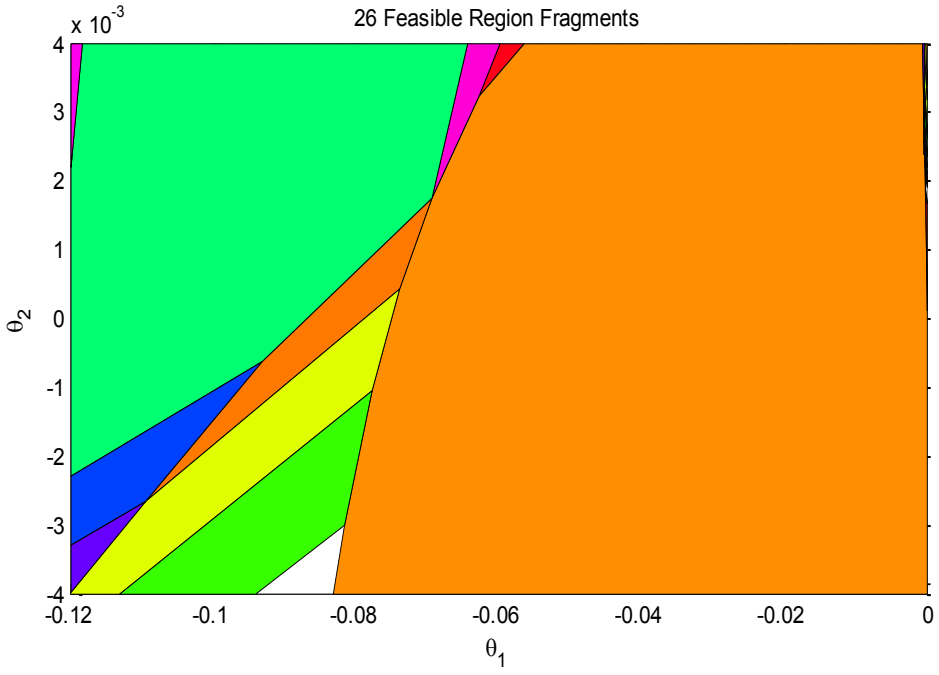

Figure 5.8: Volatile Anaesthesia mp-MPC

5.4.5 Validation

Figure 5.9 and Figure 5.10 summarise the closed loop validation results. Once an accurate estimation of the states is obtained, this can be used to design the mp-MPC controller based on the nominal patient model. It is observed that (i) as shown in Figure

5.10, using the drug infusion as control action, the controller drives the anaesthesia process to the desired set point – Figure 5.9; (ii) from Figure 5.9 we can observe that the controller shows good performance with fast settling time and no significant overshoot or undershoot; (iii) also the mp-MHE based on the reduced model exhibits satisfactory performance with no significant mismatch between the states despite the presence of measurement noise; (iv) the estimator provides sufficiently accurate information to the parametric controller in order to drive the system to the desired set point based only on measurement information –Figure 5.9.

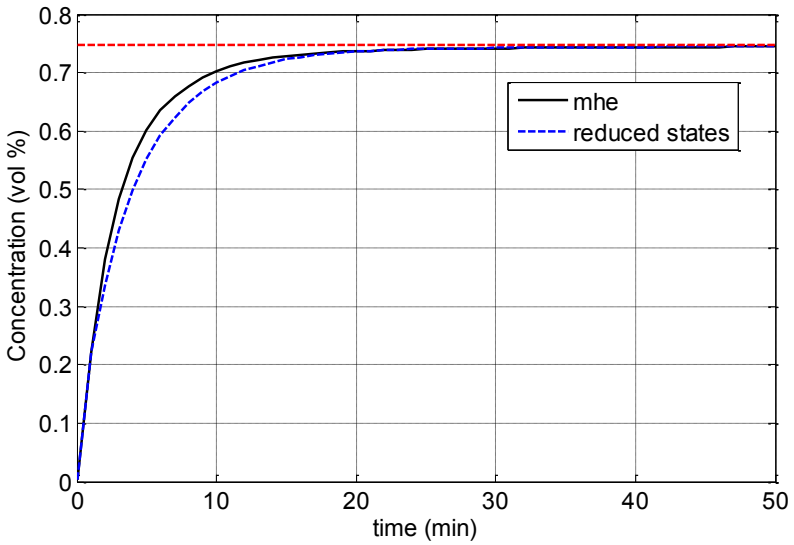

Figure 5.9: Volatile anaesthesia - Close loop simulation of a set-point change operated through simultaneous mp-MHE and mp-MPC

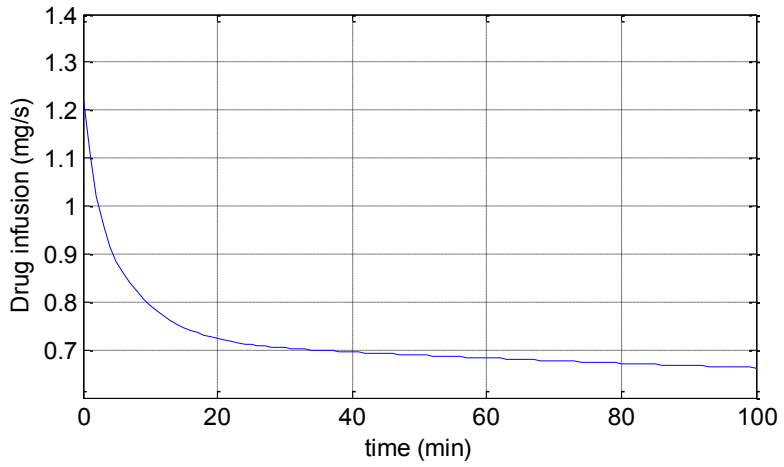

Figure 5.10: Volatile anaesthesia - Evolution of the control input variable

5.5 Discussion

This chapter presents a framework for the development of simultaneous multi-parametric model predictive control and estimation for the anaesthesia process. Starting from the development of a high fidelity model of the anaesthesia process, suitable model reduction techniques provide, if necessary, an approximate model which is used in combination with state-of-the-art simultaneous explicit model predictive control and estimation algorithms to solve the underlying optimal control problem offline. The solution is validated against the original high fidelity model in a closed-loop in silico fashion. The PAROC framework is applied both to the intravenous as well as the volatile anaesthesia process for the induction phase.

State estimation techniques are designed to estimate the states for the intravenous and volatile anaesthesia process. The estimation techniques are designed for different cases and they are tested comparatively. Furthermore the state estimators are implemented simultaneously with mp-MPC.

For volatile anaesthesia model reduction techniques performed on the model before applying the control studies. The focus is on analysing different estimation techniques and their performances when used simultaneously with multiparametric model predictive

control, with or without noise influencing the output as well as testing the inter- and intra-patient variability like in the case of intravenous anaesthesia. The main aim for this case is to analyse the performances of the simultaneous multiparametric model predictive controller and state estimation using the reduced order model. This was tested against the high fidelity model

In both intravenous and volatile process, the designed methodologies show good performances: fast settling time and no significant overshoot or undershoot. The moving horizon estimator exhibits better performance compared to the other estimation techniques especially under the influence of noise and constraints. Moreover since the BIS output is influenced by strong noise, the use of the mp-MHE brings improvements to the control strategies. The estimators provide sufficiently accurate information to the parametric controllers to induce and maintain the desired Bispectral Index reference based only on the measured information. The volatile anaesthesia process underlines the importance of using model order reduction for simultaneous multi-parametric moving horizon estimation and multi-parametric model predictive control.

Furthermore the proposed strategies are able to deal with two of the main challenges in controlling the depth of anaesthesia: (i) nonlinearity by using the inverse of the Hill function and (ii) inter- and intra- patient variability by using estimation techniques to estimate the state of each individual patient.

5.6 Conclusions

In this chapter we have presented PAROC, a comprehensive framework and software platform for the development and validation of explicit MPC controllers. The presented framework targets complex issues in a step-by-step procedure including advanced modelling, approximation and state-of-the-art multiparametric programming and explicit control techniques. An important characteristic of the framework is the closed-loop validation of the advanced controller against the high fidelity model. Some of the key

features of the PAROC framework are: (i) it is easily implemented on fundamentally different classes of problems, (ii) it follows a multiparametric approach for the controller design that transfers the computational burden offline, (iii) the validation of the exact solution against the high fidelity model through the interconnectivity of the different software packages, (iv) due to its decomposed nature it allows for different advanced applications in the different steps.

The capabilities and applicability of the framework are highlighted through the intravenous and volatile anaesthesia process during induction and maintenance phase. Overcoming challenges such as nonlinearity and inter- and intra- patient variability as well as the advantages of using the framework on such a system are presented in detail.

Chapter 6

Conclusions and Future Directions

6.1 Project Summary

As the role of the anaesthetist has become more complex and indispensable to maintain the patients' vital functions before, during and after surgery, the automation of the drug/anaesthetic administration may reduce workload while offering additional support during critical situations. Optimization and control of the depth of anaesthesia is also important for the safety of the patient and reduction of potential side-effects.

The main objective of this thesis was to develop advanced explicit/multi-parametric model predictive (mp-MPC) control strategies for the anaesthesia process.

Chapter 2 describes the mp-MPC framework based on a mathematical model for intravenous anaesthesia featuring a pharmacokinetic (PK) and pharmacodynamic (PD) compartment model structure. Different strategies were applied to overcome issues related to the nonlinear part of the model, the Hill curve of the PD model. Specialised linearization techniques were employed for this purpose.

Chapter 3 describes the simultaneous mp-MPC and state estimation strategies for the intravenous anaesthesia. Different estimation techniques to estimate the state of each individual patient were implemented and tested. The estimators were applied simultaneous with the mp-MPC to overcome challenges related to the inter- and intra-patient variability and, unmeasurable and noisy outputs.

Chapter 4 describes a piece-wise linearization of the Hill curve leading to a hybrid formulation of the patient model and thus the development of hybrid mp-MPC. An estimation technique and different robust algorithms are implemented with the hybrid mp-MPC to deal with the inter- and intra- patient variability issue.

Chapter 5 describes an integrated software platform for the development of advanced mp-MPC, PAROC, that is applied to both intravenous and volatile anaesthesia. All the theoretical developments presented in this thesis were included as part of the framework.

6.2 Key Contributions

The contributions of the work presented in this thesis can be summarised as follows:

- Novel advanced model predictive control strategies were developed for intravenous anaesthesia and implemented for the control of depth of anaesthesia (DOA) in the induction and maintenance phases
- Inter- and intra- patient variability has been successfully addressed by employing different estimation techniques and implemented with the mp-MPC control strategy – for both intravenous and volatile anaesthesia process.
- A nominal hybrid explicit/multiparametric MPC structure was developed based on a piece-wise affine approximation of the intravenous anaesthesia model, which efficiently addresses the nonlinearity of the Hill curve.
- Robust hybrid mp-MPC strategies were developed and simultaneously implemented and tested.
- Simultaneous hybrid mp-MPC and multiparametric moving horizon strategy was developed and implemented for the intravenous anaesthesia.
- The strategies and methods developed were incorporated as part of the PARametric Optimization and Control (PAROC) framework and software platform, thereby paving the way for personalized healthcare systems.

6.3 Future Directions

Three main general future direction can be employed on modelling, control and automation, for anaesthesia and general biomedical systems.

Modelling

Despite the advances made in the development of models for anaesthesia there is vast room for improvements. The compartmental model used in this work, while it addresses some of the issues pertaining to anaesthesia there are still important issues that still need to be addressed. General disturbances generated by external stimuli are still a long way for being well captured within a model. Developing a good model of these disturbances could bring significant improvements in controlling the maintenance phase of anaesthesia and moreover in helping the anaesthesiologist dealing with critical situations.

General anaesthesia consists of three components acting simultaneously on the patient's biological signals: hypnosis, analgesia and neuromuscular blockade. Hypnosis is relatively well characterized and sensors to measure it by means of electroencephalogram (EEG) data are currently employed in standard clinical practice. Neuromuscular blockade ensures that the patient remains paralyzed during surgical procedures and is also a relatively well-characterized process with standard sensors available. However, analgesia is not at all characterized and no sensor is available for measuring the pain level that the patient may experience during general anaesthesia. The challenge originates from the fact that perception of nociceptives in the neural dynamics and hence in the subsequent biological feedback is not understood properly since models to characterize this complex biological process are not available. In contrast to the well-understood dose-response relationship for the hypnotic component of sedation, the dose-response relationship for the analgesic component of sedation needs further study. The development of models for analgesia will significantly improve the derivation of more accurate control strategies for anaesthesia.

Control

As presented throughout the thesis, the control of anaesthesia poses a manifold of challenges: (i) inter- and intra-patient variability, (ii) multivariable characteristics, (iii) variable time delays, (iv) dynamics depending on the hypnotic agent, (v) model analysis variability and (vi) agent and stability issues (Haddad et al., 2003), (Absalom et al.,

2011), (Morley et al., 2000). While in this thesis we have addressed issues related to the nonlinearity and inter- and intra- patient variability there are still more challenges that need to be overcome. Employing robust techniques and/or simultaneous hybrid estimators and mp-MPC can lead to a more systematic characterisation of the uncertainty, therefore paving the way to personalized health care systems.

As mentioned previously, analgesia modelling will play a key role to the design of controllers for anaesthesia. Determining a second output that will originate from the effect of the analgesic agent will lead to the implementation of multivariable multiparametric model predictive control strategies that will significantly improve the control of anaesthesia. Therefore we will be able to tackle the synergic effects of several drugs induced in the patient during general anaesthesia, thus bringing us closer to a fully automated anaesthesia process.

Automation

Other applications of the developed strategies and of the PAROC framework for the anaesthesia process lie in the areas of:

- patient simulators or mannequins for training of nurses, medical students or anaesthetists,
- on-line computation of the current drug concentrations and effect on the patient during surgery

One of the most advanced patient simulators on the market is the CAE Healthcare© HPS®, (Healthcare, 2013a). This patient simulator shows all vital functions and inhales and exhales oxygen and anaesthetic agents according to a mathematical model (Meurs, 2011). Several software for training are available, the most well-known tool is Gas Man®, (MMSI, 2006) a computer tool for teaching, simulating and experimenting with anaesthesia uptake and distribution. The SmartPilot View by Drager, (Herbst, 2010) or the Navigator Applications Suite software by GE Healthcare, (Healthcare, 2013c) are software tools that enable a frequently updated state of the patient calculated based on drug infusions and boluses and the measured variables e.g. the exhaled and inhaled gases

and the vital functions. The aim of these tools is to provide the anaesthetist with a decision support. The anaesthetist can follow the moving state of the patient in a 2D graph and see the future states for the given infusions and inhalations.(Grunberg, 2009).

A fully automated anaesthesia process will bring great advantages to both: (i) the patient by increasing their safety as well as reducing the side effects by optimizing the drug infusion rates, and (ii) the anaesthesiologist by acting as a teaching and testing platform and offering in depth understanding of the process. There is still a long way to go to a fully automated operation theatre since all three main components of anaesthesia (hypnosis, analgesia and muscle relaxation) have to be simultaneously controlled. Moreover there is still no established solution in measuring analgesia. Nevertheless, the intensive research in this field is undoubtedly paving the way to overcoming these challenges and achieving a fully operational automated anaesthesia process.

Nowadays, embedded systems are used in many applications in the medical field for controlling various biomedical parameters. Several embedded systems can be found in anaesthesia monitoring systems but not yet in control of anaesthesia. By using mp-MPC the expensive online computation of the optimal control action is bypassed (online optimization via offline optimization) resulting in just the implementation of a simple look up table and simple function evaluation. This will facilitate the implementation of the control of DOA on embedded devices (MPC-on-a-chip).(Pistikopoulos, 2009).

Publications from this thesis

Journal Publications

[1] Nascu, I., A. Krieger, C. M. Ionescu and E. N. Pistikopoulos (2015). "Advanced Model-Based Control Studies for the Induction and Maintenance of Intravenous Anaesthesia." Biomedical Engineering, IEEE Transactions on 62(3): 832-841

[2] Pistikopoulos, E. N., N. A. Diangelakis, R. Oberdieck, M. M. Papathanasiou, I. Nascu and M. Sun (2015). "PAROC-An integrated framework and software platform for the optimisation and advanced model-based control of process systems." Chemical Engineering Science., pp. 115-138

[3] Naşcu, I., and E.N. Pistikopoulos, "A Multiparametric Model-Based Optimization Control Approach to Anaesthesia", in Canadian Journal of Chemical Engineering, in print.

Conference Publications

[1] Nascu, I., R.S.C. Lambert, and E.N. Pistikopoulos. A combined estimation and multi-parametric model predictive control approach for intravenous anaesthesia. in Conference Proceedings - IEEE International Conference on Systems, Man and Cybernetics. 2014.

[2] Nascu, I., R. S. C. Lambert, A. Krieger and E. N. Pistikopoulos (2014). Simultaneous multi-parametric model predictive control and state estimation with application to distillation column and intravenous anaesthesia. Computer Aided Chemical Engineering. 33: 541-546.

[3] Naşcu, I., R. Oberdieck and E. N. Pistikopoulos (2015). A framework for hybrid multi-parametric model-predictive control with application to intravenous anaesthesia. Computer Aided Chemical Engineering. 37: 719-724.

[4] Nascu, I., R. Oberdieck, and E. Pistikopoulos, Offset-free explicit hybrid model predictive control of intravenous anaesthesia . IEEE International Conference on Systems, Man, and Cybernetics, 2015. in press.

[5] Nascu, I., N. A. Diangelakis, R. Oberdieck, M. M. Papathanasiou and E. Pistikopoulos (2015). "Explicit MPC in real-world applications: the PAROC framework." The American Control Conference, accepted.

[6] Naşcu, I., R. Oberdieck, and E.N. Pistikopoulos, A framework for Simultaneous State Estimation and Robust Hybrid Model Predictive Control in Intravenous Anaesthesia, in Computer Aided Chemical Engineering, accepted.

[7] Lambert, R.S.C., I. Nascu, and E.N. Pistikopoulos. Simultaneous reduced order multi-parametric moving horizon estimation and model based control. in IFAC Proceedings Volumes (IFAC-PapersOnline). 2013.

Oral Presentations

[1] Naşcu, I., Romain S. C. Lambert, Efstratios N. Pistikopoulos, A framework for Model Reduction, State Estimation and Multi-Parametric Model Predictive Control in Anaesthesia, AIChE 2014, Atlanta, USA,

[2] Naşcu, I., R. Oberdieck, and E.N. Pistikopoulos, A framework for State Estimation and Robust Hybrid Multi-Parametric Model Predictive Control in Anaesthesia, AIChE 2015, Salt Lake City, USA, Oral presentation

Publications submitted

Naşcu, I., and E.N. Pistikopoulos, Simultaneous Multiparametric Moving Horizon Estimation and Model Predictive Control for the Anaesthesia Process, in Computers and Chemical Engineering.

Naşcu, I., R. Oberdieck, and E.N. Pistikopoulos, Robust Hybrid Model Predictive Control and State Estimation in Intravenous Anaesthesia, in Automatica.

Bibliography

(Pse), P. S. E. L. 2010. gPROMS Model Developer Guide. *Release v3.3.0*.

Absalom, A. R., De Keyser, R. & Struys, M. M. R. F. 2011. Closed loop anaesthesia: are we getting close to finding the Holy Grail? *Anesth Analg,* 112**,** 516-518.

Acevedo, J. & Pistikopoulos, E. N. 1997a. A Multiparametric Programming Approach for Linear Process Engineering Problems under Uncertainty. *Industrial and Engineering Chemistry Research,* 36**,** 717-728.

Acevedo, J. & Pistikopoulos, E. N. 1997b. A Multiparametric Programming Approach for Linear Process Engineering Problems under Uncertainty. *Industrial & Engineering Chemistry Research,* 36**,** 717–728.

Acevedo, J. N. & Pistikopoulos, E. N. 1999. An algorithm for multiparametric mixed-integer linear programming problems. *Operations Research Letters,* 24**,** 139-148.

Adamjan, V. M., Arov, D. Z. & Krein, M. G. 1971. Analytic properties of Schmidt pairs for a Hankel operator and the generalized Schur-Takagi problem. *Math. USSR Sbornik,* 15**,** 31-73.

Agarwal, A. & Biegler, L. T. 2013. A trust-region framework for constrained optimization using reduced order modeling. *Optimization and Engineering,* 14**,** 3-35.

Alamo, T., RamíRez, D. R. & Camacho, E. F. 2005. Efficient implementation of constrained min–max model predictive control with bounded uncertainties: a vertex rejection approach. *Journal of Process Control,* 15**,** 149-158.

Antoulas, A. C. 2005. An overview of approximation methods for large-scale dynamical systems. *Annual Reviews in Control,* 29**,** 181-190.

Antoulas, A. C. & Sorensen, D. C. 2001. Lyapunov, Lanczos, and inertia. *Linear Algebra and Its Applications,* 326**,** 137-150.

Arnoldi, W. E. 1951. The principle of minimized iterations in the solution of the matrix eigenvalue problem. *Quarterly of Applied Mathematics,* 9**,** 17-29.

Asa 2006. Practice advisory for intraoperative awareness and brain function monitoring: A report by the American Society of Anesthesiologists Task Force on Intraoperative Awareness. *Anesthesiology,* 104**,** 847-864.

Asteasuain, M., Kouramas, K., Sakizlis, V. & Pistikopoulos, E. N. 2006. Explicit parametric controller for a batch polymerization system. *In:* Marquardt, W. & Pantelides, C. (eds.) *Computer Aided Chemical Engineering.* Elsevier.

Axehill, D., Besselmann, T., Raimondo, D. M. & Morari, M. 2011. Suboptimal Explicit Hybrid MPC via Branch and Bound. *IFAC World Congress.* Milano.

Axehill, D., Besselmann, T., Raimondo, D. M. & Morari, M. 2014a. A parametric branch and bound approach to suboptimal explicit hybrid MPC. *Automatica,* 50**,** 240-246.

Axehill, D., Besselmann, T., Raimondo, D. M. & Morari, M. 2014c. A parametric branch and bound approach to suboptimal explicit hybrid MPC. *Automatica,* 50**,** 240–246.

Bailey, J. M. & Haddad, W. M. 2005. Drug dosing control in clinical pharmacology. *IEEE Control System Magazine,* 25**,** 35-31.

Baotic, M. 2002. An Efficient Algorithm for Multiparametric Quadratic Programming. AUT02-05.

Barash, P. G., Cullen, B. F., Stoelting, R. K., Cahalan, M. & Stock, M. C. 2009. *Clinical Anesthesia*.

Bemporad, A., Borrelli, F. & Morari, M. 2002a. Model predictive control based on linear programming - the explicit solution. *IEEE Transactions on Automatic Control,* 47**,** 1974–1985.

Bemporad, A., Borrelli, F. & Morari, M. 2003. Min-Max Control of Constrained Uncertain Discrete-Time Linear Systems. *IEEE Transactions on Automatic Control,* 48**,** 1600-1606.

Bemporad, A. & Morari, M. 1999a. Control of systems integrating logic, dynamics, and constraints. *Automatica,* 35**,** 407-427.

Bemporad, A. & Morari, M. 1999b. Control of systems integrating logic, dynamics, and constraints. *Automatica,* 35**,** 407–427.

Bemporad, A., Morari, M., Dua, V. & Pistikopoulos, E. N. 2002c. The explicit linear quadratic regulator for constrained systems. *Automatica,* 38**,** 3–20.

Bemporad, A., Morari, M., Dua, V. & Pistikopoulos, E. N. 2002g. The explicit linear quadratic regulator for constrained systems. *Automatica,* 38**,** 3-20.

Benallou, A., Seborg, D. E. & Mellichamp, D. A. 1986. DYNAMIC COMPARTMENTAL MODELS FOR SEPARATION PROCESSES. *AIChE Journal,* 32**,** 1067-1078.

Bibian, S., Dumont, G. A. & Zikov, T. 2011. Dynamic behavior of BIS, M-entropy and neuroSENSE brain function monitors. *Journal of Clinical Monitoring and Computing,* 25**,** 81-87.

Blatman, G. & Sudret, B. 2010. An adaptive algorithm to build up sparse polynomial chaos expansions for stochastic finite element analysis. *Probabilistic Engineering Mechanics,* 25**,** 183-197.

Bogle, I. D. L. 2012. Recent developments in Process Systems Engineering as applied to medicine. *Current Opinion in Chemical Engineering,* 1**,** 453-458.

Bonis, I., Xie, W. & Theodoropoulos, C. 2012. A linear model predictive control algorithm for nonlinear large-scale distributed parameter systems. *AIChE Journal,* 58**,** 801-811.

Borgeat, A., Wilder-Smith, O. H. G., Saiah, M. & Rifat, K. 1992. Does propofol have an anti-emetic effect? [5]. *Anaesthesia and Intensive Care,* 20**,** 260-261.

Borrelli, F. 2003. *Constrained optimal control of linear and hybrid systems,* Berlin; New York, Springer.

Borrelli, F., Baotić, M., Bemporad, A. & Morari, M. 2005. Dynamic programming for constrained optimal control of discrete-time linear hybrid systems. *Automatica,* 41**,** 1709-1721.

Bruhn, J., Bouillon, T. & Shafer, S. L. 2000. Bispectral index (BIS) and burst suppression: revealing a part of the BIS algorithm. *Journal of Clinical Monitoring and Computing,* 16**,** 593-596.

Buhmann, M. D. 2003. Radial Basis Functions: Theory and Implementations. *Cambridge University Press, ISBN: 978-0-521-63338-3*.

Caiado Daniela, V., Lemos João, M. & Costa Bertinho, A. 2013. Robust control of depth of anesthesia based on H∞ design. *Archives of Control Sciences.*

Chang, H., Krieger, A., Astolfi, A. & Pistikopoulos, E. N. 2014a. Robust multi-parametric model predictive control for LPV systems with application to anaesthesia. *Journal of Process Control,* 24**,** 1538-1547.

Chang, H., Pistikopoulos, E. N. & Astolfi, A. Robust multi-parametric model predictive control for discrete-time LPV systems. Proceedings of the American Control Conference, 2013. 431-436.

Chang, H. J., Lee, K. J., Jeong, G. M. & Moon, C. 2014c. Two case studies of robust multi-parametric model predictive control algorithm. *International Journal of Control and Automation,* 7**,** 293-302.

Clarke, D. W., Mohtadi, C. & Tuffs, P. 1987. Generalized predictive control—Part I. The basic algorithm. *Automatica,* 23**,** 137-148.

Curatolo, M., Derighetti, M., Petersen-Felix, S., Feigenwinter, P., Fischer, M. & Zbinden, A. M. 1996. Fuzzy logic control of inspired isoflurane and oxygen concentrations using minimal flow anaesthesia. *British Journal of Anaesthesia,* 76**,** 245-250.

Darby, M. L. & Nikolaou, M. 2007. A parametric programming approach to moving-horizon state estimation. *Automatica,* 43**,** 885-891.

De Keyser, R. 2003. Model Based Predictive Control *Invited Chapter in UNESCO Encyclopaedia of Life Support Systems (EoLSS),* 6.43.16.1**,** 30p.

De Keyser, R. M. C. & Van Cauwenberghe, A. R. EXTENDED PREDICTION SELF-ADAPTIVE CONTROL. IFAC Proceedings Series, 1985. 1255-1260.

Diangelakis, N. A., Panos, C. & Pistikopoulos, E. N. 2014. Design optimization of an internal combustion engine powered CHP system for residential scale application. *Computational Management Science,* 11**,** 237-266.

Diangelakis, N. A. & Pistikopoulos, E. N. 2015. A Decentralised Multi-parametric Model Predictive Control Study for a Domestic Heat and Power Cogeneration System. *In:* Krist V. Gernaey, J. K. H. & Rafiqul, G. (eds.) *Computer Aided Chemical Engineering*. Elsevier.

Dua, V., Bozinis, N. A. & Pistikopoulos, E. N. 2002a. A multiparametric programming approach for mixed-integer quadratic engineering problems. *Computers & Chemical Engineering,* 26**,** 715–733.

Dua, V., Bozinis, N. A. & Pistikopoulos, E. N. 2002i. A multiparametric programming approach for mixed-integer quadratic engineering problems. *Computers and Chemical Engineering,* 26**,** 715-733.

Dua, V. & Pistikopoulos, E. N. 1999. Algorithms for the Solution of Multiparametric Mixed-Integer Nonlinear Optimization Problems. *Industrial & Engineering Chemistry Research,* 38**,** 3976–3987.

Dua, V. & Pistikopoulos, E. N. 2000. An Algorithm for the Solution of Multiparametric Mixed Integer Linear Programming Problems. *Annals of Operations Research,* 99**,** 123-139.

Dumont, G. A., Martinez, A. & Ansermino, J. M. 2009. Robust control of depth of anesthesia. *International Journal of Adaptive Control and Signal Processing,* 23**,** 435-454.

Eger, E. I. 1974. *Anesthetic uptake and action,* Baltimore, Williams & Wilkins.

Feller, C. & Johansen, T. A. 2013a. Explicit MPC of higher-order linear processes via combinatorial multi-parametric quadratic programming. *Control Conference (ECC), 2013 European.*

Feller, C., Johansen, T. A. & Olaru, S. 2013b. An improved algorithm for combinatorial multi-parametric quadratic programming. *Automatica,* 49**,** 1370–1376.

Foster, B. L., Bojak, I. & Liley, D. T. J. 2008. Population based models of cortical drug response: Insights from anaesthesia. *Cognitive Neurodynamics,* 2**,** 283-296.

Franklin, D. W., Powell, D. J. & Emami-Naeini, A. 2001a. Feedback Control of Dynamic Systems. *Englewood Cliffs, NJ,USA*.

Franklin, G. F., Powell, D. J. & Emami-Naeini, A. 2001c. *Feedback Control of Dynamic Systems*, Prentice Hall PTR.

Fuentes-Garí, M., Velliou, E., Misener, R., Pefani, E., Rende, M., Panoskaltsis, N., Mantalaris, A. & Pistikopoulos, E. N. 2015. A systematic framework for the

design, simulation and optimization of personalized healthcare: Making and healing blood. *Computers & Chemical Engineering,* 81**,** 80-93.

Gal, T. & Nedoma, J. 1972. Multiparametric linear programming. *Management Science,* 18**,** 406–

744 422.

Gallivan, K., Grimme, E. & Van Dooren, P. Pade approximation of large-scale dynamic systems with Lanczos methods. Proceedings of the IEEE Conference on Decision and Control, 1994. 443-448.

Gan, T. J., Glass, P. S., Windsor, A., Payne, F., Rosow, C., Sebel, P., Manberg, P., Howell, S., Sanderson, I., Ray, J., Elidrissi, C., Wilkes, N., Calhoun, P., Connors, P., Alfille, P., Shapiro, L., Denman, W., Dershwitz, M., Clifford, J., Embree, P. & Sigl, J. 1997. Bispectral index monitoring allows faster emergence and improved recovery from propofol, alfentanil and nitrous oxide anesthesia. *Anesthesiology,* 87**,** 808-815.

Gentilini, A., Rossoni-Gerosa, M., Frei, C. W., Wymann, R., Morari, M., Zbinden, A. M. & Schnider, T. W. 2001. Modeling and closed-loop control of hypnosis by means of bispectral index (BIS) with isoflurane. *IEEE Transactions on Biomedical Engineering,* 48**,** 874-889.

Glass, P. S., Bloom, M., Kearse, L., Rosow, C., Sebel, P. & Manberg, P. 1997. Bispectral analysis measures sedation and memory effects of propofol, midazolam, isoflurane, and alfentanil in healthy volunteers. *Anesthesiology,* 86**,** 836-847.

Grunberg, F. 2009. Navigating through Anesthesia. *Technical Report MAy, Dr□ager Review.*

Gupta, A., Bhartiya, S. & Nataraj, P. S. V. 2011a. A novel approach to multiparametric quadratic programming. *Automatica,* 47**,** 2112-2117.

Gupta, A., Bhartiya, S. & Nataraj, P. S. V. 2011c. A novel approach to multiparametric quadratic programming. *Automatica,* 47**,** 2112–2117.

Haddad, W. M., Hayakawa, T. & Bailey, J. M. Nonlinear Adaptive Control for Intensive Care Unit Sedation and Operating Room Hypnosis. 2003. 1808-1813.

Hahn, J. & Edgar, T. F. 2002. An improved method for nonlinear model reduction using balancing of empirical gramians. *Computers and Chemical Engineering,* 26**,** 1379-1397.

Healthcare, C. 2013a. HPS with Muse - The only simulator that truly breathes - for anesthesia, respiratory, emergency and critical care.

Healthcare, G. 2013c. Navigator Applications Suite Software.

Hedengren, J. D. & Edgar, T. F. 2005. In situ adaptive tabulation for real-time control. *Industrial and Engineering Chemistry Research,* 44**,** 2716-2724.

Heemels, W. P. M. H., Schutter, B. D. & Bemporad, A. 2001. Equivalence of hybrid dynamical models. *Automatica,* 37**,** 1085–1091.

Herbst, V. 2010. Anaesthesia Pilot - Drager Press Release. *Drager PressRelease v3.3.0,* 2**,** 1-2.

Hodrea, R., Morar, R. & Nascu, I. 2012. Predictive Control of Neuromuscular Blockade. *Automation Computers Applied Mathematics,* 21.

Homma, T. & Saltelli, A. 1996. Importance measures in global sensitivity analysis of nonlinear models. *Reliability Engineering and System Safety,* 52**,** 1-17.

Hovland, S., Gravdahl, J. T. & Willcox, K. E. 2008. Explicit model predictive control for large-scale systems via model reduction. *Journal of Guidance, Control, and Dynamics,* 31**,** 918-926.

Ibrahim, A. E., Taraday, J. K. & Kharasch, E. D. 2001. Bispectral index monitoring during sedation with sevoflurane, midazolam, and propofol. *Anesthesiology,* 95**,** 1151-1159.

Ionescu, C. M., Keyser, R. D., Torrico, B. C., Smet, T. D., Struys, M. M. R. F. & Normey-Rico, J. E. 2008. Robust predictive control strategy applied for propofol dosing using BIS as a controlled variable during anesthesia. *IEEE Transactions on Biomedical Engineering,* 55**,** 2161-2170.

Ionescu, C. M., Nascu, I. & De Keyser, R. 2011a. Robustness Tests of a Model Based Predictive Control Strategy for Depth of Anesthesia Regulation in a Propofol to Bispectral Index Framework. *In:* Vlad, S. & Ciupa, R. (eds.) *International*

Conference on Advancements of Medicine and Health Care through Technology. Springer Berlin Heidelberg.

Ionescu, C. M., Nascu, I. & De Keyser, R. Towards a multivariable model for controlling the depth of anaesthesia using propofol and Remifentanil. 2012. 325-330.

Ionescu, C. M., Nascu, I. & Keyser, R. 2011c. Robustness Tests of a Model Based Predictive Control Strategy for Depth of Anesthesia Regulation in a Propofol to Bispectral Index Framework. *In:* Vlad, S. & Ciupa, R. (eds.) *International Conference on Advancements of Medicine and Health Care through Technology.* Springer Berlin Heidelberg.

Irwin, M. G., Hui, T. W., Milne, S. E. & Kenny, G. N. 2002. Propofol effective concentration 50 and its relationship to bispectral index. *57*.

Iselin-Chaves, I. A., Flaishon, R., Sebel, P. S., Howell, S., Gan, T. J., Sigl, J., Ginsberg, B. & Glass, P. S. A. 1998. The effect of the interaction of propofol and alfentanil on recall, loss of consciousness, and the Bispectral Index. *Anesthesia and Analgesia,* 87**,** 949-955.

Ivakhnenko, A. G. & Muller, J. A. 1995. Self-organization of nets of active neurons. *SAMS,* 20**,** 93-106.

Jensen, E. W., Litvan, H., Revuelta, M., Rodriguez, B. E., Caminal, P., Martinez, P., Vereecke, H. & Struys, M. M. R. F. 2006. Cerebral state index during propofol anesthesia: A comparison with the Bispectral Index and the A-Line ARX Index. *Anesthesiology,* 105**,** 28-36.

Johansen, J. W. 2006. Update on Bispectral Index monitoring. *Best Practice and Research: Clinical Anaesthesiology,* 20**,** 81-99.

Johansen, J. W. & Sebel, P. S. 2000a. Development and clinical application electroencephalographic bispectrum monitoring. *Anesthesiology,* 93**,** 1336-1344.

Johansen, J. W., Sebel, P. S. & Sigl, J. C. 2000b. Clinical impact of hypnotic-titration guidelines based on EEG bispectral index (BIS) monitoring during routine anesthetic care. *Journal of Clinical Anesthesia,* 12**,** 433-443.

Keyser, R. D. 2003. Model based predictive control for linear systems. *UNESCO Encyclopedia of Life Support Systems.* Oxford: Eolss Publishers Co Ltd.

Khajuria, H. & Pistikopoulos, E. N. 2011. Dynamic modeling and explicit/multi-parametric MPC control of pressure swing adsorption systems. *Journal of Process Control,* 21**,** 151-163.

Kiparissides, A., Kucherenko, S. S., Mantalaris, A. & Pistikopoulos, E. N. 2009. Global sensitivity analysis challenges in biological systems modeling. *Industrial and Engineering Chemistry Research,* 48**,** 7168-7180.

Kolmogorov, A. N. 1957. On the representation of continuous functions of many variables by superpositions of continuous functions of one variable and addition. *Doklay Akademii Nauk USSR,* 14 953-956.

Kontoravdi, C., Asprey, S. P., Pistikopoulos, E. N. & Mantalaris, A. 2005. Application of global sensitivity analysis to determine goals for design of experiments: An example study on antibody-producing cell cultures. *Biotechnology Progress,* 21**,** 1128-1135.

Kontoravdi, C., Pistikopoulos, E. N. & Mantalaris, A. 2010. Systematic development of predictive mathematical models for animal cell cultures. *Computers and Chemical Engineering,* 34**,** 1192-1198.

Kouramas, K. & Pistikopoulos, E. 2011a. Wind Turbines Modeling and Control. *Wiley-VCH,* 5.

Kouramas, K. I., Faísca, N. P., Panos, C. & Pistikopoulos, E. N. 2011b. Explicit/multi-parametric model predictive control (MPC) of linear discrete-time systems by dynamic and multi-parametric programming. *Automatica,* 47**,** 1638-1645.

Krieger, A., Panoskaltsis, N., Mantalaris, A., Georgiadis, M. C. & Pistikopoulos, E. N. Analysis of an individualized physiologically based model for anesthesia control. 2012. 385-390.

Krieger, A., Panoskaltsis, N., Mantalaris, A., Georgiadis, M. C. & Pistikopoulos, E. N. 2014. Modeling and analysis of individualized pharmacokinetics and pharmacodynamics for volatile anesthesia. *IEEE Transactions on Biomedical Engineering,* 61**,** 25-34.

Krylov, A. N. 1931. On the Numerical Solution of Equation by Which are Determined in Technical Problems the Frequencies of Small Vibrations of Material Systems.

Izvestija AN SSSR (News of Academy of Sciences of the USSR), Otdel. mat. i estest. nauk, 7**,** 491-539.

Kucherenko, S., Rodriguez-Fernandez, M., Pantelides, C. & Shah, N. 2009. Monte Carlo evaluation of derivative-based global sensitivity measures. *Reliability Engineering and System Safety,* 94**,** 1135-1148.

Lall, S., Marsden, J. E. & Glavaski, S. 1999. Empirical Model reduction for controlled nonlinear systems. *Proceedings of the IFAC World Congress***,** 473-478.

Lambert, R. S. C., Rivotti, P. & Pistikopoulos, E. N. 2013. A Monte-Carlo based model approximation technique for linear model predictive control of nonlinear systems. *Computers and Chemical Engineering,* 54**,** 60-67.

Lanczos, C. 1950. An iteration method for the solution of the eigenvalue problem of linear differential and integral operatorsJ. . *Res. Nat. Bureau Stan,* 45**,** 255-282.

Lemke, F. 1997. Knowledge Extraction from Data Using Self-Organizing Modeling Technologies. *eSEAM'97 conference, MacSciTech organization*

Li, G., Hu, J., Wang, S. W., Georgopoulos, P. G., Schoendorf, J. & Rabitz, H. 2006. Random Sampling-High Dimensional Model Representation (RS-HDMR) and orthogonality of its different order component functions. *Journal of Physical Chemistry A,* 110**,** 2474-2485.

Li, G., Wang, S. W. & Rabitz, H. 2002. Practical approaches to construct RS-HDMR component functions. *Journal of Physical Chemistry A,* 106**,** 8721-8733.

Litvan, H., Jensen, E. W., Revuelta, M., Henneberg, S. W., Bernardo, P., Paniagua, P., Campos, J. M., Martinez, P., Caminal, P. & Villar Landeira, J. M. 2002. Comparison of auditory evoked potentials and the A-line ARX index for monitoring the hypnotic level during sevofluane and propofol induction. *Acta Anaesthesiologica Scandinavica* 46:3**,** 245-251.

Liu, J., Singh, H. & White, P. F. 1996. Electroencephalographic bispectral analysis predicts the depth of midazolam induced sedation. *Anesthesiology,* 84**,** 64-69.

Liu, J., Singh, H. & White, P. F. 1997. Electroencephalographic bispectral index correlates with intraoperative recall and depth of propofol-induced sedation. *Anesthesia and Analgesia,* 84**,** 185-189.

Lorentz, G. 1966. Approximation of functions. *Approximation of functions*.

Mccormick, G. P. 1976. Computability of global solutions to factorable nonconvex programs: Part I — Convex underestimating problems. *Mathematical Programming,* 10**,** 147–175.

Meurs, V. 2011. Modeling and Simulation in Biomedical Engineering: Applications in Cardiorespiratory Physiology. *McGraw Hill Professional*.

Mi, W. D., Sakai, T., Singh, H., Kudo, T., Kudo, M. & Matsuki, A. 1999. Hypnotic endpoints vs. the bispectral index, 95% spectral edge frequency and median frequency during propofol infusion with or without fentanyl. *European Journal of Anaesthesiology,* 16**,** 47-52.

Minto, C. F., Schnider, T. W., Egan, T. D., Youngs, E. J., Lemmens, H. J., Gambus, P. L., Billard, V., Hoke, J. F., Moore, K. H., Hermann, D. J., Muir, K. T., Mandema, J. W. & Shafer, S. L. 1997. Influence of age and gender on the pharmacokinetics and pharmacodynamics of reminfetanil. I. Model development. *Anesthesiology,* 86**,** 10-23.

Mmsi 2006. Med Man Simulations. *Inc. (MMSI), Gas Man®.*

Mohtadi, C., Clarke, D. & Tuffs, P. 1987. Generalized predictive control-part II. Extensions and Interpretations. *Automatica,* 23**,** 149-160.

Morley, A., Derrick, J., Mainland, P., Lee, B. B. & Short, T. G. 2000. Closed loop control of anaesthesia: An assessment of the bispectral index as the target of control. *Anaesthesia,* 55**,** 953-959.

Morris, M. D. 1991. Factorial sampling plans for preliminary computational experiments. *Factorial sampling plans for preliminary computational experiments,* 33.

Muñoz De La Peña, D., Alamo, T., Bemporad, A. & Camacho, E. F. 2006. A decomposition algorithm for feedback min-max model predictive control. *IEEE Transactions on Automatic Control,* 51**,** 1688-1692.

Muñoz De La Peña, D., Ramírez, D. R., Camacho, E. F. & Alamo, T. 2005. Application of an explicit min-max MPC to a scaled laboratory process. *Control Engineering Practice,* 13**,** 1463-1471.

Narciso, D. & Pistikopoulos, E. 2008. A combined Balanced Truncation and multi-parametric programming approach for Linear Model Predictive Control. *Computer Aided Chemical Engineering.*

Nascu, I., Diangelakis, N. A., Oberdieck, R., Papathanasiou, M. M. & Pistikopoulos, E. 2015a. Explicit MPC in real-world applications: the PAROC framework. *The American Control Conference,* submitted.

Nascu, I., Ionescu, C. M., Nescu, I. & De Keyser, R. Evaluation of three protocols for automatic DOA regulation using Propofol and Remifentanil. 2011. 573-578.

Nascu, I., Krieger, A., Ionescu, C. & Pistikopoulos, E. 2014a. Advanced Model Based Control Studies for the Induction and Maintenance of Intravenous Anaesthesia. *IEEE Transactions on Biomedical Engineering* 01-10.

Nascu, I., Krieger, A., Ionescu, C. & Pistikopoulos, E. N. 2014c. Advanced Model Based Control Studies for the Induction and Maintenance of Intravenous Anaesthesia. *Biomedical Engineering, IEEE Transactions on,* PP**,** 1-1.

Nascu, I., Krieger, A., Ionescu, C. M. & Pistikopoulos, E. N. 2015c. Advanced Model-Based Control Studies for the Induction and Maintenance of Intravenous Anaesthesia. *Biomedical Engineering, IEEE Transactions on,* 62**,** 832-841.

Nascu, I., Lambert, R. S. C., Krieger, A. & Pistikopoulos, E. N. 2014e. Simultaneous multi-parametric model predictive control and state estimation with application to distillation column and intravenous anaesthesia. *Computer Aided Chemical Engineering.*

Nascu, I., Lambert, R. S. C. & Pistikopoulos, E. N. A combined estimation and multi-parametric model predictive control approach for intravenous anaesthesia. Conference Proceedings - IEEE International Conference on Systems, Man and Cybernetics, 2014j. 2458-2463.

Nascu, I., Nascu, I., Ionescu, C. M. & De Keyser, R. Adaptive EPSAC predictive control of the hypnotic component in anesthesia. 2012. 103-108.

Nascu, I., Oberdieck, R. & Pistikopoulos, E. 2015e. A framework for hybrid multi-parametric model-predictive control with application to intravenous anaesthesia. *PSE 2015/ESCAPE 25,* In press.

Nascu, I. & Pistikopoulos, E. Simultaneous Multiparametric Moving Horizon Estimation and Model Predictive Control Studies for the Anaesthesia Process. *Computers & Chemical Engineering,* to be submitted.

Nikandrov, A. & Swartz, C. L. E. 2009. Sensitivity analysis of LP-MPC cascade control systems. *Journal of Process Control,* 19**,** 16-24.

Niño, J., De Keyser, R., Syafiie, S., Ionescu, C. & Struys, M. 2009. EPSAC-controlled anesthesia with online gain adaptation. *International Journal of Adaptive Control and Signal Processing,* 23**,** 455-471.

Nunes, C. S., Mendonça, T., Lemos, J. M. & Amorim, P. 2009. Feedforward adaptive control of the Bispectral Index of the EEG using the intravenous anaesthetic drug propofol. *International Journal of Adaptive Control and Signal Processing,* 23**,** 485-503.

Oberdieck, R. & Pistikopoulos, E. N. 2015. Explicit hybrid model-predictive control: The exact solution. *Automatica,* 58**,** 152-159.

Oberdieck, R., Wittmann-Hohlbein, M. & Pistikopoulos, E. N. 2014a. A branch and bound method for the solution of multiparametric mixed integer linear programming problems. *Journal of Global Optimization,* 59**,** 527–543.

Oberdieck, R., Wittmann-Hohlbein, M. & Pistikopoulos, E. N. 2014g. A branch and bound method for the solution of multiparametric mixed integer linear programming problems. *Journal of Global Optimization,* 59**,** 527-543.

Olaru, S. & Ayerbe, P. R. Robustification of explicit predictive control laws. Decision and Control, 2006 45th IEEE Conference on, 13-15 Dec. 2006 2006. 4556-4561.

Panos, C., Kouramas, K. I., Georgiadis, M. C. & Pistikopoulos, E. N. 2010. Dynamic optimization and robust explicit model predictive control of hydrogen storage tank. *Computers & Chemical Engineering,* 34**,** 1341-1347.

Panos, C., Kouramas, K. I., Georgiadis, M. C. & Pistikopoulos, E. N. 2012. Modelling and explicit model predictive control for PEM fuel cell systems. *Chemical Engineering Science,* 67**,** 15-25.

Papathanasiou, M. M., Steinebach, F., Stroehlein, G., Müller-Späth, T., Nascu, I., Oberdieck, R., Morbidelli, M., Mantalaris, A. & Pistikopoulos, E. N. 2015. A

control strategy for periodic systems – application to the twin-column MCSGP. *In:* Krist V. Gernaey, J. K. H. & Rafiqul, G. (eds.) *Computer Aided Chemical Engineering*. Elsevier.

Paros 2004. Parametric optimization programming (pop).

Patrinos, P. & Sarimveis, H. 2010. A new algorithm for solving convex parametric quadratic programs based on graphical derivatives of solution mappings. *Automatica,* 46**,** 1405–1418.

Patrinos, P. & Sarimveis, H. 2011. Convex parametric piecewise quadratic optimization: Theory and algorithms. *Automatica,* 47**,** 1770–1777.

Pistikopoulos, E., Faísca, N. P., Kouramas, K. & Panos, C. 2009. Explicit robust model predictive control. *Proceedings of the international symposium on advanced control of chemical processes ADCHEM'09***,** 249-254.

Pistikopoulos, E., Georgiadis, M. & Dua, V. 2007. Multi-parametric Programming: Theory, Algorithms and Applications. *Wiley-VCH*.

Pistikopoulos, E., Georgiadis, M. & Dua, V. 2007b. Multi-parametric Programming: Theory, Algorithms and Applications. *Wiley-VCH,* 2.

Pistikopoulos, E. N. On-line Optimization via Off-line Optimization - A Guided Tour to Parametric Programming. AspenWorld, 2000.

Pistikopoulos, E. N. 2009. Perspectives in multiparametric programming and explicit model predictive control. *AIChE Journal,* 55**,** 1918-1925.

Pistikopoulos, E. N., Bozinis, N. A. & Dua, V. 1999. POP: A Matlab implementation of multi-parametric quadratic programming algorithm. *London, UK: Centre for Process System Engineering, Imperial College*.

Pistikopoulos, E. N., Diangelakis, N. A., Oberdieck, R., Papathanasiou, M. M., Nascu, I. & Sun, M. 2015. PAROC-An integrated framework and software platform for the optimisation and advanced model-based control of process systems. *Chemical Engineering Science*.

Pistikopoulos, E. N., Georgiadis, M. & Dua, V. 2007a. Multi-parametric Programming: Theory, Algorithms and Applications. *Wiley-VCH*.

Pse 1997-2014. gPROMS ModelBuilder (R). Process Systems Enterpise.

Raković, S. V., Barić, M. & Morari, M. Max-min control problems for constrained discrete time systems. Proceedings of the IEEE Conference on Decision and Control, 2008. 333-338.

Rampil, I. J. 1998. A primer for EEG signal processing in anesthesia. *Anesthesiology,* 89**,** 980-1002.

Rao, C. V. 2000. Moving horizon strategies for the constrained monitoring and control of nonlinear discrete-time systems. *Moving horizon strategies for the constrained monitoring and control of nonlinear discrete-time systems*.

Rawlings, J. B. & Mayne, D. Q. 2009. Model Predictive Control: Theory and Design. *Nob Hill Publishing*.

Rewieński, M. & White, J. A trajectory piecewise-linear approach to model order reduction and fast simulation of nonlinear circuits and micromachined devices. IEEE/ACM International Conference on Computer-Aided Design, Digest of Technical Papers, 2001. 252-257.

Ricardez Sandoval, L. A., Budman, H. M. & Douglas, P. L. 2008. Simultaneous design and control of processes under uncertainty: A robust modelling approach. *Journal of Process Control,* 18**,** 735-752.

Rivotti, P., Lambert, R. S. C. & Pistikopoulos, E. N. 2012. Combined model approximation techniques and multiparametric programming for explicit nonlinear model predictive control. *Computers and Chemical Engineering,* 42**,** 277-287.

Robertson, D. G. & Lee, J. H. 2002. On the use of constraints in least squares estimation and control. *Automatica,* 38**,** 1113-1123.

Rosenblatt, M. & Van Ness, J. W. 1972. Estimation of the bispectrum. *Annali Mathematical Statistical,* 36**,** 1120-1136.

Sakizlis, V., Dua, V., Perkins, J. D. & Pistikopoulos, E. 2004a. Robust model-based tracking control using parametric programming. *Computers & Chemical Engineering,* 28**,** 195-207.

Sakizlis, V., Kakalis, N. M. P., Dua, V., Perkins, J. D. & Pistikopoulos, E. N. 2004c. Design of robust model-based controllers via parametric programming. *Automatica,* 40**,** 189-201.

Saltelli, A. 2004. Global Sensitivity Analysis: An Introduction *Proceeding of 4th International Conference on Sensitivity Analysis of Model Output (SAMO '04)*.

Saltelli, A., Annoni, P., Azzini, I., Campolongo, F., Ratto, M. & Tarantola, S. 2010. Variance based sensitivity analysis of model output. Design and estimator for the total sensitivity index. *Computer Physics Communications,* 181**,** 259-270.

Saltelli, A., Ratto, M., Tarantola, S. & Campolongo, F. 2006. Sensitivity analysis practices: Strategies for model-based inference. *Reliability Engineering and System Safety,* 91**,** 1109-1125.

Sartori, V., Schumacher, P. M., Bouillon, T., Luginbuehl, M. & Morari, M. On-line estimation of propofol pharmacodynamic parameters. Annual International Conference of the IEEE Engineering in Medicine and Biology - Proceedings, 2005. 74-77.

Schnider, T. W., Minto, C. F., Gambus, P. L., Andresen, C., Goodale, D. B., Shafer, S. L. & Youngs, E. J. 1998. The influence of method of administration and covariates on the pharmacokinetics of propofol in adult volunteers. *Anesthesiology,* 88**,** 1170-1182.

Schnider, T. W., Minto, C. F., Shafer, S. L., Gambus, P. L., Andresen, C., Goodale, D. B. & Youngs, E. J. 1999. The influence of age on propofol pharmacodynamics. *Anesthesiology,* 90**,** 1502-1516.

Seron, M. M., De Doná, J. A. & Goodwin, G. C. Global analytical model predictive control with input constraints. Proceedings of the IEEE Conference on Decision and Control, 2000. 154-159.

Sigl, J. C. & Chamoun, N. G. 1994. An introduction to bispectral analysis for the electroencephalogram. *Journal of Clinical Monitoring,* 10**,** 392-404.

Singh, A. K. & Hahn, J. 2005. State estimation for high-dimensional chemical processes. *Computers and Chemical Engineering,* 29**,** 2326-2334.

Sobol, I. M. 1993. Global sensitivity indices for nonlinear mathematical models and theirMonte Carlo estimates. *Mathematical Modeling Computation* 407-414.

Sobol, I. M. 2001. Global sensitivity indices for nonlinear mathematical models and their Monte Carlo estimates. *Mathematics and Computers in Simulation,* 55**,** 271-280.

Sobol, I. M. & Kucherenko, S. S. 2005. On Global sensitivity analysis of quasi-Monte Carlo algorithms. *Monte Carlo Methods and Applications,* 11**,** 83-92.

Söderström, T. 2002. *Discrete-time Stochastic Systems*, Springer.

Spjøtvold, J., Kerrigan, E. C., Jones, C. N., Tøndel, P. & Johansen, T. A. 2006. On the facet-to-facet property of solutions to convex parametric quadratic programs. *Automatica,* 42**,** 2209–2214.

Struys, M. M. R. F., De Smet, T., Versichelen, L. F. M., Van De Velde, S., Van Den Broecke, R. & Mortier, E. P. 2001. Comparison of closed-loop controlled administration of propofol using Bispectral Index as the controlled variable versus "standard practice" controlled administration. *Anesthesiology,* 95**,** 6-17.

Struys, M. M. R. F., Vereecke, H., Moerman, A., Jensen, E. W., Verhaeghen, D., De Neve, N., Dumortier, F. J. E. & Mortier, E. P. 2003. Ability of the Bispectral Index, autoregressive modelling with exogenous input-derived auditory evoked potentials, and predicted propofol concentrations to measure patient responsiveness during anesthesia with propofol and remifentanil. *Anesthesiology,* 99**,** 802-812.

Su, Q. L., Hermanto, M. W., Braatz, R. D. & Chiu, M. S. 2016. Just-in-Time-Learning based Extended Prediction Self-Adaptive Control for batch processes. *Journal of Process Control,* 43**,** 1-9.

Sudret, B. 2008. Global sensitivity analysis using polynomial chaos expansions. *Reliability Engineering and System Safety,* 93**,** 964-979.

Sumner, T., Shephard, E. & Bogle, I. D. L. 2012. A methodology for global-sensitivity analysis of time-dependent outputs in systems biology modelling. *Journal of the Royal Society Interface,* 9**,** 2156-2166.

Tøndel, P., Johansen, T. A. & Bemporad, A. 2003. An algorithm for multi-parametric quadratic programming and explicit MPC solutions. *Automatica,* 39**,** 489–497.

Torrico, B. C., De Keyser, R., Ionescu, C. & Normey-Rico, J. E. Predictive control with robust dead-time compensation: Application to drug dosing during anesthesia. IFAC Proceedings Volumes (IFAC-PapersOnline), 2007. 402-407.

Trifkovic, M., Sheikhzadeh, M., Nigim, K. & Daoutidis, P. 2014. Modeling and control of a renewable hybrid energy system with hydrogen storage. *IEEE Transactions on Control Systems Technology,* 22**,** 169-179.

Velliou, E., Fuentes-Garí, M., Misener, R., Pefani, E., Rende, M., Panoskaltsis, N., Mantalaris, A. & Pistikopoulos, E. N. 2014. A framework for the design, modeling and optimization of biomedical systems. *In:* Mario R. Eden, J. D. S. & Gavin, P. T. (eds.) *Computer Aided Chemical Engineering.* Elsevier.

Viertö-Oja, H., Maja, V., Särkelä, M., Talja, P., Tenkanen, N., Tolvanen-Laakso, N., Paloheimo, M., Vakkuri, A., Yli-Hankala, A. & Meriläinen, P. Description of the entropy algorithm as applied in the Datex- Ohmeda S/5 Entropy Module. *Acta Anaesthesiol Scandinavica,* 48**,** 154-161.

Voelker, A., Kouramas, K. & Pistikopoulos, E. N. 2013. Simultaneous design of explicit/multi-parametric constrained moving horizon estimation and robust model predictive control. *Computers and Chemical Engineering,* 54**,** 24-33.

Welch, G. & Bishop, G. 2001. An introduction to the Kalman filter: SIGGRAPH 2001 Course 8. *Proc. Comput. Graph., Annu. Conf. Comput Graph., Interact. Techn.***,** 12-17.

West, N., Dumont, G. A., Van Heusden, K., Petersen, C. L., Khosravi, S., Soltesz, K., Umedaly, A., Reimer, E. & Ansermino, J. M. 2013. Robust closed-loop control of induction and maintenance of propofol anesthesia in children. *Paediatric Anaesthesia,* 23**,** 712-719.

Westenskow 1997. Fundamentals of Feedback Control: PID, Fuzzy Logic, and Neural Networks. *Journal of Clinical Anesthesia,* 9**,** 33S-35S.

Wittmann-Hohlbein, M. & Pistikopoulos, E. N. 2012. A two-stage method for the approximate solution of general multiparametric mixed-integer linear programming problems. *Industrial and Engineering Chemistry Research,* 51**,** 8095-8107.

Wittmann-Hohlbein, M. & Pistikopoulos, E. N. 2013. On the global solution of multi-parametric mixed integer linear programming problems. *Journal of Global Optimization,* 57**,** 51-73.

Wong, E. 1971. Stochastic Process in Informaion and Dynamical Systems. *McGraw-Hill*.

Xie, W., Bonis, I. & Theodoropoulos, C. 2011. Off-line model reduction for on-line linear MPC of nonlinear large-scale distributed systems. *Computers and Chemical Engineering,* 35**,** 750-757.

Xie, W., Bonis, I. & Theodoropoulos, C. 2012. Linear MPC based on data-driven Artificial Neural Networks for large-scale nonlinear distributed parameter systems. *Computer Aided Chemical Engineering.*

Yelneedi, S., Samavedham, L. & Rangaiah, G. P. 2009. Advanced Control Strategies for the Regulation of Hypnosis with Propofol. *Industrial & Engineering Chemistry Research,* 48**,** 3880-3897.

Yue, H., Brown, M., He, F., Jia, J. & Kell, D. B. 2008. Sensitivity analysis and robust experimental design of a signal transduction pathway system. *International Journal of Chemical Kinetics,* 40**,** 730-741.

Zavitsanou, S., Mantalaris, A., Georgiadis, M. C. & Pistikopoulos, E. N. 2014. Optimization of Insulin Dosing in Patients with Type 1 Diabetes Mellitus. *In:* Jiří Jaromír Klemeš, P. S. V. & Peng Yen, L. (eds.) *Computer Aided Chemical Engineering.* Elsevier.

Zavitsanou, S., Mantalaris, A., Georgiadis, M. C. & Pistikopoulos, E. N. 2015. <italic>In Silico</italic> Closed-Loop Control Validation Studies for Optimal Insulin Delivery in Type 1 Diabetes. *Biomedical Engineering, IEEE Transactions on,* 62**,** 2369-2378.

Ziogou, C., Panos, C., Kouramas, K. I., Papadopoulou, S., Georgiadis, M. C., Voutetakis, S. & Pistikopoulos, E. N. 2011. Multi-Parametric Model Predictive Control of an Automated Integrated Fuel Cell Testing Unit. *In:* E.N. Pistikopoulos, M. C. G. & Kokossis, A. C. (eds.) *Computer Aided Chemical Engineering.* Elsevier.

Appendix A
Sensitivity Analysis

The use of sensitivity analysis in the context of biomedical engineering is of critical importance. Sensitivity analysis has been increasingly used for the assessment of the robustness of complex biological and biomedical models and in uncertainty quantification (Kontoravdi et al., 2005, Kontoravdi et al., 2010, Yue et al., 2008, Kiparissides et al., 2009, Kucherenko et al., 2009). This is particularly relevant in the field of pharmacometrics when trying to estimate the relative influence of pharmacokinetic, pharmacodynamics and other uncertain parameters. Sensitivity analysis is also used in model simplification as an approach to decrease the parametric dimensionality of biological systems. It could also be used to remove some parts of a model that do not significantly affect its response. This is usually done by fixing non-essential parameters to their mean value so that more attention can be dedicated to critically important factors to perform tasks like parameter estimation or optimal design of experiment. In recent years, global sensitivity analysis has gained considerable attention due to its advantages over local sensitivity analysis approaches (Homma et al., 1996, Saltelli, 2004). Global sensitivity analysis (SA) can be used to quantify the variability in model predictions resulting from the uncertainty in multiple parameters and to shed light on the biological mechanisms driving system behaviour (Sumner et al., 2012). It is model-independent by design and has the capability of detecting parametric interactions, unlike one factor at a time (OAT) local methods (Saltelli et al., 2010). An eminent class of global sensitivity analysis techniques is that of variance based method, which include the well-known Sobol' method of sensitivity indices (Sobol, 1993, Sobol, 2001). One of the disadvantages of such methods that are based on Monte-Carlo sampling is the necessity to repeatedly run potentially expensive simulations. This is exacerbated in the case of high dimensional input spaces for which exploration may become computationally intractable. One way to reduce the computational expense of performing sensitivity analysis has been the use of surrogate-models or meta-models. This approach consists of using relatively simpler models that emulate the dynamic behaviour of the original computationally intensive models. Various surrogate modelling approaches has been suggested such as Gaussian process modelling, polynomial chaos expansion (Sudret, 2008), radial basis function (Buhmann, 2003), and High Dimensional

model representation (Li et al., 2002)(actually a particular instance of PCE). The two main difficulties of these approaches are: The ability to handle higher dimension spaces and the sampling requirements to achieve convergence. For example regression based PCE approaches are better suited for systems with no more than 10 input variables (Blatman et al., 2010). Methods based on numerical integration like HDMR are able to perform in high dimensional spaces but may require a significant amount of sampling realization in order to achieve convergence. An efficient solution is the combined use of low computational screening methods to discards non-essential variables prior to the use of a variance-based method on the remaining parameters. One of the most commonly used screening methods is the Morris method (Morris, 1991). A very powerful set of data-driven approaches is the class of inductive modelling methods, in particular group method of data handling (Ivakhnenko et al., 1995). Group method of Data handling is based on the cybernetic principle of self-organization and has the ability to perform with limited data samples and in very high dimensional spaces, by selecting important parameters in an adaptive fashion. Another advantage of the approach is its immunity to noise. This is a very relevant aspect as in many cases, the sensitivity analysis practitioner does not necessarily have access to a model but only noisy field data.

A1 The Sobol's Sensitivity Analysis

The Sobol's sensitivity analysis method is a variance based approach based on the ANOVA decomposition(Sobol, 2001, Sobol et al., 2005). If f is an integrable function defined on the unit hypercube $I^n$and $x\epsilon I^n$, $x = (x_1, \dots, x_n)$ the input variables, the output $f(x)$ of the function may be expressed as:

$$f(x) = f_0 + \sum_{s=1}^{n} \sum_{i_1<\cdots<i_s}^{n} f_{i_1 \dots i_s}(x_{i_1}, \dots, x_{i_s}) \qquad \text{(Equation A.1)}$$

f_0 is the mean response of $f$and the terms $f_i(x_i)$ and $f_{ij}(x_i,x_j)$ represent the first and second order terms and so on. The formula above is termed ANOVA decomposition. The component functions may then be expressed as integrals of$f$:

$$\int f(x)dx = f_0 \qquad \text{(Equation A.2)}$$

$$\int f(x)\prod_{k\neq i} dx_k = f_0 + f_i(x_i)$$

$$\int f(x)\prod_{k\neq i,j} dx_k = f_0 + f_i(x_i) + f_{ij}(x_i, x_j)$$

One of the most known global sensitivity analysis methods was introduced by (Sobol, 2001). If it is assumed that$f$ is square integrable over I^n, we have:

$$\int f^2(x)dx - f_0 = \sum_{s=1}^{n}\sum_{i_1<\cdots<i_s}^{n}\int f_{i_1\ldots i_s}dx_1 \ldots dx_s \qquad \text{(Equation A. 3)}$$

$$D = \int f^2(x)dx - f_0 \text{and} D_{i_1\ldots i_s} = \int f_{i_1\ldots i_s}dx_1 \ldots dx_s$$

The terms represent the variance and partial variance respectively. The Sobol's sensitivity indices (SI) can be given by:

$$S_{i_1\ldots i_s} = \frac{D_{i_1\ldots i_s}}{D} \qquad \text{(Equation A. 4)}$$

where:

$$\sum_{s=1}^{n}\sum_{i_1<\cdots<i_s}^{n} S_{i_1\ldots i_s} = 1 \qquad \text{(Equation A. 5)}$$

If a set of variables $y = (x_1, \ldots, x_s)$is considered and z a set of the complementary variables, we note $x = (y, z)$. Using the previous definition of the variance the total variance of the subset y can be computed as:

$$D_y^{tot} = D - D_z \quad \text{(Equation A. 6)}$$

and:

$$S_y^{tot} = \frac{D_y^{tot}}{D} \quad \text{(Equation A.7)}$$

The following inequality holds:

$$0 \leq S_y \leq S_y^{tot} \leq 1 \quad \text{(Equation A. 8)}$$

If $S_y = S_y^{tot} = 0$ then f does not depend on y.

If $S_y = S_y^{tot} = 1$ then f only depends on y.

The indices enable us to rank variables and discard unessential variables. Sensitivity analysis indices are usually computed through Monte-Carlo numerical integration (Sobol, 2001).

$$D_y = \int f(x) f(y,z) dx dz - f_0^2 \quad \text{(Equation A. 9)}$$

Using low discrepancy sequences have shown to increase the efficiency of the technique especially the Sobol's sequence for uniform sampling.

2.2.1.2 High Dimensional Model Representation (HDMR)

In order to efficiently build the map of the input-output behavior of a model function involving high dimensional inputs, (typically $n \sim 10^2 - 10^3$), the HDMR approach was introduced as a set of quantitative tools. In most engineering problems the expansion of functions can be truncated to the second order component function by Li *et al.*(Li et al., 2006, Li et al., 2002)

$$f(x) \approx h(x) = f_0 + \sum_{i=1}^{n} f_i(x_i) + \sum_{1 \leq i < j \leq n} f_{ij}(x_i, x_j) \quad \text{(Equation A. 10)}$$

A particular way of deriving an HDMR representation through monte-carlo sampling is the Random Sampling HDMR technique (RS-HDMR). Since the computation of multidimensional integrals may become prohibitive (Sobol, 1993), an alternative technique based on the use of interpolation of over families over low order component

functions has been introduced by Rabitz and co-workers(Li et al., 2002). If a set of piecewise continuous component functions $\{\varphi\}$ is considered, we can derive:

$$f_i(x_i) = \sum_{r=1}^{k} \alpha_r^i \varphi_r(x_i) \qquad \text{(Equation A. 11)}$$

$$f_{ij}(x_i, x_j) = \sum_{p=1}^{l} \sum_{q=1}^{m} \beta_{pq}^{ij} \varphi_p(x_i) \varphi_q(x_j)$$

Once a family of component functions has been selected the coefficients

$$\forall r \epsilon [1, k], \alpha_r^i = \int_0^1 f_i(x_i) \varphi_r(x_i) dx_i \qquad \text{(Equation A. 12)}$$

$$\forall p \epsilon [1, l], \forall q \epsilon [1, m], \beta_{pq}^{ij} = \int_0^1 \int_0^1 f_{ij}(x_i, x_j) \varphi_p(x_i)\, \varphi_q(x_j) dx_i dx_j$$

In practice these calculations are done through Monte-Carlo Integration. There is a direct relationship between the HDMR expansion coefficients and the Sobol's sensitivity analysis technique:

$$D_i = \sum_{r=1}^{k_i} \left(\alpha_r^i\right)^2 \qquad \text{(Equation A. 13)}$$

And

$$D_{ij} = \sum_{p=1}^{l_i} \sum_{q=1}^{l_j} \left(\beta_{pq}^{ij}\right)^2 \qquad \text{(Equation A. 14)}$$

The sensitivity indices are obtained by dividing with the total variance. Even though, the total effect coefficients and the total variance, involving interaction order greater than three will still require the use of the Sobol original approach.

Although, HDMR has been very successful in a number of sensitivity analysis studies, it can be problematic in the case of a large number of parameters. The calculation of its component often require large sampling sets even though the method is able of presenting high dimensional input-output relationships. In the case of computationally intensive simulation models this may become very impractical.

2.2.1.3 Group Method of Data Handling (GMDH)

Group Method of Data Handling (GMDH) is based on the principle of self-organization and is sometimes referred to as Polynomial Neural Networks. This technique is based on representing complex functions through networks of elementary expressions, like other advanced surrogate-modelling approaches such as neural networks or the HDMR approach.(Lorentz, 1966) and (Kolmogorov, 1957) have shown that any continuous function $f(x_1, \ldots, x_d)$ of dimension d on $[0,1]^d$ can be exactly represented as a composition of sums and continuous one-dimensional functions. The GMDH approach is very efficient in data-driven modelling of complex systems with several advantages over conventional neural networks. We can refer to(Ivakhnenko and Muller, 1995, Lemke, 1997)for more ample theoretical description of the method. An advantage over the classical neural networks is that GMDH is inductive, adaptively creating models from data under the form of networks of optimized active neurons in an evolutionary manner. The aim is to estimate an optimal structure of a network that self-organizes itself during training making this a combined structure and parameter estimation procedure that starts from a basic structure the mean value of the time series output data.

A first layer is built by considering all possible variables pair and inductively self-constructing and validating neurons made of simple expressions, usually within linear or second order polynomials.

This will result in a set of transfer functions for the first network layer. A number of fittest and best generalizing models consisting of neurons are then selected via an external criterion. After each single induction step model validation is performed as integrated critical part of model self-organization. In the classical approach, in order to create a new layer the selected neurons are subsequently used as inputs, while other neurons are discarded. More complex organizations can be generated by using the selection criterion and using the cybernetics inheritance principle. The final optimal complex structure consists of a single network. There is no need to predefine the number of neurons or layers to be used since they are adaptively determined through the learning process.

The model self-organization stops itself when an optimal complex model has been found, i.e., further increasing model complexity would result in over-fitting the design data by starting adapting to noise. This is an important advantage over the RS-HDMR approach or regression based PCE that require the computation of a full set of predefined parameters. HDMR requires the computation of a large number of α_r^i coefficients through numerical integration β_{pq}^{ij}, for many combinations of parameters (x_i,x_j) and polynomial orders and unessential parameters can only be weeded-out a posteriori upon

calculation of these coefficients.

2.2.1.4 GMDH-HDMR

As shown previously, GMDH holds a number of advantages that are essential to global sensitivity analysis. The method is able to handle high dimensionalities, this being important in the context of biomedical engineering. Moreover, GMDH is, by design, a very efficient screening procedure in itself by adaptively weeding out unessential parameters in a computationally tractable manner. Also, it has good performance for small data samples. The presented method is based on the direct construction of the HDMR expansion by using GMDH inductive modelling. If a set of parameters $(x_i)_{i\in[\![1,n]\!]}$ is considered, additional 'synthetic' variables are built.

These correspond to Legendre orthogonal polynomials of up to a predefined order n and evaluated on the original variables: $X_{r,i} = \varphi_r(x_i), r = 1..n$.

The GMDH algorithm is performed only on these variables, imposing a multi-linear relationship between the variables. For the calculation of the Sobol's sensitivity indices the coefficient of the GMDH expression are used.

The main advantage of this method is its inductive ability to eliminate unessential parameters during the modelling process leading to the elimination of the calculation of coefficients for parameters that do not contribute to the variance of the output. The method, indeed incorporates the screening step and calculation of sensitivity indices in a single procedure.

Appendix B
Model Reduction

Model order reduction (MOR) describes a methodology intended to reduce the dimensionality of a dynamical system while preserving its input-output behaviour (Figure B.1). The main purpose of model order reduction originally stemmed from a need to derive approximations of large-scale dynamical systems for simulation purposes. One major area of application has concerned the reduction of finite element models originating from the discretization of large-scale systems of ordinary differential equations (ODEs), differential algebraic equations (DAE), partial differential equations (PDEs) and partial differential algebraic equations (PDAEs). In effect, sophisticated discretization techniques yield computationally prohibitive high dimensional systems. These discretized systems tend to be extremely complex and sometimes intractable for the purpose of prediction and simulation, and even more so, in the case of the resolution of inverse problems characterizing optimization, parameter estimation and model predictive control. In the context of multiparametric/explicit model predictive control, this complexity takes a very specific meaning. Indeed, complexity directly materializes in steep increase in the number of critical regions, which results from the compounded effect of a high number of state variables (parameters) and constraints (dependent on the length of the prediction horizon)

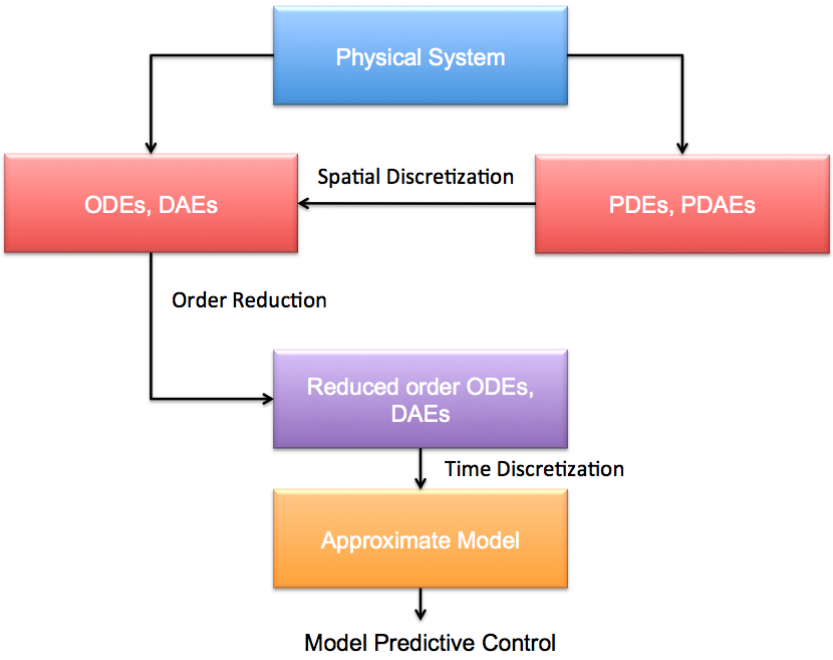

Figure B. 1: Schematic representation of the MOR approximation procedure

Linear Model Order Reduction

An important class of model reduction techniques concern linear systems. A major area of application of this class of problem has been the reduction of large-scale microelectromechanical systems(Antoulas, 2005). Most MOR techniques are projection based i.e., consist of projecting the dynamics of the original system on a lower dimensional subspace. One major class of methods is that of singular value decomposition methods (SVD) and is based on the more general concept of principal component analysis (PCA). PCA is a procedure concerned with inferring the covariance structure of a system by converting a set of observations of possibly correlated variables into a set of values of linearly uncorrelated variables called the principal components. The transformation results in a hierarchized set of principal components ordered by decreasing variance. In particular, it allows the identification of the principal directions (e.g. state variables) in which the data varies. The two main classes of MOR techniques are SVD methods and moment matching approaches. In balanced truncation, a transformation is operated that project the system dynamics in a space where the most observable systems correspond to the most controllable ones. Following the procedure described in (Antoulas, 2005), we formulate a dynamical system in an equivalent balanced form:

$$\begin{aligned} x_{t+1} &= Ax_t + Bu_t \\ y_t &= Cx_t \end{aligned} \qquad \text{(Equation B. 1)}$$

The linear gramians controllability and observability gramians W_C and W_O are defined as the unique positive definite solution to the Lyapunov equations:

$$AW_C + W_C A^T = -BB^T$$
$$AW_C + W_C A^T = -BB^T \qquad \text{(Equation B. 2)}$$

Finding a balanced form for these gramians consists of finding a diagonal matrix Σ such that:

$$\bar{W}_O = \bar{W}_C = \Sigma = diag\left(\sigma_i\right)_{i \in [1,n]} \qquad \text{(Equation B. 3)}$$

Where

$$\bar{W}_C = TW_C T^T$$
$$\bar{W}_O = \left(T^{-1}\right)^T W_O T^{-1} \qquad \text{(Equation B. 4)}$$

T is a transformation matrix and the σ_i are the Hankel singular values. The transformation matrix is then used to reformulate the dynamical system in an equivalent balanced form:

$$\bar{x}_{t+1} = TAT^{-1}\bar{x}_t + TBu_t$$
$$y_t = CT^{-1}x_t \qquad \text{(Equation B. 5)}$$

It is possible to truncate the system by retaining the states accounting for most of its dynamical behaviour by partitioning the balanced system: Noting $\bar{A} = TAT^{-1}$ and $\bar{B} = TB$ a reduced order LTI is obtained:

$$\bar{x}_{1t+1} = A_{11}\bar{x}_{1t} + B_1 u_t$$
$$y_t = C_1 \bar{x}_{1t} \qquad \text{(Equation B. 6)}$$

where:

$$\bar{A} = \begin{bmatrix} A_{11} & A_{12} \\ A_{21} & A_{22} \end{bmatrix}, \bar{B} = \begin{bmatrix} B_1 \\ B_2 \end{bmatrix}, \bar{C} = \begin{bmatrix} C_1 & C_2 \end{bmatrix}, \bar{x} = \begin{bmatrix} \bar{x}_1 \\ \bar{x}_2 \end{bmatrix} \qquad \text{(Equation B. 7)}$$

Those synthetic i.e., physically meaningless states form an ordered set of decreasing controllability and observability. Another very important class of linear MOR techniques is that of moment-matching approaches. This class of method consists of the interpolation of the transfer function of a system, usually via the Pade approximation(Gallivan et al.,

1994). It also belongs to the wider class of projection techniques known under the name of Krylov subspace methods(Krylov, 1931). Two widely used moment matching methods are the method of (Arnoldi, 1951) and (Lanczos, 1950). Current research concerns the combination of the two paradigms(Antoulas et al., 2001). These techniques are commonly referred to as 'SVD-Krylov' methods. For a thorough overview of linear MOR techniques, the reader will refer to (Antoulas, 2005). In some cases, a linear system is not sufficient to accurately capture the dynamics of a dynamical system. As linearization potentially leads to a significant loss of information, nonlinear model reductions approaches were introduced.

Nonlinear Model Reduction

The second approach employed is nonlinear balanced truncation, which is a snapshots based technique and an empirical extension of the linear balanced truncation technique. Consider a nonlinear system of ODEs of the following form:

$$\begin{aligned} \dot{x}(t) &= f(x(t),u(t)) \\ y(t) &= h(x(t),u(t)) \end{aligned} \qquad \text{(Equation B. 8)}$$

As in linear balanced truncation, the method consists of finding a transformation matrix T in order to project the state vector on a lower order subspace $\bar{x} = Tx$. In order to compute these matrices, empirical gramians or covariance matrices are derived from simulation data from the system.

Defining the following sets:

$$\begin{aligned} T^n &= \left\{T_1,...,T_r; T_i \in \Re^{n\times n}, T_i^T T_i = I, i = 1,...,r\right\} \\ M &= \left\{c_1,...,c_s; c_i \in \Re, c_i \geq 0 = I, i = 1,...,s\right\} \\ E^n &= \left\{e_1,...,e_n\right\} \text{standard unit vectors in } \Re^n \end{aligned} \qquad \text{(Equation B. 9)}$$

where r is the number of matrices for perturbation directions; s the number of different perturbation sizes for each direction and n the number of inputs of the system. Using the sets above it is possible to derive empirical controllabity and observability gramians as follows:

$$W_C = \sum_{l=1}^{r}\sum_{m=1}^{s}\sum_{i=1}^{p}\frac{1}{rsc_m^{\,2}}\int_0^\infty \Phi^{ilm}(t)dt \qquad \text{(Equation B. 10)}$$

Where $\Phi^{ilm}(t) \in \Re^{n\times n}$

is given by $\Phi^{ilm}(t) = \left(x^{ilm}(t) - x_0^{\,ilm}\right)\left(x^{ilm}(t) - x_0^{\,ilm}\right)^T$ and $x^{ilm}(t)$ is the state of the nonlinear system corresponding to the impulse input:

$u(t) = c_m T_l e_i \delta(t) + u_0$ and x_0^{ilm} corresponds to the steady state of the system. Similarly an empirical observability gramian is defined by:

$$W_C = \sum_{l=1}^{r}\sum_{m=1}^{s} \frac{1}{rsc_m^{\,2}} \int_0^\infty T_l \Psi^{lm}(t) T_l^{\,T} dt \qquad \text{(Equation B. 11)}$$

$\Psi^{lm}(t) \in \Re^{n \times n}$

Is defined as

$\Psi^{lm}{}_{ij}(t) = \left(y^{ilm}(t) - y_0^{ilm}\right)\left(y^{jlm}(t) - y_0^{jlm}\right)$ and $y^{ilm}(t)$ is the output of the system corresponding to the initial condition $x_0 = c_m T_l e_i + x_0$

The y_0^{ilm} corresponds to the output measurement when the system is at steady state. A balanced system is then obtained from the previously defined empirical gramians as:

$$\begin{aligned} \dot{\bar{x}}(t) &= Tf(T^{-1}\bar{x}(t), u(t)) \\ y(t) &= g(T^{-1}\bar{x}, u) \end{aligned} \qquad \text{(Equation B. 12)}$$

Using a Garlekin projection $P = [I, 0]$ matrix with the same rank as the reduced system, the unimportant states may be set a nominal steady state value and the nonlinear reduced order model:

$$\begin{aligned} \dot{\bar{x}}_1(t) &= PTf(T^{-1}P^T\bar{x}(t), u(t)) \\ \dot{\bar{x}}_2(t) &= \bar{x}_{2ss}(0) \\ y &= g(T^{-1}\bar{x}, u) \end{aligned} \qquad \text{(Equation B. 13)}$$

Note that in the case of the presence of parametric uncertainty, the system may be reduced by treating the parameters as exogenous inputs in a similar way as the method described above:

$$\begin{aligned} \dot{x}(t) &= f(x(t), u(t), \theta(t)) \\ y(t) &= h(x(t), u(t), \theta(t)) \end{aligned} \qquad \text{(Equation B. 14)}$$

Simply by posing $\tilde{u} = \begin{pmatrix} u \\ \theta \end{pmatrix}$

A classification of linear and nonlinear model reduction techniques can be found in Table B. 1 and Table B. 2 presents a Summary of the literature on model order reduction for mp-MPC applications.

Table B. 1: Classification of the main order reduction techniques (Antoulas, 2000)

Moment Matching Methods	SVD Methods	
Linear Systems		Nonlinear Systems
Arnoldi(Arnoldi, 1951) Lanczos(Lanczos, 1950)	Balanced Truncation (Moore, 1982) Hankel Approximation (Adamjan et al., 1971), (Antoulas and Sorensen, 2001))	POD (Wong, 1971); Astrid, 2004) Empirical Balanced Truncation (Lall et al., 1999, Hahn et al., 2002) TPWL (Rewieński et al., 2001)

Table B. 2: Summary of the literature on model order reduction for mp-MPC applications

Authors	Methodologies	Key Features
(Narciso and Pistikopoulos, 2008)	Balanced Truncation, mp-MPC	Combines linear balanced truncation and explicit MPC incorporating the error bound into the control formulation.
(Singh and Hahn, 2005)	Empirical Balanced Truncation, Luenberg type observers	State estimation on nonlinear reduced order models obtain through empirical balanced truncation
(Hovland et al., 2008)	POD, mp-MPC, Kalman filters	Implementation of a 'goal-oriented' model constrained optimization framework to determine the optimal POD reduction projection basis.

		Simultaneous use of Kalman state estimation on the reduced order systems.
(Bonis et al., 2012)	Successive linearization, Krylov Methods	'Equation-free' successive linearization of nonlinear systems of ODEs to which an Arnoldi order reduction scheme is applied.
(Agarwal et al., 2013)	POD	Implementation of a trust-region framework to guarantee optimality conditions with respect to the original system in optimization problems defined on reduced order POD models.
(Hedengren et al., 2005)	Empirical balanced truncation, ISAT	Order reduction through empirical balanced truncation coupled to complexity reduction and linearization via ISAT
(Xie et al., 2012)	ANNs, POD	A hybrid, data-driven approach, constructing POD approximate models with $a_i(t)$ time varying coefficient determined via ANN black-box models and the basis function in POD from data plant 'snapshots'.
(Lambert et al., 2013)	Empirical balanced truncation	Empirical balanced balance truncation combined to linearization and balanced truncation for application of mp-MHE
(Rivotti et al., 2012)	Empirical balanced	Empirical balanced truncation combined to nonlinear mp-NMPC

	truncation	
(Lambert et al., 2013)	Variance-based model reduction	Use numerical integration for a variance based approximation technique using global sensitivity analysis principles
(Xie et al., 2011)	POD,TPWL, mp-MPC	POD model order reduction of the dimensionality with respect to the spatial coordinate and use of TPWL to linearize the time dependent coefficients in the POD expansion.

Appendix C
Multiparametric Programming

C1. Multiparametric programming

Multiparametric programming is a technique for solving any optimization problem, where the objective is to minimize or maximize a performance criterion subject to a given set of constraints and where some of the parameters vary between specified lower and upper bounds. The main characteristic of multiparametric programming is its ability to obtain: (i) the objective and optimization variable as a function of the varying parameters, and (ii) the regions in the space of the parameters where these functions are valid [critical regions (CR)] (Kouramas et al., 2011b).

The advantage of using multiparametric programming to address these problems is that for problems pertaining to plant operations, such as for process planning, scheduling, and control one can obtain a complete map of all the optimal solutions. Hence, as the operating conditions vary, one does not have to reoptimize for the new set of conditions(Pistikopoulos et al., 2007a).

A general multiparametric programming problem may be formulated as follows.

$$\begin{aligned} &\min_{x} f(x,\theta) \\ &s.t.\ g_i(x,\theta) \le 0, \quad \forall i = 1,..,p \\ &\quad h_j(x,\theta) = 0, \quad \forall j = 1,...,q, \\ &\quad x \in X \subseteq \Re^n, \\ &\quad \theta \in \Theta \subseteq \Re^m, \end{aligned} \qquad \text{(Equation C.1)}$$

Where *f, g* and *h* are twice continuously differentiable in *x* and θ.

If (Equation C.1) has a quadratic objective function, linear constraints, and the parameters appear on the right-hand side of the constraints the equation will have the following form

$$
\begin{aligned}
z(\theta) = \min_{x} \; & fc^T x + \frac{1}{2} x^T Q x \\
s.t. \quad & \\
& Ax \le b + F\theta \\
& x \in X \subseteq \Re^n, \\
& \theta \in \Theta \subseteq \Re^m,
\end{aligned}
\qquad \text{(Equation C.2)}
$$

where c is a constant vector of dimension *n, Q* is an *(n x n)* symmetric positive definite constant matrix, *A* is a *(p x n)* constant matrix, *F* is a *(p x m)* constant matrix, *b* is a constant vector of dimension *p*, and *X* and *Θ* are compact polyhedral convex sets of dimensions n and m, respectively. Note that a term of the form $\theta^T P x$ in the objection function can also be addressed in the following formulation, as it can be transformed into the form given in (Equation C.2) by substituting $x = s - Q^{-1}P^T\theta$, where s is a vector of arbitrary variables of dimensions n and P is a constant matrix of dimension *(m x n)*.

If we apply the basic sensitivity theorem to (Equation C.2) at $[x(\theta_Q),\theta_Q]$ we will obtain the following result:

$$
\begin{pmatrix} \dfrac{dx(\theta_Q)}{d\theta} \\ \dfrac{d\lambda(\theta_Q)}{d\theta} \end{pmatrix} = -(M_Q)^{-1} N_Q, \qquad \text{(Equation C.3)}
$$

Where

$$M_Q = \begin{bmatrix} Q & A_1^T & . & . & . & A_p^T \\ -\lambda_1 & A_1 - V_1 & & & & \\ . & & . & & & \\ . & & & . & & \\ . & & & & . & \\ -\lambda_p A_p & & & & & -V_p \end{bmatrix}, \qquad \text{(Equation C.4)}$$

$$N_Q = [Y, \lambda_1 F_1, ..., \lambda_p F_p]^T,$$

$$V_i = A_i x(\theta_Q) - b_i - F_i \theta_Q,$$

and Y is a null matrix of dimension *(n x m)*. Thus, in the linear-quadratic optimization problem, the Jacobian reduce to a mere algebraic manipulation of the matrices declared in (Equation C.2)

$$\begin{bmatrix} x_Q(\theta) \\ \lambda_Q(\theta) \end{bmatrix} = -(M_Q)^{-1} N_Q(\theta - \theta_Q) + \begin{bmatrix} x_Q(\theta_Q) \\ \lambda_Q(\theta_Q) \end{bmatrix} \qquad \text{(Equation C.5)}$$

The space of θ where this solution remains optimal is defined as the critical region, CR^Q, and can be obtained by using feasibility and optimality conditions. The notation *CR* will be used to denote the set of points in the space of θ that lie in *CR* as well as to denote the set of inequalities which define CR. Feasibility is ensured by substituting $x_Q(\theta)$ into the inactive inequalities given in (Equation C.2), whereas the optimality condition is given by $\tilde{\lambda}_Q(\theta) \geq 0$, where $\tilde{\lambda}_Q(\theta)$ corresponds to the vector of active inequalities, resulting in a set of parametric constraints. This is represented by

$$CR^R = \left\{ \breve{A} x_Q(\theta) \leq \breve{b} + \breve{F}\theta, \tilde{\lambda}_Q(\theta) \geq 0, CR^{IG} \right\}, \qquad \text{(Equation C.6)}$$

where $\breve{A}$, $\breve{b}$, and $\breve{F}$ correspond to the inactive inequalities and CR^{IG} represents a set of linear inequalities defining an initial given region. A compact representation of CR^Q is obtained from the parametric inequalities by removing the redundant inequalities:

$$CR^{Q} = \Delta\{CR^{R}\}, \qquad \text{(Equation C.7)}$$

where Δ is an operator which removes redundant constraints(Pistikopoulos et al., 2007a). Once CR^{Q}, which is a polyhedral region, has been defined for a solution, $[x(\theta_Q), \theta_Q]$, the next step is to define the rest of the region, CR^{rest}, as proposed in(Pistikopoulos et al., 2007b)]:

$$CR^{rest} = CR^{IG} - CR^{Q} \qquad \text{(Equation C.8)}$$

We then obtain another set of solutions in each of these regions and their corresponding *CRs*. The algorithm terminates when there are no more regions to be explored, namely when the solution of the differential equation (Equation C.3) has been fully approximated by first-order expansions.

Table C. 1: mp-QP algorithm

Step 1	In a given region solve (Equation C.2) by treating θ as a free variable to obtain a feasible point $[\theta_Q]$
Step 2	Fix $\theta = \theta_Q$ and solve (Equation C.2) to obtain $[x(\theta_Q), \lambda(\theta_Q)]$
Step 3	Compute $[-(M_Q)^{-1}N_Q]$ from (Equation C.3)
Step 4	Obtain $[x_Q(\theta),\lambda_Q(\theta)]$ from (Equation C.5)
Step 5	Form a set of inequalities, CR^{R}, as described in (Equation C.6)
Step 6	Remove redundant inequalities from this set of inequalities and define the corresponding CR^{Q} as given in (Equation C.7)
Step 7	Define the rest of the region, CR^{rest}as given in (Equation C.8)
Step 8	If no more regions to explore, go to the next step, otherwise go to Step 1

Step 9	Collect all the solutions and unify the regions having the same solution to obtain a compact representation

The main steps of the algorithm are presented in Table C. 1. While defining the rest of the regions, some of the regions are split and hence the same optimal solutions may be obtained in more than one region. Therefore, the regions with the same optimal solutions are united and a compact representation of the final solution is obtained.

C.2 Multiparametric mixed-integer programming

The solution of mp-MIP problems is very challenging. The additional complications introduced by the presence of integer variables are (i) combinatorial complexity and (ii) nonconvexity. In the following, the problem and solution characteristics of mp-MIP problems are described, before approaches are reviewed which have been proposed to solve certain mp-MIP problems. Based upon these, a general framework for the solution of a certain class of mp-MIP problems is presented, as well as a novel strategy on how to handle the presence of nonconvexity in the description of the critical regions.

Remark C.1 *The most common mp-MIP problems, and thus the ones considered here, are multiparametric mixed-integer linear and quadratic programming (mp-MILP and mp-MIQP, respectively) problems, whereas mp-MILP problems are a subclass of the mp-MIQP problems with a linear objective function.*

C 2.1 Problem and Solution Characterization

In the following, the following mp-MIQP problem is considered

$$z(\theta) = \min_{x,y} (Q\omega + H\theta + c)^T \omega$$

$$s.t. \quad Ax + Ey \leq b + F\theta$$

$$x \in R^n, y \in \{0,1\}^p, \omega \in [x^T, y^T]^T$$
$$\theta \in \Theta := \left\{\theta \in R^q \middle| \theta_l^{min} \leq \theta_l \leq \theta_l^{max}, l = 1, \dots, q\right\} \quad \text{(Equation C.9)}$$

where Θ is a polyhedral subset of the parameter space, and the matrices have appropriate dimensions. Note that this formulation only includes binary variables. Furthermore, only $Q > 0$ is considered.

When the integer combination $y = \bar{y}$ is fixed in problem (Equation C.9), the following mp-QP problem results

$$\begin{aligned} z(\theta) = \min_x\ & (Q_x x + H_x \theta + \tilde{c}_x)^T x + f(\theta) \\ s.t.\quad & Ax \leq (b - E\bar{y}) + F\theta \\ & x \in R^n, \\ & \theta \in \Theta := \left\{\theta \in R^q \middle| \theta_l^{min} \leq \theta_l \leq \theta_l^{max}, l = 1, \dots, q\right\}, \end{aligned} \quad \text{(Equation C.10)}$$

where the index x denotes the part of the matrix or variable associated with the continuous variable x, and $\tilde{c}_x = c_x + Q_{xy}\bar{y}$, where Q_{xy} is the part of Q associated with the combination of continuous and binary variables. Note that $f(\theta)$ does not influence the solution $x(\theta)$, as it is a scaling factor of the objective function value.

The solution of problems of type (Equation C.10) has been studied extensively, and its solution characteristics are reported in the following definition and theorem.

Definition C.1 (Piecewise affinity and critical regions (Bemporad et al., 2002c)) *A function $x(\theta): \Theta \mapsto R^n$, where $\Theta \subseteq R^q$ is a polyhedral set, is piecewise affine if it is possible to partition Θ into convex polyhedral regions, called critical regions, CR_i, and $x(\theta) = K_i\theta + r_i, \forall\theta \in CR_i$.*

Remark C.3 *The definition of a piecewise quadratic function is analogous.*

Definition C.2 (Parametric profile) *The solution of a mp-P problem is referred to as a parametric profile, and it consists of the closure of the critical regions and the solutions associated with them.*

Theorem C.1 (Properties of mp-QP solution (Bemporad et al., 2002c, Dua et al., 2002a)) *Consider the optimal solution mp-QP problem (3.7) and let* Q_x *be positive definite,* Θ *convex. Then the set of feasible parameters* $\Theta_f \subseteq \Theta$ *is convex, the solution* $x(\theta)$ *is piecewise affine and the optimizer solution* $z(\theta): \Theta_f \mapsto R$ *is continuous, convex and piecewise quadratic.*

In the case of mp-MIQP problems of type (Equation C.9), the solution properties are given by the following theorem and lemma.

Theorem C.2 (Properties of mp-MIQP solution (Borrelli et al., 2005)) *Consider the optimal solution of problem* (Equation C.9) *and let* Q *be positive definite. Then, the solution* $x(\theta)$ *is piecewise affine, and the set* CR_i *has the following form*

$$CR_i = \{\theta: \theta^T G_{i,j} \theta + h_{i,j}^T \theta \leq w_{i,j}, j = 1, \dots, t_i\} \qquad \text{(Equation C.11)}$$

where t_i *is the number of constraints that describe* CR_i.

Lemma C.1 (Quadratic boundaries (Borrelli et al., 2005)) *Consider the solution of problem* (Equation C.9) *as a combination of solutions of the mp-QP problems associated with all possible combinations of binary variables. Then, quadratic boundaries arise from the comparison of quadratic objective functions associated with feasible combinations of binary variables.*

C.2.3 A general framework for the solution of mp-MIQP problems

Based on the similarities highlighted in the comments, it is possible to formulate a unified framework for the solution of mp-MIQP problems of type (Equation C.9). This framework incorporates all approaches presented so far and shows their underlying

similarities. This does not only lead to a good theoretical understanding, but also is the basis for a unified software implementation of all the approaches.

This framework is based on the following 5 key components:

Initialization: The algorithm is initialized.

Integer Handling: A candidate integer solution is found, which is fixed in the original problem thus transforming it into a mp-QP problem. The three options to find a suitable candidate are (i) global optimization (Dua et al., 2002a), (ii) branch-and-bound (Acevedo et al., 1997b, Axehill et al., 2011, Axehill et al., 2014c, Oberdieck et al., 2014a) and (iii) exhaustive enumeration (Borrelli, 2003).

mp-QP solution: The mp-QP problem is solved using available solvers (e.g. (Bemporad et al., 2002c, Dua et al., 2002a, Spjøtvold et al., 2006, Tøndel et al., 2003)).

Comparison procedure: The objective function values of the mp-QP problem and the upper bound in the critical region considered are compared against each other to form a new, tighter upper bound. The four comparison procedures are (i) no comparison of the objective function (Dua et al., 2002a, Borrelli, 2003), (ii) comparison of the objective function over the entire critical region considered (Axehill et al., 2011, Axehill et al., 2014c), (iii) linearization of the nonlinearities in the objective function using McCormick relaxations (Oberdieck et al., 2014a) and (iv) calculation of the exact solution via piecewise outer approximation of quadratically constrained critical regions, a procedure which will be explained in detail in section 3.2.5. Note that the approaches (i)-(iii) might result in envelopes of solutions.

Termination: The algorithm terminates if a termination criterion is reached.

A schematic representation of the framework is shown in Figure C.1: The general framework for the solution of mp-MIQP problems..

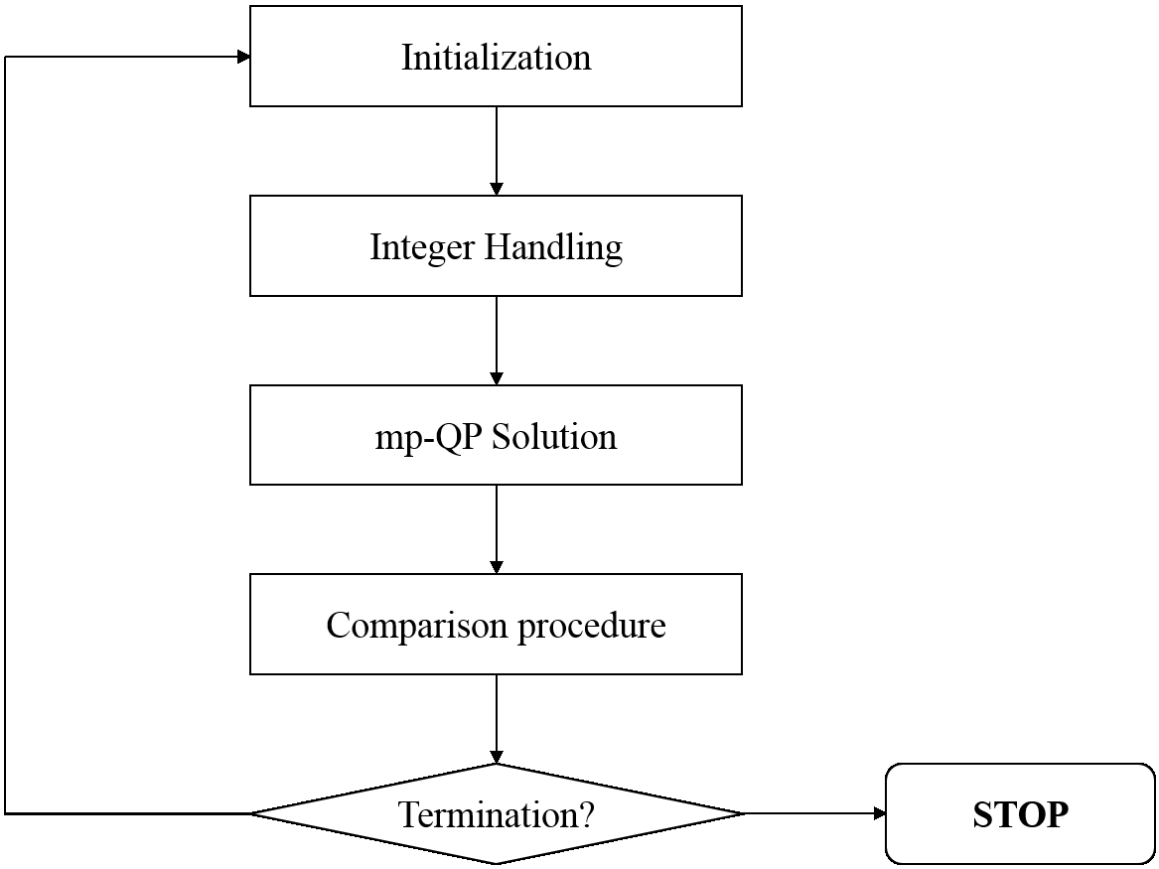

Figure C.1: The general framework for the solution of mp-MIQP problems.

The framework presented presents several options for the way integer variables are handled and the comparison procedures are done. Since the integer handling has a greater influence on the structure of the algorithm, as it changes how the problem is approached, this will be used to distinguish the way the unit operations are approached by the integer handling method chosen.

In the following, each aspect of the framework is discussed and suggestions for their implementation are presented.

C.2.4 Detailed analysis of the general framework

Initialization

The aim of the initialization procedure is to convert the input data efficiently into a suitable form such that the main algorithm can solve the problem. The initialization procedures for mp-MIQP problems presented so far involve initializing the binary search tree (in the case of a branch-and-bound procedure) (Acevedo and Pistikopoulos, 1997b, Axehill et al., 2011, Axehill et al., 2014c, Oberdieck et al., 2014a), creating a list of all possible integer variable combinations (in the case of an exhaustive enumeration procedure) (Borrelli, 2003) and setting the upper bound to ∞ (Acevedo and Pistikopoulos, 1997b, Dua et al., 2002a, Oberdieck et al., 2014a).

Remark C.9 *Notably this part could also be used for other tasks such as upper bound creation of initialization of parallelization strategies. These topics are subject to ongoing research and provide possibilities of lowering the computational burden.*

Integer Handling

The aim of this unit operation is to (i) find a candidate integer variable combination and (ii) fix it in the original mp-MIQP resulting in a mp-QP. As previously mentioned, three different approaches have been presented:

- **Global Optimization (Dua et al., 2002a):** A candidate binary variable solution is found by solving the global optimization problem.
- **Branch-And-Bound (Acevedo and Pistikopoulos, 1997b, Axehill et al., 2011, Axehill et al., 2014c, Oberdieck et al., 2014a):** The branch-and-bound procure relies on relaxing the binary variables $y \in \{0,1\}^p$ to continuous variables $\bar{y} \in [0,1]^p$, which results in a mp-QP problem. Based on this relaxation a binary search tree , and at each node one binary variable is fixed to either 0 or 1. Additionally, each node inherits a parameter space from its parent node, where the mp-QP is solved. This parameter space is based on the original parameter space Θ, after the following fathoming criteria have been applied

- The problem is infeasible
- An integer solution is found
- The optimal objective function value of the parent node is greater than the current best upper bound in the entire parameter space considered.

- **Exhaustive Enumeration (Borrelli, 2003):** All possible combinations of binary variables, a total of 2^p, are considered exhaustively. Note that this approach is identical to considering the final depth of a binary search tree.

Solution of the mp-QP problem

The solution of mp-QP problem has been discussed extensively in the open literature. The two main approaches are thereby:

- Geometrical approach (Bemporad et al., 2002c, Dua et al., 2002a, Spjøtvold et al., 2006, Tøndel et al., 2003, Patrinos et al., 2010, Patrinos et al., 2011): A geometrical interpretation of the polyhedral regions as half spaces is used to successively explore the initial parameter space. Different techniques discussing different exploration and redundancy checks have thereby been discussed.
- Combinatorial approach (Gupta et al., 2011c, Feller et al., 2013a, Feller et al., 2013b): The solution of the mp-QP problem is viewed at via the Karush-Kuhn-Tucker conditions, where a certain combination of the inequality constraints is active and inactive, thus leading to a system of linear equations. The consideration of all combinations of all constraints thereby exhaustively solves the problem. The different approaches presented aim at limiting this combinatorial complexity.

Comparison procedure

After the solution to the mp-QP problem has been obtained, it has to be compared against the current upper bound. The need for such a comparison procedure arises from the fact that it is not possible to explore the parameter space like performed for the solution of the mp-QP problem due to the presence of the integer variables.

Mathematically, this comparison procedure can be described as

$$PP_{sol} = \min_{\theta \in \Theta} PP_1 \cup PP_2 \qquad \text{(Equation C.12)}$$

Where PP_i refers to the i-th parametric profile (see Definition C.2) and $PP_1 \cup PP_2$ represents the union of the two parametric profiles. The main challenges to solve (Equation C.12) are thereby:

- Combinatorial complexity: In order to obtain PP_{sol}, each critical region of PP_1 has to be compared to each critical region of PP_2, thus leading to combinatorial complexity.
- Nonconvexity: the possibly quadratic nature of the objective functions might lead to nonconvexities. As the handling of nonconvex critical regions is a challenging problems, other ways have to be found to deal with this issue.

Remark C.10 *All comparison procedures presented to date focus on how to deal with the nonconvexity, while little attention has been given to the combinatorial complexity of the problem. At the end of this section we will present a first analysis of the problem. Additionally, in the next section a new comparison procedure resulting in the exact partitioning of the parameter space is presented.*

In the open literature, three different comparison procedures have been presented:

- **No objective function comparison (Dua et al., 2002a):** This approach, first presented in (Dua et al., 1999), does not compare the objective functions of the two parametric profiles, but directly creates an envelope of solutions (see Definition C.3).
- **Objective function comparison over entire CR (Axehill et al., 2011, Axehill et al., 2014c):** This approach was first presented in the realms of multiparametric dynamic programming (mp-DP) problems (Borrelli et al., 2005), and later on applied to mp-MIQP problems. It consists of classifying the situation in the currently considered intersect of critical regions and eq. (3.14). If case (c) is

realized, then an envelope of solutions (Definition C.3) is created over the entire critical region.

- **Direct objective function comparison via McCormick relaxations (Oberdieck et al., 2014a):** In this procedure, the difference $\Delta z(\theta)$ between the objective functions in the considered intersect of critical regions is directly considered. If quadratic terms are present in $\Delta z(\theta)$, then affine under- and overestimators using McCormick relaxations (McCormick, 1976) are calculated. These estimators generate polyhedral regions, in which either the objective function of one of the parametric profiles is optimal or an envelope of solutions is created.

In order to lessen the combinatorial complexity of the system, it is necessary to incorporate additional information into the solution of problem. In particular, it is necessary to classify each critical region CR_k of parametric profile i according to the following criteria:

Case (a): CR_k does not overlap with any critical region from the other parametric profile, PP_j.

Case (b): CR_k partially overlaps with one or multiple critical regions from the other parametric profile, PP_j.

Case (c): CR_k completely overlaps with one or multiple critical regions from the other parametric profile, PP_j.

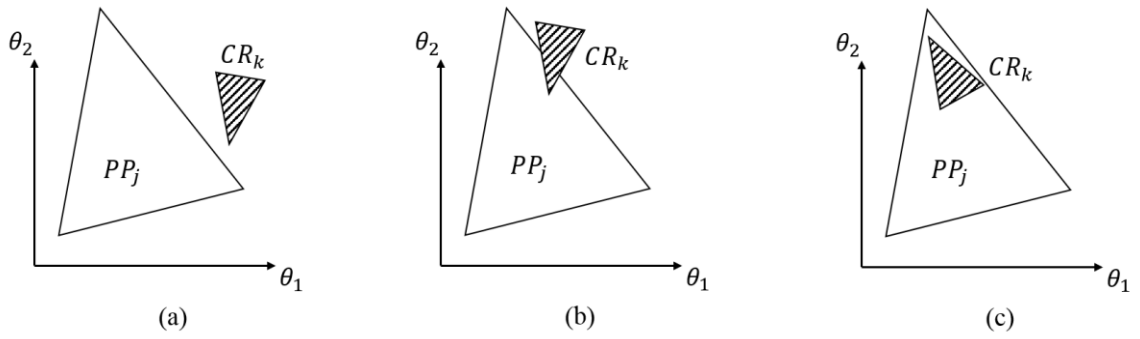

Figure C.2: The three classifications of overlap between CR_k and PP_j

Any part of CR_k that does not overlap with PP_j does not have to be considered in the comparison procedure, as it cannot be compared to anything. Thus, the number, or volume, of critical regions considered can be reduced, thus lessening the impact of the combinatorial complexity. However, in order perform the classification, the union of all critical regions in PP_j has to be calculated, a procedure which also is subject to combinatorial complexity. However, this complexity is lower than the previous one, as it only requires the comparison of all critical regions associated with one parametric profile, and not with two.

Termination

In order to conclude the framework description, a suitable way of defining the termination criterion has to be outlined. The structure of this termination criterion depends on the integer handling approach chosen:

- **Global optimization:** If the problem is infeasible in every critical region.
- **Branch-and-bound:** If the list of nodes N is empty.
- **Exhaustive Enumeration:** If all combinations of binary variables have been explored.

As previously mentioned, the exhaustive enumeration approach is thereby the only approach which allows for an *a priori* determination of the number of problems that will be solved in the course of the algorithm.

Comments

Based on the proposed framework, the following comments are made.

- Any of the comparison procedures presented can be combined with any of the integer handling strategies to create an algorithm which is most suitable to ones needs. Among these combinations are also the mp-MIQP algorithms that have been presented so far. Thus, the presented framework sheds a light on the development of these algorithms and gives great theoretical insight.

- It is possible to include relative and absolute suboptimality into this framework (the first description of which was presented in (Axehill et al., 2011, Axehill et al., 2014c)). However, it does not significantly add to the scientific content presented and is thus omitted.
- If any advances are made in any of the components of the framework, e.g. initialization, integer handling or comparison procedure, then these advances can be readily incorporated into the existing framework. Thus it is a flexible account not of a specific algorithm, but rather of a general solution approach for this class of problems.

Appendix D

Advanced Model Based Control Strategies

Model Predictive Control (MPC) is a control methodology based on two main principles: explicit on-line use of a *process model* to *predict* the process output at future time instants and the computation of an optimal control action by minimizing one or more *cost functions*, possibly including *constraints* on the process variables.

For a better understanding of the MBPC principle, the concept is presented in Figure D.1

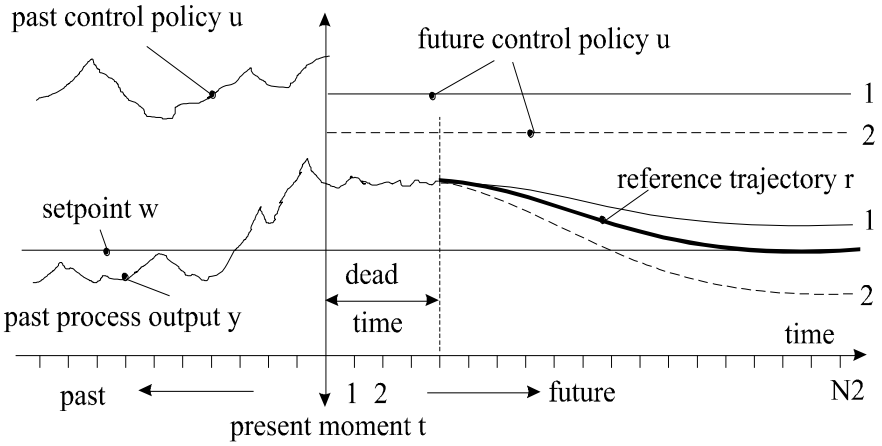

Figure D.1: Strategy of MBC principle

The process output $y(t+k)$ is predicted over a time horizon k=1..N_2 at each 'current' moment t. The predicted values are indicated by $y(t+k/t)$ and the value N_2 is called the *prediction horizon*. Assuming that the model is available, the prediction will be done by means of a model of the process. The forecast depends on the past inputs and outputs, but also on the future control scenario $\{u(t+k/t),k=0...N_2-1\}$. Starting at $r(t/t)=y(t)$ we define a *reference trajectory* $\{r(t+k/t),k=0...N_2-1\}$ over the prediction horizon, describing how we want to guide the process output from its current value $y(t)$ to its setpoint $w(t)$. The *control vector*$\{u(t+k/t),k=0...N_2-1\}$ is calculated in order to minimize a specified *cost function*. This cost function depends on the predicted control errors $\{r(t+k/t)-y(t+k/t)\ k=1...N_2-1\}$. All other elements of the calculated control vector, except the first one, $u(t/t)$, that is *actually* applied to the real process can be forgotten, because at the next sampling instant all time-sequences are shifted, a new output measurement $y(t+1)$ is obtained and the whole procedure is repeated. This leads to a new

control input $u(t+1/t+1)$, which is generally different from the previously calculated $u(t+1/t)$; this principle is called the *'receding horizon'* strategy. The MBPC strategy can be visualized in the following block-scheme:

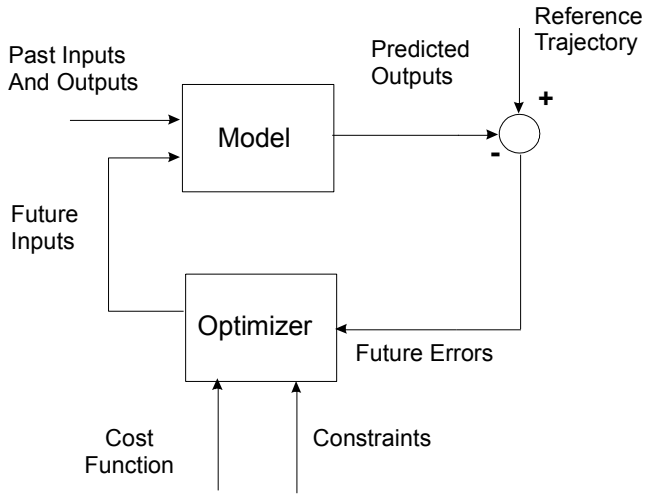

Figure D.2: MBC block-scheme.

EPSAC Strategy – Theoretical Background

The EPSAC - MPC strategy, as described in detail in (De Keyser, 2003), for linear models is based on a generic process model:

$$y(t) = x(t) + n(t) \qquad \text{(Equation D.1)}$$

The disturbance $n(t)$ includes the effects in the measured output $y(t)$ which do not come from the model input $u(t)$ via the available model. These non-measurable disturbances have a stochastic character with non-zero average value, which can be modelled by a coloured noise process:

$$n(t) = \left[C(q^{-1}) / D(q^{-1}) \right] \cdot e(t) \qquad \text{(Equation D.2)}$$

with: $e(t)$ - uncorrelated (white) noise with zero mean value; $C(q^{-1})$ and $D(q^{-1})$ - monic polynomials in the backward shift operator q^{-1} of orders n_c and n_d. This design filter can be used to improve the quality of the control performance, by supplying information to the controller about the type of disturbances. In this application, the disturbance filter $C(q^{-1})/D(q^{-1})$ is defined as a pure integrator, used to remove the steady-state error, similarly to the effect of the integrator in case of PID controller.

The relationship between $u(t)$ and $x(t)$ is given by the generic dynamic system model:

$$x(t) = f\left[x(t-1), x(t-2), \cdots \quad \cdots\right] \qquad \text{(Equation D.3)}$$

In our case the input applied to the patient, $u(t)$, is a scalar containing the Propofol delivery rate. The process output is predicted at time instant t over the prediction horizon, N_2 based on the measurements available at that moment and the future outputs of the control signal. The predicted values of the output are:

$$y(t+k \mid t) = x(t+k \mid t) + n(t+k \mid t) \qquad \text{(Equation D.4)}$$

Prediction of $x(t+k|t)$ and of $n(t+k|t)$ can be done respectively by recursion of the process model and by using filtering techniques on the noise model (Equation D.2) (De Keyser, 2003).

In EPSAC for linear models, the future response is then considered as being the cumulative result of two effects:

$$y(t+k \mid t) = y_{\text{base}}(t+k \mid t) + y_{\text{optimize}}(t+k \mid t) \qquad \text{(Equation D.5)}$$

The component $y_{\text{base}}(t+k \mid t)$ is a sum of the effects of:

- past control $\{u(t\text{-}1), u(t\text{-}2), \ldots\}$,
- a *base* future control scenario, defined *a priori* (a simple choice being $\{u_{\text{base}}(t+k \mid t) \equiv 0, \quad k \geq 0\}$)
- future (predicted) disturbances $n(t+k|t)$.

The vector $y_{\text{base}}(t+k\,|\,t)$ can be easily obtained using (Equation D.2) - (Equation D.4) taking $u_{base}(t+k\,|\,t)$ as the model input for (Equation D.3).

The vector $y_{\text{optimize}}(t+k\,|\,t)$ represents the effect of the *optimizing* future control actions

$$\{\delta u(t\,|\,t),\ \delta u(t+1\,|\,t),\ \ldots\ \ \mathrm{V}_u-1\,|\,t)\} \qquad \text{(Equation D.6)}$$

With

$$\delta u(t+k\,|\,t)=u(t+k\,|\,t)-u_{\text{base}}(t+k\,|\,t) \qquad \text{(Equation D.7)}$$

The vector $y_{\text{optimize}}(t+k\,|\,t)$ is given by:

$$y_{\text{optimize}}(t+k\,|\,t)=h_k\,\delta u\,(t\,|\,t)+h_{k-1}\delta u\,(t+1\,|\,t)+ \\ +\ldots+g_{k-N_u+1}\,\delta u\,(t+N_u-1\,|\,t) \qquad \text{(Equation D.8)}$$

The parameters $g_1,g_2,\ldots g_k,\ldots g_{N_2}$ are the coefficients of the *unit step response* of the system, i.e., the response of the PK-PD system for a stepwise change of the input (with amplitude 1). The parameters $h_1,h_2,\ldots h_k,\ldots h_{N_2}$ are the coefficients of the *unit impulse response* of the system and can be easily calculated from the step response coefficients and vice versa: $h_k=g_k-g_{k-1}$

(and $h_0=h_{-1}=\ldots=g_0=g_{-1}=\ldots\equiv 0$).

The key EPSAC-MPC equation:

$$\mathbf{Y}=\bar{\mathbf{Y}}+\mathbf{GU} \qquad \text{(Equation D.9)}$$

is obtained, where:

$$
\begin{aligned}
\mathbf{Y} &= \left[y(t+N_1 \mid t) \cdots \quad {}_2 \mid t) \right]^T \\
\bar{\mathbf{Y}} &= \left[y_{\text{base}}(t+N_1 \mid t) \cdots \quad \cdot N_2 \mid t) \right]^T \\
\mathbf{U} &= \left[\delta u(t \mid t) \cdots \quad \mathrm{V}_u - 1 \mid t) \right]^T \\
\mathbf{G} &= \begin{bmatrix}
h_{N_1} & h_{N_1-1} & h_{N_1-2} & \cdots & g_{N_1-N_u+1} \\
h_{N_1+1} & h_{N_1} & h_{N_1-1} & \cdots & \cdots \\
\cdots & \cdots & \cdots & \cdots & \cdots \\
\cdots & \cdots & \cdots & \cdots & \cdots \\
h_{N_2} & h_{N_2-1} & h_{N_2-2} & \cdots & g_{N_2-N_u+1}
\end{bmatrix}
\end{aligned}
\qquad \text{(Equation D.10)}
$$

with the *horizons* N_1, N_2 being design parameters, N_1 being equal to the time-delay, in samples.

The controller output is obtained by minimizing a cost function:

$$
J(\mathbf{U}) = \sum_{k=N_1}^{N_2} [r(t+k \mid t) - y(t+k \mid t)]^2 \qquad \text{(Equation D.11)}
$$

where *r(t+k|t)* is the desired *reference trajectory*.

The cost function (Equation D.11) is a quadratic form in **U,** having the following structure using the matrix notation from (Equation D.10) and with **R** defined similarly to **Y**:

$$
J(\mathbf{U}) = [\mathbf{R} - \bar{\mathbf{Y}} - \mathbf{G}\mathbf{U}]^{-1}[\mathbf{R} - \bar{\mathbf{Y}} - \mathbf{G}\mathbf{U}] \qquad \text{(Equation D.12)}
$$

which leads after minimization w.r.t. **U** to the optimal solution:

$$
\mathbf{U}^* = [\mathbf{G}^T\mathbf{G}]^{-1}\mathbf{G}^T(\mathbf{R} - \bar{\mathbf{Y}}) \qquad \text{(Equation D.13)}
$$

Only the first element $\delta u(t/t)$ in $\mathbf{U}^*$ is required in order to compute the actual control and this represents the control signal which will be applied to the patient:

$$u(t) = u_{\text{base}}(t \mid t) + \delta u(t \mid t) = u_{\text{base}}(t \mid t) + \mathbf{U}^*(1) \qquad \text{(Equation D.14)}$$

At the next sampling instant t+1, the whole procedure is repeated taking into account the new measurement information $y(t+1)$.

The cost function can be extended in order to penalize excessive control actions:

$$J(\mathbf{U}) = (\mathbf{R} - \mathbf{Y})^T (\mathbf{R} - \mathbf{Y}) + \rho \mathbf{U}^T \mathbf{U} \qquad \text{(Equation D.15)}$$

$$\mathbf{Y} = \overline{\mathbf{Y}} + \mathbf{G} \cdot \mathbf{U}$$

and the control input is calculated by

$$\mathbf{U}^* = (\mathbf{G}^T \mathbf{G} + \rho \mathbf{I})^{-1} \cdot \mathbf{G}^T \cdot (\mathbf{R} - \overline{\mathbf{Y}}) \qquad \text{(Equation D.16)}$$

It is worthwhile to notice that optimization with input constraints (on the manipulated variable) are accepted only if the control horizon N_u >1. Since in this paper the control horizon is unitary, the input is constrained using *clipping*.

D.2 mp-MPC Strategy – Theoretical Background

We consider the mp-MPC problem of a linear discrete-time system with state and input constraints:

$$\min_{u_k} \left\| x_{N_{MPC}} \right\|_{P_{MPC}}^2 + \sum_{k=1}^{N_{MPC}} \left\| x_k \right\|_{Q_{MPC}}^2 + \sum_{k=0}^{N_{MPC}-1} \left\| u_k \right\|_{R_{MPC}}^2 \qquad \text{(Equation D.17)}$$

$$x_{k+1} = Ax_k + Bu_k, y = Cx_k$$

$$x_k \in X \subseteq \mathbb{R}^p, u_k \in U \subseteq \mathbb{R}^s$$

where x, y, u are the states, outputs and inputs of the system, respectively. X, U are the sets defining the state and input constraints and that contain the origin in their interior. $Q_{MPC} \succ 0, P_{MPC} \succ 0$ are positive semi definite matrices and $R_{MPC} \succ 0$ is a symmetric positive matrix, N_{MPC} is the horizon length of the MPC.

The reformulation as a multiarametric quadratic problem is given by:

$$\begin{aligned} U(\theta) = \arg\min_{U} \frac{1}{2} U^T H U + xFU + \frac{1}{2} x^T Y x \\ s.t.\ G\mathrm{U} \le \mathrm{W} + \mathrm{Ex} \\ x_{\mathrm{k}+1} = Ax_k + Bu_k,\ k = 1..N \\ y_{\mathrm{k}} = Cx_k \end{aligned} \qquad \text{(Equation D.18)}$$

where U is the vector contain the control moves sequence. The quadratic optimization problem in (Equation D.18) can be converted to a multi-parametric programming problem by performing the linear transformation:

$$z = u + H^{-1}F^T x \qquad \text{(Equation D.19)}$$

The resulting mp-QP has the following form:

$$\begin{aligned} \min_z \frac{1}{2} z^T H z \\ Gz \le W + Sx \\ x_k \in X \subseteq \mathbb{R}^p, z \in U \\ \subseteq \mathbb{R}^s \end{aligned} \qquad \text{(Equation D.20)}$$

where z represents the new decision variable while S is defined as:

$$S = E + GH^{-1}F^T \qquad \text{(Equation D.21)}$$

In this new formulation, x is now acting as a parameter of the optimization problem and only appears in the constraints. Next, local sensitivity analysis is performed on the Karush-Kuhn-Tucker (KKT) conditions of the mp-QP:

$$Hz + G^T \lambda = 0 \qquad \text{(Equation D.22)}$$

$$\lambda_i(G_i z - W_i - S_i x) = 0, i = 1..q$$
$$\lambda \geq 0 \qquad \text{(Equation D. 23)}$$

$$\begin{bmatrix} z(x) \\ \lambda(x) \end{bmatrix} = -(M_0)^{-1} M_0 (x - x_0) + \begin{bmatrix} z(x_0) \\ \lambda(x_0) \end{bmatrix} \qquad \text{(Equation D.24)}$$

$$M_0 = \begin{bmatrix} H & G_1^T & \dots & G_q^T \\ -\lambda_1 G_1 & -V_1 & & \\ \vdots & & \ddots & \\ -\lambda_q G_q & & & -V_q \end{bmatrix} \qquad \text{(Equation D.25)}$$

$$N_0 = \begin{bmatrix} Y & \lambda_1 S_1 & \dots & \lambda_p S_p \end{bmatrix}^T \qquad \text{(Equation D.26)}$$

The parameter space i.e., the set of x values for which the explicit relationship between $[z(x), \lambda(x)]$ and the parameter around the point $[z(x_0), \lambda(x_0)]$ remains optimal is termed a critical region, which is of the following form:

$$\mathcal{CR}_i = \{x \in \mathbb{R}^n | H_i x \leq b_0\} \qquad \text{(Equation D.27)}$$

Each of these critical regions contains an affine expression describing the optimal control value of the states:

$$u = f(x) = \begin{bmatrix} K_1 x + c_1 & \text{if } x \lfloor CR^1 \\ \dots & \\ K_s x + c_s & \text{if } x \lfloor CR^s \end{bmatrix} \qquad \text{(Equation D.28)}$$

where s is the number of critical regions.

As explained before, this reduces the online implementation of MPC to simple function evaluation, facilitating real time applications. One of the main difficulties when attempting to design a multi-parametric/explicit controller is the increase in the number of critical regions with the number of states and constraints, the latter being function of the control prediction horizon. Here we give the worst-case computational complexity for an mp-QP controller:

$$N_r = \sum_{k=0}^{\eta} k!\, l^k \qquad \text{(Equation D. 29)}$$

$$\eta = \sum_{i=0}^{h} \frac{l!}{(l-i)!\, i!}$$

where h is the number of optimization variables and l is the number of inequalities.

Another issue is the transposition of mp-MPC techniques to nonlinear systems. This is the topic of the next paragraph.

One of the advantages of model predictive control is the ability to handle generic constraints. Additional constraints, specific to the application being considered, may be easily added without loss of generality.

The reformulation presented in this section may be adapted in a straightforward way to different model predictive control strategies, such as reference output tracking, constraint softening, or to include penalties to the rate of change in the input vector

Appendix E
Estimation Techniques

E.1 Kalman Filter

The Kalman filter is a standard method for unconstrained state estimations and it follows a two-step procedure to calculate the maximum a-posteriori Bayesian estimate (Rawlings et al., 2009, Rao, 2000, Welch and Bishop, 2001). The first step is the time update which uses the system model to predict the current state of the system based on the last estimate. The second step is the measurement update. The prediction from the previous step is updated by using the sensor information. Therefore, we can say that the Kalman filter is predictor-corrector type estimator that is optimal in the sense that it minimizes the estimated error covariance .

Time update (prediction step)

Prediction of the state:

$$\hat{x}_{k/k-1} = A\hat{x}_{k-1/k-1} + Bu_{k-1} \qquad \text{(Equation E.1)}$$

Projection of the error covariance:

$$P_{k/k-1} = AP_{k-1}A^T + Q_{kal} \qquad \text{(Equation E.2)}$$

Measurement update (correction step)

Computation of the Kalman gain:

$$K_k = P_{k/k-1}C^T(CP_{k/k-1}C^T + R_{kal})^{-1} \qquad \text{(Equation E.3)}$$

Update of the estimate with measurement:

$$\hat{x}_{k/k} = \hat{x}_{k/k-1} + K_k(y_k - Cx_{k/k-1}) \qquad \text{(Equation E.4)}$$

Update of the error covariance

$$P_k = (I - K_k C) P_{k/k-1} \qquad \text{(Equation E.5)}$$

Where Q_{kal} and R_{kal} represent the measure of confidence in the model and the measurement.

The solution of the discrete algebraic Riccati equation (Söderström, 2002).

$$P = A^T PA - A^T PB(B^T PB + R_{kal})^{-1} B^T PA + Q_{kal} \qquad \text{(Equation E.6)}$$

Can be used for the calculation of the steady-state gain which makes $P_{k+1}=P_k=P$ constant.

E.2 Moving Horizon Estimation

The idea of moving horizon estimation is to estimate the state using a moving and fixed-size window of data. Once a new measurement becomes available, the oldest measurement is discarded and the new measurement is added. The concept is to penalize deviations between measurement data and predicted outputs. In addition – for theoretical reasons - a regularization term on the initial state estimate is added to the objective function. There are two main characteristics that distinguish MHE from other estimation strategies, such as Kalman filter: (i) prior information in the form of constraints on the states, disturbances and parameters can be included; (ii) since MHE is optimization based it is able to handle explicitly nonlinear system dynamics through the use of approximative nonlinear optimization algorithms. In (Haseltine and Rawlings (2005)) MHE was shown to possess superior estimation properties compared to the Extended Kalman Filter .

The Kalman filter considers only one set of measurements at a time. In (Rawlings and Mayne, 2009) is shown that the Kalman filter is the algebraic solution to the following unconstrained least-square optimization problem:

$$\Phi(x_0,\{w\}) = \left\|\hat{x}_0 - \underline{x}_0\right\|^2_{P_0^{-1}} + \sum_{k=0}^{T-1}\left\|\hat{w}_k\right\|^2_{Q_k^{-1}} + \sum_{k=0}^{T}\left\|\hat{v}_k\right\|^2_{R_k^{-1}} \qquad \text{(Equation E.7)}$$

Where

$$\begin{aligned} x_{k-1} &= Ax_k + Bu_k + Gw_k \\ y_k &= Cx_k + v_k \end{aligned} \qquad \text{(Equation E. 8)}$$

And Qk>0, Rk>0, P0 >0 are positive definite matrices. This optimization problem now opens the possibility to add system knowledge in the form of constraints. The constraints might for example capture the fact that a leak is always an outflowing stream or account for non-zero non-Gaussian noise (Robertson et al., 2002).

The optimization problem (Equation E.7) is then not equivalent to the Kalman filter any more. If all the available past measurements are used for the estimation as in (Equation E.7), the estimation problem grows unbounded with time. This is referred to as the *full information estimator (Rao, 2000)*. The derivation is based on the maximization of the a-posteriori Baysian estimate. In order to keep the estimation problem computationally tractable it is necessary to limit the processed data, for example by discarding the oldest measurement once a new one becomes available. This essentially slides a window over the data, leading to the *moving horizon estimator* (MHE). The data that is not considered any more can be accounted for by the so called *arrival cost* so that the information is not lost. The MHE then considers only a limited amount of data so that the constrained optimization problem becomes:

$$\begin{aligned} &\min_{\hat{x}_{T-N/T},\hat{W}_T} \left\|\hat{x}_{T-N/T} - \underline{x}_{T-N/T}\right\|_{P^{-1}_{T-N/T-1}} + \left\|Y^{T-1}_{T-N} - O\hat{x}_{T-N/T} - \bar{c}bU^{T-2}_{T-N}\right\|^2_{P-1} \\ &+ \sum_{k=T-N}^{T-1}\left\|\hat{w}_k\right\|_{Q_k^{-1}} + \sum_{k=T-N}^{T-1}\left\|\hat{v}_k\right\|_{R_k^{-1}} \end{aligned}$$

st: (Equation E.9)

$$\begin{aligned} \hat{x}_{k+1} &= A\hat{x}_k + Bu_k + G\hat{w}_k \\ y_k &= C\hat{x}_k + \hat{v}_k \\ \hat{x}_k &\in X, \hat{w}_k \in \Theta, \hat{v}_k \in V \end{aligned}$$

where T is the current time, $Q_k \succ 0, R_k \succ 0, P_{T-N/T-1} \succ 0$ are the covariances of w_k v_k x_{T-N} assumed to be symmetric, N is the horizon length of the MHE, $Y^{T-1}_{T-N} = \left[y^T_{T-N},...,y^T_T\right]^T$ is a

vector containing the past $N+1$ measurements and $U_{T-N}^{T-1} = \left[u_{T-N}^{T},...,u_{T-1}^{T}\right]^{T}$ is a vector containing the past N inputs. x, v, w denotes the variables of the system and $\hat{x}, \hat{v}, \hat{w}$ denote the estimated variable of the system and $\hat{x}_{T/T-N}$ and $\hat{W}_T = W_{T-N}^{T-1} = \{\hat{w}\}_{T/T-N}^{T-1}$ $\hat{x}_{T-N/T}, \hat{w}_T$ denote the decision variable of the optimization problem, respectively the estimated state variable and the noise sequence.

$$\left\|\hat{x}_{T-N/T} - \underline{x_{T-N/T}}\right\|_{P_{T-N/T-1}}^{2} + \left\|Y_{T-N}^{T-1} - O\hat{x}_{T-N/T} - \bar{c}bU_{T-N}^{T-2}\right\|_{P-1}^{2} \quad \text{(Equation E.10)}$$

is described as the smoothed arrival cost. For steady-state MHE $Q_k = Q$, $R_k = R$, and $P_{T-N|T-1} = P$ are time invariant.

The current state of the system can be calculated from the initial state $x_{T|T-N}$ by forward programming using the discrete time linear system if the deterministic input U^{T-1}_{T-N} and the noise sequence W_{T-N}^{T-1} are known. It is thus sufficient to estimate the initial state $\hat{x}^{*}_{T|T-N}$ and the noise $\hat{W}^{*}_{T}$ .The concept of MHE is illustrated in Figure E. 1 where $(\cdot)_{T-k|T}$ denotes the sample at time T − k obtained at time T

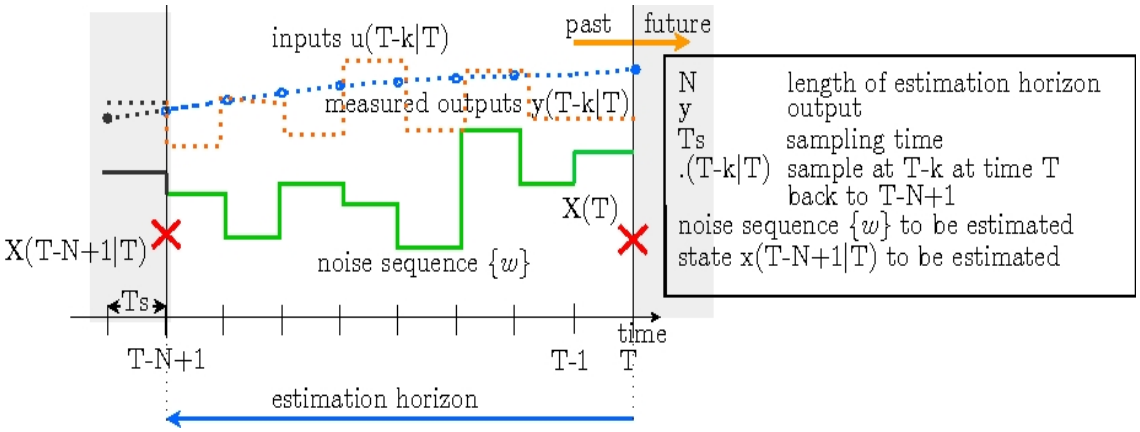

Figure E. 1: Concept of MHE

The MHE is applied with the following steps:

1. The optimization problem (Equation E.9) is solved to obtain $\hat{x}^{*}_{T/T-N}$ and $\hat{W}^{*}_{T}$.

2. The current state estimate $\hat{x}^*_{T/T}$ is obtained by substituting $\hat{x}^*_{T/T-N}$ and $\hat{W}^*_T$ into the system dynamics $\hat{x}_{k+1} = A\hat{x}_k + Bu_k + G\hat{w}_k$ and projecting the state values forward from time T − N to the current time T by $\hat{x}^*_{T/T} = A^N \hat{x}^*_{T-N/T} + \sum_{j=T-N}^{T-1} A^{T-1-j} G\hat{w}_k$

3. When the next measurement becomes available (at the next sampling instance), steps 1 and 2 are repeated.

Remark E.1*In the case* T ≤ N*, the full information estimator is solved using the arrival cost* $\|\hat{x}_{T-N/T} - \underline{x}_{T-N/T}\|^2_{P_0^{-1}}$. *The horizon 'fills up' and no data is discarded (Rao, 2000).*

Remark E.2 *(Rao, 2000) points out that wrongly posed constraints might lead to an infeasible optimization problem and that constraints on* $\hat{v}_k$ *could be problematic due to the possibility of outliers in the measurement. Any constraints posed in* (Equation E.9) *should hence be chosen such that the real system does not violate them (Rao, 2000).*

This observation leads to the following assumption for the work in this thesis:

Assumption E.1*The real system does not violate the constraints posed to the MHE:* $x \in \hat{X}, v \in \hat{V}, w \in \hat{W}$ *which contain the origin in their interior.*

Multiparametric Moving Horizon Estimation

The formulation of the MHE with the smoothed arrival cost is still an open issue which will be addressed here. In order to formulate and solve the constrained moving horizon estimator with multi-parametric programming, the optimization problem needs to be reformulated into the standard multi-parametric quadratic form.

Darby and Nikolaou(Darby and Nikolaou, 2007) have re-formulated the MHE with the filtered arrival cost.

The multiparametric formulation of the constrained MHE is obtained by substituting the state space formulation of the estimated system $\hat{x}_{t+1} = A\hat{x}_t + Bu_k + G\hat{w}_t$, $\hat{v}_t = y_t - C\hat{x}_t$ into:

$$[\hat{x}_{T-N+1}, \{\hat{w}\}_{T-N+1}^{T-1}] = \min_{x_{T-N+1}, \{w\}_{T-N+1}^{T-N}} \sum_{k=T-N+1}^{T-N} (w_k - \overline{w})^T \cdot Q^{-1} \cdot (w_k - \overline{w}) + \sum_{k=T-N+1}^{T} (v_k^T \cdot R^{-1} \cdot v_k) + (x_{T-N+1} - \overline{x}_{T-N+1/T-N})^T \cdot P_{SS}^{-1} \cdot (x_{T-N+1} - \overline{x}_{T-N+1/T-N}) \quad \text{(Equation E.11)}$$

subject to

$$x_{k+1} = A \cdot x_k + B \cdot u_k + G \cdot w_k \qquad \text{discrete state-space formulation}$$
$$y_k = C \cdot x_k + v_k \qquad \rightarrow v_k = y_k - C \cdot x_k$$
$$Hx \cdot x \le h \qquad \text{path constraints on state variables}$$
$$Kw \cdot w \le k \qquad \text{path constraints on the noise w}$$
$$Lv \cdot v \le l \qquad \text{path constraints on the noise v}^{1}$$
$$\bar{x}_{T-N+1/T-N} = A \cdot \hat{x}_{T-N/T-N} + B \cdot u_k + G \cdot \overline{w} \qquad \text{update of the cost to arrive}$$

Where N is the length of the horizon, T is the current point in time, Q and R are positive definite diagonal weighting matrices on the noises, P_{SS} is the steady state solution for the Kalman filter. $\{\hat{w}\}_{T-N+1}^{T-N}$ and $\{v\}_{T-N+1}^{T}$ are sequences of independent, normally distributed random numbers with mean values $\overline{w}$ for *{w}* and zero-mean for *{v}*. $\bar{x}_{T-N+1/T-N}$ is the arrival costwhich captures the previous measurements that are not considered any more. $\hat{x}_{T-N+1}$ is the solution of the MHE at the previous time step.

$$\min_{\hat{x}_{T-N+1},\{\hat{w}\}_{T-N+1}^{T-1}} \frac{1}{2}\left[\hat{x}_{T-N+1}, \{\hat{w}\}_{T-N+1}^{T-1\quad T}\right] H \begin{bmatrix} \hat{x}_{T-N+1} \\ \{\hat{w}\}_{T-N+1}^{T-1} \end{bmatrix} + \theta.f. \begin{bmatrix} \hat{x}_{T-N+1} \\ \{\hat{w}\}_{T-N+1}^{T-1} \end{bmatrix}$$

(Equation E.12)

where

$$\theta = \left[\underline{x}_{T-N/T}^T, y_{T-N}^T, \ldots, y_T^T, u_{T-N}^T, \ldots, u_{T-1}^T\right]^T,$$

$$H\begin{bmatrix} 2P^{-1} - 2O^T \cdot W^{-1} \cdot O + 2ca^T \cdot diag(R^{-1}) \cdot ca & 2ca \cdot diag(R^{-1}) \cdot cg \\ 2cg^T \cdot diag(R^{-1}) \cdot ca & 2diag(Q^{-1}) + 2cg^T \cdot diag(R^{-1}) \cdot cg \end{bmatrix},$$

$$f = \begin{bmatrix} [-2P^{-1}, 0] \\ 2diag(R^{-1} \cdot C) \cdot [a, g] \\ 2b^T \cdot diag(C^T \cdot R^{-1} \cdot C) \cdot [a, g] \end{bmatrix}, \qquad (13)$$

$$a = \begin{bmatrix} I \\ A \\ A^2 \\ \vdots \\ A^{N-1} \end{bmatrix}, \quad \mathrm{g} = \begin{bmatrix} 0 & 0 & \cdots & 0 \\ G & 0 & \cdots & 0 \\ A \cdot G & G & \cdots & 0 \\ A^2 \cdot G & A \cdot G & \cdots & 0 \\ \vdots & & \ddots & \\ A^{N-2} \cdot G & A^{N-2} \cdot G & \cdots & G \end{bmatrix},$$

$$b = \begin{bmatrix} 0 & 0 & \cdots & 0 \\ B & 0 & \cdots & 0 \\ A \cdot B & B & \cdots & 0 \\ A^2 \cdot B & A \cdot G & \cdots & 0 \\ \vdots & & \ddots & \\ A^{N-2} \cdot B & A^{N-3} \cdot B & \cdots & B \end{bmatrix}, \quad \begin{aligned} \mathrm{ca} &= \mathrm{diag(C)} \cdot \mathrm{a}, \\ \mathrm{cg} &= \mathrm{diag(C)} \cdot \mathrm{g}, \\ \mathrm{cb} &= \mathrm{diag(C)} \cdot \mathrm{b}, \end{aligned}$$

(Equation E.13)

where *diag(·)* denotes a matrix denotes a matrix of appropriate size with (·) on its main diagonal and zero everywhere else. Further details can be found in (Darby and Nikolaou, 2007) and (Voelker et al., 2013).

The optimal solution to the MHE optimization (Equation E.12)

$\left[\hat{x}_{T-N+1}^*(\theta), \{\hat{w}\}_{T-N+1}^{T-1}{}^*(\theta)\right]^T$ (* denotes the the optimizer of problem (Equation E.12)) is a piecewise affine function of the measurements, inputs, and the arrival cost.

$$\begin{bmatrix} \hat{x}_{T-N+1}^*(\theta) \\ \{\hat{w}\}_{T-N+1}^{T-1}{}^*(\theta) \end{bmatrix} = F(\theta) = \begin{cases} K_1\theta + c_1 & if\ \theta \in CR^1 \\ \vdots & \vdots \\ K_l\theta + c_l & if\ \theta \in CR^l \end{cases} \qquad \text{(Equation E.14)}$$

where l is the number of critical regions (CR).

Remark E.3 *Often only the state estimate* $\hat{x}_{T/T}$ *is of interest and hence it might be sufficient if only* $\hat{x}_{T/T}$ *has to fulfil the constraints rather then all* $\hat{x}_{k/T}$ *for all* k = T − N, . . . , T. *It might therefore suffice to pose constraints only on* $\hat{x}_{T/T}$ *rather than the whole horizon by replacing* t*he matrix* $\mathrm{col}(\hat{d}_x)$ *with* dx *and the matrix* $\mathrm{diag}(\hat{D}_x)$ *with* $\begin{bmatrix} 0 & \dots & \hat{D}_x \end{bmatrix}$ *. This reduces the number of parameters in the optimization problem .*

Appendix F
Distillation Column

F.1 Distillation Column model

This example considers the design of a controller for a simplified model of a distillation column (Benallou et al., 1986). The motivation for this example is to demonstrate how nonlinear model reduction techniques may be used to overcome the limitations of multiparametric programming algorithms for systems with high dimensionality. The assumptions in this example do not intend to describe an industrial situation and, at the current state of the art, explicit multiparametric controllers are not suitable for large scale applications such as industrial distillation columns (Pistikopoulos, 2009). The system is schematically depicted in Figure F. 1 and the underlying equations presented in Table F. 1 and

Table F. **2**. It may be noted that the system is mostly linear, with nonlinearities arising only from the equilibrium relations. The control problem consists of regulating the product purity to a fixed set-point of **y(t-1)** = 0.935, using the reflux ratio as the manipulated variable. The system states, $x_i, i = 1..3$ are assumed to be measured and no external disturbances are considered. A constraint is imposed on the manipulated variable, which is allowed to vary in the interval RR ∈ [0 ; 5]. Due to the high dimensionality of the model, the mp-NMPC algorithm cannot be directly applied and a model order reduction step should be included beforehand. For the purposes of this example, reduced order models with 1 and 2 states were derived, using the technique presented in Appendix B. The discrete-time representation of the reduced system of ODEs was obtained using an implicit Runge–Kutta method. For the discretization, 3 collocation points were used, and the number of finite elements was set to 9 and 6 for the reduced order controllers with 1 state and 2 states, respectively. The number of collocation points and finite elements may be determined performing off-line simulations. Even though a larger number of finite elements would lead to a finer approximation, and have impact on the control performance, it is limited by the corresponding increase in computational burden. The resulting control law consists of an expression for the manipulated variable, **u**, as an explicit function of the reduced states of

the system.

Condenser	$$\frac{dx_{A,1}}{dt} = \frac{1}{A_{cond}} V(y_{A,2} - x_{A,1})$$
Trays in the rectification section $i = 2..16$	$$\frac{dx_{A,i}}{dt} = \frac{1}{A_{Tray}} \left[L_1 \left(x_{A,i-1} - x_{A,i} \right) - V \left(y_{A,i} - y_{A,i+1} \right) \right]$$
Feed Tray:	$$\frac{dx_{A,17}}{dt} = \frac{1}{A_{Tray}} \left[F x_{A,Feed} + L_1 x_{A,16} - L_2 x_{A,17} - V \left(y_{A,17} - y_{A,18} \right) \right]$$
Trays in the stripping section $i = 2..16$:	$$\frac{dx_{A,i}}{dt} = \frac{1}{A_{Tray}} \left[L_2 \left(x_{A,i-1} - x_{A,i} \right) - V \left(y_{A,i} - y_{A,i+1} \right) \right]$$
Reboiler:	$$\frac{dx_{A,32}}{dt} = \frac{1}{A_{Reboiler}} \left[L_2 x_{A,31} - (F - D) x_{A,32} - V y_{A,32} \right]$$
Mass balances	$$V = L_1 + D \quad L_2 = L_1 + F$$ $$RR = \frac{L_1}{D}$$
Volatilility	$$\alpha_{A,B} = \frac{y_A (1 - x_A)}{x_A (1 - y_A)}$$

Table F. 1: Schematic of the distillation column example model

A_{cond}	total molar holdup in the condenser
A_{Tray}	total molar holdup in each tray
$A_{Reboiler}$	total molar holdup in each tray
F	Feed flowrate
D	Distillate flowrate
L_1	Flowrate of the liquid in the rectification section
L_2	Flowrate of the liquid in the stripping section
V	Vapour flowrate in the column
RR	reflux ratio
$x_{A,i}$	liquid composition of component A on the i^{th} stage
$x_{A,Feed}$	Feed composition of component A
$y_{A,i}$	vapour composition of component A on the i^{th} stage
$\alpha_{A,B}$	relative volatility (assumed constant)

Table F. 2: variables description Distillation column

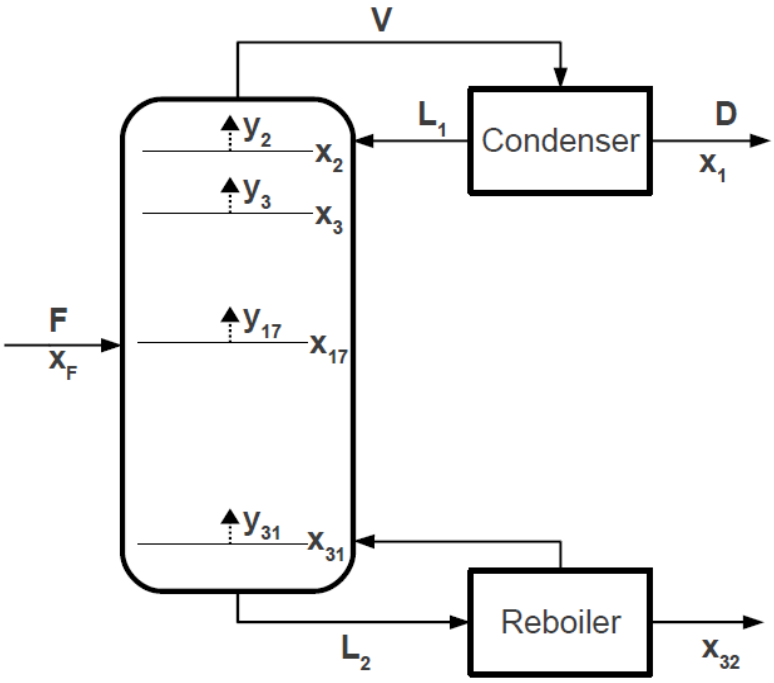

Figure F. 1: Schematic of the distillation column example model

Multiparametric moving horizon estimators were built for the following approximated models:

Case 1: The original distillation column model was first linearized, thus yielding a 32 states linear time invariant system. This latter was subsequently reduced to two states via balanced truncation.

Case 2: The original distillation column model was reduced to two states by using empirical nonlinear balanced truncation. The resulting two states system of ODEs was then linearized.

Relative performance of both reduced order model is shown in Figure F.2. It is evident that the transient response of in case 1 gives a better fidelity to the original model.

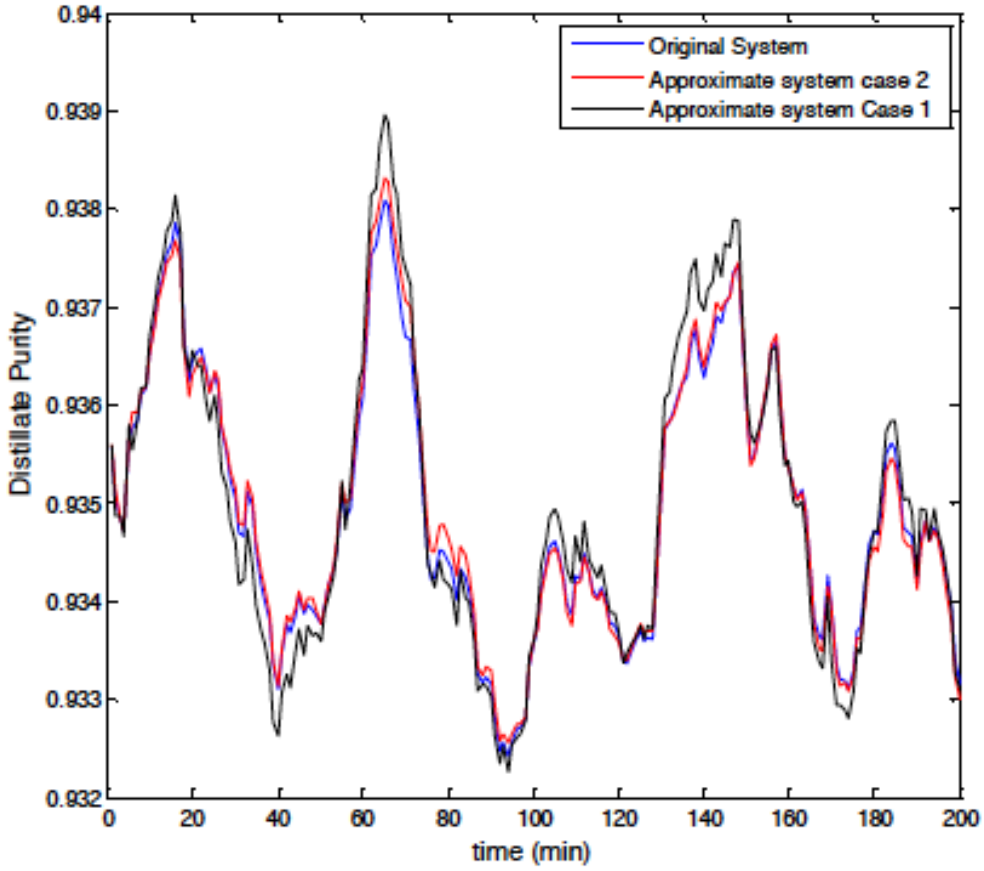

Figure F.2: Dynamic simulations of the original system compared to reduced order models

In this work we do not intend to have the original state information for the physical system. Note that the 32-states model cannot be directly used to derive multiparametric controllers/estimators. Also note that the remaining states are also those required to compute optimal control laws when deriving a mp-MPC controller. Although the first state of the original system of ODEs is measured, it is also possible to reconstruct it from the estimated reduced states. This is shown inFigure F.3 . One can notice that case 2 offers a significantly better estimation than case 1 although both systems are linear. The comparison is also performed on the reduced states. The two lower dimensional subspaces onto which the original states are projected are not the same since the linearization in case 1 is performed around the steady states values of the original states

while the linearization in case 2 is carried out on the steady state values for the nonlinear reduced order model. In Figure F.4 we show the critical regions for the moving horizon

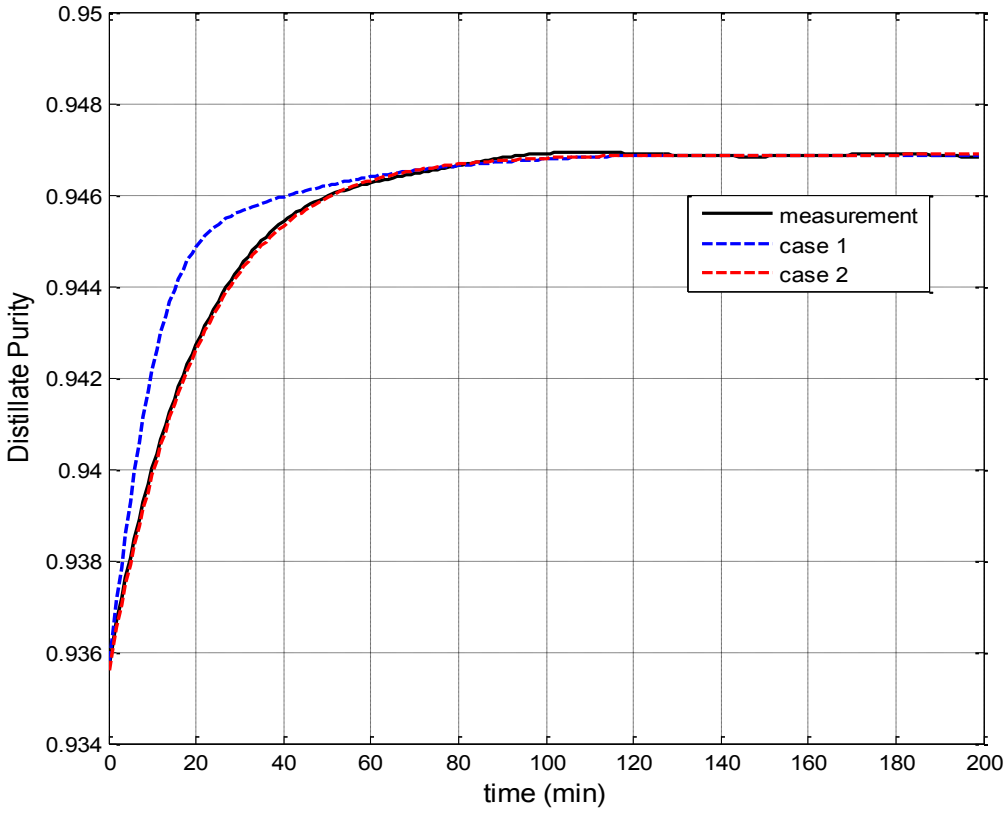

Figure F.3: Comparison of reconstructed states for both reduced order models.

estimator based on case 2, which will be used for simultaneous mp-MPC/MHE.

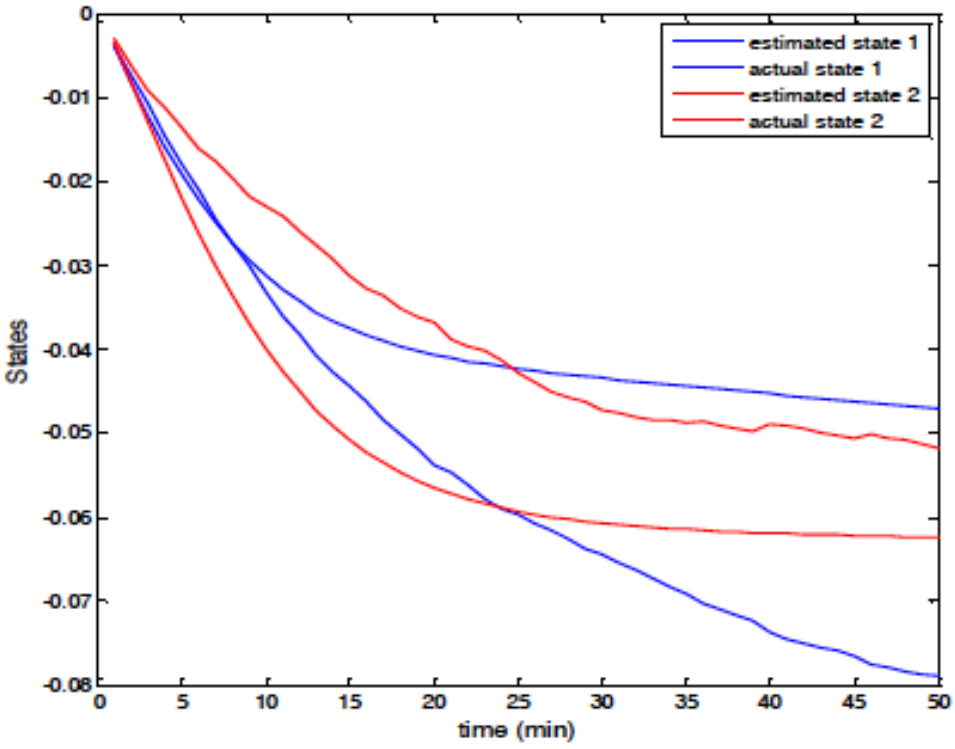

Figure F.4: actual and estimated reduced order state information for case 1

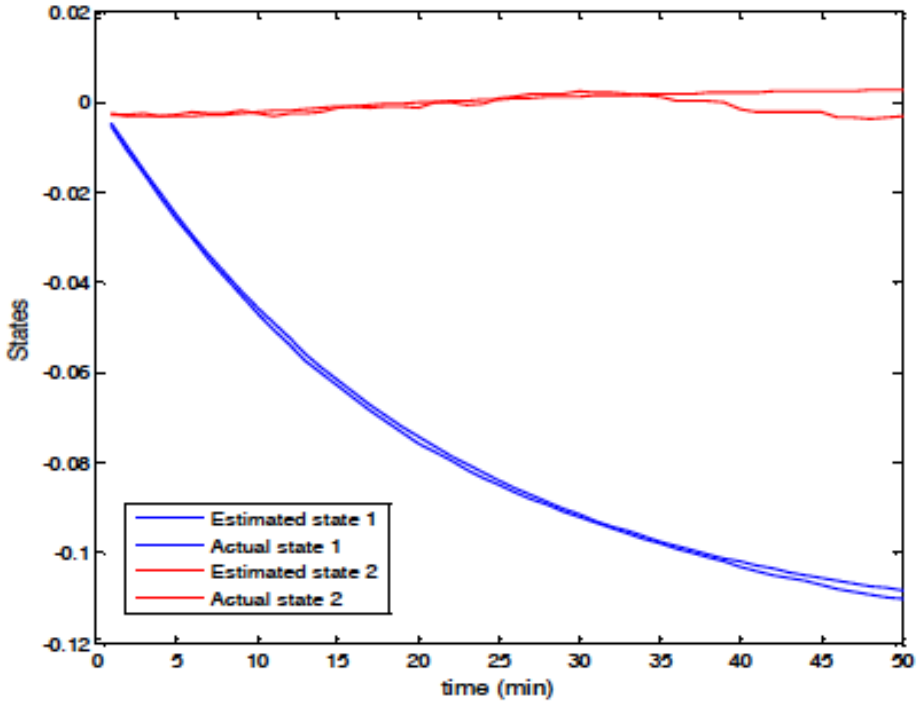

Figure F. 5: actual and estimated reduced order state information for case 2

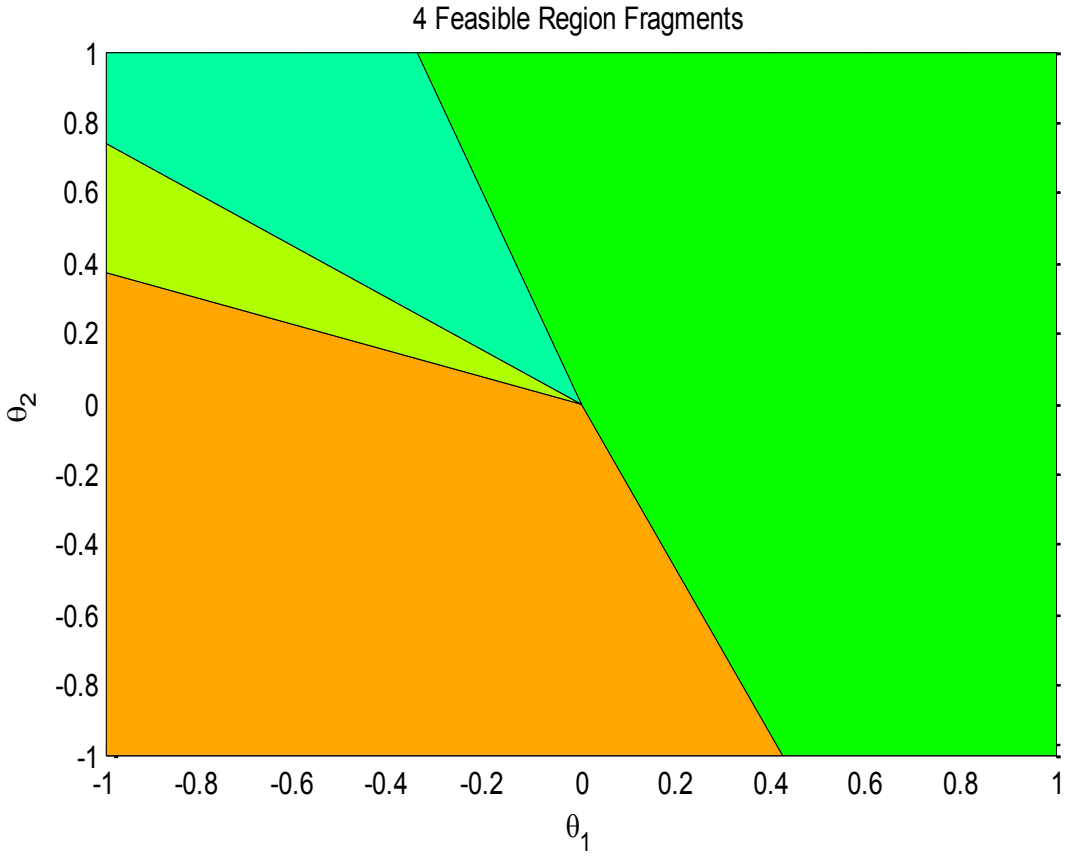

Figure F.4: Multiparametric critical region maps for the estimator built based on case 2: Projection on the first two parameters, which are the two past measurements in the estimation problem.

Figure F. and Figure F. show the performance of both reduced order estimators in their respective subspace. One observation that can be made, having used similar reduction techniques both based on singular value decomposition and balancing of the system, is that the order in which the linearization and reduction steps are performed does matter and nonlinear model order reduction seems to perform better if employed prior to linearization

mp-MHE and mp-MPC were combined and a close-loop simulation, shown in Figure F.5, was performed to evaluate the performance of the methodology. It can be seen that the estimator provides sufficiently accurate information to the parametric controller to drive the system to the desired set point based only on measurement information. The combination of two reduced order parametric maps is then sufficient to operate a control policy for high order chemical process. A slight offset is observed around the set-point and is mainly due to the noise or uncertainty of the inlet concentration of the column. In the case of high measurement noise (Figure F.6 and Figure F.7), the control profiles are more erratic but the simultaneous implementation of mp-MPC and mp-MHE still achieve the desirable set-point change.

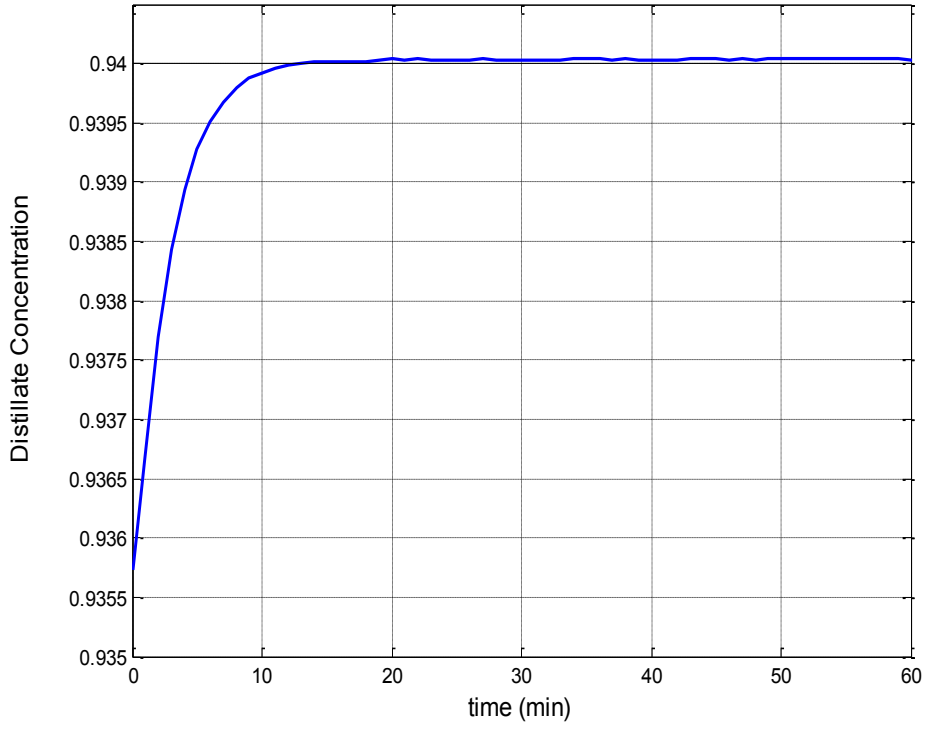

Figure F.5: Close loop simulation of a set-point change operated through simultaneous mp-MHE and mp-MPC.

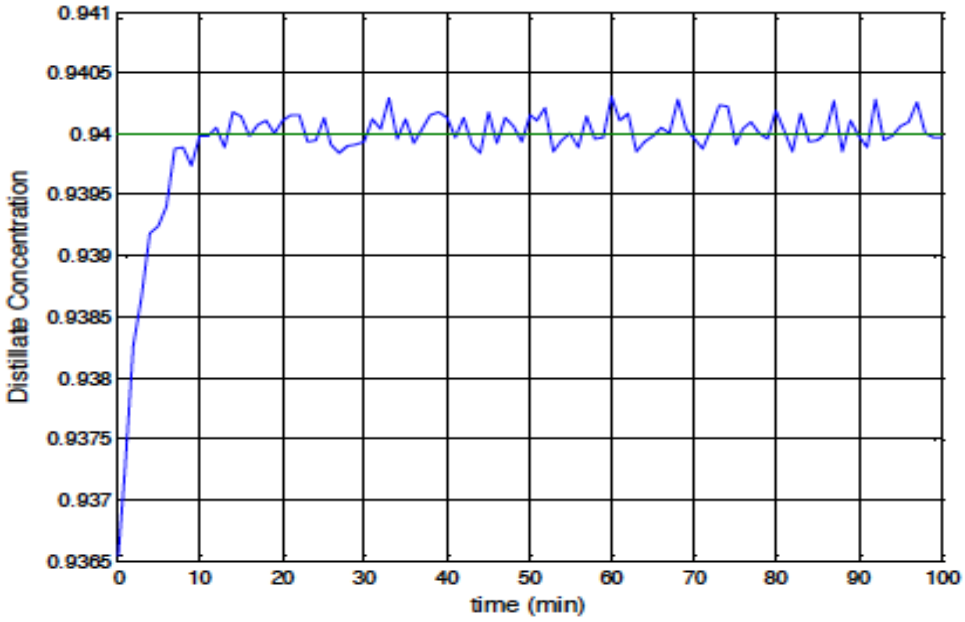

Figure F.6: Evolution of the control input variable in the case of high measurement noise

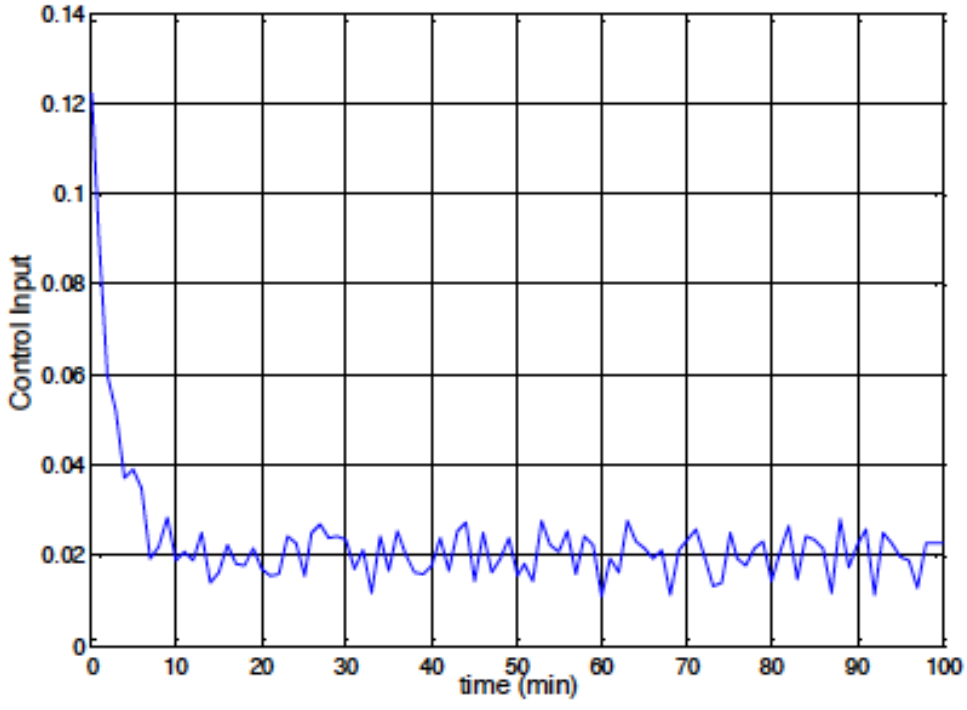

Figure F.7: Evolution of the output variable input variable in the case of high measurement noise

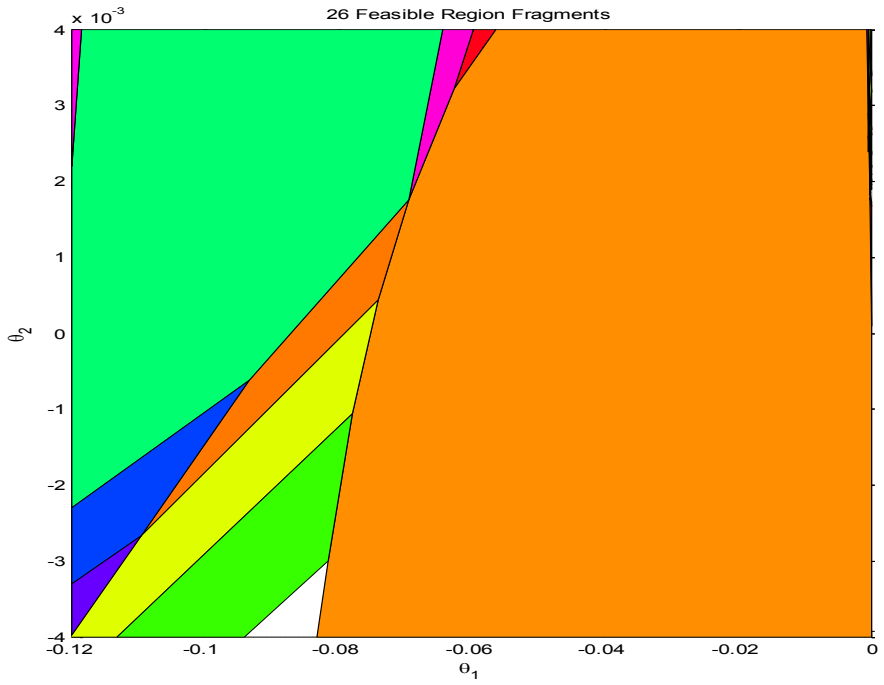

Figure F.8: Critical regions for the mp-MPC controller implemented simultaneously to mp-MHE

Case 1	**Case 2**
$A=\begin{pmatrix}0.97902 & -0.051464\\ 0.03223 & 0.92291\end{pmatrix}$	$A=\begin{pmatrix}0.9546 & 0.05113\\ -0.04809 & 0.3834\end{pmatrix}$
$B=\begin{pmatrix}-0.06874\\ -0.039587\end{pmatrix}$	$B=\begin{pmatrix}-0.09323\\ -0.0596\end{pmatrix}$
$C=\begin{pmatrix}-0.096179 & -0.10013\end{pmatrix}$	$C=\begin{pmatrix}-0.1009 & 0.06461\end{pmatrix}$
$G=\begin{pmatrix}0.066148324\\ -0.09309532\end{pmatrix}$	$G=\begin{pmatrix}0.0097686\\ 0.045933\end{pmatrix}$

Table F. 3: LTI system for case 1 and case 2